

**Camera Traps as Sensor Networks for
Space-Time Monitoring of Terrestrial
Mammal Communities**

Elsa M S Bussi re

UCT Research in Biological Sciences



Camera Traps as Sensor Networks for Space-Time Monitoring of Terrestrial Mammal Communities

Elsa Marion Sylvie Bussière
15 December 2017

Thesis submitted to the University of Cape Town
in candidacy for the degree of
Doctor of Philosophy

Supervisor: Les G. Underhill
Co-supervisor: Greg Distiller

To those who believed in me,
even when I did not believe in myself

To all scientists,
who do not only wish to make sense of
the natural world intellectually, but also
wish to experience nature emotionally and
viscerally

Mathematics, rightly viewed, possesses not only truth, but supreme beauty; a beauty cold and austere, like that of sculpture, without appeal to any part of our weaker nature, without the gorgeous trappings of painting or music, yet sublimely pure, and capable of a stern perfection such as only the greatest art can show. The true spirit of delight, the exaltation, the sense of being more than Man, which is the touchstone of the highest excellence, is to be found in mathematics as surely as in poetry.

Bertrand Arthur William Russell

Nature was Humboldt's teacher and the greatest lesson that nature offered was that of freedom. Nature is the domain of liberty, Humboldt said, because nature's balance was created by diversity which might in turn be taken as a blueprint for political and moral truth. Everything, from the most unassuming moss or insect to elephants and towering oak trees, has its role, and together they made the whole. Humankind was just one small part. Nature itself was a republic of freedom.

Andrea Wulf, *The Invention of Nature*

Contributors

PhD Candidate

Elsa M. S. Bussière, Animal Demography Unit, Department of Biological Sciences, University of Cape Town, South Africa

Supervisor

Les G. Underhill, Animal Demography Unit, Department of Biological Sciences, University of Cape Town, South Africa

Co-supervisor

Greg Distiller, Department of Statistical Sciences, University of Cape Town, South Africa

Institutions

University of Cape Town, Private Bag X3, Rondebosch 7701, South Africa

CapeNature, Scientific Services, Private Bag X5014 Stellenbosch 7599,
Assegaaibosch Nature Reserve Jonkershoek, South Africa

Sponsors



Disclaimer

I declare that this thesis has been composed solely by myself and that it has not been submitted, in whole or in part, in any previous application for a degree. Except where states otherwise by reference or acknowledgement, the work presented is entirely my own.

Elsa M. S. Bussière

A handwritten signature in black ink, appearing to read 'Elsa M. S. Bussière', written in a cursive style with a horizontal line underneath.

Abstract

Most of the conservation issues which ecologists are called on to help resolve are essentially about ecological communities. Camera trapping technology has led to a surge in the collection of large ecological datasets, which provides an unmissable opportunity to attain deeper knowledge of animal community assembly and structure. Using extensive camera trap data, this thesis examines whether camera traps can be used as sensor networks for a space-time monitoring of the terrestrial mammal community that occurs in the Little Karoo of South Africa.

In Chapter 1, the species-habitat relationship along a ruggedness gradient was studied. Using resource selection functions and multivariate statistics, this chapter showed that the strength of affinities, which mammals developed with specific terrain roughness, varied among species. It also enabled the recognition of subtle and continuous nuances in the spectrum of habitat preferences, providing a novel tool to explore the forces driving species coexistence in local animal communities.

The theme of Chapter 2 was to consider patterns of seasonal occurrence within species circadian rhythms. Using kernel density functions with descriptive and multivariate statistics, this chapter showed that most mammal species responded to the ecological variability brought about by seasonality by adjusting their diel activity rhythms between winter and summer, resulting in a reduction of time exposure to a physiologically stressful environment caused by high temperatures in summer. It also highlighted that while some shifts only result from photoperiodism alignment, most are driven by other factors too.

Chapter 3 examined temporal-partitioning as a mechanism driving sympatry. Using kernel density functions and multivariate statistical analyses, this chapter enabled subtle nuances in the spectrum of diel activity rhythms to be visualised, highlighting the variety of temporal niche breadths and of

activity onset/offset timings, which allowed diel activity rhythms to diversify and the mammal community to partition the temporal resources.

Finally, in Chapter 4, topics dealing with leopard habitat preferences and leopard population density were explored. Using spatially explicit capture-recapture models, this chapter showed that leopard density remained low but varied with topographic relief; it increased with ruggedness of the terrain up to an optimum, and followed a reversed trend as the terrain roughness kept increasing. The population was composed of two groups of individuals with significantly different home range sizes, potentially explained by gender duality in movement. The chapter provided leopard density estimates ranging from 0.49 to 0.82 individual per 100 km².

Local communities, such as that of the mammal species of the Little Karoo, are neither closed nor isolated. Therefore, it would be insightful if future studies were to embrace the metacommunity concept and explain these patterns of species distribution, abundance and interaction at multiple scales of spatio-temporal organisation.

Acknowledgements

A PhD is a high job demand with low job control. As a prospective PhD student, I was not so naive as to take on the journey expecting an easy ride. While I prepared myself for the intellectual challenges, I did not anticipate the psychological ones. The overwhelming feeling of being cut adrift really pushed me to the edge. I could write an entire thesis on my PhD setbacks and on how, independent research felt like a lonely assignment, sowing the idea of being an incompetent fraud. During my darkest days, I could barely remember the passionate and driven version of myself, bustling with energy and chasing galvanizing dreams. Getting this PhD cost me an awful lot of time and heartache, but, rather than demonizing my detractors, I would like to celebrate my support network:

I would like to thank the University of Cape Town, its Animal Research Ethics Committee as well as CapeNature for granting the necessary research permits in order to carry out my PhD research project. Coral Birss and Corne Claassen, your support, encouragement and advice have been extremely helpful.

I am hugely grateful to all my generous sponsors who believed in this exploratory project: the University of Cape Town, the Hans Hoheisen Charitable Trust, the Cape Leopard Trust, the Explorer's Club, the National Geographic Conservation Trust, the National Research Foundation, KWay and The Rufford Foundation. Quinton Martin, you lent me a hand when I was about to give it all up, your camera traps revealed the presence of many Cape mountain leopards as you wished it would.

I would like to thank my supervisors, Prof. Les Underhill and Dr. Greg Distiller. Les, the journey was long and strenuous. More than once I doubted your commitment to me and to my work; however, you are one of the few people who never ceased to believe in me, no matter what went on in the space between my ears (or behind my eyes). You gave me an unimaginable freedom,

difficult to handle and worrisome at times, but forging my greatly needed self-reliance. Thank you for placing your unwavering trust and confidence in my abilities to pull through the myriad of obstacles that rised up against us. Greg, I am grateful for the patient guidance, encouragement and advice you have provided throughout my time as your student. I have been extremely lucky to have you responding to my questions and queries so promptly.

Marius Brand and the entire field team at Anysberg Nature Reserve, I am appreciative of your keen interest in the project and of your help to facilitate data collection as much as possible. A special thank to ranger Nkosinathi Moyo, your house was an enjoyable shelter during the coldest nights of winter. I still cannot believe that you did not run away as you witnessed my full distress and discomposure firsthand, when twenty camera traps got washed away after the summer flood! George Moggach and Megan McLaren, your stunning house in the middle of the arid and rugged Karoo desert, surrounded with gemsboks, springboks and kudu was surreal!

Sanbona Wildlife Reserve provided much support in terms of accommodation, time, fuel and man power to carry out the research study on its large property. I would like to thank Mario Wildman, Bradwill Petersen, Ruan Erasmus and Andy Hughes for assisting me with camera trap deployment. Mario, I thoroughly enjoyed your friendship and your cheerfulness, which always dampened my stress. I am thankful to the workshop for helping me with all the car troubles, and, of course, to Paul Vorster and Liesl Eichenberger for their trust, guidance and help throughout the project. Paul, a very special thank for your unswerving support throughout the animal captures, it made all the difference.

Hanscel Vosloo, thank you for making MontEco part of the study area, especially as it turned out to be an important space for brown hyenas. Thanks for allowing me to live on the farm and for my brother to visit. Ben Jakobus Booysen, you were such a wonderful assistant. Although we could not communicate with words, you always smiled and observed my gestures carefully. You learned very quickly and I could rely on you whenever needed.

Danie Pretorius, you really went out of your way to help me with my research. Koktyls, at the foot of the Warmwaterberg Mountains, was a splendid base to organise my field trips, even though your pet crow persisted in trying to puncture my eyes!

Xanet and Morne Postma, your energy, passion and kindness was wonderful. I cannot thank you enough for your tremendous warmth, hospitality and fantastic food, which make African Game Lodge a special place in the Little Karoo.

Frik Linde, your home – the Witteberg Nature Reserve – is undoubtedly one of the prettiest areas I got the chance to visit in the Little Karoo. Your 4×4 tracks were a bit of a challenge for my Land Rover, but your cottages were the perfect place to unwind after a long day under the sun.

Kevin Jolliffe, your enthusiasm and the freedom you immediately gave me to move freely on Drie Kuilen Nature Reserve and collect valuable data, was delightful. I adored your excitement when we first photo-captured an aardwolf!

Jonathan and Sharon Deal, thank you for making Gecko Rock Nature Reserve part of the study area.

This project would have never been possible without the collaboration of all the farmers and other landowners who granted me access to their land, guided me through the endless two-track road network, and often welcomed me into their warmly home. A very special thank to Michael Meiring, Elrie Roux, Larissa Green and Kent Cooper, Steyn and Ellen Joubert, Evan and Christelle Johnson, Dirk and Ronel Steyn, Koos van der Merwe, Martin Mauermann, Juna Phillips, Wouter Stemmet, Ralph Müller, Jan Meintjies, Roelf Louw, Abri Meiring, Albert Kuhn, Susan Gie, Helene Cloete, Philip and Ronel Fouché, Tom Garvin, Derek Bowman and Pankie Kellerman, for your participation and for smoothing my way.

Marika and Johan Bell, I cannot possibly thank you enough for your warmth, affection and support. Your old farmhouse, with its olive trees, is a safe heaven and the Cape mountain leopards know all about it. Lodewyk Galant, thank you for your kindness.

Willem and Schalk Burger, I thank you from the bottom of my heart for making sure that every brown hyena walked away safely after being captured under your supervision.

Sue Kuyper, you were always there with wide open arms when I felt stuck in the corner of anxiety and dread. Thank you for handling all the frustrating administrative duties that usually come with postgraduate studies.

Nicholas Lindenberg and Thomas Slingsby, you are my favourite GIS consultants. I could hardly follow your train of thoughts, although you never made me feel dull or slow. Thanks for always making yourselves available, and for providing solutions to all my troubles.

Guy Palmer and Jerome Ainsley, you took the time to go through hundreds of camera trap photographs to help me identify hares and birds, thank you very much for your expertise.

XX

ELSA M. S.
BUSSIÈRE

Dennis Laidler, you are kindness itself! I am always thrilled to share my dearest Zimbabwean memories with you, and to hear your incredible stories and adventures in this fabulous country. I owe you my most beautiful Cape mountain leopard photos, thanks for helping me build this fancy camera trap.

Arnold van der Westhuizen, Guy Balme, Anita Meyer and Tom McLaughlin, you helped me in the development of research ideas that I could not pursue. My thesis ended up being very different from that I had in mind when I started a few years back and I thank you very much for your understanding.

Res Altwegg, you have always been upfront and honest with me, which are qualities I value dearly. Thank you for helping me solve many of my R troubles, for providing relevant bibliography and for always accepting to listen when I needed it.

Robert Thomson, Thanks for being the friend I needed when starting my research in the Kalahari, as well as for trusting me with your pygmy falcons.

Jeremy Bolton, your knowledge about camera trapping was a valuable source of information as I was getting started in this field of research.

Jaco Mattheus, you always understood the worries which came with purchasing costly research equipment. Your background in conservation makes you a trust-worthy salesman, as you understand the challenges and risks coming with wildlife research. Thank you for your help and guidance.

Matthew Wijers, I am eternally grateful for your unconditional support and encouragement throughout the years. Your wholehearted trust in me often gave me the courage to move forward when I was fearful. Thanks for your genuine and sincere interest in my work and struggles, as well as for going the extra mile when you sensed I needed it. I hope this thesis will give you ideas to analyse your own camera trap data; the Zimbabwean lions are lucky to have you on their side.

Herman and Melanie Joubert, no words can possibly express the extent of my gratitude for the day my life crossed paths with yours. You have helped me in so many ways and welcomed me into your home as part of your family. Thanks to you, Montagu and your sweet little house on top of the hill overlooking the orchards, hold a special place in my heart. With Bennie, Carla and the children, you gave me the most magnificent gift: a sense of belonging. While most people act as if I were a foreigner in a country I consider to be home, you made me feel part of your lives and triggered in me the need to give, and receive attention to, and from you. You saw my cultural differences as an opportunity to travel without leaving home, and you forever changed my understanding of yours. Thank you for the delightful

stories of your wanderings in the Kgalagadi and the Kruger, while devouring exquisite malva puddings by the fire place.

Karin and Derick Müller, you never fail to make me smile. Thank you for welcoming me into your home in Serpentine and for always lending me a helping hand when I need it. Your generosity and encouragement always made me feel special, and your joyful minds are an absolute pleasure. You find success in all your endeavours, and I strongly believe that part of this fortune lies in your ability to share it all with your loved ones.

Lauren de Vos, Dane Lee Marx and Megan Loftie-Eaton, what amazing people you are! Your boundless love and unlimited sensitivity for the natural world and its wonders are a real inspiration. I adore listening to all your adventures as you have the precious skill to foster emotional synchrony between people. Megan, you are a nature encyclopedia on legs; nonetheless, you always explore the wilderness as if you were to see it for the first time, never doubt the beauty of this gift of yours, and never cease to share it with all. Lauren, I thought no PhD student could face more setbacks than I did until I heard your journey. I admire your resilience, your benevolence and, overall, your irrepressible drive to bring your artistic impulse into the world. Thank you for listening and sharing your struggles; the finish line is close and your mind has the sharpness to cross it as fast as the shortfin mako shark (what a cute toothy torpedo)! Dane, we hope you come back home soon!

Fernand Sieber, we make a great team! I save your plants from dehydration while you bring me comics and make me laugh in the evening. Your witty sense of humour is the only thing that proved to be more efficient than Bikram yoga to sculpt my six-pack. Thank you for your friendship and positive energy, for truckloads of good times, as well as for all the small chocolates left on my pillow. You have no idea how much your friendship and moral support helped keep my head above water!

Margaux Rat, you once told me that independent and smart women are a pain in the ass, so I guess that is exactly what you are! Your limitless energy is contagious. Thank you for being a safe place I could confide in.

Herman Mynhardt, you introduced me to a facet of Cape Town that was vastly foreign to me. Thanks for guiding me down a path of curiosity and novelty, for taking me pick mussels, catch crayfish and explore Betty's Bay.

Laetitia Borgomano, Fanny Dallenne, Guillaume Vanpée, Maxime Chardonnerau, Alexandra Bordes, Juliette Protino and Marion Hurel Ménard, your friendship is precious to me. You remind me of my "douce France,

cher pays de mon enfance”. Thank you for the messages of support and encouragement. I hope we meet again under the African sun.

Helena Salgueiro and Patrick Thommen, you are the most amazing biology lecturers I ever had. Your dedication and passion were an inspiration. You were two of my rocks during the frightfully challenging years of Classes Préparatoires aux Grandes Ecoles. You broadened my mind and fueled my dreams of conducting wildlife research in Africa.

Debra and the whole team at yogazone, you introduced me to your hot yoga styles that you have been teaching and developing for many years. I always felt invigorated, relaxed and centred after immersing myself into your classes. Yogazone became a safe place – a sanctuary – during the last months of the PhD write-up.

To my running shoes and swimming costume, thank you for keeping me sane and healthy, both on land and at sea! To my books, thanks for the delightful imaginary adventures that lulled me away from my fears.

Papa, maman, Romain and Annouck, you mean the world to me. You are my parents, my brother, my sister, but also my friends. I cannot thank you enough for all the wonderful travels and thrilling experiences that took us off the beaten tracks, into some of the world’s remotest regions, and ignited in me a passion for the wonders of the natural world. Thank you for passing on your love for science and Africa to me, it became the general thrust of my life journey. Your unquestioning love and trust gave me the confidence to follow my dearest dreams, you are my greatest source of mental and emotional support. I am eternally thankful to you two – papa and maman – for tirelessly helping me put brick upon brick to rebuild myself during these past months. Romain and Annouck, I long to be and laugh with you again. Please, come visit me all in Cape Town, I cannot wait for us all to be standing together at the southern tip of the African continent.

Infinite thanks to Annouck Bussièrè for the fabulous illustrations found throughout the thesis. With them, the chances to have people reading it all through increased substantially :)

My late papi Dé, I wish you were still with us, as I know how proud you would be to see me complete this journey. With mamie Jo, you passed on to me your passion for investigation and story telling. I hope it is a little bit what I have achieved here.

To the red Karoo mountains and its wild inhabitants, you made my PhD so special. Your unobtrusiveness and apparent desolation challenged me at first, you, one of the world’s most biodiverse places. It took me time to get

to know you, and I will forever cherish the gifts you spoiled me with: my encounter with a Cape clawless otter at the river, my face-to-face with a juvenile caracal, the glimpse of a small spotted genet and the company of a Cape porcupine during my nocturnal travels. But above all, I will never forget the distressing look that every captured brown hyena gave me. A call for freedom. An irresistible drive to remain hidden in the darkness of the night. What an extraordinary animal!

Finally, I would like to thank all the great minds in scientific history who carry me, as well as everyone else, on their shoulders. As Bernard of Chartres used to say: “we are like dwarves perched on the shoulders of giants, and thus we are able to see more and farther than the latter. And this is not at all because of the acuteness of our sight or the stature of our body, but because we are carried aloft and elevated by the magnitude of the giants”.

Five years ago, if I had some notion of what it would really be like to complete this PhD, I probably would have run for the hills. Today I am immensely proud to see how far I have come, and it would have never been possible without you all.

Thank you.

*So damn
cute!*



Abbreviations and symbols

Abbreviations

ADM: Activity-shift Distance Matrix
AIC: Akaike Information Criterion
ETA: Effective Trapping Area
EWT: Endangered Wildlife Trust
CCM: Count Community Matrix
CEPF: Critical Ecosystem Partnership Fund
HPC: High Performance Computing
ICTS: Information and Communication Technology Services
IUCN: International Union for the Conservation of Nature
MammalMAP: African Mammal Atlas Project
NMDS: Non-metric Multi-Dimensional Scaling
ODM: Overlap Distance Matrix
RDM: Ruggedness-preference Distance Matrix
RSF: Resource Selection Function
SANBI: South African National Biodiversity Institute
SECR: Spatially Explicit Capture-Recapture
SCM: Smoothed Community Matrix
TRI: Terrain Ruggedness Index

Logic symbols

\exists Existential quantification. “There exists at least one ...”
 \forall Universal quantification. “Whatever ...”
 \in Membership. “... is an element of ...”
 \mapsto Arrow function. $r \mapsto A(r)$ with A being the function and r the variable.
 C^o Class of all continuous functions.
 $[x, y]$ Continuous domain that contains the set of all real numbers r satisfying $x \leq r \leq y$.
 $\{x_1, x_2, x_3\}$ Discrete domain that contains the set of values x_1, x_2 and x_3 .

Notation

Chapter 1 to 3 deal with numerous species. The $,s$ notation was used as a reading tool to simplify mathematical formulas. $X_{,s}$ was the annotation used to name the X variable which refers to species s .

Contents

Abstract	xiii
Acknowledgements	xvii
Abbreviations and symbols	xxv
Introduction	3
1 Understanding the role of topographic relief in the sympatry of mammal species	15
2 Seasonal plasticity of mammalian diel activity rhythms: patterns and control	43
<i>Splendours of the Little Karoo</i>	93
3 Multivariate analyses enable visualisation of temporal resource partitioning in local mammal communities	129
4 Estimating leopard population density in relation to terrain ruggedness with spatially explicit capture-recapture models	159
Conclusion	193
References	197
Appendix	219



Introduction

Around two centuries ago, Alexander von Humboldt – described as the lost hero of ecological science – revolutionised the way we perceived the natural world, as Andrea Wulf explains beautifully in her book *The invention of nature* [368]. Humboldt observed patterns, similarities and connections everywhere, prompting him to write “In this great chain of causes and effects, no single fact can be considered in isolation”. The web of life, the concept of nature as we know it today, was invented for the first time. Concomitantly, nature’s vulnerability became obvious because pulling on one thread would cause the whole tapestry to unravel. Ernst Haeckel, greatly inspired by Humboldt’s evocative writing [368], named this new discipline: *Oecologie*. In his book *Generelle morphologie* [132], Haeckel wrote “All the Earth’s organisms belonged together like a family occupying a dwelling; and like the members of a household they could conflict with, or assist, one another. Organic and inorganic nature made a system of active forces”.

Biocoenosis, the importance of community ecology

In ecological studies, biocoenosis is the emphasis on relationships between species co-occurring at a given time and space. These relationships are considered in addition to the interaction of each species with the physical environment [234]. All organisms exist as an intrinsic component of a community, and yet relatively few experiments investigate the web of species interactions within the context of multi-species coexistence [187, 308, 323]. The significance of the community context is highlighted by the observation that the intensity and often the direction of the interactions between a set of species may vary in the presence of others [323]. John Lawton said, in a commonly cited paper, “community ecology is a mess” and “why [do] ecologists continue to devote so much time and effort to traditional studies in community ecology?” [187]. Natural communities are indeed extremely com-

plex and understanding the processes governing them often requires tedious and laborious elaboration of details, often not transferable to broadly similar systems [134, 186].

Community ecology investigates the nature of the biological interactions between organisms, their origins and their ecological, as well as evolutionary, outcomes [60]. To achieve these objectives, one must take account not only of the dynamics of the target species and/or process, but also of the variations within the biotic and abiotic environments. This requires studies, which cover larger geographical areas than are usually done and which emphasise the role of historical factors in order to consider evolution in the community assembly process [6, 60, 63].

Most of the conservation issues which ecologists are called on to help resolve are essentially about ecological communities; it is therefore crucial to pursue and advance ecological studies at various scales and to analyse community assembly and structure over space and time [98, 112, 308].

Camera trap, a revolutionary tool

Accessing a large amount of ecological data about animal communities, collected unobtrusively over vast spatial and temporal scales, has always been a consequential challenge for ecologists. Observing wildlife without interfering with it was an activity first developed by hunter-gatherers who constructed blinds and other smokescreens aiming to conceal themselves. Today, the desire for undisturbed observations of wildlife is still highly sought-after, both for recreation and aesthetic appreciation of nature, and for scientific understanding of animal populations and their relationships to their environment [252]. Today, modern photographic devices, camera-triggering systems and compact power sources allow us unequalled, non-invasive access into wildlife habitats using automated digital camera traps.

Wildlife photography became famous in the late nineteenth century, and the first animal-triggered photograph was that of a galloping horse, taken in 1877 with a dozen of cameras triggered by breaking strings [129]. Other successful attempts to have animals taking their own pictures took place during the first decades of the twentieth century. Using trip wires and a flash system, George Shiras photographed a myriad of North-American wild species, and developed innovative methods, sometimes using bait and sometimes positioning cameras at strategic places with frequent animal movement [302–304]. Shiras' methods were then adapted by the German Carl Georg Schillings to photograph the Eastern African wildlife, which produced striking photographs of leopards *Panthera pardus*, black-backed jackals *Canis*

mesomelas, spotted hyenas *Crocuta crocuta*, African lions *Panthera leo*, black rhinoceros *Diceros bicornis*, all taken by the subjects themselves [296, 297].



Figure 1: Camera trap photographs of George Shiras

Five of the 74 published photographs of George Shiras, father of wildlife photography, showing the North American fauna. Shiras, who began photographing in 1889, was the first to use camera traps and flash photography when photographing animals.

It did not take long before this newly developed photographic tool attracted the attention of scientists wishing to document the species diversity of a specific area. For example, in 1927, using trip wires and bait, Frank M. Chapman photographed ocelots *Leopardus pardalis*, mountain lions *Puma concolor* and white-lipped pecaries *Tayassu pecari* among many other species on the Barro Colorado Island in Panama [62]. He also used the photographs to make inferences about animal behaviour and to attempt individual identification.

Since the earliest models that used traditional film and a one-shot trigger function, the remote cameras advanced significantly. The trip wire fell into disuse and the camera trigger evolved, becoming a treadle placed in runways, before turning into a beam of deep red light activating the photographic device once interrupted by animals [72, 259]. The practicability of remote cameras improved with thriving technology; they became digital, portable, affordable, easy to use, long lasting and reliable. Weather and water-proof housings were designed to protect the equipment from damage and to camouflage it for minimal disturbance [127]. Remote photography has a deep-seated background in ecological research [72]. It is the develop-

ment, in 1991, of infrared-triggered camera systems – which are described as digital and automatic photographic devices, employing a pulsed infrared beam as a triggering device [59] – that induced its use to surge. Remote camera systems for detecting wildlife, also called camera traps, became so attractive that from 1993 onwards, they matured into commercially available products [182].

Ecological studies benefited greatly from the use of camera trap systems. The primary advantage was the large savings in time and money by forgoing labor-intensive direct observations, the ability to gather information in inclement weather as well as throughout the night [68, 99], and to record data in inaccessible locations and rugged terrain [54, 202]. These benefits became all the more profitable when the research was conducted on multiple sites [265, 321]. Chronic mechanical problems (battery failure and programming errors) could however cause data loss, especially because it often took time for the investigator to become aware of the issue [278]. Remote photographic systems also enabled ecologists to collect reliable data and to get insights into the ecology of rare, secretive and sometimes aggressive species [202], which would have been challenging to observe otherwise. However, several scientists highlighted the possibility for camera traps to alter animal behaviour [148, 207, 221, 261, 358]. Initially lacking, the number of surveys attempting to evaluate the impacts of camera trapping on animals increased and provided guidelines on how to minimise the risks of bias [141, 278]. Through the years, the variety of camera traps exploded; they differed in terms of their aspect, zones of detection, sensitivity and performances under contrasting environmental conditions [330]. As camera traps kept developing, their reliability increased and their disturbance became minimal [3, 41, 128]; they alleviated problems associated with observer bias, making the study of rare, protected and sensitive species, feasible.

Camera traps have received wide exposure in both the scientific and popular literature because they bring opportunities to collect a colossal amount of data where little information was previously available and because they provide engaging images useful for education and promotion [166, 331]. In a purely scientific framework, camera traps were employed to investigate animal activity patterns [8, 59, 72, 77, 127, 128, 288, 348], nest ecology [67, 185, 207], habitat preferences [83, 172, 312, 315], species richness [1, 44, 279], as well as species abundance and density [33, 137, 203–205, 314, 349]. Camera traps can be utilised to address far-reaching questions in community ecology by collecting systematic data on an assemblage of wide-ranging species [331]. Remaining continuously on and being deployed across large areas, camera trap networks offer opportunities to evaluate spatial and temporal inter-species dynamics [2, 331].

Camera traps and statistical ecology

Scientific and technical jargon define camera traps as ‘proximity detectors’ [29], meaning that they have the potential to register the animals’ presence and identity without any animal detention. The surge in mass camera trap development provided the scientific scene with a new tool, which led researchers to revisit commonly used ecological methods such as capture-mark-recapture. Bringing technology into the ecological framework made the field of statistical ecology a flourishing discipline. Among the myriad of statistical developments, one stands out: Spatially-Explicit Capture-Recapture (SECR) models [89]. SECR is a newly-developed statistical analysis which provides reliable population density estimates from camera trap data, and which is used worldwide to gain insights into the population ecology of wide-ranging and elusive species; often those of the greatest conservation concern [33, 55, 84, 137, 171]. While conventional capture-recapture methods provides abundance estimates, the SECR approach takes account of the spatial history of the photo-captures and skips the intermediate step of estimating an Effective Trapping Area (ETA) to access density estimates [90].

The Little Karoo, a unique landscape

The mingling of unsustainable consumption in developed countries and unceasing poverty in developing nations is threatening the natural world with non-reversible species extinction, proceeding at an ever-increasing pace, exceeding greatly conservation resources [231, 241]. In developing countries, the Critical Ecosystem Partnership Fund (CEPF) safeguards, by promoting working alliances and circumventing effort duplications as well as *ad hoc* actions, the internationally recognised hotspots: places where outstanding concentrations of endemic species are undergoing phenomenal loss of habitat [70, 241].

The Little Karoo of South Africa is a semi-arid inter-montane basin falling into the Cape Floristic Region [Appendix 1A], where succulent Karoo (dwarf, succulent shrublands), subtropical thicket (discreet bush clumps) and fynbos (fire-prone shrublands and heathlands) [199] – three globally-recognised biodiversity hotspots – intermingle [230, 231, 240]. The succulent Karoo biome is one of two international biodiversity hotspots located in arid regions [230]. In South Africa, although these semi-arid rangelands contain some of the most biodiversity rich landscapes in the country, they are also some of the least conserved spaces; falling under the national average of 6% of their area under protection [253].

The bedrock of biodiversity conservation strategies has been the use of statutory conservation areas; it is however becoming increasingly clear that this global network alone is not going to be adequate to reach its goal of comprehensively conserving biodiversity [47, 238, 247, 289]. Alternative recourses for biodiversity conservation merit closer attention.

From the 1730s onwards, the European settlement subjected the Little Karoo ecosystem to major anthropomorphic forces. The main form of land use was extensive livestock husbandry with ostriches, sheep and goats, due to unfertile landscapes [144]. The region has since experienced a regression of the agricultural economy because of substantial actual and perceived economic losses due to livestock depredation, which has been to the benefit of tourism and second-home industries. The Little Karoo is sparsely populated and the landscape is now a mosaic of extensive farms, small protected areas, and secondary properties. Being rugged, scenic and one of the least productive agricultural systems [34, 270] of the Cape landscape, it makes for an extensive grazing/browsing area with a substantial wild mammal presence, despite few statutory conservation areas [115].

Embryonic research motivations and collateral benefits

Landowners, especially farmers and nature enthusiasts, show a keen interest in knowing their property and understanding its biological functioning. Throughout the years and generations, they learnt to read the signs that nature leaves behind: spoor, droppings, pastings, etc. Nowadays, it is fairly common to see them use camera traps as an additional source of information [183]. All the knowledge gathered in this way is shared, discussed and debated within the local community; it is nonetheless lost to science and conservation, despite an ever-increasing effort to develop open-access atlas projects where data can be submitted and explored by anyone, from anywhere at anytime [81, 307, 342]. The camera trap survey that was led as part of this PhD study, was initially motivated by the desire to investigate and document the potential presence of the brown hyena *hyaena brunnea* in the western section of the Little Karoo. No mammal atlases remotely mentioned the presence of the species in this area, although multiple local farmers were convinced of its occurrence. The data collected enabled to identify at least 18 individuals and to record the population within the Red List of mammals of South Africa, Lesotho and Swaziland [369], which was revised in 2016 by EWT (Endangered Wildlife Trust), SANBI (South African National Biodiversity Institute), IUCN (International Union of Conservation of Nature) and MammalMAP (African Mammal Atlas Project).

The camera trap survey also documented the presence of a rare species, one of the most endangered mammal in the world, the riverine rabbit *Bunolagus monticularis*. Three unknown sites, located in riverine vegetation adjacent to seasonal rivers, were revealed. The information was passed on to CapeNature – the statutory institution with responsibility for biodiversity conservation in the Western Cape – so that it gets incorporated into the Western Cape Biodiversity Assessment report.

On a less positive note, the survey also revealed the presence of non-native species, such as warthog *Phacochoerus africanus* and fallow deer *Dama dama*, most likely introduced to the ecosystem by landowners themselves. The observation of bushpigs *Potamochoerus larvatus* was unexpected and could be explained by a gradual migration of the species from the Eastern Cape region of South Africa.

Timeline of research fieldwork

Given the vastness of the study area (4,327 km²), the camera trap study was conducted as a series of six three-month long surveys. The initial scientific design for camera trap deployment was to use a regular grid and rotate it so that the number of camera stations falling onto roads, river beds and animal paths was maximised. The first camera trap survey was conducted using this design and camera grids placed at random locations provided few to no data at all. However, camera stations located on roads and major animal paths were successful, providing large datasets with a rich species diversity. Camera stations located along river beds were not nearly as successful as that on roads, both in terms of capture frequency and capture diversity.

On the 6th of January 2014, two months after initial deployment of the field equipment, the Little Karoo was hit by the worst flooding since the terrible 1981 flood that then wiped out half the buildings in nearest towns. This time, the water level did not rise as dramatically as it used to 35 years earlier, but roads were washed away and 20 camera traps (a third) were never to be found again.

The first survey led to redraw the scientific design and camera trap deployment protocol of the project. Camera trap stations were then all deployed on roads and animal paths, with a density of two camera trap stations per 50 km². Although the first survey should be considered to be a preliminary stage of the study, valuable data were gathered and included into the analysis as well as into the thesis whenever it was relevant. The sixth survey of the series consists of a replicate of the first, using the newly chosen and standardised protocol which was then used throughout the project.

Research rationale and thesis overview

Considering the ever-increasing pace at which biodiversity erosion is happening, and the expectation for continued increase in pressure on the natural world, it is crucial to gain insights into the mechanisms behind species responses to their environment, so that we can effectively manage biodiversity in a rapidly changing environment, where all biological equilibrium is jeopardised. Camera trapping technology has led to a surge in the collection of animal information, which provides an unmissable opportunity to help resolve numerous of the burning ecological questions that are essentially dealing with ecological communities. This thesis aims to develop new analytical methods enabling to explore large camera trap datasets and to attain deeper knowledge of the mammal community assembly and structure, over space and time, in the Little Karoo, in South Africa.

The thesis is built as a series of stand-alone chapters, which explains the redundancies in the introduction and method sections.

Chapter 1: *Understanding the role of topographic relief in the sympatry of mammal species.*

This chapter first develops – for 27 species within the mammal community – a quantitative approach to relate species distribution to roughness of the terrain in the Little Karoo. Using the Jacob’s Index, the species preference/avoidance for all gradual ruggedness levels is estimated on a scale ranging from -1 (strict avoidance of this habitat) to $+1$ (strict preference, the species is always found in this habitat). Values close to zero indicate that the habitat is used in proportion to its availability. The Jacob’s preference index is then used to produce choropleth maps: shaded graphical representations showing the preferred habitat maps for 27 mammal species. Then, using Non-metric Multi-Dimensional Scaling (NMDS), I estimate the dissimilarities of habitat preferences in relation to terrain ruggedness for each pair of species within the mammal community. The output of the analysis is summarised into a two-dimensional graphical display, gathering species with similar habitat preferences, and keeping away those that demonstrate opposite trends.

Chapter 2: *Seasonal plasticity of mammalian diel activity rhythms: patterns and control.*

This chapter initially searches for seasonal shifts in species activity patterns by comparing the diel activity rhythms of 25 mammal species between the winter and summer seasons. These rhythms are estimated for every

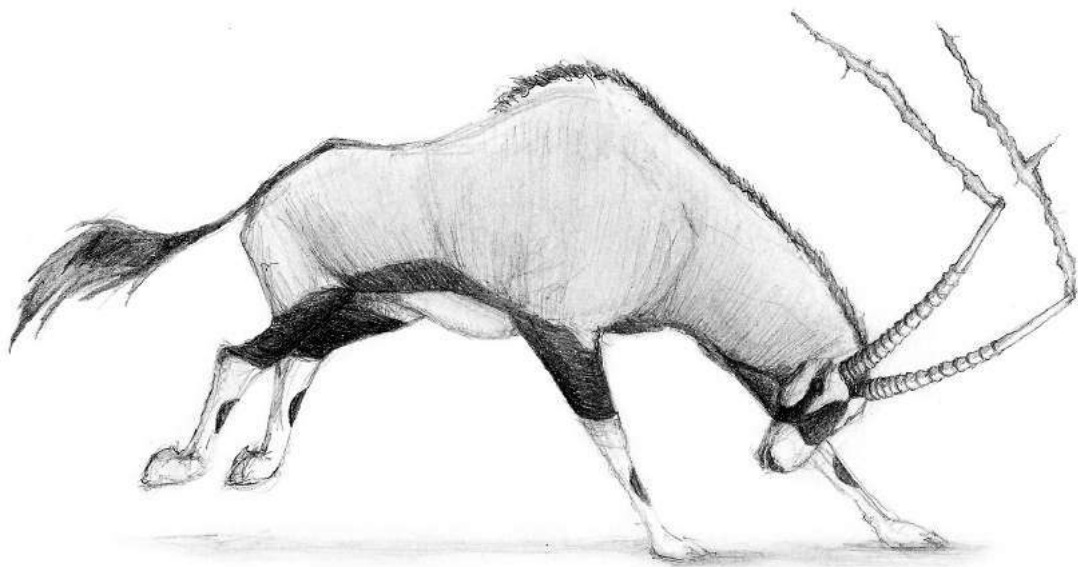
species, using circular kernel density functions. A bootstrap analysis is used to test whether any seasonal change in species' diel activity rhythm was observed. This process was repeated, using three different time metrics to build three density functions for every species, with the objective to test whether seasonal shifts in diel activity rhythms are a consequence of photoperiodism alignment. Variations in diel activity rhythms were then quantified throughout the 24-hour cycle, and compared among all species of the community by running an NMDS dissimilarity analysis.

Chapter 3: *Multivariate analyses enable visualisation of temporal resource partitioning in local mammal communities.*

This chapter uses circular kernel density functions to describe – for 27 mammal species with the mammal community – the species' diel activity rhythm averaged throughout the year. Using three multivariate analyses, the rhythms are compared among all species of the mammal community to differentiate species strategies on how they use the different periods of the 24-hour sleep-wake cycle, and to describe the partitioning of temporal resources among sympatric species.

Chapter 4: *Estimating leopard population density in relation to terrain ruggedness with spatially explicit capture-recapture models.*

This chapter uses newly-developed likelihood-based statistical methods to estimate the population density of Cape mountain leopards in the Little Karoo. Several submodels are built; each allows model parameters to vary with a different combination of covariates. Relative goodness of fit is assessed using model averaging. Using additional habitat information, predictable density maps are plotted from the model estimates having received heaviest weight.



Understanding the role of topographic relief in the sympatry of mammal species

1.1 Abstract

A sound understanding of the forces driving species-habitat relationships is critical to address ecological and biogeographical questions. The patterns of species distribution within a community are the result of the different habitat affinities, which every species has evolved within the landscape to adapt to their environment. A landscape can be defined as a portion of the Earth's surface, formed by a complex of biotic and abiotic systems, and made of spatially heterogeneous habitats. Both landscape and habitat should be viewed as species-specific concepts so that patterns of habitat-use can be interpreted as individualistic responses to spatial gradients in the environment. In this study, camera trap systems were used to record patterns of habitat-use among sympatric mammals of the Little Karoo in South Africa. A resource selection function was then used to quantify species' preferences along the ruggedness gradient, and multivariate statistics were applied to gain insight into spatial partitioning within the mammal community of the Little Karoo. The results show that heterogeneous topographic relief was likely to be an essential constituent of a species' niche and a crucial variable to predict species' habitat-use. The strength of affinities animals developed with specific terrain roughness varied between species; most of them strongly avoided highly-rugged terrain, whereas moderately- and slightly-rugged terrains were usually used in proportion to their availability. The Non-metric multidimensional scaling

plot spatially separated habitat-specialist from habitat-generalist species, as well as grouped species showing similar terrain affinities. The analysis enabled to recognise subtle and continuous nuances in the spectrum of habitat preferences, providing a novel tool to explore the forces driving species coexistence in local animal communities.

1.2 Introduction

Describing patterns of species distributions and habitat selection is a fundamental goal in ecology. A sound understanding of the forces driving species-habitat relationships is critical to address ecological and biogeographical questions, especially for species of conservation concern [130]. At the beginning of the 19th century, Alexander van Humboldt [350] showed interest in the spatial patterning and geographic distribution of organisms, as he described the latitudinal and altitudinal distribution of vegetation zones. His work triggered many more studies of the geographic distribution of various taxa throughout the rest of the century [78, 227, 228].

The patterns of species distribution in a community are the result of the varying habitat affinities, which every species has evolved to adapt to their environment [218]. The general assumption is that animals utilise the minimum economically defensible area (fitness maximization) [159, 206, 267], which is large enough to satisfy their metabolic needs [219, 276].

A landscape can be defined as a portion of the Earth's surface, formed by a complex of biotic and abiotic (geological, hydrological, meteorological, ecological and anthropological) systems [373]. It is made of spatially heterogeneous areas (habitats), which are characterised by structure, function and change (alteration through time) [343]. Habitat description consists of evaluating qualitatively and/or quantitatively landscape heterogeneity. Although much effort has been concentrated on developing vegetation indices (e.g. Ratio Vegetation Index, Vegetation Index Number, Normalised Difference Vegetation Index) [18], numerous landscape features (vegetation, soils, climate, geomorphology, land use) can be used to identify – in a discrete and/or continuous manner – different habitats over a surface [237]. Landscapes can be observed from many points of view and at different spatial and temporal scales [222, 229, 287, 344]. A 'landscape' for a large, mobile predator is a geographically larger area than that for a small rodent, therefore a landscape, just as habitats, should be viewed as species-specific concepts [237].

Gleason [119, 120] claimed that patterns of habitat-use are important and that they should be interpreted as individualistic responses to spatial gradients in the environment [153, 215, 225, 360]. Numerous studies have highlighted the fact that terrestrial mammal distribution and abundance vary along elevational gradients [214–216], especially in mountainous landscapes [48, 197, 282, 305]. For example, in 1971, at a study site close to that being used for this paper – in the Swartberg and Baviaanskloof Mountains – the Saasveld Forestry Research Station studied the ecology of the small mammal fauna, and showed that species composition as well as habitat variables (vegetation structure and cover) varied according to altitude [28]. Although elevation above sea level, like degree of latitude, is not itself of importance to organisms, the correlated environmental variables (both past and present, abiotic and biotic) drive patterns of abundance, distribution and diversity.

Nearly all mountainous areas are shaped by the erosion of exposed (due to uplift) and discontinuous geological substrates, to form ridges, valleys, stream networks and other geomorphological features, which makes for a heterogeneous topographic relief. Terrain heterogeneity is often an essential constituent of the niche of a species [50, 246, 361] and a crucial variable to predict species' habitat-use [101, 177]. Riley et al. (1999) developed the terrain ruggedness index (TRI) – a spatial gradient – which quantifies topographic heterogeneity [284].

Assessing habitat preferences in wild, free-ranging, elusive and often low-density species presents a number of challenges. Methods for defining animals' habitat preferences commonly use Resource Selection Functions (RSFs) that compare resource attributes in areas where animals are observed with those in areas that are considered available [37]. These methods traditionally depended on direct observations [178] and/or spoor transects [337] and/or tracking of radio-collared individuals [104, 165]. Observational studies can alter natural behaviour and activity patterns of the target animals, and can also be limited by sample sizes due to the secretive nature of the target species or to logistical constraints [42]. Spoor transects are feasible on malleable substrates only; they are time consuming and logistical constraining, especially due to habitat inaccessibility. Telemetry studies gather data remotely thereby preventing the biases that may result from observer presence, however the results remain reduced to those individuals that can be physically captured. Camera traps (also called remotely triggered cameras) are now commonly used worldwide in wildlife research, and are one of the newest tools in the ethologist's toolkit [42]. Remaining continuously active, each device is typically capable of generating large datasets and is particularly

useful for detecting elusive and low-density species. The disturbance caused by camera traps, despite some sounds and flashes [221], is minimal [3,41,128]. The non-selectivity of camera traps allows researchers to potentially sample a statistical population of the target and non-target species, which accurately reflect the members of the entire population. Several research teams have used camera traps with a single study design to collect information on habitat selection of sympatric species [36,167], and sometimes at the larger community level [125].

In this study, camera trap systems were used to record patterns of habitat-use among sympatric mammals of the Little Karoo in South Africa. A resource selection function was then used to quantify species' preferences along the ruggedness gradient. Finally, multivariate statistics were applied to gain insight into spatial partitioning within the mammal community of the Little Karoo.

1.3 Material and methods

1.3.1 Study area

The Little Karoo is a semi-arid desert located at the southern tip of the African continent [Appendix 1A], within the Cape Fold Belt. It is hemmed in by the Langeberg Mountains in the south, the Swartberg Mountains in the north and the Outeniqua Mountains in the east. This desert is part of a unique biogeographic region because it belongs to one of the 36 internationally recognised biodiversity hotspots [230,241] [Introduction]. It has a mean annual rainfall of 200 to 300 mm, falling primarily in winter [198]. The topography is a patchwork of mountains, valleys, rolling hills, rocky mesas, flat plains, and a network of small drainage lines. The average temperature varies from 23.7°C in January to 11.2°C in July, and the seasonality varies greatly due to the dry continental desert climate to the north, and the cool, moist oceanic climate to the south [198]. The land is sparsely populated and the landscape is a mosaic of farms and small protected areas: Anysberg Nature Reserve and Sanbona Wildlife Reserve being the two largest ones. The northern section of the Sanbona Wildlife Reserve represents 6% of the whole sampling area, and is delineated by a high voltage game fence with the objective of limiting the movements of medium to large animals [195]. The game fence enables the presence of species not found in the rest of the study area, lion *Panthera leo*, cheetah *Acynonyx jubatus*, African elephant *Loxodonta africana*, African buffalo *Syncerus caffer*, Burchell's zebra *Equus quagga*

burchellii, giraffe *Giraffa camelopardalis*, and white rhinoceros *Ceratotherium simum*.

The Little Karoo can also be described as a mega-ecotone, where the succulent Karoo and the Cape Floristic Provinces intermingle. 41% of the study area falls into the succulent Karoo biome, in which the dominant plant life-form is dwarf shrubs (absence of trees and grasses). The remainder (59%) is part of the fynbos biome, with presence increasing with elevation [319]. Within those biomes, different vegetation types can be identified: fynbos (13.6%), thicket (29.3%), renoster (16.9%) and succulent Karoo (32.0%); the remaining 8.2% falling into the source and drainage vegetation categories. The vegetation and topographic maps (Fig. 1.1) suggest a strong association between terrain roughness and vegetation type; and the boxplots (Fig. 1.2) show that averaged ruggedness varies between all four different biomes.

1.3.2 Data collection

Camera traps were deployed between March 2014 and August 2015 as part of a research project on large carnivores – brown hyenas *Hyaena brunnea* and leopards *Panthera pardus* – within a study area of 4,327 km² (minimum convex polygon). Digital automated cameras (Cuddeback Attack and Ambush, Cuddeback Inc., Green Bay, Wisconsin, USA) were set to take photos with a one-second delay between consecutive triggers, and with an incandescent flash at night [Chapter 1 section 1.3.3].

The sampling design was selected to estimate the population density of leopards and brown hyenas within the study site. Given the vastness of the study area, the camera trap study was undertaken as a series of six regional surveys (spatially and temporally separated). Using QGIS 2.10.1 software [268], a 7 × 7 km grid was designed and placed across the study site. The final camera trap positions were selected by identifying two locations in every grid square that were expected to maximise chances of photo-capturing medium to large-bodied animals. Grid size and camera spacing were selected in order to ensure relatively even sampling effort and to satisfy data collection protocols used to estimate population density using Spatially Explicit Capture-Recapture models (SECR) [163] [Chapter 4 section 4.3].

Camera trap stations consisted of a pair of camera traps facing each other (slightly off-set to avoid simultaneous flash triggers), positioned at a 90° angle with a linear channel such as gravel roads, animal paths and riverlines, and at an average height of 40 cm. Each sampling block (one per survey) ran for *c.* three months, and consisted of between 30 and 61 camera trap stations

with a mean inter-site distance of 3.5 km. The camera trap stations were checked once (*c.* 1.5 months, halfway through the survey) to change batteries. Data entry was facilitated by the software Camera Base [338], and the final database was exported into Excel and analysed in R Studio, using the R software 3.2.4 [269].

1.3.3 Analysis

Sampling with camera traps provided detection/non-detection information for all medium to large species that could be photo-captured. Using these data to make inferences about species occupancy at the sampling sites assumed that the species' detection probabilities were known. There was no uncertainty at locations where the species was photo-captured, but it became ambiguous at locations where the species was not detected. Imperfect observation made naïve estimates of occupancy (proportion of sites at which the species was detected) negatively biased [10]. However, assuming that a species detection probability did not vary from one habitat type to another, naïve estimates of occupancy offered a means to make inferences about the species' habitat preferences.

Datasets tend to be sparse for low density species and those with low detection probabilities. Species with at least 50 photo-captures and 10 capture sites, were included for this study. Small photo-capture rates can be explained in two ways: **1)** a small species detection probability (e.g. the camera setup is inadequate for small mammals such as mice) or **2)** a low species density (e.g. riverine rabbit *Bunolagus monticularis* [85]).

Social species moving in groups such as antelopes, generated a series of photographs when they encountered a camera trap station. Another example was with chacma baboon *Papio ursinus*, a primate which often took a curious interest in the cameras, leading the troop to play around the setup for several minutes, generating hundreds of photographs. This could considerably inflate the photo-capture counts per habitat type, which become no longer comparable between different species and between different locations. To work around this issue, every photo-capture was either defined as a capture-event or as a duplicate. When a species was photographed at the same location multiple times, the first photograph was considered to be the capture-event. Photo-events that occurred more than one hour apart were considered to be independent. All photographs of the same species collected within one hour after a capture-event, at the same location, were considered

to be duplicates; in other words, non-independent events. Duplicates were discarded for this study.

1.3.3.1 Active site detection

Every camera trap station operated for c . three months and collected detection/non-detection information in relation to spatial covariates such as the TRI. When species s was photo-captured at least once at a camera trap station, the latter was considered to be an active site for the species. Understanding the detection process of active sites is a first step in understanding the spatial dataset collected with camera traps.

In practice, the number of operating camera trap stations after the 85th camera trap night dropped rapidly, i.e. after 2.8 months (Fig. 1.3), which is why data collected from the 85th night were discarded. A camera trap night variable n could then be defined for all camera trap stations: $n \in [1 .. 85]$. Five camera trap stations failed (due to flooding, animal damage, technical malfunctioning) before the 30th camera trap night; the data from these cameras were discarded.

For every species s , and for every camera trap night n , the cumulative number of active sites $C_{n,s}$ (camera trap stations where species s was photo-captured from night 1 to n), weighted by the number of operating camera trap stations N_n , was calculated:

$$C'_{n,s} = \frac{C_{n,s}}{N_n} = \frac{C_{n-1,s} + S_{n,s}}{N_n} \quad \text{with} \quad C_{0,s} = 0 \quad (1.1)$$

In (1.1), $S_{n,s}$ is the number of new active sites registered on night n .

For every species s , the resulting cumulative curve was weighted by the total number of active sites ($C'_{85,s}$) revealed between the 1st and the 85th camera trap night:

$$C''_{n,s} = \frac{C'_{n,s}}{C'_{85,s}} \cdot 100 \quad (1.2)$$

Three capture-speed indexes $V_{,s}^1$, $V_{,s}^2$ and $V_{,s}^{\text{end}}$ were calculated for every species s :

$$\begin{aligned} V_{,s}^1 &= C''_{28,s} \\ V_{,s}^2 &= C''_{56,s} \\ V_{,s}^{\text{end}} &= C''_{85,s} - C''_{70,s} \end{aligned} \quad (1.3)$$

In (1.3), $V_{,s}^1$ and $V_{,s}^2$ give the percentage of active sites revealed after 28 and 56 camera trap nights (four and eight weeks), compared to the number revealed after 85 camera trap nights.

In (1.3), $V_{,s}^{\text{end}}$ gives the percentage of active sites revealed in the last two weeks of the study, compared to the number revealed at the end of the study (after 85 camera trap nights).

1.3.3.2 Effects of topography

Terrain data for the study area were downloaded as Digital Elevation Model (DEM) data files from Shuttle Radar Topography Mission (SRTM) [242] and analysed using QGIS 2.10.1 software [268]. The 30×30 m DEM data provide accurate information about the shape and features of the surface of the Earth. The change in elevation was measured using the Terrain Roughness (ruggedness) Index (TRI) [284]. TRI is calculated by summing change in elevation between a grid cell and its eight neighbours:

$$\text{TRI} = [\sum (x_{ij} - x_{00})^2]^{\frac{1}{2}}$$

where x_{ij} = elevation of each neighbour cell and,
 x_{00} = elevation in the central grid cell [284].

TRI was then averaged over a 2-km radius circle around each camera trap station and used as a spatial covariate r in further analytical work (Fig. 1.4).

R_A is a vector storing the r value of each camera trap station within the study area. $R_{U,s}$ stores the r values associated with each photo-capture of species s , depending on the camera trap station where the photo-capture event took place. Applying a kernel density estimation to R_A and $R_{U,s}$, the ruggedness profile $r \mapsto A(r)$ of the study area (habitat available), as well as the ruggedness profile $r \mapsto U_{,s}(r)$ of the area used by species s (habitat used), were produced [309]. An example is provided for the leopard *Panthera pardus* in Fig. 1.5.

From each of the A and $U_{,s}$ kernel density functions, 512 points were extracted at regular intervals along the ruggedness r -axis. The species preference in terrain ruggedness was measured by the Jacob's preference index $r \mapsto D_{,s}(r)$ [155]:

For every value r along the ruggedness r -axis:

$$D_{,s} = \frac{A - U_{,s}}{U_{,s} + A - 2 \cdot U_{,s} \cdot A} \quad (1.4)$$

U_s being the proportion of habitat used, and A the proportion of habitat available.

The Jacob's index provides an adjustment for the relative abundance of each habitat available to the animals [155]. $D_{,s}$ lies between -1 (complete avoidance of a habitat) and $+1$ (complete preference for a single habitat). Values close to zero indicate that the habitat is used in proportion to its availability. Negative values indicate that the species is recorded in that habitat, but disproportionately few times considering the extent of that habitat which is available.

Using the Jacob's preference index, preferred habitat maps were built in QGIS 2.10.1 [268]. The ruggedness topographic indexes were averaged r_k within each square-polygon k of a 1.4×1.4 km regular grid covering the whole study area. For every species s , the corresponding values of the Jacob's preference index $D_{,s}(r_k)$ were then georeferenced $D_{k,s}$ to produce choropleth maps; these are graphical representations in which each geographical area (grid cell k) was shaded according to its associated $D_{k,s}$ value.

Two choropleth maps, representing the same variable $D_{k,s}$, but using two different colour schemes, were built for every species s . The appearance of the map pattern could vary substantially between the two maps, further to the use of 1) different colour gradients and 2) different classification decisions (classification method and number of classes employed) for the variable of interest.

For the first choropleth map, a species-specific colour scheme was used. The colour gradient ranges from white – matching the lowest value $\min(D_{k,s})$ of the georeferenced Jacob's index for species s – to dark red – matching the largest value $\max(D_{k,s})$ of the georeferenced Jacob's index for species s . The number of classes employed matched the number of distinctive values taken by $D_{k,s}$. All grid cells k having averaged ruggedness values r_k falling outside the spectrum of sampled ruggedness values ($3.54 \leq r \leq 33.08$), and for which inferences about habitat preferences could not be made, were shaded in black.

For the second choropleth map, a colour scheme standardised across all species was used. The colour gradient is made of 100 classes ranging from white – matching the lowest possible values of the Jacob's index ($-1.00 \leq D_{k,s} \leq -0.98$) – to dark blue – matching the largest possible values of the georeferenced Jacob's index ($0.98 \leq D_{k,s} \leq 1.00$). All grid cells k having averaged ruggedness values r_k falling outside the spectrum of sampled ruggedness values ($3.54 \leq r \leq 33.08$), and for which inferences about habitat preferences could not be made, are shaded in black.

1.3.3.3 Spatial partitioning

Non-metric Multi-Dimensional Scaling (NMDS) is a statistical tool which provides a means of displaying and summarising a square symmetric matrix of dissimilarities into a low-dimensional Euclidean space [126, 180, 181]. The objective in NMDS is to find a configuration of points in Euclidean space so that the ordering of the interpoint distances matches, as closely as possible, the ordering of the dissimilarities in the matrix of dissimilarities. Summarising a set of data into a two-dimensional graph might not be feasible and a certain amount of distortion might be created. The measure of lack of fit in NMDS is known as the ‘stress’ of the configuration. Non-zero stress values occur with insufficient dimensionality, and as the number of dimensions increases, the stress value will either decrease or remain stable [32].

NMDS was applied to a matrix of dissimilarity data which estimated the dissimilarities of habitat preferences in relation to terrain ruggedness for each pair of species in the mammal community of the Little Karoo. The spatial information for the 27 mammal species was compiled into a matrix M with $n = 27$ rows (species) and $p = 512$ columns (ruggedness values selected at regular intervals between 3.54 and 33.08). Every element $M[s, r]$ gave the Jacob’s preference index $D_{,s}(r)$ of species s for the ruggedness value r .

$$M[s, r] = D_{,s}(r)$$

Using the *dist* function from the *stats* R-package [22, 32, 209], M was computed to return a distance matrix with distances being measured between rows of M using the Manhattan method; the output distance matrix was a symmetric matrix with 27 rows and columns, and was referred to as the Ruggedness-preference Distance Matrix (RDM). Every element $\text{RDM}[s_1, s_2]$ quantified the dissimilarity between the Jacob’s Indexes of species s_1 and s_2 .

$$\text{RDM}[s_1, s_2] = \text{dist}(D_{,s_1}(r), D_{,s_2}(r))$$

An NMDS ordination was then performed on RDM, using the *isoMDS* function from the *MASS* R-package [285]. The objective of the ordination is to find the configuration with minimum ‘stress’ for a given number of dimensions. The operation was therefore repeated several times, each time with a different number of chosen dimensions k , and a screeplot (stress versus k) was plotted in order to identify the point beyond which additional dimensions do not substantially lower the stress value.

The output data information was then summarised into a two-dimensional graphical display, which maximised the rank correlation between the calculated species dissimilarities/distances and the plotted distances between species [32].

1.4 Results

The trapping effort of 17,631 camera trap nights resulted in 26,312 photo-captures (11,742 independent photo-capture events) of 91 wild species, including 51 mammals, 39 birds and 1 reptile. Of the 51 mammal species, 27 had more than 50 photo-captures and at least 10 active sites to father the analysis [Appendix 2A].

1.4.1 Active site detection

For the 27 mammal species, the cumulative percentages of active sites are illustrated in Fig. 1.6, and the daily detection rate of new active sites in Fig. 1.7. The capture-speed indexes are provided in Table 1.1.

The speed at which active sites were added decreased through time ($V_{,s}^1 > V_{,s}^2$). For the 27 species, the first month was most productive. For 21 species, it took 28 camera trap nights to discover at least 50% of all study-revealed active sites, and 56 nights to discover at least 75%.

$V_{,s}^{\text{end}}$, the percentage of active sites uncovered during the last two weeks of the camera operating time (70th to 85th camera trap nights) varied from 0 to 25%, according to species. For eleven of them, $V_{,s}^{\text{end}}$ was less than or equal to 5% – brown hyena *Hyaena brunnea*, Cape mountain zebra *Equus zebra zebra*, chacma baboon, grey duiker *Sylvicapra grimmia*, grysbok *Raphicerus melanotis*, steenbok *Raphicerus campestris*, African wildcat *Felis silvestris*, Cape hare *Lepus capensis*, klipspringer *Oreotragus oreotragus*, greater kudu *Tragelaphus strepsiceros* and Cape porcupine *Hystrix africaeaustralis* – suggesting that the asymptote of the cumulative curve was nearly reached by the 85th camera trap night.

1.4.2 Ruggedness preferences

The patterns of ruggedness preferences vary significantly among the 27 mammal species, and are displayed in Fig. 1.8.

The ruggedness values r , ranging from 3.54 (smooth, level ground) to 33.08 (rough ground), were categorised into three groups of equal length:

Slightly-rugged terrain:	$3.54 \leq r_l \leq 13.39$
Moderately-rugged terrain:	$13.39 < r_m \leq 23.24$
Highly-rugged terrain:	$23.24 < r_h \leq 33.08$

Table 1.2 shows that although 23 of the 27 species strongly avoided certain types of rugged terrain, 5 strongly favoured some.

Strong avoidance: $\exists r, D_{,s}(r) < -0.5$

Strong preference: $\exists r, D_{,s}(r) > +0.5$

Highly-rugged terrain: 18 of the 27 species strongly avoided highly-rugged terrain. Indeed, four species – brown hyena, steenbok, springbok *Antidorcas marsupialis* and Cape hare – strictly avoided highly-rugged terrain: $\forall r_h, D_{,s}(r_h) < -0.5$. Honey badger *Mellivora capensis*, grysbok and rock hyrax *Procavia capensis*, were the three species that strongly favoured highly-rugged terrain.

Moderately-rugged terrain: 23 of the 27 species used moderately-rugged terrain in proportion to its availability (no preference or avoidance); however, the remaining four species – steenbok, springbok, Cape hare and rock hyrax – strongly avoided it.

Slightly-rugged terrain: Two species – springbok and Cape hare – strongly preferred slightly-rugged terrain, whereas seven others – Cape gray mongoose *Galerella pulverulenta*, grysbok, Cape mountain zebra, Hewitt's red rock rabbit *Pronolagus saundersia*, klipspringer, leopard and rock hyrax – strongly avoided it. The 18 remaining species used slightly-rugged terrain in proportion to its availability.

Most species showed strong preference and/or avoidance for certain types of rugged terrain, except three – chacma baboon, African wildcat and Cape porcupine – for which the Jacob's index curve lay almost along the horizontal line $y = 0$ (Fig. fig. 1.6(c), 1.6(i) and 1.6(k)), meaning that $\forall r, D_{,s}(r) \simeq 0$. The range of values taken by the Jacob's index $[\max(D_{,s}), \min(D_{,s})]$, for those three species, was therefore small (respectively 0.13, 0.14 and 0.35), whereas it was large for species showing both strong preference and strong avoidance for different terrain roughness, which was the case for springbok, Cape hare and rock hyrax (respectively 1.58, 1.68 and 1.87) (Fig. 1.2).

Chloropleth maps: The preferred habitat maps for the 27 mammal species are provided in appendix 3A.

Chloropleth maps built with a species-specific colour scheme, have the two extreme colours found at the opposite ends of the gradient matching the extreme **observed** values of the Jacob's index. Therefore, these maps always displayed the full colour spectrum of the applied gradient (white to dark red), and emphasised the contrast between preferred and avoided terrain, independently of the range of values taken by the Jacob's index. However,

grid cells with the same colour value between two different choropleth maps (from two different species) might not indicate the same Jacob's index value.

Choropleth maps built with a standardised colour scheme, have the two extreme colours found at the opposite ends of the gradient matching the extreme **possible** values of the Jacob's index (-1 and 1). Therefore, these maps did not necessarily display the full colour spectrum of the applied gradient (white to dark blue). The map's colour spectrum broadened with the range of values taken by the Jacob's index, and grid cells with the same colour values between two different choropleth maps (from two different species) indicated the same Jacob's index values.

When the range of values taken by the Jacob's index [$\max(D_{k,s})$, $\min(D_{k,s})$] gets close to the range of **possible** values $[-1, 1]$, the two choropleth maps become nearly identical (e.g. rock hyrax, Fig. 3A.23). On the contrary, their appearances vary greatly as the range of values taken by the Jacob's index shrinks (e.g. African wildcat, Fig. 3A.3).

1.4.3 Habitat partitioning

The NMDS iterative algorithm captured, in two dimensions, the essential structure of the dissimilarity data. It also produced the graph shown in Fig. 1.9, which represents, as closely as possible, the dissimilarity between species' ruggedness preferences in a two-dimensional Euclidean space. In other words, points close together represent species that favoured more similar terrain (in terms of ruggedness) than species represented by points farther apart; however, the graph does not provide quantitative information regarding this difference. Whenever possible, the species' ruggedness preferences were illustrated with the Jacob's index curve (thin black line in Fig. 1.9).

A screeplot (Fig. 1.10) shows the decrease in ordination stress with an increase in the number of ordination dimensions allowed – revealed that attempting an ordination with one NMDS axis yielded high stress (0.108) whereas two or three dimensions was adequate. The stress value equaled 0.047 in two dimensions and, like all stress values equal to or below 0.050, it indicated good fit. Allowing the algorithm to use more than two dimensions reduced the stress slightly (e.g. 0.032 in three dimensions) suggesting that the NMDS plot in two dimensions was adequate.

In the NMDS plot, the 27 species were spatially placed along a convex arch showing a clear and gradual left-right transition along the arch, from species favouring slightly-rugged terrain (e.g. Cape hare) to species favouring highly-

rugged terrain (e.g. rock hyrax). In the middle part of the arch there was a gradual bottom-top transition along the second axis from species favouring moderately-rugged terrain (e.g. Hewitt's red rock rabbit), to species showing no particular preferences for any type of terrain (e.g. African wildcat). The honey badger was the species showing a slightly convex Jacob's index curve, which explains its isolation in the plot.

1.5 Discussion

Examining habitat preferences among 27 terrestrial mammals of the Little Karoo in South Africa, I found that heterogeneous topographic relief was likely to be an essential constituent of the niche of a species and a crucial variable to predict species' habitat-use. The distribution of most species showed a continuum of variations along the ruggedness gradient; this has already been observed with numerous terrestrial mammals [7, 106, 107, 118, 295, 333, 359]. The analysis revealed that most species strongly avoided highly-rugged terrain, whereas moderately-rugged terrain was usually used in proportion to its availability. Although slightly-rugged terrain was also mainly used in proportion to its availability by most species, the trend was not as clear with a third of them strongly avoiding or favouring this habitat.

The strength of affinities animals developed with specific terrain roughness varied between species and can be quantified with the range of values taken by the Jacob's preference index $[\max(D_{,s}), \min(D_{,s})]$; species were positioned along a transitional gradient of habitat specialisation. Habitat-generalist species – chacma baboon and African wildcat – were at the lower end, and habitat-specialist species – rock hyrax and Cape hare – at the upper end.

The study showed that choropleth maps are useful tools to geographically visualise species' habitat-use. The choice of two different colour schemes resulting from two different classification rules, enabled to produce, for every species, two maps providing complementary insights into space-use and space partitioning. The standardised choropleth maps (blue) provide a quick visual interpretation of the intensity of habitat specialisation and how it varies between species of the same community; habitat-generalist species will tend to have homogeneous monochrome maps, whereas habitat-specialist species will tend to have kaleidoscopic and contrasted maps. The standardised colour scaling failed to distinguish nuanced variations in habitat preferences. A second choropleth map, built with a stretched colour scaling (red), emphasised those nuances, which is especially insightful for habitat-generalist species.

The selected method for studying habitat preference among the mammal community of the Little Karoo, relied on data collected throughout the year (series of three-month long surveys) and was therefore less sensitive to seasonal variations. Although the detection rate of new active sites decreased substantially for most species after 56 sampling nights, it remained non-negligible for some species even after completion of the three-month sampling period. Inferences about habitat preferences could however still be made because it is the relative frequency of habitat-use which is of importance, assuming that species detection probability does not vary from one habitat type to another.

Space-partitioning could be a mechanism by which sympatric species co-exist in a stable manner. Interspecific competition takes place when resources are limiting, but coexistence can still be achieved if sympatric species evolved different behaviours and morphologies, allowing them to use different food sources and/or to use them in different areas and/or at different times [49, 75, 76, 298].

The analysis of the dissimilarity of habitat-use patterns among the mammal community of the Little Karoo, led to a collapse and summary of a complex ecological database, allowing an intuitive and visual exploration of the data. The NMDS plot spatially separated habitat-specialist from habitat-generalist species, as well as grouped species showing similar terrain affinities. This method does not only allow one to classify species as habitat-specific or generalist but to also recognise nuances in the spectrum of preferences, have a more continuous approach and be able to compare species to one another for a better understanding of the forces driving species coexistence in local animal communities.

It would be precarious to extrapolate these results and findings to a broader landscape. However, if similar studies were conducted on habitat-use patterns within mammal communities inhabiting variant study sites in the Western, Eastern and Northern Cape Provinces, it should be possible to build a distribution map with suitable habitat for each species, based on ruggedness preferences. Additional camera trap studies would then need to be implemented in order to ground truth projections but it ought to be feasible to delimit the area in which there is a probability greater than zero that a species, e.g. leopard, occurs.

1.6 Tables

Table 1.1: Capture-speed indexes

For 27 mammal species in the Little Karoo: CE is the total number of photo-captures; AS , the total number of active sites (where species s was photo-captured); $V_{,s}^1$, the percentage of active sites revealed after 28 camera trap nights; $V_{,s}^2$, the percentage of active sites revealed after 56 camera trap nights; $V_{,s}^{\text{end}}$, the percentage of active sites revealed during the last two weeks of the study. r gives the ranking position and Δr gives the ranking change between $V_{,s}^1$ and $V_{,s}^2$.

Species	CE	AS	$V_{,s}^1(r)$	$V_{,s}^2(\Delta r)$	$V_{,s}^{\text{end}}$
brown hyena	89	33	86 (01)	96 (-1)	4
scrub hare	508	60	77 (02)	89 (-8)	7
gemsbok	1006	96	75 (03)	91 (-2)	7
Cape mountain zebra	105	24	75 (04)	89 (-5)	0
chacma baboon	1696	172	71 (05)	93 (1)	3
grey duiker	1109	108	70 (06)	91 (0)	3
black backed jackal	1034	113	70 (07)	86 (-6)	6
grysbok	127	14	69 (08)	91 (1)	0
red hartebeest	150	22	68 (09)	94 (6)	6
steenbok	275	37	68 (10)	86 (-4)	4
African wildcat	465	119	66 (11)	87 (0)	2
Cape hare	106	18	64 (12)	100 (11)	0
klipspringer	365	75	64 (13)	90 (5)	2
eland	417	68	63 (14)	79 (-4)	10
greater kudu	283	57	62 (15)	84 (0)	5
Cape porcupine	445	115	60 (16)	87 (4)	4
rock hyrax	57	14	60 (17)	82 (1)	10
aardwolf	127	34	59 (18)	80 (1)	16
grey rhebuck	228	57	56 (19)	76 (-4)	9
leopard	215	78	52 (20)	78 (-1)	7
springbok	105	16	51 (21)	69 (-5)	16
aardvark	162	62	47 (22)	78 (2)	11
caracal	381	98	47 (23)	76 (1)	8
Cape gray mongoose	341	68	47 (24)	65 (-3)	16
small spotted genet	73	26	46 (25)	70 (0)	25
Hewitts red rock rabbit	77	20	45 (26)	79 (7)	7
honey badger	99	54	38 (27)	70 (3)	12

Table 1.2: Ruggedness preferences

For 27 mammal species in the Little Karoo: *range* is the range of Jacob's index values $\max(D_{,s}) - \min(D_{,s})$; + indicates a strong preference; - indicates a strong avoidance; -- indicates a strict avoidance. r_l , r_m and r_h consist of slightly-, moderately- and highly-rugged terrain.

Species	<i>range</i>	r_l	r_m	r_h
chacma baboon	0.13			
African wildcat	0.14			
Cape porcupine	0.35			
caracal	0.78			-
honey badger	0.79			+
Cape gray mongoose	0.85	-		
aardvark	1.05			-
grey rhebuck	1.05			-
greater kudu	1.11			-
scrub hare	1.11			-
aardwolf	1.12			-
grey duiker	1.14			-
gemsbok	1.16			-
small spotted genet	1.16			-
black backed jackal	1.20			-
eland	1.20			-
grysbok	1.23	-		+
red hartebeest	1.23			-
Cape mountain zebra	1.24	-		-
Hewitts red rock rabbit	1.28	-		-
brown hyena	1.33			--
steenbok	1.43		-	--
klipspringer	1.44	-		
leopard	1.45	-		
springbok	1.58	+	-	--
Cape hare	1.68	+	-	--
rock hyrax	1.87	-	-	+

1.7 Figures

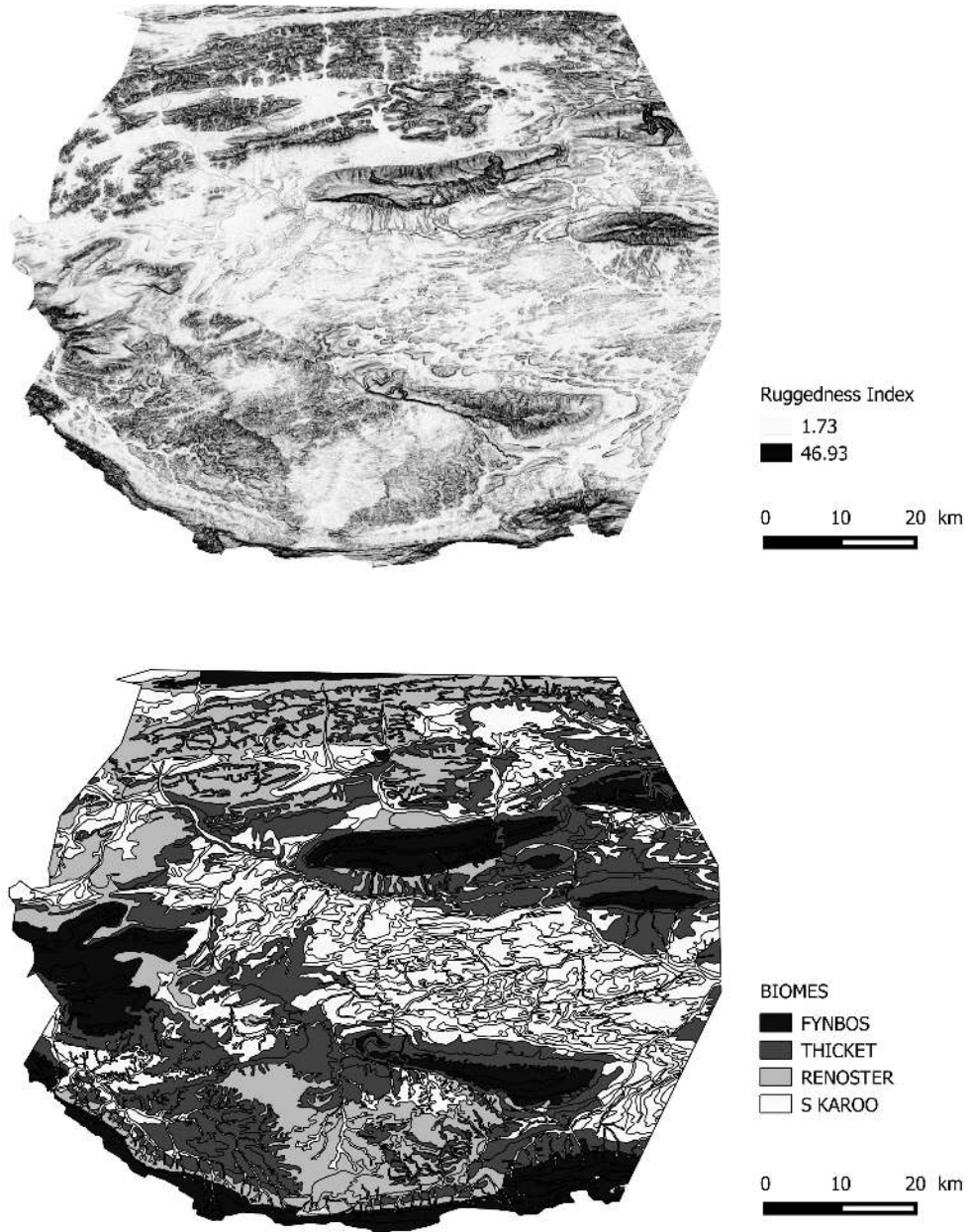


Figure 1.1: Topographic and vegetation maps of the study area

Four main vegetation types can be identified within the study area located in the Little Karoo: fynbos (13.6%), thicket (29.3%), renoster (16.9%) and succulent Karoo (32.0%). The two maps suggest a strong association between terrain roughness and vegetation.

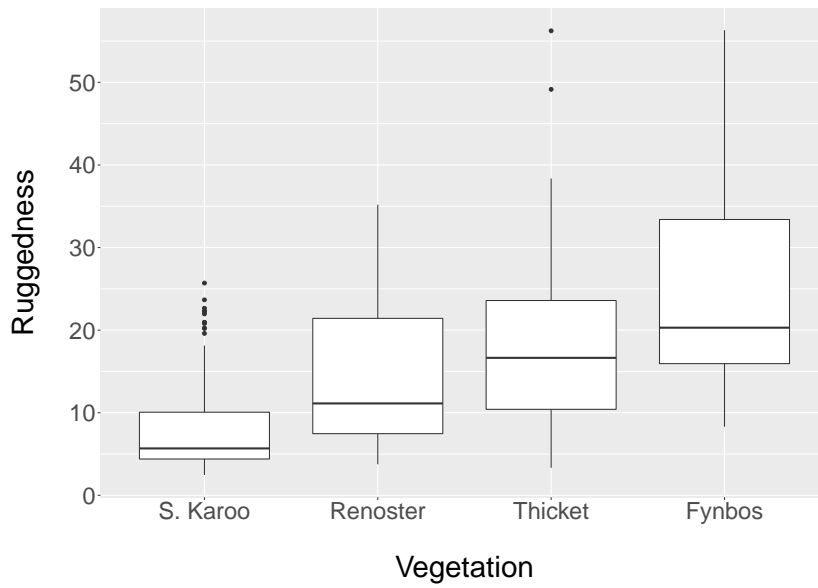


Figure 1.2: Ruggedness Index in each vegetation patch

Using QGIS 2.10.1 software [268], the ruggedness index was averaged in each vegetation polygon, before being displayed with boxplots, in order to illustrate the strong association between terrain roughness and vegetation.

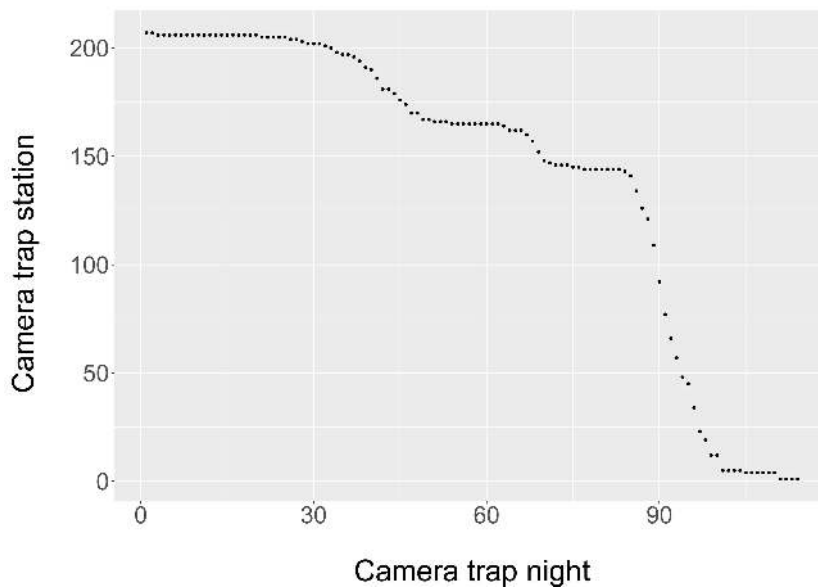


Figure 1.3: Operating camera trap stations

Most of the camera trap stations ran for *c.* three months, which explains why the number of operating camera trap stations after the 85th camera trap night drops significantly.

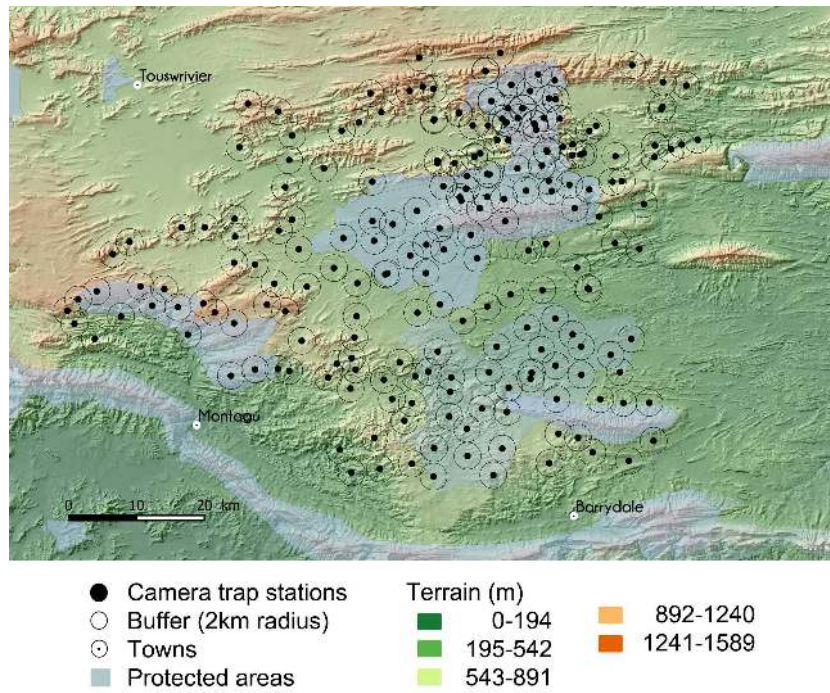


Figure 1.4: Study area

30×30 m Digital Elevation Model (DEM) data provide accurate information about the shape and features of the surface of the study area in the Little Karoo. The change in elevation was measured using the Terrain Roughness (ruggedness) Index (TRI) in QGIS 2.10.1 software [268]. The latter was averaged throughout a 2-km radius circle around every camera trap station and used as a spatial covariate.

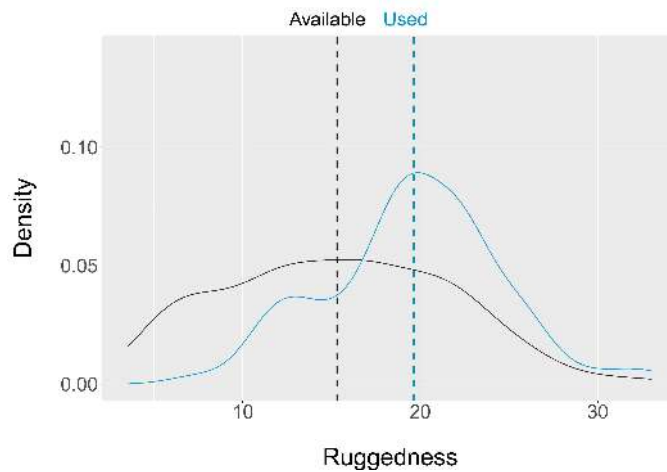


Figure 1.5: Ruggedness profiles: available and used by leopards

The ruggedness profile A (black line) of the study area describes the habitat available to all species s , whereas the ruggedness profile $U_{leopard}$ (blue line) describes the habitat used by leopards.

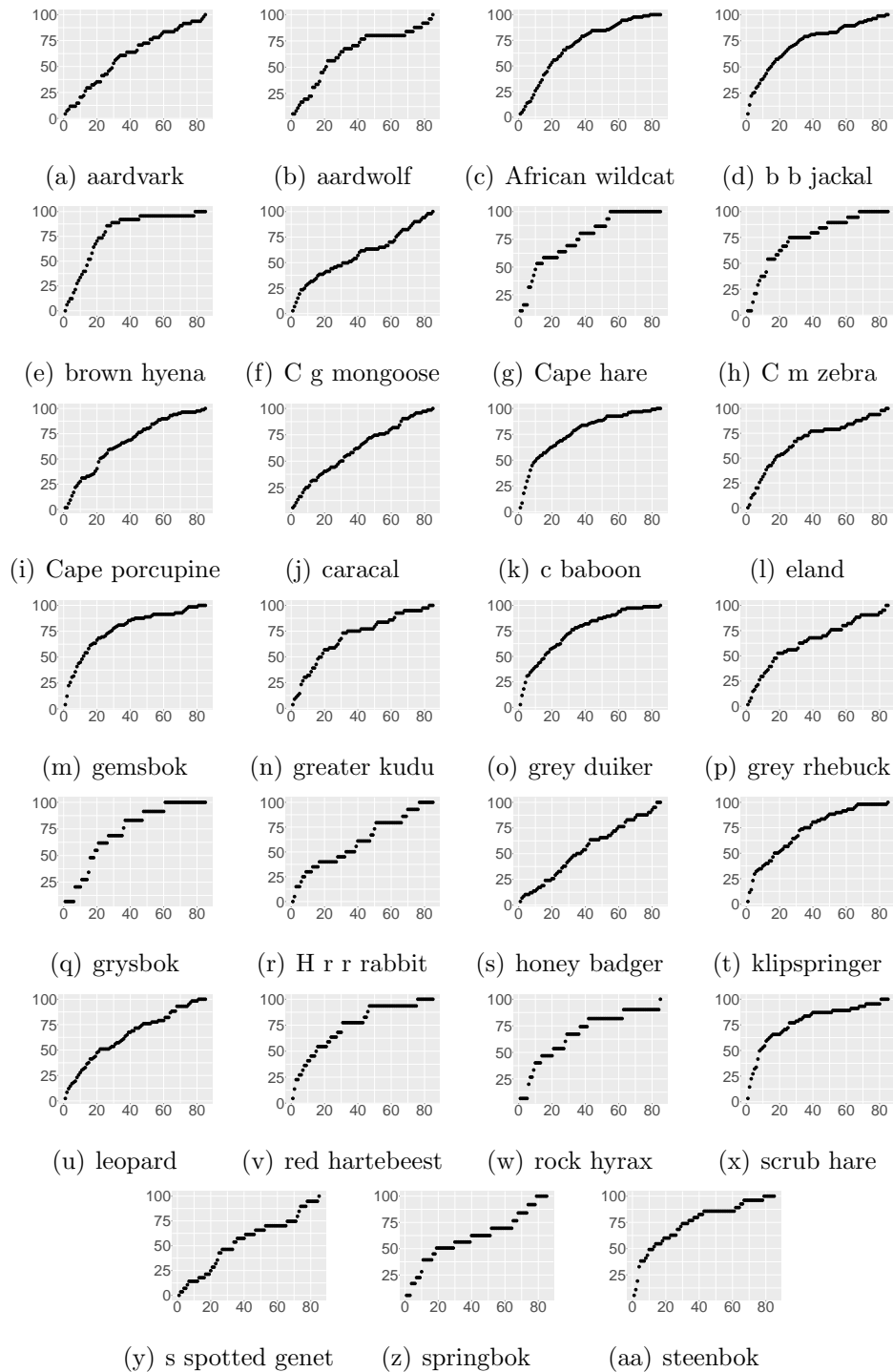


Figure 1.6: Cumulative number of active sites

The plots show the cumulative number of active sites for 27 mammal species in the Little Karoo. The discrete first axis ranges from 0 to 85 camera trap nights; and the second axis gives the percentage of active sites revealed after x camera trap nights, in relation to the total number revealed after three months.

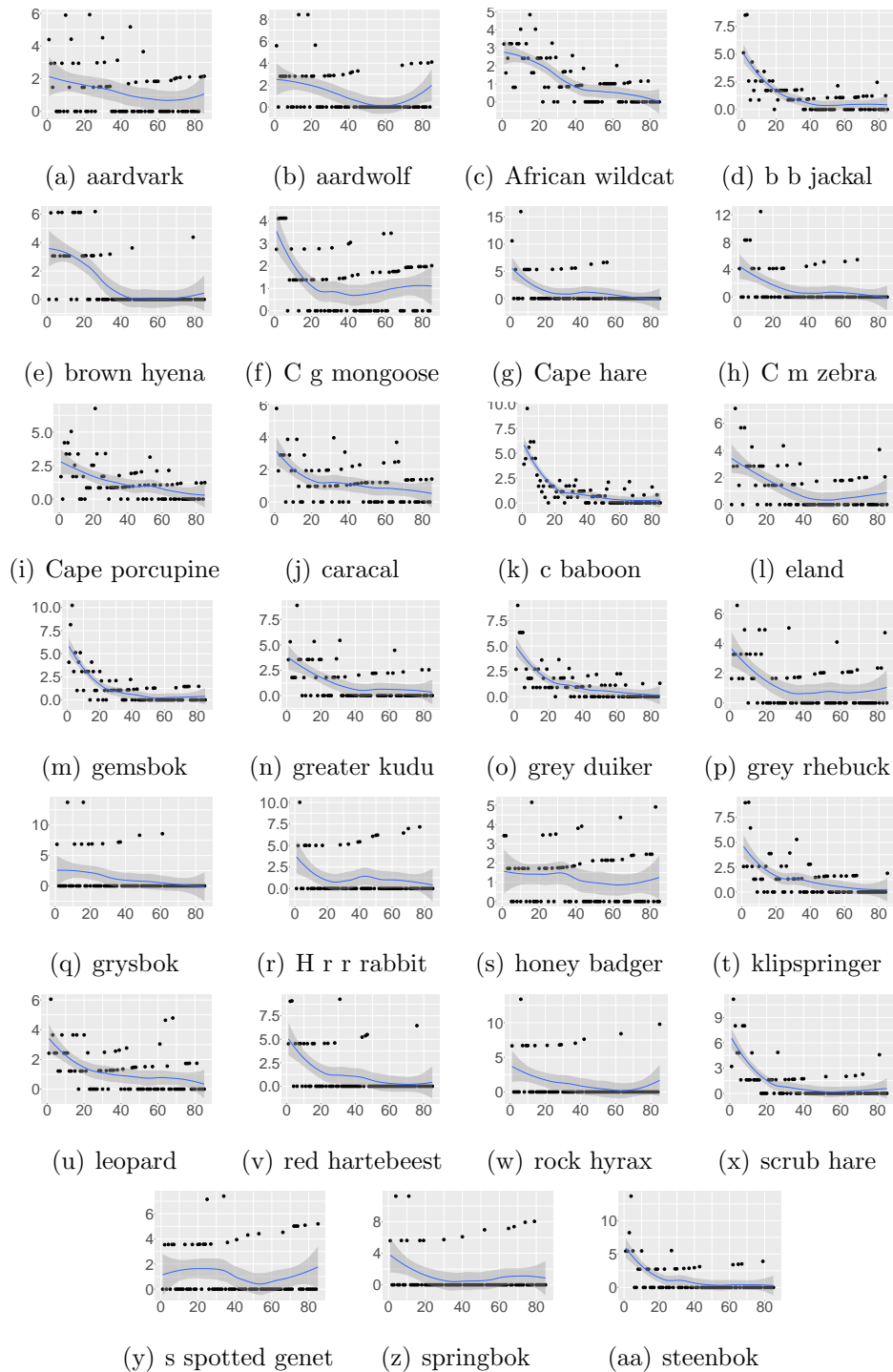


Figure 1.7: Detection rate of new active sites

The plots show the detection rate of new active sites for 27 mammal species in the Little Karoo. The discrete first axis ranges from 0 to 85 camera trap nights; and the second axis gives the percentage of active sites revealed on each camera trap night x , in relation to the total number revealed after three months. The area shaded in blue is the confidence interval of the detection rate function.

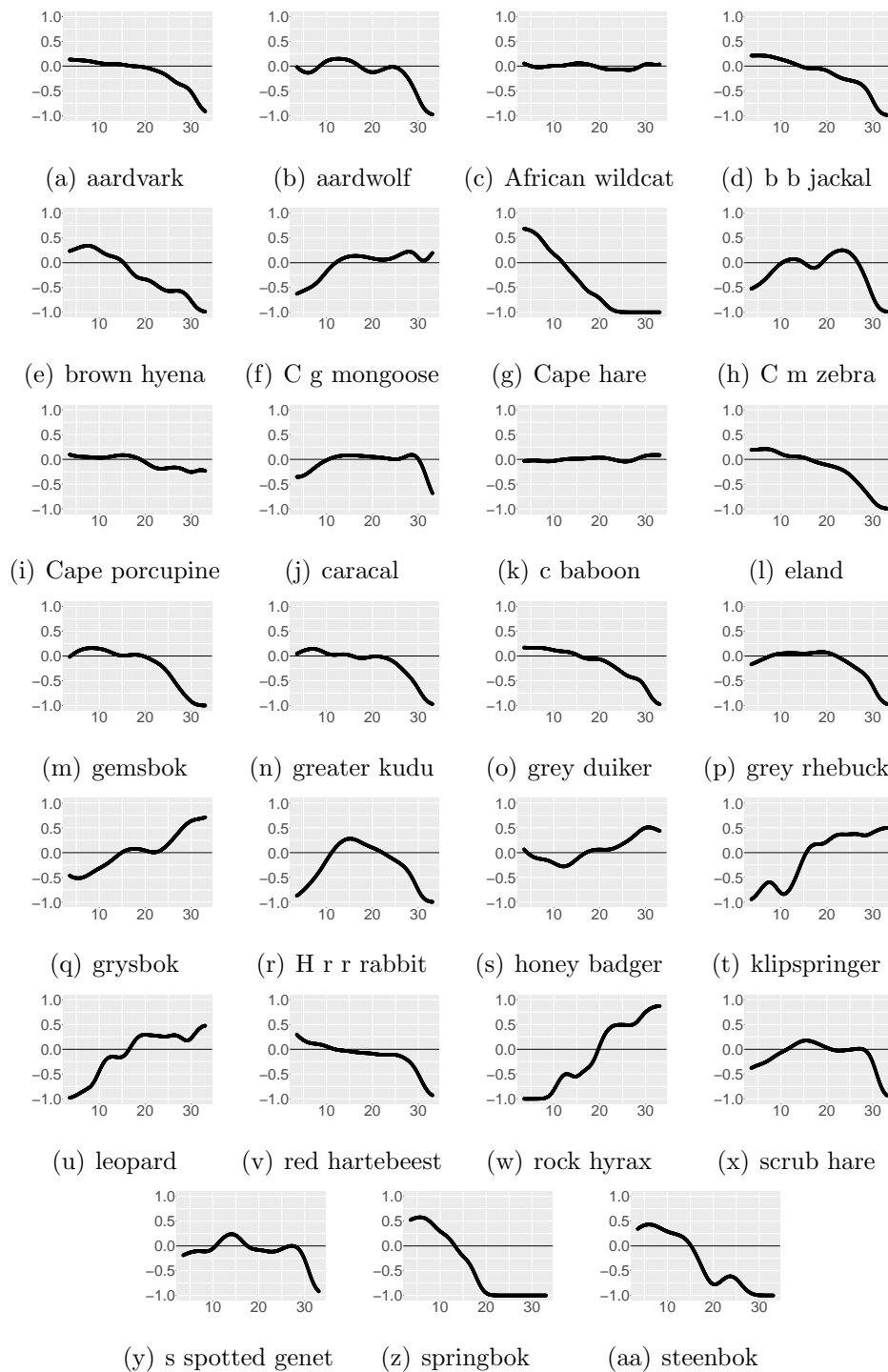


Figure 1.8: Jacob's Index curve

The plots show the Jacob's Index curve for 27 mammal species in the Little Karoo. The Jacob's preference index is independent of the relative abundance of each habitat available to the animals [155]. It varies from -1 (strong avoidance) to $+1$ (strong preference), and values close to zero indicate that the habitat is used in proportion to its availability.

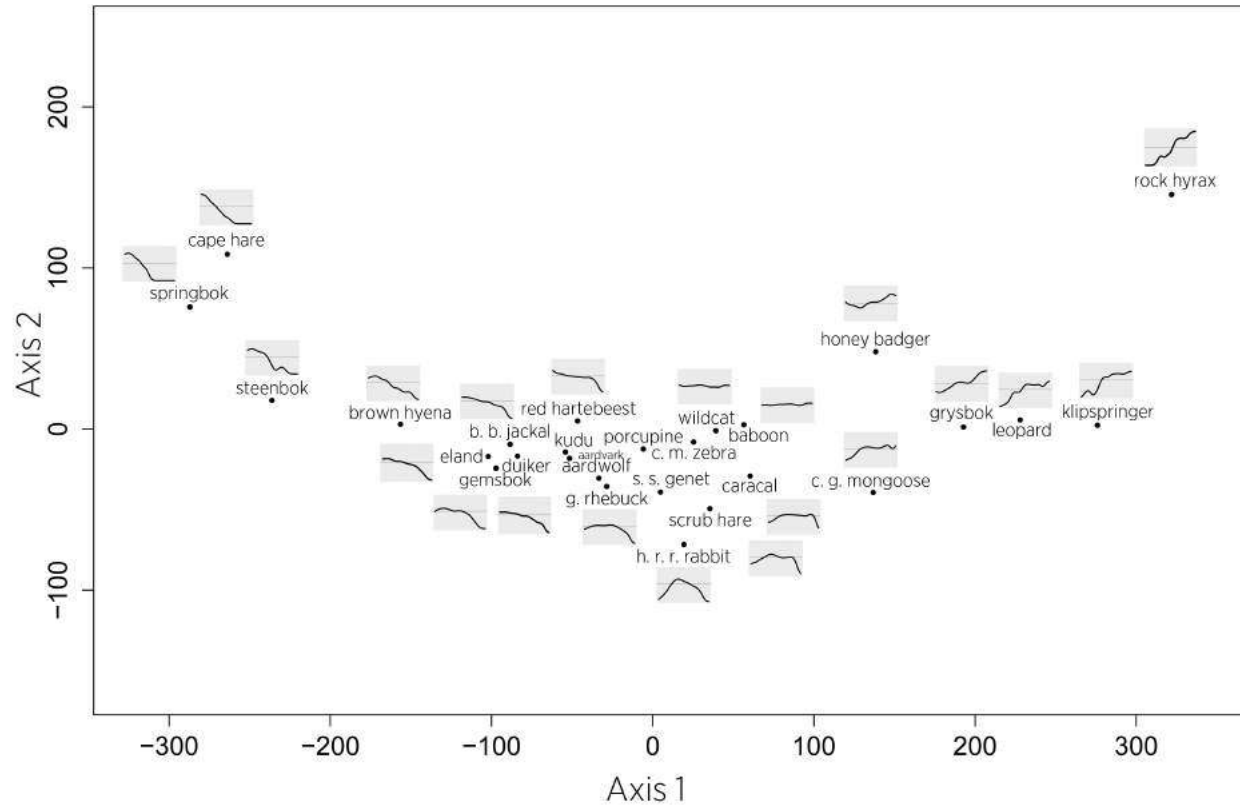


Figure 1.9: Non-metric multidimensional scaling (NMDS) of the Ruggedness-preference Distance Matrix (RDM). The NMDS analysis includes 27 mammal species of the Little Karoo. Axis one is interpreted as a left-right gradient from species favouring slightly-rugged terrain to species favouring highly-rugged terrain. Axis two is interpreted as a bottom-top gradient from species favouring moderately rugged terrain to species showing no particular preferences, and finally to the three strictly habitat-specialised species (either for slightly- or highly-rugged terrain).

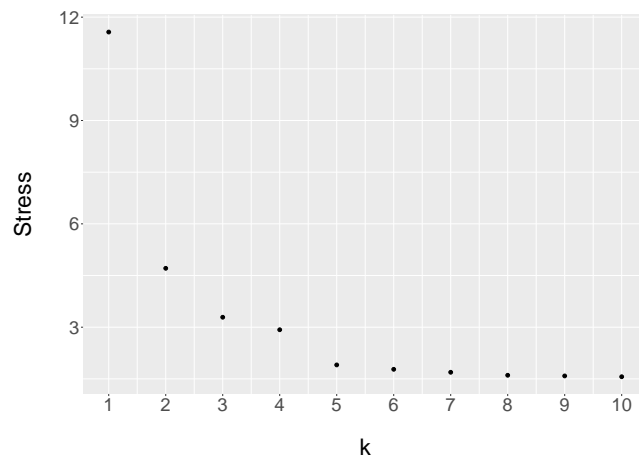
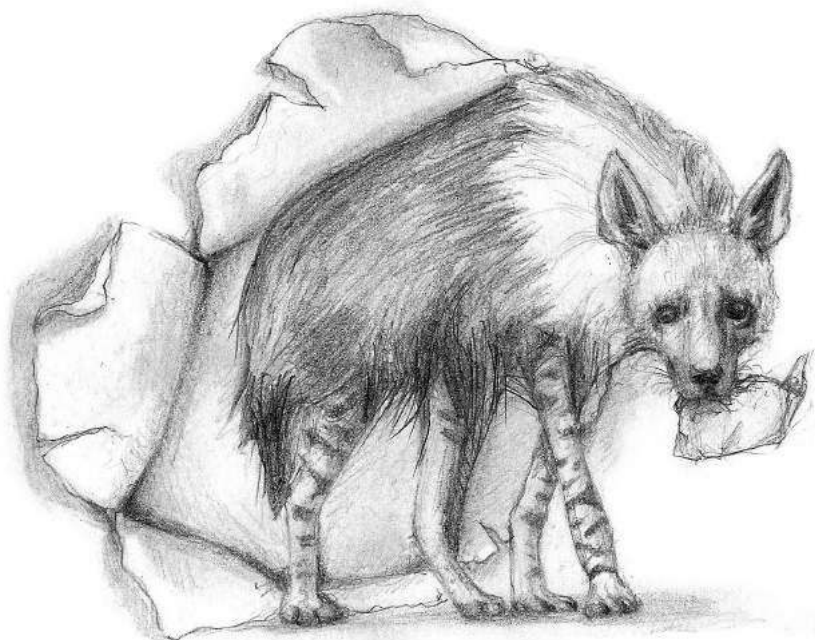


Figure 1.10: Stress values in relation to the number of dimensions k

The measure of lack of fit in NMDS is known as the 'stress' of the configuration. Non-zero stress values occur with insufficient dimensionality, and as the number of dimensions increases, the stress value will either decrease or remain stable.



Seasonal plasticity of mammalian diel activity rhythms: patterns and control

2.1 Abstract

The world is seasonal with animals subjected to predictable and periodic variations of the environment. Keeping track of these oscillations is relevant for reproduction and survival, and animals have evolved genetically programmed timing mechanisms, also called endogenous biological clocks, enabling circadian (24-hour) and circannual (365 days) rhythms to align with geophysical cycles; they use these to develop phenologies and to adapt to the time structure of the environment. Being essential to life but also energetically costly, activity level (movement) must be optimised throughout the day, and endogenous schedules are adjusted by environmental (exogenous) conditions. Among the numerous factors that influence the 24-hour circadian rhythm of a species, photoperiodism – which takes account of the measure of daylength and of the direction of change in daylength – is the most reliable environmental cue providing temporal information to synchronise circannual rhythms. In this study, camera trap systems were used to record patterns of seasonal occurrence within circadian rhythms of the mammal species of the Little Karoo in South Africa. The seasonal plasticity of the diel activity rhythm – defined in three time metrics: traditional 24-hour human clock-time and two ecological times with standardised sunrise and sunset times – is then quantified and compared among the species in the community. Most mammal species responded to the ecological variability brought about by seasonality

by adjusting their diel activity rhythms between winter and summer. Comparison of intraspecific shifts in diel activity rhythms – before and after time standardization in respect to annual sunrise and sunset times – showed that, while some shifts only result from photoperiodism alignment, most are driven by other factors too. Ten species shifted, in summer compared to winter, proportions of their daily activity from warmer daily time periods to cooler ones; this supports a behavioural strategy leading to a reduction of time exposure to a physiologically stressful environment caused by high temperatures in summer.

2.2 Introduction

The world is seasonal and, in most places, animals are subject to predictable and periodic variations of the environment; keeping track of these oscillations is relevant for reproduction and survival [109]. Resource availability or suitability often varies through the annual cycle, and is likely to influence species with lifespans of the order of a year or more [79, 200, 281, 299, 371]. Animals have evolved genetically programmed timing mechanisms, also called endogenous biological clocks, enabling circadian (24-hour) and circannual (365 days) rhythms, to align with geophysical cycles; they use these to develop phenologies and to adapt to the time structure of the environment [122, 139, 345]. Several species have been shown to have a persistent circannual cycles, sometimes throughout their lives, in the complete absence of temporal information, highlighting the underlying endogenous control [5, 52, 131, 194, 232]. However, under natural conditions, these rhythms vary between sympatric species as well as within species, depending on geographical location [12, 236, 258]. This suggests that these endogenous schedules can be adjusted by environmental (exogenous) conditions [73, 160, 370].

The diel activity rhythms of terrestrial mammals usually coincide with the hours of daylight, darkness, and/or twilight [19, 26, 151], and therefore they are usually grouped into four categories: diurnal, nocturnal, crepuscular (active in twilight) and cathemeral (irregularly active at any time of night or day) [8, 151]. Strictly nocturnal and strictly diurnal are two extremes of a continuum of temporal partitioning strategies over the 24-hour cycle [151]. Numerous factors influence the 24-hour circadian rhythm of a species [121, 190, 191, 275]. Ultimate factors provide the selective basis for biological seasonality, such as annual food and water availability, temperature [26] and interspecies interactions (predation and competition). Other factors (proximate factors), such as daylength [26, 74], are not themselves of

major importance to mammalian reproductive fitness but are employed to help time an organism's seasonal cycles and to anticipate and adapt to important changes in ultimate factors [122]. The most reliable environmental cue providing temporal information to synchronise circannual rhythms is the photoperiod, which takes account of the measure of daylength and of the direction of change in daylength [26, 38, 39, 109, 122, 244]. An encoded melatonin signal, secreted in concentrations inversely proportional to daylength, allows organisms to track time-of-year [122, 345].

Being essential to life but also energetically costly, activity level (movement) must be optimised throughout the day [82]. Defining the influence of seasonality on the diel activity of terrestrial mammals requires a large amount of data, collected among numerous individuals within the species community throughout the whole spectrum of the 24-hour and 365-day cycles. Animal activity level was traditionally measured through direct observations [25], or from data collected by telemetry devices [42, 165], such as speed of movement [257] and variance in signal strength [327]. More recently, multi-axial accelerometers have been used to collect high-resolution data on activity level [243]. Camera traps combine many advantages of the observational and telemetry-based techniques, while offering a number of improvements. Automation, miniaturization and networked systems are all features of modern camera traps, which enable ethologists to sample a variety of individuals and species within a community under greatly different environmental conditions. The disturbance caused by camera traps, despite some sounds and flashes [221], is likely to be minimal [3, 41, 128]. Time-of-detection data from remote sensors has been used to make inferences about animal activity level for many years [42, 59, 260, 290], and newly-developed analytical tools provide robust methods to quantify many aspects of animal behaviour from camera trap data [254, 283].

In this study, camera trap systems were used to record patterns of seasonal occurrence within circadian rhythms of the mammal species of the Little Karoo in South Africa. I then quantify and compare, for 25 frequently recorded mammal species, the seasonal plasticity of the diel activity rhythm defined in three time metrics: the traditional 24-hour human clock-time and two ecological times, in which the time of sunrise and sunset are transformed to be standardised throughout the 365-day cycle. The chapter finally shows whether seasonal shifts in animal diel activity rhythms are due to photoperiodism and/or to other factors.

2.3 Material and methods

2.3.1 Study area

The Little Karoo is a semi-arid desert located at the southern tip of the African continent [Appendix 1A], within the Cape Fold Belt [Introduction, Chapter 1 section 1.3.1]. Seasonality here involves the familiar temperate sequence of summer, autumn, winter and spring, but is largely driven by the cycle of a hot-dry summer, and a cool-wet winter [188]. Due to the inclination angle of the rotation axis of the Earth (as compared to its orbital plane), daylength varies with seasons on the planet's surface, depending on the observer's latitude. The study area in the Little Karoo is positioned in a grid cell with latitude-longitude coordinates for the north-west and south-east corners being respectively (33.296745°S ; 19.974518°E) and (33.916654°S ; 20.990753°E). The variation range of daylength in this area, between the southern summer solstice (14.40 hours on 21 December) and the southern winter solstice (9.92 hours on 22 June) is 4.48 hours.

2.3.2 Data collection

Camera traps were deployed between March 2014 and August 2015 [Chapter 1 section 1.3.2] as part of a research project on large carnivores – brown hyenas *Hyaena brunnea* and leopards *Panthera pardus* – within a study area of 4,327 km² (minimum convex polygon).

2.3.3 Analysis

2.3.3.1 Kernel density estimation

This analysis was designed to explore the seasonal plasticity of the diel activity of terrestrial mammals in the Little Karoo between winter (period of the year with daylength varying within the shortest third of its annual range), and summer (daylength varying within the longest third) (Fig. 2.1). The rest of the year, in which daylength varies within the middle third of its range, consists of two transitional time intervals; data collected for this period were discarded for this study.

The clock-times t recorded for every photo-capture i provided information on the diel activity rhythms of species s in winter and in summer. Season-specific diel activity rhythms were displayed using a 24-hour kernel density function k (flexible circular distribution [309]), which produced

the probability density function $A_{l,s}$ of the diel activity rhythm of species s throughout season l :

$$A_{l,s} = \sum_{i=1}^n k(t_{i,s}) \quad \text{with} \quad \int_0^{24} A_{l,s} \cdot dt = 1 \quad (2.1)$$

In winter, $l = w$

In summer, $l = e$ (estival)

The probability density functions $A_{l,s}$ are representations of circular distributions. Circular variables such as time-of-day are substantially different from linear variables because they do not behave like numbers on a number line (the ‘distance’ between 23:59 and 00:01 is the same as that between 10:41 and 10:43). The graphical display of circular distributions can therefore look very different depending on the selected time origin. For example, the diel activity rhythm of a strictly nocturnal species appears either as a unimodal or a U-shaped distribution, depending whether the display is centred around midnight or around noon (Fig. 2.4(a)). The graphical display of the probability density functions $A_{l,s}$ was either noon- or midnight-centred, depending on the time period of the 24-hour cycle in which most of the species’ daily activity was allocated.

Every photo-capture was either defined as a capture-event or as a duplicate [Chapter 1 section 1.3.3]. All duplicates were discarded for this study because they inflate the photo-capture counts per unit of time and therefore distort the kernel density functions.

For this study, mammal species for which at least 15 photo-captures were made both in winter and in summer were included [Chapter 1 section 1.3.3]. The data collected within the northern section of the Sanbona Wildlife Reserve were discarded for this study due to the high game fence delimitating its border, which makes the reserve a biological system suspected to have evolved fairly independently and to differ from the rest of the study area [Chapter 1 section 1.3.1].

2.3.3.2 Data pre-processing

The diel activity rhythms of the mammals of the Little Karoo were analysed using three time metrics:

clock-time

In a first analysis, the unit of time t was the second (International System

of Units), defined in terms of oscillations of the caesium atom ^{55}Cs [220]. It is the common unit for timekeeping used in human societies and it can unambiguously be defined as ‘what a clock reads’.

Annual daylength standardisation

In human clock-time, sunrise and sunset times vary through the year and across study areas. Because the dark-light cycle is one of the most predictable environmental cue to which animals are subjected to, light entrainment is likely to be a significant driver of the endogenous circadian clock and associated diel activity rhythm [277]; analyses based on clock-time therefore result in ‘fuzziness’ of the activity timing, likely to particularly impact crepuscular species. In a second analysis, the time variable t was transformed so that daily sunrise and sunset times (SR , SS) were standardised to 06:38 (annual average of sunrise times \overline{SR}) and to 18:38 (annual average of sunset times \overline{SS}). However, the transformation did not affect true midday \overline{MD} or midnight \overline{MN} , which were reached at 12:38 and 00:38 respectively, given the location of the study area on the Earth’s surface.

$$\begin{aligned}\overline{SR} &= 06:38 \text{ (6.63 h)} & \overline{MD} &= 12:38 \text{ (12.63 h)} \\ \overline{SS} &= 18:38 \text{ (18.63 h)} & \overline{MN} &= 00:38 \text{ (0.63 h)}\end{aligned}$$

This adjustment was achieved by pre-processing clock-time in both summer and winter datasets, by a pre-processing function f which varies with time of day t and date of year T :

$$t' = f(t, T)$$

Although both winter and summer datasets were pre-processed according to the same set of rules, the variations of daylength between the two seasons resulted in two opposite time adjustments: time in summer was contracted around \overline{SS} and \overline{SR} , whereas it was expanded in winter. However, \overline{MD} and \overline{MN} remained untransformed throughout the year and the magnitude of the time adjustment gradually decreased as t got closer to those two constant hours (Fig. 2.3 and Fig. 2.5).

The resulting t' was a 24-hour circular variable such that daylength equaled 12 hours, for all dates of winter and summer.

$$\text{With } t' : \forall T, \text{ daylength} = \overline{SS} - \overline{SR} = 12 \text{ h}$$

The sequential order of ‘time distances’ (or elapsed time) between different photo-capture events also remained the same before and after data pre-processing.

$$\forall (t_1, t_2) \in [0, 24], |t_1 - SR| \leq |t_2 - SR| \Leftrightarrow |t'_1 - \overline{SR}| \leq |t'_2 - \overline{SR}|$$

The pre-processing function f was defined by a set of four equations, applied to domains of t values, related to intervals between midnight and sunrise, sunrise and midday, midday and sunset, and sunset and midnight. SR and SS were respectively the sunrise and sunset times on the date T of the photo-capture, and t the time of the photo-capture event.

$$\begin{aligned}
 \overline{MN} \leq t \leq SR & \quad t' = \overline{MN} + K_1 \cdot (t - \overline{MN}) & \quad K_1 = \frac{6}{SR - \overline{MN}} \\
 SR \leq t \leq \overline{MD} & \quad t' = \overline{MD} - K_2 \cdot (\overline{MD} - t) & \quad K_2 = \frac{6}{\overline{MD} - SR} \\
 \overline{MD} \leq t \leq SS & \quad t' = \overline{MD} + K_3 \cdot (t - \overline{MD}) & \quad K_3 = \frac{6}{SS - \overline{MD}} \\
 SS \leq t \leq \overline{MN} & \quad t' = \overline{MN} - K_4 \cdot (\overline{MN} - t) & \quad K_4 = \frac{6}{\overline{MN} - SS}
 \end{aligned} \tag{2.2}$$

Replacing \overline{MD} and \overline{MN} by their quantitative values for the study site yields:

$$\begin{aligned}
 0.63 \leq t \leq SR & \quad t' = 0.63 + K_1 \cdot (t - 0.63) & \quad K_1 = \frac{6}{SR - 0.63} \\
 SR \leq t \leq 12.63 & \quad t' = 12.63 - K_2 \cdot (12.63 - t) & \quad K_2 = \frac{6}{12.63 - SR} \\
 12.63 \leq t \leq SS & \quad t' = 12.63 + K_3 \cdot (t - 12.63) & \quad K_3 = \frac{6}{SS - 12.63} \\
 SS \leq t \leq 0.63 & \quad t' = 0.63 - K_4 \cdot (0.63 - t) & \quad K_4 = \frac{6}{0.63 - SS}
 \end{aligned} \tag{2.3}$$

Time-of-day is a circular variable; under certain circumstances, the equations returned inappropriate time values for t' . For example, if a species got photo-captured on 3 March at 23:00, four hours after sunset, then:

$$\left. \begin{aligned} t &= 23.00 \\ SS &= 19.00 \end{aligned} \right\} t' = -6.67$$

To overcome this issue, the daily periodicity was defined as the 24-hour cycle starting at 00:38 (0.63) and finishing at 24:38 (24.63). Consequently, the fourth equation was then split up into two;

$$\begin{aligned}
 SS \leq t \leq 24 & \quad t' = 24.63 - K_{4.1} \cdot (24.63 - t) & \quad K_{4.1} = \frac{6}{24.63 - SS} \\
 24 \leq t \leq 24.63 & \quad t' = 24.63 - K_{4.2} \cdot (24.63 - t) & \quad K_{4.2} = \frac{6}{24.63 - SS_p}
 \end{aligned} \tag{2.4}$$

where SS_p is the sunset time on the previous day ($T - 1$) of the photo-capture.

In the five equations (Eq. 2.3 and 2.4), the distortion of t was mainly defined by the value of the coefficient K_λ which, depending on the season, was either greater or smaller than 1. Fig. 2.3 shows the pre-processing of t for events that took place on the days of the winter and summer solstices. It highlights

the standardisation of daylength to exactly 12 hours throughout the 365-day cycle. Fig. 2.5 provides a different approach to showing the results of the pre-processing function f for all values of t within the 24-hour cycle, but this time for events that took place on six dates of the year T , including on the vernal and fall equinoxes T_4 as well as on the southern summer and winter solstices (T_1, T_6). Photo-capture events that took place during winter mornings saw their times t adjusted to earlier values (blue points below the black line $y = x$), whereas events that took place during winter afternoons, saw their times t adjusted to later values (blue points above the black line), resulting in an expansion of daylength (grey area in Fig. 2.5). The opposite transformation took place in summer with a contraction of daylength (white area in Fig. 2.5).

$$\left. \begin{array}{l} \text{winter} \quad \overline{MN} < t < \overline{MD} \Rightarrow t' < t \\ \text{winter} \quad \overline{MD} < t < \overline{MN} \Rightarrow t' > t \end{array} \right\} \text{daylength expansion}$$

$$\left. \begin{array}{l} \text{summer} \quad \overline{MN} < t < \overline{MD} \Rightarrow t' > t \\ \text{summer} \quad \overline{MD} < t < \overline{MN} \Rightarrow t' < t \end{array} \right\} \text{daylength contraction}$$

t' values greater than 24.00 ($24 \leq t \leq 24.63$) were then re-adjusted by subtracting 24.00, so that all t' values belonged to the 24-hour cycle starting at 00:00 and finishing at 24:00.

Using t' as circular data, the probability density functions describing the diel activity rhythms $A_{l,s}$ of species s during season l , in relation to sunrise and sunset, were computed.

Seasonal daylength standardisation

Finally, in a third analysis, the time variable t was also transformed so that summer and winter activity patterns could be compared, by standardising daily sunrise times SR to 07:25 (winter average of sunrise times \overline{SR}_w) or to 05:40 (summer average of sunrise times \overline{SR}_e), and daily sunset times SS to 17:53 (winter average of sunset times \overline{SS}_w) or to 19:31 (summer average of sunset times \overline{SS}_e). However, the transformation did not affect true midday \overline{MD} and night \overline{MN} , which were reached at 12:38 and 00:38 respectively, given the location of the study area on the Earth's surface.

$$\begin{array}{lll} \overline{SR}_e = 05:40 \text{ (5.67 h)} & \overline{SR}_w = 07:25 \text{ (7.42 h)} & \overline{MD} = 12:38 \text{ (12.63 h)} \\ \overline{SS}_e = 19:31 \text{ (19.52 h)} & \overline{SS}_w = 17:53 \text{ (17.88 h)} & \overline{MN} = 00:38 \text{ (0.63 h)} \end{array}$$

This adjustment was achieved by pre-processing clock-time according to a similar method, except that in this case, two different and seasonal pre-

processing functions f_l were applied to winter (f_w) and summer (f_e) datasets:

$$f_l(t, T) \begin{cases} T \in \text{winter}, & t' = f_e(t, T) \\ T \in \text{summer}, & t' = f_w(t, T) \end{cases}$$

Winter and summer datasets were pre-processed according to different sets of rules: time in summer was slightly contracted around \overline{SR}_e and \overline{SS}_e , whereas it was slightly expanded in winter around \overline{SR}_w and \overline{SS}_w .

The resulting t'' was a 24-hour circular variable, and the difference of daylength between any winter and summer days was always equal to exactly 3.37 hours.

$$(\overline{SS}_e - \overline{SR}_e) - (\overline{SS}_w - \overline{SR}_w) = 3.37 \text{ h}$$

The sequential order of ‘time distance’ between different photo-capture events remained the same before and after data pre-processing.

$$\begin{aligned} \forall l \in \{w, e\}, \forall (t_1, t_2) \in [0, 24], \\ |t_1 - SR_l| \leq |t_2 - SR_l| \Leftrightarrow |t'_1 - \overline{SR}_l| \leq |t'_2 - \overline{SR}_l| \end{aligned}$$

The pre-processing function f_l of season l only differed from its sister function f by the numerator n_λ of the K_λ coefficients in all five equations (Eq. 2.3 and 2.4). $\lambda \in \{1, 2, 3, 4, 5\}$:

$$\begin{array}{lll} 0.63 \leq t \leq SR & n_{1,w} = 6.79 & n_{1,e} = 5.06 \\ SR \leq t \leq 12.63 & n_{2,w} = 5.21 & n_{2,e} = 6.94 \\ 12.63 \leq t \leq SS & n_{3,w} = 5.25 & n_{3,e} = 6.89 \\ SS \leq t \leq 24.00 & n_{4,w} = 6.74 & n_{4,e} = 5.10 \\ 24.00 \leq t \leq 24.63 & n_{5,w} = 6.74 & n_{5,e} = 5.10 \end{array} \quad (2.5)$$

t'' values greater than 24.00 ($24 \leq t \leq 24.63$) were then re-adjusted by subtracting 24.00, so that all t'' values belonged to the 24-hour cycle starting at 00:00 and finishing at 24:00.

Using t'' as circular data, the probability density functions describing the diel activity rhythms $A''_{l,s}$ of species s during season l , in relation to seasonal times of sunrise and sunset, were computed.

2.3.3.3 Bootstrapping

A statistical bootstrap method (resampling technique) [235] was used to compare, for every mammal species s , its diel activity rhythm from the data collected during winter $A_{w,s}$ to that collected during summer $A_{e,s}$.

Kernel density functions such as $A_{l,s}$ have an under-curve area equal to 1, which offers the opportunity to compare them against one another, by calculating their coefficient of overlap ranging from 0 (no overlap) to 1 (identical curves) [283]. Using the *overlapEst* function from the *overlap* R-package [226], the coefficient of overlap $O_{,s}$ in diel activity rhythms of species s , between winter and summer was calculated:

$$\begin{aligned} O_{,s} &= O_v(A_{w,s}, A_{e,s}) \\ &= \int_0^{24} \min(A_{w,s}, A_{e,s}) \cdot dt \end{aligned} \quad (2.6)$$

The process of bootstrapping consists of random sampling without replacement (also called permutation). In this study, $r = 10,000$ permutations were created by randomly splitting the camera trap dataset into two samples ($A_{w_p,s}, A_{e_p,s}$) with sizes matching those of the two datasets obtained during the winter and summer seasons. Similarly, the coefficient of overlap of the two newly created density functions was calculated, prior to storing it into a species vector $V_{,s}$:

$$\begin{aligned} O_{,s}^p &= O_v(A_{w_p,s}, A_{e_p,s}) \\ V_{,s} &= (O_{,s}^1, O_{,s}^2, \dots, O_{,s}^p, \dots, O_{,s}^r) \\ r &= 10,000 \end{aligned} \quad (2.7)$$

The percentage of overlap coefficients stored in $V_{,s}$ that are greater than the observed one $O_{,s}$ was calculated for every species s , along with the p-value $P_{,s}$:

$$\begin{aligned} V_{g,s} &= \text{subset}(V_{,s}, O_{,s}^p > O_{,s}) \\ P_{,s} &= \frac{L(V_{g,s})}{L(V_{,s})} \quad L = \text{length}() \end{aligned} \quad (2.8)$$

The bootstrap analysis was applied to the three pre-processed datasets, built with three different time variables t , t' and t'' , producing $O_{,s}$, $O'_{,s}$, $O''_{,s}$ and $P_{,s}$, $P'_{,s}$, $P''_{,s}$.

2.3.3.4 Circular statistics

The statistical analysis of circular data is a specialised field [108, 156]. Batschelet (1981) [21] deals with circular statistics specifically within a biological framework. When standard statistical measures, such as the arithmetic mean and variance are applied to circular variables, inappropriate

and nonsensical results are obtained, depending on the arbitrary time origin [21]. Batschelet (1981) [21] provides mathematical tools (vector algebra and trigonometric functions) to measure location and dispersion within a circular distribution. These mathematical tools offer an opportunity to profile species' diel activity rhythms and to quantify their seasonal shifts. However, this methodology provides meaningful results under the assumption that data are symmetric and unimodal, and very few mammal species of the Little Karoo have their diel activity rhythms meet those criteria (Fig. 2.4(b)), which is why other routes had to be explored.

2.3.3.5 Seasonal shift in diel activity rhythms

The seasonal shift in diel activity rhythms between summer and winter was quantified in the three different time metrics t , t' and t'' , for the 25 mammal species s :

$$\begin{aligned} S_{,s} &= A_{e,s} - A_{w,s} \\ S'_{,s} &= A'_{e,s} - A'_{w,s} \\ S''_{,s} &= A''_{e,s} - A''_{w,s} \end{aligned} \quad (2.9)$$

$S_{,s}$, $S'_{,s}$ and $S''_{,s}$ could also be defined as:

$$\int_0^{24} S_{,s} \cdot dt = \int_0^{24} S'_{,s} \cdot dt' = \int_0^{24} S''_{,s} \cdot dt'' = 0 \quad (2.10)$$

$$\begin{aligned} \int_0^{24} |S_{,s}| \cdot dt &= 2 \cdot (1 - O_{,s}) \\ \int_0^{24} |S'_{,s}| \cdot dt' &= 2 \cdot (1 - O'_{,s}) \\ \int_0^{24} |S''_{,s}| \cdot dt'' &= 2 \cdot (1 - O''_{,s}) \end{aligned} \quad (2.11)$$

The area under the curve of probability density functions is, by definition, equal to 1; the definite integrals of the difference between two such functions is compulsorily equal to 0 (Eq. 2.10). The demonstration of Eq. 2.11 is provided in Appendix 4A.

Descriptive statistics

In Chapter 3 section 3.4, it was shown that, after daylength standardisation

(t') and within the 24-hour cycle, the time-profile (summary of the activity level of all species in the community at time t') went through a periodic cycle characterised by four periods θ . Two stable ones ϕ_n and ϕ_d , matching the darkest and brightest hours of the cycle. Outside those hours, the time-profile went through two transitional periods ρ_m and ρ_e during which it varies rapidly to get from ϕ_n to ϕ_d and vice versa. The early morning and late evening periods (ρ) are therefore considered to be the crepuscular hours of the daily cycle.

$$\theta \begin{cases} \phi_n & : & (\overline{SS} + 1.37 \text{ h}, \overline{SR} - 1.63 \text{ h}) \\ \phi_d & : & (\overline{SR} + 3.37 \text{ h}, \overline{SS} - 2.63 \text{ h}) \\ \rho_m & : & (\overline{SR} - 1.63 \text{ h}, \overline{SR} + 3.37 \text{ h}) \\ \rho_e & : & (\overline{SS} - 2.63 \text{ h}, \overline{SS} + 1.37 \text{ h}) \end{cases} \quad (2.12)$$

ρ_m , ϕ_d , ρ_e and ϕ_n respectively last five, six, four and nine hours.

Several descriptive statistics were then defined and calculated for every species s and for the four daily time periods θ defined above. These statistics were annotated with an apostrophe to highlight the fact that there were calculated after annual daylength standardisation of the data (t'):

$$\begin{aligned} \text{Total rhythm variation (\%):} & \quad \text{TRV}'_{,s} = \frac{1}{2} \cdot 100 \cdot \int_0^{24} |S'_{,s}| \cdot dt' \\ \text{Local rhythm variation (\%):} & \quad \text{LRV}'_{,s}(\theta) = 100 \cdot \frac{\int_\theta |S'_{,s}| \cdot dt'}{\int_0^{24} |S'_{,s}| \cdot dt'} \\ \text{Local activity shift (\%):} & \quad \text{LAS}'_{,s}(\theta) = 100 \cdot \int_\theta S'_{,s} \cdot dt' \\ \text{Compensation index:} & \quad I'_{,s}(\theta) = \frac{\int_\theta S'_{,s} \cdot dt'}{\int_\theta |S'_{,s}| \cdot dt'} \end{aligned} \quad (2.13)$$

The mathematical relationships between $A'_{l,s}$, $O'_{,s}$ and $S'_{,s}$ are defined in Fig. 2.6.

The total rhythm variation of species s ($\text{TRV}'_{,s}$) provides the percentage of diel activity rhythm that shifted between the two seasons. The local rhythm variation of species s during time period θ ($\text{LRV}'_{,s}(\theta)$) provides the percentage of $\text{TRV}'_{,s}$ explained during θ . The local activity shift of species s during time period θ ($\text{LAS}'_{,s}(\theta)$) provides the resulting shift in daily activity proportions allocated by species s throughout θ . Finally, the compensation index of species s during time period θ ($I'_{,s}(\theta)$) will be equal to 1 if $\text{LRV}'_{,s}(\theta)$ is entirely converted into a shift in activity. However, if compensation effects (activity

increases compensated by activity decreases throughout θ) occur, $I'_s(\theta)$ will take values greater than one.

After this species-specific work, the same analysis was applied to the whole mammal community c , using the following probability density functions:

$$\int_0^{24} A_{l,c} \cdot dt = \int_0^{24} A'_{l,c} \cdot dt' = \int_0^{24} A''_{l,c} \cdot dt'' = 1 \quad (2.14)$$

$A_{l,c}$, $A'_{l,c}$ and $A''_{l,c}$ were calculated using the data for the 25 mammal species within the community c . The following variables $S_{,c}$, $S'_{,c}$ and $S''_{,c}$, as well as descriptive statistics $\text{TRV}'_{,c}$, $\text{LRV}'_{,c}$, $\text{LAS}'_{,c}$ and $I'_{,c}$, were calculated. The weight a species s had on the diel activity rhythms of the mammal community c , was proportional to its photo-capture frequency.

At a second stage, diel activity rhythms $A_{l,\bar{c}}$, $A'_{l,\bar{c}}$ and $A''_{l,\bar{c}}$ were built using equal weight for the 25 mammal species within the community \bar{c} . This was achieved by extracting, for every species s , 128 points at regular time intervals from each of the three kernel density functions $A_{l,s}$, $A'_{l,s}$ and $A''_{l,s}$, before averaging:

$$\begin{aligned} i \in [1..128], \quad A_{l,\bar{c}}(t_i) &= \frac{\sum_{s_j=1}^{25} A_{l,s_j}(t_i)}{25} \\ i \in [1..128], \quad A'_{l,\bar{c}}(t'_i) &= \frac{\sum_{s_j=1}^{25} A'_{l,s_j}(t'_i)}{25} \\ i \in [1..128], \quad A''_{l,\bar{c}}(t''_i) &= \frac{\sum_{s_j=1}^{25} A''_{l,s_j}(t''_i)}{25} \end{aligned} \quad (2.15)$$

Applying the same analysis once more, following variables $S_{,\bar{c}}$, $S'_{,\bar{c}}$ and $S''_{,\bar{c}}$, as well as descriptive statistics $\text{TRV}'_{,\bar{c}}$, $\text{LRV}'_{,\bar{c}}$, $\text{LAS}'_{,\bar{c}}$ and $I'_{,\bar{c}}$, were calculated.

Non-metric Multi-Dimensional Scaling (NMDS)

Non-metric approach to multi-dimensional scaling is a statistical tool which provides a means of displaying and summarising a square symmetric matrix of dissimilarities into a low-dimensional Euclidean space [126, 180, 181]. A dissimilarity matrix was computed to estimate the dissimilarities of seasonal shifts in diel activity rhythm for each pair of species in the mammal

community of the Little Karoo [32]. The objective in NMDS is to find a configuration of points in Euclidean space so that the ordering of the interpoint distances matches, as closely as possible, the ordering of the dissimilarities in the matrix of dissimilarities [32].

The information contained in $S'_{,s}$ was compiled into a matrix M with $n = 25$ rows (species) and $p = 128$ columns (t' values selected at regular intervals between 00:38 and 24:38). Every element $M[s, t']$ gave the seasonal change in diel activity rhythm $S'_{,s}(t')$ of species s at time t' .

$$M[s, t'] = S'_{,s}(t')$$

Using the *dist* function from the *stats* R-package [22, 32, 209], M was computed to calculate a distance matrix with distances being measured between rows of M using the Manhattan method; the output distance matrix was a symmetric matrix with 25 rows and columns, and was referred to as the Activity-shift Distance Matrix (ADM). Every element $ADM[s_1, s_2]$ quantified the dissimilarity between the seasonal shift in diel activity rhythm of species s_1 and s_2 .

$$ADM[s_1, s_2] = \text{dist}(S'_{,s_1}, S'_{,s_2})$$

An NMDS ordination was performed on ADM, using the *isoMDS* function from the *MASS* R-package [285]. Summarising a dissimilarity matrix into a two-dimensional plot might not be feasible and a certain amount of distortion might be created. The measure of lack of fit in NMDS is known as the ‘stress’ of the configuration. Non-zero stress values occur with insufficient dimensionality, and as the number of dimensions increases, the stress value will either decrease or remain stable [32]. The objective of the ordination is to find the configuration with minimum ‘stress’ for a given number of dimensions. The operation was therefore repeated several times with a different number of chosen dimensions k , and a screeplot (stress versus k) was plotted in order to identify the point beyond which additional dimensions do not substantially lower the stress value.

2.4 Results

The trapping effort of 14,331 camera trap nights resulted in 21,469 photo-captures which were reduced to 9,057 independent photo-capture events; these involved 80 wild species, including 46 mammals, 33 birds and one reptile. Of the 46 mammal species, 25 had more than 15 photo-captures in both summer and winter to enable the analysis to be conducted [Appendix 2A].

2.4.1 Diel activity rhythms

The probability density functions, built with the three time metrics, described the noon- or midnight-centred diel activity rhythms $A_{l,s}$, $A'_{l,s}$ and $A''_{l,s}$ of species s during season l , and showed the nocturnal-diurnal dichotomy that provides a temporal axis of niche segregation and that has facilitated coexistence among sympatric species [40] [Chapter 3 section 3.4] (Fig. 2.7). Similarly, Fig. 2.9 displays the diel activity rhythms $A_{l,c}$, $A'_{l,c}$ and $A''_{l,c}$, as well as $A_{l,\bar{c}}$, $A'_{l,\bar{c}}$ and $A''_{l,\bar{c}}$ of the mammal community c and \bar{c} during season l .

2.4.2 Overlap coefficients

The associated overlap coefficients calculated between seasonal diel activity rhythms were shaded in grey (Fig. 2.7 and 2.9), and summarised in Table 2.1.

The diel activity rhythms of the 25 mammal species s were nearly identical before and after **seasonal** daylength standardisation ($A_{l,s}$, $A'_{l,s}$). The average difference between their associated overlap coefficients $O_{,s}$ and $O'_{,s}$ was equal to 0.8% (Table 2.1).

The average difference in overlap $O_{,s}$ and $O'_{,s}$ between the diel activity rhythms of the 25 mammal species s , produced before and after **annual** daylength standardisation $A_{l,s}$ and $A'_{l,s}$, was however substantial and equal to 7.3%. The graphs in Fig. 2.7 illustrate the distortion t' of the linearity of clock-time t around sunrise and sunset (contraction in summer, expansion in winter), due to annual daylength standardisation. For 20 of the 25 mammal species, standardising daily times of sunrise and sunset (SR , SS) to the annual average times of sunrise and sunset (\overline{SR} , \overline{SS}) prompted an increase in overlap $O'_{,s}$, sometimes as high as 15% (e.g. leopard and grey duiker *Sylvicapra grimmia*). Aardvark *Orycteropus afer*, Cape hare *Lepus capensis*, red hartebeest *Alcelaphus buselaphus* and scrub hare *Lepus saxatilis* were the four species having their overlap coefficients decreasing after annual daylength standardisation, that of aardwolf *Proteles cristatus* remained constant. $O'_{,s}$ ranged from 0.46 (rock hyrax *Procavia capensis*, greatest seasonal change) to 0.89 (greater kudu *Tragelaphus strepsiceros*, smallest seasonal change).

2.4.3 Bootstrapped p-values

The results of the bootstrap analysis are summarised in Table 2.1 and Fig. 2.10. They showed that the significant seasonal shift in clock-timed diel

activity rhythms between winter and summer ($P_{,s} < 0.05$) for African wildcat *Felis silvestris*, Cape mountain zebra *Equus zebra zebra*, greater kudu and leopard, was no longer observed after annual daylength standardisation ($P'_{,s} > 0.05$). It however remained observed ($P_{,s} < 0.05$ and $P'_{,s} < 0.05$) for 15 other species: aardwolf, black-backed jackal *Canis mesomelas*, Cape gray mongoose *Galerella pulverulenta*, Cape porcupine *Hystrix africaeaustralis*, caracal *Caracal caracal*, chacma baboon *Papio ursinus*, eland *Taurotragus oryx*, gemsbok *Oryx gazella*, grey duiker, honey badger *Mellivora capensis*, Hewitt's red rock rabbit *Pronolagus saundersia*, klipspringer *Oreotragus oreotragus*, rock hyrax *Procavia capensis*, scrub hare *Lepus saxatilis* and steenbok *Raphicerus campestris*.

The bootstrap analysis also showed that three of the six species which displayed no significant seasonal change in their clock-timed diel activity rhythms between winter and summer ($P_{,s} > 0.05$), did display a significant change after annual daylength standardisation ($P'_{,s} < 0.05$): aardvark *Orycteropus afer*, Cape hare *Lepus capensis* and red hartebeest *Alcelaphus buselaphus*.

2.4.4 Seasonal shift in diel activity rhythm

Seasonal shift in diel activity rhythm were displayed using S -curves (Fig. 2.8 and 2.9), before being explored using descriptive statistics (Table 2.2).

2.4.4.1 Graphical display: S -curves

The summer-winter seasonal shifts in diel activity rhythms for each of the 25 mammal species s , were quantified for the three time metrics, and represented as noon- or midnight-centred curves $S_{,s}$, $S'_{,s}$ and $S''_{,s}$ in Fig. 2.8. Similarly, Fig. 2.9 displays the summer-winter seasonal shifts in diel activity rhythms $S_{,c}$, $S'_{,c}$ and $S''_{,c}$ as well as $S_{,\bar{c}}$, $S'_{,\bar{c}}$ and $S''_{,\bar{c}}$, of the mammal community c and \bar{c} . In each two-dimensional Euclidean space, the signed area of the plane that was bounded by the S' -curve, the horizontal line $y = 0$, and the vertical lines $t' = 0$ and $t' = 24$, was shaded in black over the darkest hours of the cycle (ϕ_n), dark grey over the crepuscular hours (ρ) and light grey over the brightest hours (ϕ_d). The species-specific seasonal shifts $S_{,s}$, $S'_{,s}$ and $S''_{,s}$ were positive when the proportion of daily activity, allocated by species s at time t , t' and t'' , was higher in summer than in winter. On the contrary, they were negative when the proportion was lower in summer than in winter. The same observations applied to communal seasonal shifts $S_{,c}$, $S'_{,c}$ and $S''_{,c}$ as well as $S_{,\bar{c}}$, $S'_{,\bar{c}}$ and $S''_{,\bar{c}}$.

2.4.4.2 Descriptive statistics

Table 2.2 compiles the S -curves descriptive statistics TRV' , LRV' , LAS' and I' providing insights into the seasonal shifts in diel activity rhythms of the 25 mammal species s and of the whole mammal community c and \bar{c} .

a) Total rhythm variation: $TRV'_{,s}$

The 25 mammal species were ranked in descending order of their total rhythm variation $TRV'_{,s}$ (Table 2.2). Rock hyrax, with 54% of $TRV'_{,s}$, was the species with the highest percentage of diel activity rhythm shift between summer and winter. Greater kudu was the species with the lowest percentage of diel activity rhythm shift between summer and winter (11% of $TRV'_{,s}$). High percentages of $TRV'_{,s}$ did not necessarily imply a significant seasonal shift in diel activity rhythm. With 28% of $TRV'_{,s}$, Springbok showed a substantial variation of its seasonal diel activity rhythms; however, the bootstrap analysis showed no significant change (Table 2.1).

b) Local rhythm variation: $LRV'_{,s}(\theta)$

The percentage of $TRV'_{,s}$ explained during each of the four θ time periods (ρ_m , ϕ_d , ρ_e and ϕ_n (Eq. 2.12)), was defined as the associated local rhythm variation $LRV'_{,s}(\theta)$. Divided by the number of hours in θ , it provided the hourly rhythm variation of species s throughout θ (Table 2.2). $LRV'_{,s}(\theta)$ was shaded in grey when θ was the time period of the 24-hour cycle with the highest hourly rhythm variation. The variations in diel activity rhythm took place throughout the 24-hour cycle and the time period θ that explained most of those variations varied according to the species. For eight of the 25 species, the seasonal shift mainly took place throughout the crepuscular hours of the morning (ρ_m). Eight other species showed a main shift during the darkest hours (ϕ_n), five species during the crepuscular hours of the evening (ρ_e) and four species during the brightest hours (ϕ_d). When considering all crepuscular hours together (ρ), it appeared that, for 13 species, most of the seasonal shift took place during the crepuscular hours of the 24-hour cycle. This is also true regarding the variations in diel activity rhythm of the mammal community as a whole: c and \bar{c} .

c) Local activity shift: $LAS'_{,s}(\theta)$

Variations of the diel activity rhythm can lead to local activity shifts: increases and/or decreases in the proportions of daily activity allocated to certain time periods of the 24-hour cycle. They can also result in no alteration of the proportions of daily activity during a specific time period (θ), because of compensation effects (throughout the time period in question, local increases can be compensated by local decreases).

Morning crepuscular hours, $LAS'_{,s}(\rho_m)$: Table 2.2 shows that, except for honey badger and leopard, the other 23 mammal species increased their proportions of daily activity allocated to morning crepuscular hours (ρ_m) in summer, compared with those allocated in winter. These percentages were shaded in orange.

Brightest and evening crepuscular hours, $LAS'_{,s}(\phi_d, \rho_e)$: The proportions of daily activity allocated to brightest hours (ϕ_d) and evening crepuscular hours (ρ_e) in summer, decreased (shaded in blue) or remained unchanged (no shading) for most species (23 species for ϕ_d , and 20 species for ρ_e).

Darkest hours, $LAS'_{,s}(\phi_n)$: The trends regarding the darkest hours (ϕ_n) were more nuanced with roughly the same number of species having increased (8 species) their proportions of daily activity during the darkest hours of the 24-hour cycle in summer, as the number of species having decreased (10 species) or unchanged (seven species) their proportions of daily activity during those hours.

One of the most striking seasonal shift was that of honey badger. It displayed a bimodal and crepuscular pattern in winter and a unimodal and nocturnal pattern in summer (Fig. 2.7(r)).

d) Compensation index: $I'_{,s}(\theta)$

Four species, klipspringer, steenbok, Cape porcupine and African wildcat, showed substantial compensation effects, meaning that despite large seasonal variations of their diel activity rhythms over θ , their resulting seasonal shift in activity during θ was small. The compensation index $I'_{,s}(\theta)$ highlighted these compensation effects with values appreciably greater than one, and shaded in grey in Table 2.2. For 14 species, the compensation index $I'_{,s}(\rho)$ was greater than one, meaning that the seasonal shift in activity allocated to morning and evening crepuscular hours (ρ_m and ρ_e) worked in opposite directions. When a species showed no activity during θ in both seasons, the associated $LRV'_{,s}(\theta)$ and $LAS'_{,s}(\theta)$ were zero, and $I'_{,s}(\theta)$ returned NA.

Looking at the mammal community \bar{c} , the seasonal variations in diel activity rhythm led to an increase of the proportions of daily activity allocated to morning crepuscular hours (ρ_m), a decrease of the proportions of daily activity allocated to the brightest and evening crepuscular hours (ϕ_d and ρ_e), and no shift in proportions of daily activity allocated to the darkest hours of the night (ϕ_n). However, $I'_{,\bar{c}}(\phi_n) = 11$ showed that the proportions of daily activity symmetrically increased and decreased at different periods of the darkest time period (ϕ_n), creating activity compensation. Finally, $I'_{,\bar{c}}(\rho) = 4$ showed that the proportions of daily activity varied in opposite directions be-

tween morning and evening crepuscular hours (ρ_m and ρ_e). Fig. 2.9 provides a graphical summary of those results.

2.4.5 Seasonal shift comparison in the community

The NMDS algorithm captured, in two dimensions, the essential structure of the dissimilarity data (stress = 0.159). Fig. 2.11 represents, as closely as possible, the ordering of the dissimilarities between species' seasonal shift in diel activity rhythm. In other words, points close together represent species that shifted their diel activity rhythm between winter and summer in a more similar manner than species represented by points farther apart; however, the graph does not provide quantitative information regarding this difference. Whenever possible, the noon-centred $S'_{,s}$ -curves were added to NMDS plot, next to the associated species points.

A screeplot (Fig. 2.12) revealed that attempting an ordination with one NMDS axis yielded unacceptably high stress (0.269) whereas two or three dimensions was more adequate. However, with five dimensions, the stress value dropped below 0.050, which indicated good fit. Despite a stress value greater than 0.050, the NMDS plot in two dimensions could be useful as a first exploration of the data and to gain some insights into the dissimilarities data between the seasonal shifts in diel activity rhythm of the 25 mammal species s , within the mammal community of the Little Karoo.

In the NMDS plot (Fig. 2.11), the 25 mammal species were spatially placed in a plane with a clear and gradual left-right transition along the first axis, from species with a 'diurnal' shift of their diel activity rhythms between summer and winter (e.g. rock hyrax) to species with a 'nocturnal' shift of their diel activity rhythms between summer and winter (e.g. aardwolf). The species in the centre of the plot are those which show rather little pattern and small-amplitude shifts of their diel activity rhythms between seasons (e.g. greater kudu). Species on the right hand side of the first axis are the species which are nocturnal, but switch from using hours before midnight in winter to hours after midnight in summer, of which aardwolf is the strongest example. On the edges of the plot are the species with unusual shifts: rock hyrax remains diurnal but switches a substantial proportion of its daily activity from midday hours in winter to morning twilight in summer; honey badger shifts from being crepuscular in winter to being nocturnal in summer; and red hartebeest, which is crepuscular both seasons, but switches a substantial proportion of its daily activity from night to day.

2.5 Discussion

Using camera traps set over winter and summer, this chapter documented the seasonal plasticity of the diel activity rhythms of 25 mammal species co-occurring in the Little Karoo. Most mammal species responded to the ecological variability brought about by adjusting their diel activity rhythms between winter and summer. The extent of these seasonal shifts varied among the mammal community.

2.5.1 Data pre-processing

Standardising daily times of sunrise and sunset (SR , SS) to the **annual** average times of sunrise and sunset (\overline{SR} , \overline{SS}), reshaped species' diel activity rhythms noticeably. In contrast, standardising daily times of sunrise and sunset (SR , SS) to the **seasonal** average times of sunrise and sunset (\overline{SR}_w , \overline{SR}_e ; \overline{SS}_w , \overline{SS}_e), hardly influenced species' diel activity rhythms, because of the minor time difference between t and t'' . On any day of season l , sunrise and sunset times were close to the seasonal averaged ones, which is why pre-processing the data in this manner brought no useful insights into the seasonal shifts in diel activity rhythms of the 25 sympatric mammal species.

2.5.2 Factors influencing seasonal shifts

The de-synchronised, clock-timed diel activity rhythms of African wildcat, Cape mountain zebra, greater kudu and leopard were synchronised with annual daylength standardisation, meaning that, for these species, the seasonal change in diel activity rhythms was almost entirely a consequence of photoperiodism alignment.

The de-synchronised, clock-timed diel activity rhythms of aardwolf, black-backed jackal, Cape gray mongoose, Cape porcupine, caracal, chacma baboon, eland, gemsbok, grey duiker, honey badger, Hewitt's red rock rabbit, klipspringer, rock hyrax, scrub hare and steenbok, did not re-synchronise after annual daylength standardisation, suggesting that their significant seasonal change in diel activity rhythms were not (solely) a result of photoperiodism alignment, and was driven by other factor(s). However, except for aardwolf and scrub hare, the overlap coefficients of the other 13 species increased after annual daylength standardisation ($O'_{,s} > O_{,s}$), often further to a minimisation of the seasonal de-synchronisation, which suggests that their significant seasonal change in diel activity rhythms could be a partial conse-

quence of photoperiodism alignment as well, whose contribution increased as their overlap coefficient did too.

The synchronised, clock-timed diel activity rhythms of armadillo, Cape hare and red hartebeest got de-synchronised, and their overlap coefficient decreased, after annual daylength standardisation, meaning that their diel activity rhythms did not align to photoperiodism as seasons change and that they follow clock-time.

Finally, no significant seasonal change in clock-timed and t' -adjusted diel activity rhythms was observed for brown hyena, grey rhebuck and springbok. The increase of their overlap coefficient after annual daylength standardisation suggests that their diel activity rhythms might partly align to photoperiodism. This adjustment would however not be significant given the overall versatility of the diel activity rhythm.

Comparing intraspecific shifts in diel activity rhythms – before and after time standardization in respect to annual sunrise and sunset times – this chapter found that, while some shifts only result from photoperiodism alignment, most are driven by other factors too (Table 2.3). Environmental seasonality influences processes that enable individuals to meet their metabolic needs; it drives population dynamics and community structure. It also translates into variations of numerous environmental factors such as photoperiodism, temperature, rainfall and food availability [46]. Variations in food availability are likely to prompt variations in food intakes (calories and nutrients), which are fundamental to satisfy cellular maintenance, thermoregulation and locomotion costs [45, 142]; these ecological processes have the potential to directly affect species' diel activity rhythm [105, 255, 272, 367]. A great number of mammals living in seasonally changing environment are doubtlessly seasonal breeders [294]. Two well-known seasonal predictors that prepare individuals metabolically for breeding are photoperiodism and secondary plant compounds found in newly emerging vegetation [97]. It is likely to observe variations of the diel activity rhythm of species during the course of pregnancy and nursing [372].

2.5.3 Profiling seasonal shifts

Seasonal shifts in diel activity rhythm varied in their amplitude and direction among species. Comparing the amplitude of species' seasonal shift with each other must be done carefully because their significance depends on the overall versatility of the diel activity rhythm, which might vary greatly among species (Fig. 2.10). Nineteen species showed a significant shift in clock-timed

diel activity rhythm between winter and summer, and for 15 of them, this shift could not solely be explained by photoperiodism alignment (Table 2.3). Although the analysis also showed a significant seasonal shift in diel activity rhythm after annual daylength standardisation ($P'_{,s} < 0.05$) for three other species – armadillo, Cape hare and red hartebeest – it would be misleading to attempt to interpret its meaning since the clock-timed seasonal shift was not significant ($P_{,s} > 0.05$). Following clock-time, these three species showed a significant seasonal shift, which was induced by the pre-processing of time t in order to achieve daylength standardisation.

The hourly rhythm variation ($\text{LRV}'_{,s}$) reached its highest rate during different daily time periods θ depending on the species. This time period is likely to depend on the species' temporal preferences. For example, rock hyrax and klipspringer were the two species having their hourly rhythm variation reach its highest rate during the brightest hours of the 24-hour cycle (ϕ_d). These two species also allocate a considerable amount (more than 50%) of their daily activity to ϕ_d ; in Chapter 3 section 3.4, rock hyrax and klipspringer are defined as diurnal species. As for Hewitt's red rock rabbit and Cape porcupine, defined as nocturnal species, their hourly rhythm variation reached its highest rate during the darkest hours of the daily cycle (ϕ_n).

In the case of no hourly rhythm variation observed ($\text{LRV}'_{,s}(\theta) = 0$), it was either because species s had not shifted its proportions of daily activity throughout this time period, or that species s was not active at all in both summer and winter, throughout this time period (e.g. Hewitt's red rock rabbit during the brightest hours of the day, Table 2.2).

However, nine of the 15 species, eland, caracal, scrub hare, steenbok, Cape gray mongoose, grey duiker, black-backed jackal, chacma baboon and gemsbok, had their hourly rhythm variation reach its highest rate during the crepuscular hours (ρ) of the 24-hour cycle, independently of their temporal preferences. This supports the idea that photoperiodism plays a crucial role in the adjustment of mammal diel activity rhythms in the Little Karoo.

Among the 15 mammal species that showed a significant change of their seasonal diel activity rhythms both before and after daylength standardisation, 10 shifted proportions of their daily activity from warmer daily time periods to cooler ones, in summer compared to winter. Most of the activity shifts went from the brightest and evening crepuscular hours (ϕ_d and ρ_e) towards morning crepuscular hours (ρ_m , and to a lesser extent towards the darkest hours ϕ_n). This trend could be the result of a behavioural strategy to avoid hot midday and evening hours, and consequently minimise time exposure to a physiologically stressful environment caused by high temperatures

in summer (Fig. 2.13) [113, 150, 157, 158, 201, 336]. Besides the thermoregulatory benefits of restricting activities to cooler time periods, it offers the opportunity to increase the water intake by feeding at night or before dawn when dew forms on vegetation [334]. It is less explicit to interpret the significant shift of daily activity from dark night (ϕ_n) towards morning twilight (ρ_m), which was observed between winter and summer for Hewitt's red rock rabbit, scrub hare, black-backed jackal and gemsbok. The NMDS analysis represented these four species close to one another in Fig. 2.11, suggesting little dissimilarity was observed between their seasonal shifts in diel activity rhythm.

The 4% increase of the proportions of daily activity allocated to ϕ_d by the mammal community c in summer – despite the opposite behaviour followed by most of the species within c , except red hartebeest and chacma baboon – was due to the large weight that species chacma baboon had in c . With 1,514 independent photo-capture events collected for chacma baboon over winter and summer together, the species had a 17% weight in c , compared to 4% in \bar{c} , where all 25 mammal species received equal weight.

Changes in timing of the diel activity rhythm of 25 mammal species between winter and summer, resulted into a shift in the proportions of the daily activity of community \bar{c} from the brightest and evening crepuscular hours (ϕ_d and ρ_e) towards morning crepuscular hours ρ_m , supporting furthermore the behavioural strategy leading to a reduction of time exposure to a physiologically stressful environment caused by high temperatures in summer. Although the study registered information for each season over two consecutive years, it might not be sufficient to determine stability of versatilities within seasons with respect to different years.

2.6 Tables

Table 2.1: Bootstrapped p-values

The N_w and N_s are respectively the number of photo-capture events collected across winter and summer for 25 mammal species in the Little Karoo; $O_{,s}$, $O'_{,s}$ and $O''_{,s}$ (built with t , t' and t'') are the overlap coefficients between winter and summer diel activity rhythms; $P_{,s}$, $P'_{,s}$ and $P''_{,s}$ are the bootstrapped p-values (in %) showing whether winter and summer diel activity rhythms are significantly different ($< 5\%$).

Species	N_w	N_s	$O_{,s}$	$P_{,s}$	$O'_{,s}$	$P'_{,s}$	$O''_{,s}$	$P''_{,s}$
aardvark	81	55	0.84	10	0.81	3	0.84	11
aardwolf	42	68	0.57	0	0.57	0	0.57	0
African wildcat	261	130	0.82	0	0.88	15	0.82	0
black backed jackal	484	362	0.82	0	0.86	0	0.81	0
brown hyena	50	23	0.80	18	0.81	22	0.79	18
Cape gray mongoose	229	73	0.70	0	0.81	0	0.70	0
Cape hare	23	69	0.81	18	0.76	5	0.81	15
Cape mountain zebra	37	48	0.67	1	0.80	49	0.69	3
Cape porcupine	178	187	0.76	0	0.81	0	0.77	0
caracal	226	80	0.68	0	0.80	0	0.68	0
chacma baboon	521	993	0.84	0	0.87	0	0.84	0
eland	173	143	0.67	0	0.74	0	0.67	0
gemsbok	426	372	0.82	0	0.88	0	0.81	0
greater kudu	153	90	0.78	0	0.89	76	0.78	0
grey duiker	362	644	0.70	0	0.85	0	0.70	0
grey rhebuck	62	111	0.82	11	0.85	30	0.82	9
Hewitts red rock rabbit	30	32	0.67	1	0.72	4	0.72	6
honey badger	44	32	0.54	0	0.66	1	0.56	0
klipspringer	167	136	0.73	0	0.80	0	0.74	0
leopard	95	81	0.69	0	0.84	17	0.71	0
red hartebeest	30	118	0.78	22	0.69	1	0.77	21
rock hyrax	17	33	0.36	0	0.46	0	0.36	0
scrub hare	327	81	0.82	1	0.80	0	0.85	7
springbok	20	55	0.69	9	0.72	19	0.69	9
steenbok	121	93	0.66	0	0.80	4	0.67	0

Community	N_w	N_s	$O_{,c}$	$P_{,c}$	$O'_{,c}$	$P'_{,c}$	$O''_{,c}$	$P''_{,c}$
c	4159	4109	0.88	0	0.87	0	0.88	0
\bar{c} (equal weight)	-	-	0.83	0	0.89	0	0.83	0

Table 2.2: Seasonal shift in diel activity rhythm
(Caption on following page)

Species	TRV _s '	LRV _s '					LAS _s '					I' _s				
	24-h cycle	ρ_m	ϕ_d	ρ_e	ϕ_n	ρ	ρ_m	ϕ_d	ρ_e	ϕ_n	ρ	ρ_m	ϕ_d	ρ_e	ϕ_n	ρ
rock hyrax *	54	40	53	5	2	45	45	-49	4	0	49	1	1	1	1	1
aardwolf *	43	13	2	21	64	34	9	1	-20	10	-11	1	1	1	5	2
honey badger *	34	18	8	22	52	40	-11	-6	-19	36	-30	1	1	1	1	1
red hartebeest *	31	25	32	13	30	38	6	19	-13	-12	-7	2	1	1	1	3
Hewitts red rock rabbit *	28	24	0	10	65	34	18	0	-3	-15	15	1	NA	2	2	1
springbok	28	21	43	7	29	28	8	-18	-5	15	3	1	1	1	1	5
eland *	26	23	14	32	31	55	13	-5	-21	13	-8	1	2	1	1	3
Cape hare *	24	13	0	10	76	23	8	0	6	-14	14	1	NA	1	2	1
Cape mountain zebra	20	17	25	21	37	38	2	-11	-8	17	-6	4	1	1	1	2
caracal *	20	11	20	29	40	40	7	-7	-13	13	-6	1	1	1	1	2
klipspringer *	20	18	42	26	14	44	8	0	-12	4	-4	1	202	1	1	4
scrub hare *	20	36	6	9	49	45	9	1	2	-12	11	1	2	2	2	1
steenbok *	20	42	21	10	27	52	1	-4	5	-2	5	22	2	1	6	4
aardvark *	19	24	0	4	71	28	13	0	2	-15	15	1	NA	1	2	1
brown hyena	19	3	0	13	83	16	4	0	9	-13	13	1	NA	1	2	1
Cape gray mongoose *	19	46	26	22	6	68	17	-10	-8	1	9	1	1	1	1	3
Cape porcupine *	19	17	4	13	66	30	6	1	-7	0	-1	1	2	1	287	16
leopard	16	23	6	14	57	37	-7	-2	-8	17	-15	1	1	1	1	1
grey duiker *	15	44	26	8	22	52	6	-7	-1	2	6	2	1	4	6	3
grey rhebuck	15	39	24	6	31	45	14	-3	-4	-7	10	1	3	1	1	1
black-backed jackal *	14	51	14	7	28	58	15	-4	-2	-9	13	1	1	1	1	1
chacma baboon *	13	15	44	38	3	53	3	7	-10	0	-7	2	2	1	9	2
African wildcat	12	23	11	32	34	55	7	0	-5	-2	2	1	97	1	5	7
gemsbok *	12	29	20	20	31	49	8	2	-5	-5	3	1	3	1	1	4
greater kudu	11	32	20	12	36	44	10	-6	3	-7	13	1	1	1	1	1
Community	TRV'	LRV'					LAS'					I'				
24-h cycle	ρ_m	ϕ_d	ρ_e	ϕ_n	ρ	ρ_m	ϕ_d	ρ_e	ϕ_n	ρ	ρ_m	ϕ_d	ρ_e	ϕ_n	ρ	
c	15	34	17	18	31	52	8	4	-4	-8	4	1	1	1	3	
\bar{c} (equal weight)	15	34	19	21	26	60	8	-3	-5	0	3	1	1	1	11	4

Table 2.2: Seasonal shift in diel activity rhythm

All descriptive statistics, provided above for 25 mammal species in the Little Karoo, were calculated after annual daylength standardisation of the data (t'). * is showing next to the names of species with a significant seasonal change ($P'_{,s} < 0.05$). $TRV'_{,s}$ represents the total rhythm variation of species s between winter and summer, which also consists of the percentage of diel activity rhythm that shifted between the two seasons. Time of day was divided into four θ time periods: ρ_m , ϕ_d , ρ_e and ϕ_n ($\rho = \rho_m + \rho_e$, showing in italic). $LRV'_{,s}(\theta)$ provides the local rhythm variation of species s during time period θ , which consists of the percentage of $TRV'_{,s}$ explained during θ . Divided by the number of hours in θ , the local rhythm variation highlighted the daily time period that explained most of the $TRV'_{,s}$ per hour, for species s ; it was shaded in gray. $LAS'_{,s}(\theta)$ represents the local activity shift of species s during time period θ , which consists of the resulting shift in daily activity proportions allocated by species s throughout θ . All substantial increases ($> 2\%$) of the proportions of daily activity in summer, were highlighted in orange, whereas all substantial decreases ($< -2\%$) were highlighted in blue. Finally, $I'_{,s}(\theta)$ represents the compensation index of species s during time period θ , which equaled 1 when $LRV'_{,s}(\theta)$ was entirely converted into a shift in activity. However, when compensation effects (activity increases compensated by activity decreases throughout θ) occurred, $I'_{,s}(\theta)$ took values greater than one. When a species showed no activity during θ in both seasons, the associated $LRV'_{,s}(\theta)$ and $LAS'_{,s}(\theta)$ equaled 0, and $I'_{,s}(\theta)$ returned NA. TRV' , LRV' , LAS' and I' apply similarly to the mammal community c and \bar{c} as a whole.

Reading example: 54% of rock hyrax's diel activity rhythm shifted between winter and summer. Most of the shift took place during ρ_m (40%) and ϕ_d (53%) periods of the 24-hour cycle. In summer, rock hyrax increased by 45% the proportion of its daily activity allocated to ρ_m , whereas it decreased by 49% the proportion of its daily activity allocated to ϕ_d . The seasonal shift in activity primarily went from ϕ_d to ρ_m . For Cape porcupine, 66% of the seasonal shift took place during ϕ_n . However, the resulting activity shift during ϕ_n was close to 0%, which was highlighted by $I'_{,s}(\phi_n) = 287$, meaning that throughout ϕ_n , the activity increases were compensated by symmetric activity decreases. Most of the total rhythm variation of the caracal took place during ϕ_n (40%). However, during ρ_e , the extent of rhythm variation explained per hour, was greater and shaded in gray.

Table 2.3: Summary

For 25 mammal species in the Little Karoo: $O_{,s}$ and $O'_{,s}$ (built with t and t') are the overlap coefficients between winter and summer diel activity rhythms; $P_{,s}$ and $P'_{,s}$ are the associated bootstrapped p-values and * indicates a significant seasonal change (< 0.05); Ph indicates photoperiodism alignment and F indicates the influence of other factors.

Species	$O'_{,s} - O_{,s}$	$P_{,s}$	$P'_{,s}$	Ph	F
African wildcat	+	*		x	
Cape mountain zebra	+	*		x	
greater kudu	+	*		x	
leopard	+	*		x	
aardwolf	=	*	*		x
black backed jackal	+	*	*	(x)	x
Cape gray mongoose	+	*	*	(x)	x
Cape porcupine	+	*	*	(x)	x
caracal	+	*	*	(x)	x
chacma baboon	+	*	*	(x)	x
eland	+	*	*	(x)	x
gemsbok	+	*	*	(x)	x
grey duiker	+	*	*	(x)	x
Hewitts red rock rabbit	+	*	*	(x)	x
honey badger	+	*	*	(x)	x
klipspringer	+	*	*	(x)	x
rock hyrax	+	*	*	(x)	x
scrub hare	-	*	*		x
steenbok	+	*	*	(x)	x
aardvark	-		*		
Cape hare	-		*		
red hartebeest	-		*		
brown hyena	+			(x)	
grey rhebuck	+			(x)	
springbok	+			(x)	

2.7 Figures

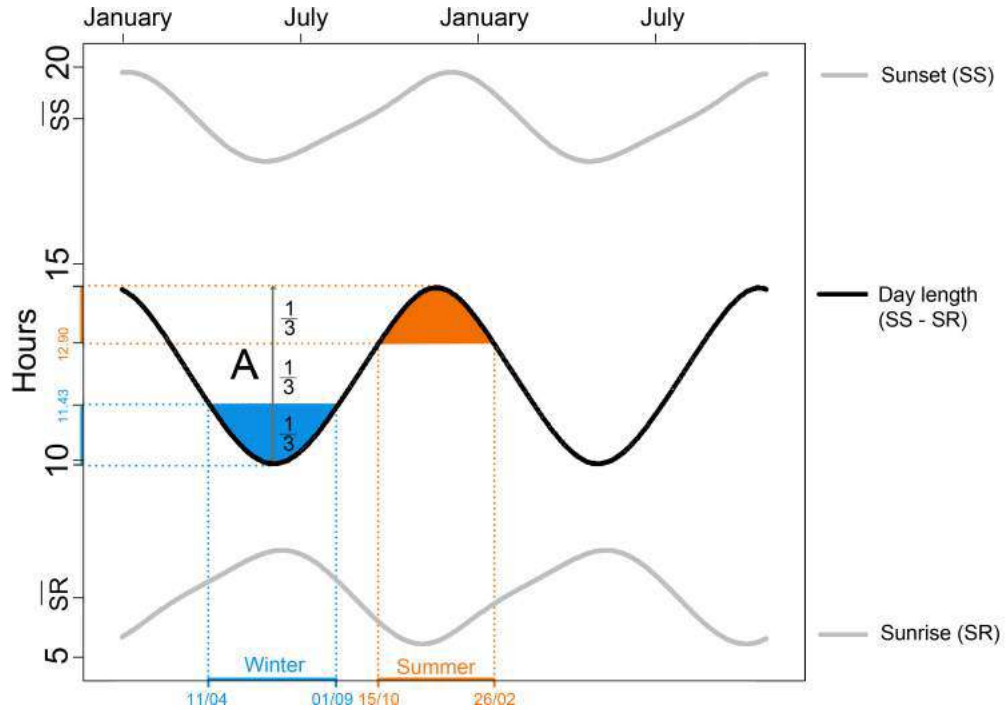


Figure 2.1: Daylength oscillations throughout the year, in the Little Karoo. Winter is defined as the period of the year with daylength D_l varying within the bottom third of its annual range A ($D_l < 11.43$), and summer as the period of the year with daylength varying within the top third ($D_l > 12.90$). Consequently, winter starts on 11 April and ends on 01 September, whereas summer starts on 15 October and ends on 26 February.

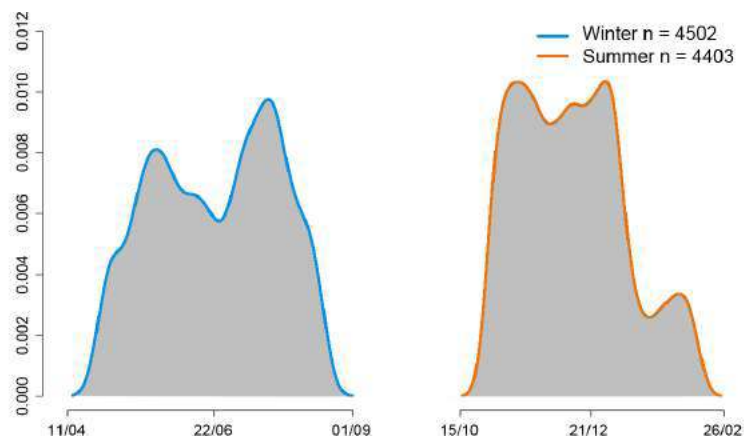


Figure 2.2: Data collection in winter and summer

The graph shows the distributions of the number of photo-captures collected in winter and in summer, in the Little Karoo.

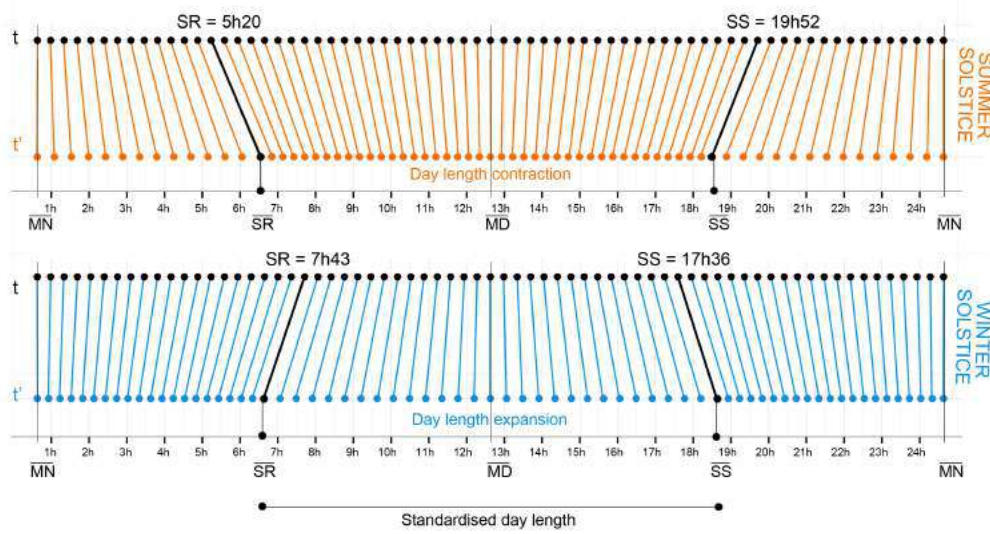
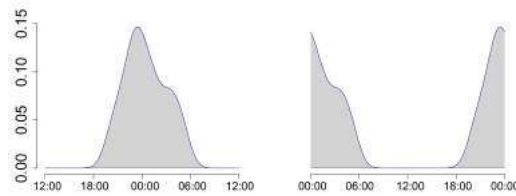
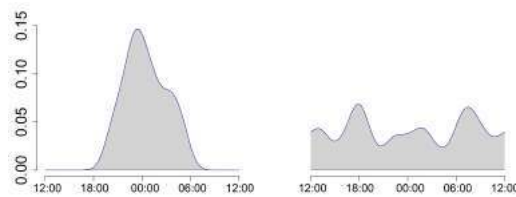


Figure 2.3: Daylength standardisation (t')
 Pre-processing of t on the days of the southern winter and summer solstices. In summer and winter, the time variable t gets distorted in opposite ways, resulting into a standardisation of daylength to 12 hours, throughout the year. Independently on the date T of the year (except on the days of the equinoxes), the adjustment ($|t' - t|$) is always greatest at sunrise ($t = SR$) and at sunset ($t = SS$).



(a) Effect of time origin: midnight vs noon



(b) Unimodal and symmetric distribution assumptions

Figure 2.4: The problems of circular data

(a) The aardvark diel activity rhythm appears either as a unimodal or a U-shaped distribution, whether the display is centred around midnight or around noon. (b) The aardvark diel activity rhythm (left density function) follows a unimodal and symmetric circular distribution, contrarily to the multimodal diel activity rhythm of the greater kudu (right density function).

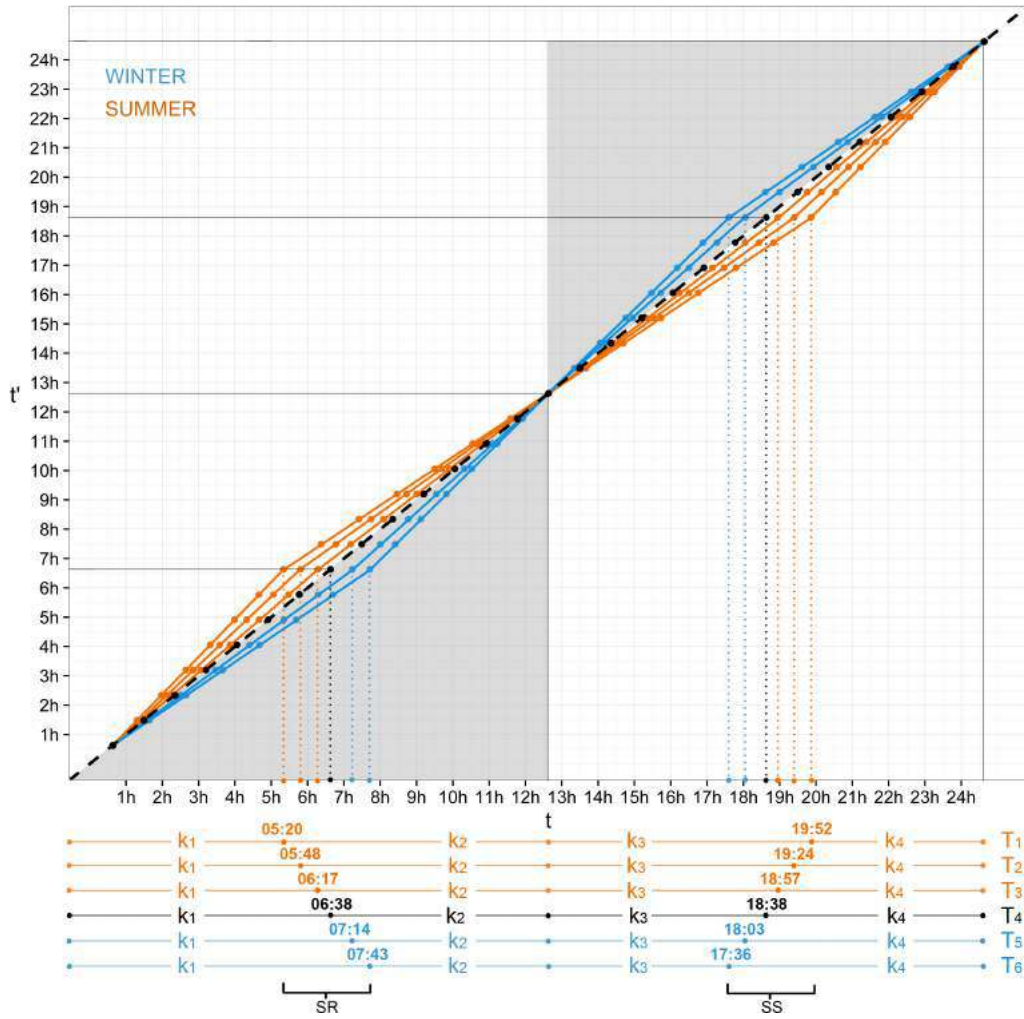


Figure 2.5: Pre-processing function $f: t' = f(t, T)$

The graph shows the pre-processing of the time variable t , on six different days of the year (T), including on the vernal and fall equinoxes (T_4) as well as on the southern winter (T_6) and summer (T_1) solstices. f is defined by four equations with domain of definition depending on sunrise (SR) and sunset (SS) times, the latter depending themselves on T . On the days of the equinoxes ($SR = \overline{SR}$ and $SS = \overline{SS}$), therefore no adjustment was computed ($t' = t$, black line). During winter mornings ($SR > \overline{SR}$), t was then adjusted to lower values ($t' < t$, blue lines), and during winter afternoons ($SS < \overline{SS}$), t was adjusted to greater values ($t' > t$, blue lines), resulting into an expansion of daylength (grey area). The opposite distortion took place in summer (orange lines), resulting into a contraction of daylength (white area).

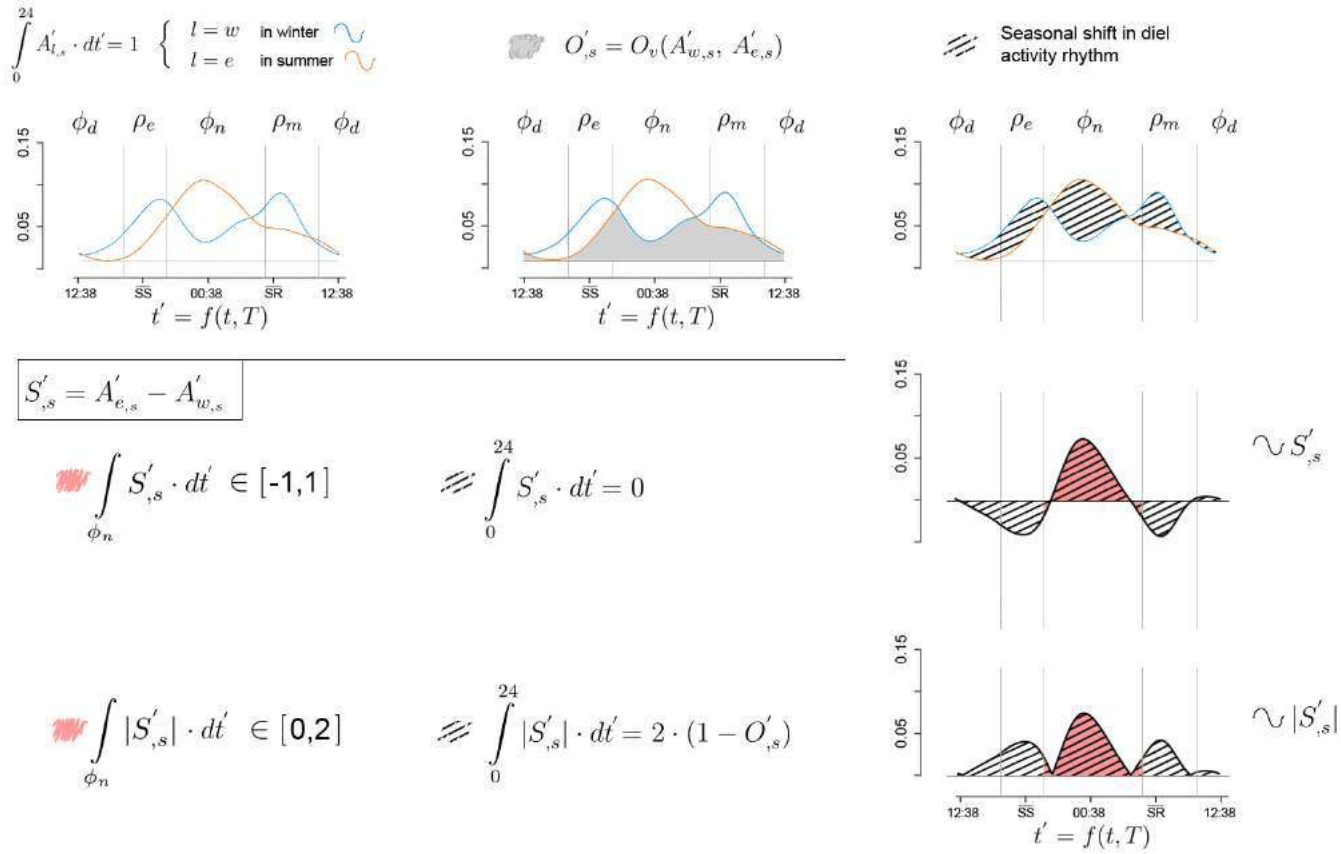
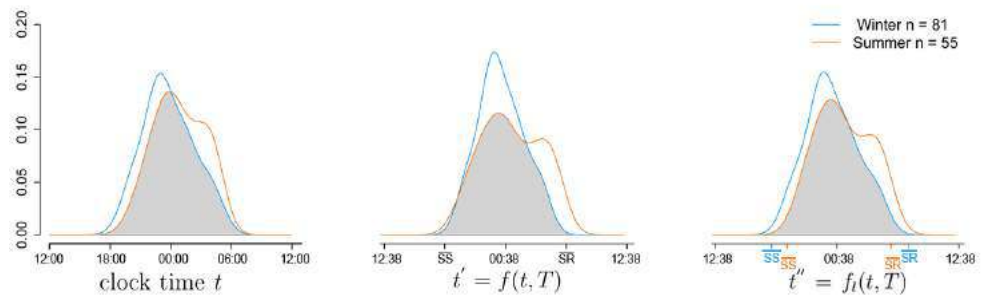
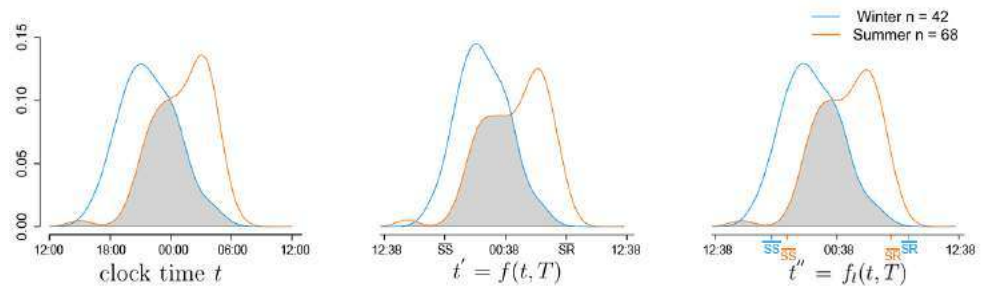


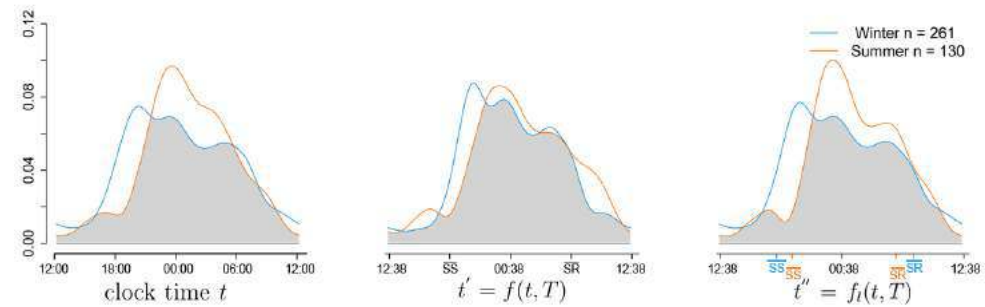
Figure 2.6: Mathematical relationships between $A'_{l,s}$, O'_{s} and $S'_{,s}$. $A'_{e,s}$ and $A'_{w,s}$ are the probability density functions representing the diel activity rhythms of species s in summer and winter. O'_{s} represents the area of overlap between the two probability density functions. Both $S'_{,s}$ and $|S'_{,s}|$ provide insights into the seasonal shift in diel activity rhythm of species s between summer and winter. $|S'_{,s}|$ illustrates the extent of the rhythm variation between summer and winter, whereas $S'_{,s}$ illustrates the resulting activity shift.



(a) Aardvark, midnight-centred diel activity rhythm



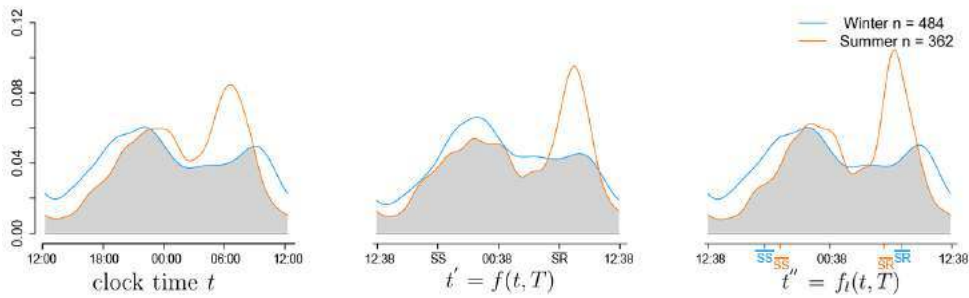
(b) Aardwolf, midnight-centred diel activity rhythm



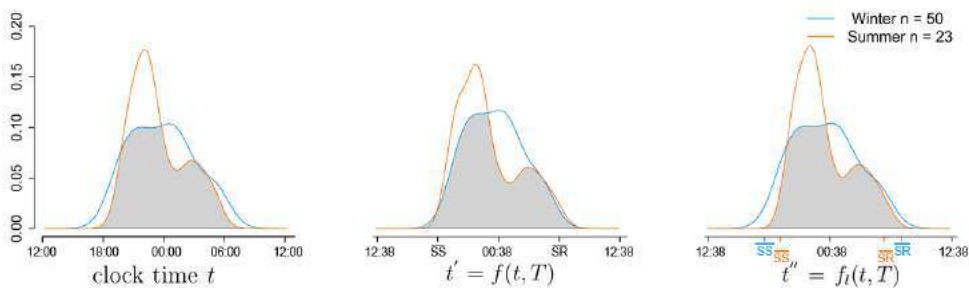
(c) African wildcat, midnight-centred diel activity rhythm

Figure 2.7: Species seasonal diel activity rhythms

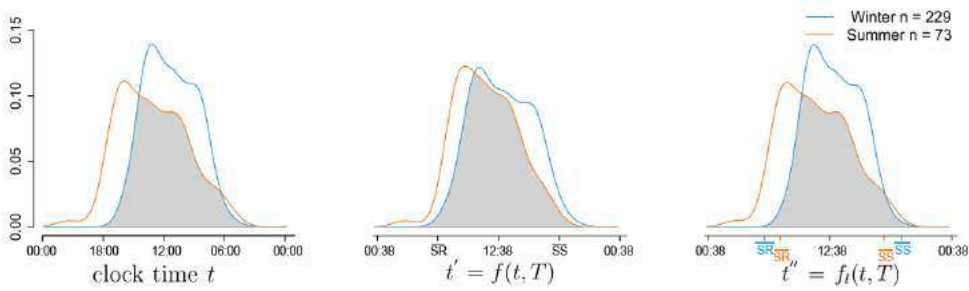
Winter and summer diel activity rhythms are displayed for 25 mammal species s in the Little Karoo, using three different time metrics: traditional 24-hour human clock-time t and two ecological times with standardised sunrise and sunset times t' and t'' . The grey areas show the overlap between the two probability density functions in each plot, for summer and winter.



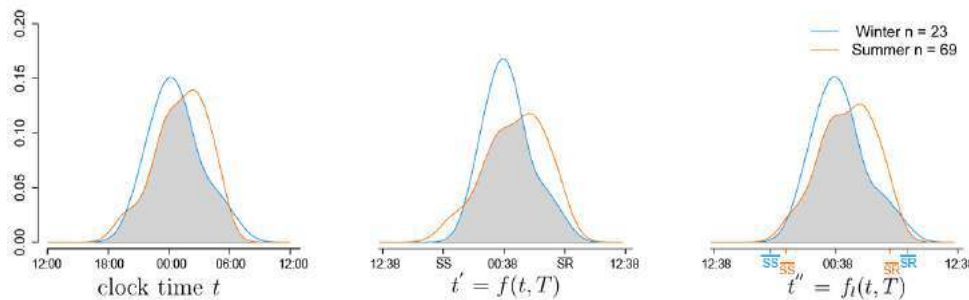
(d) black-backed jackal, midnight-centred diel activity rhythm



(e) Brown hyena, midnight-centred diel activity rhythm



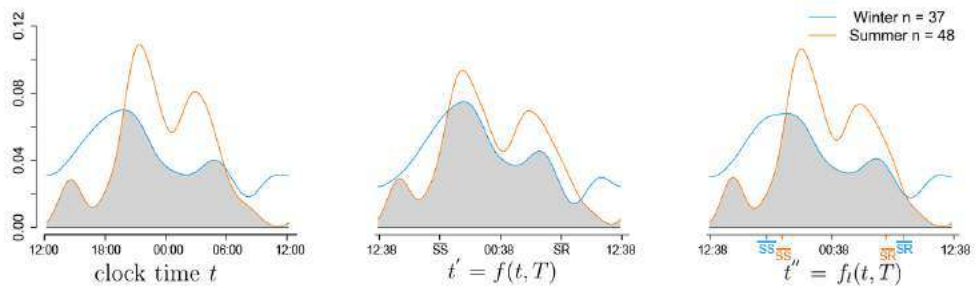
(f) Cape gray mongoose, noon-centred diel activity rhythm



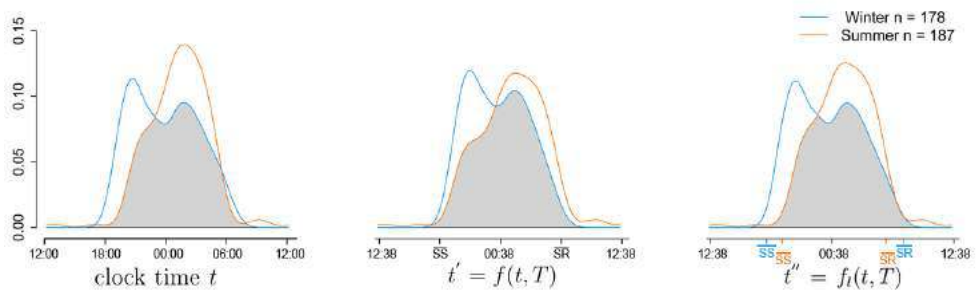
(g) Cape hare, midnight-centred diel activity rhythm

Figure 2.7: Seasonal shift in diel activity rhythms (continued)

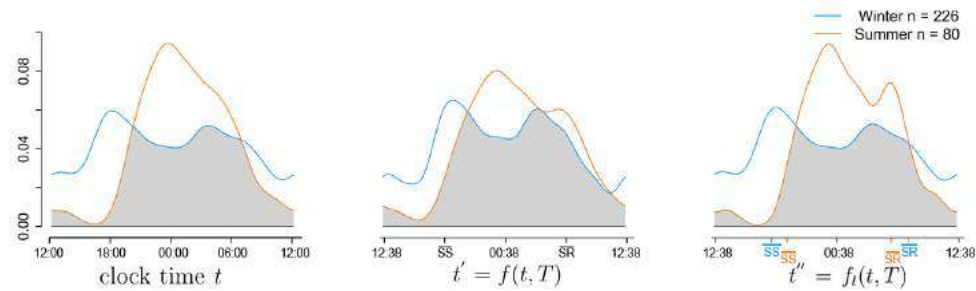
A full caption is provided on p74.



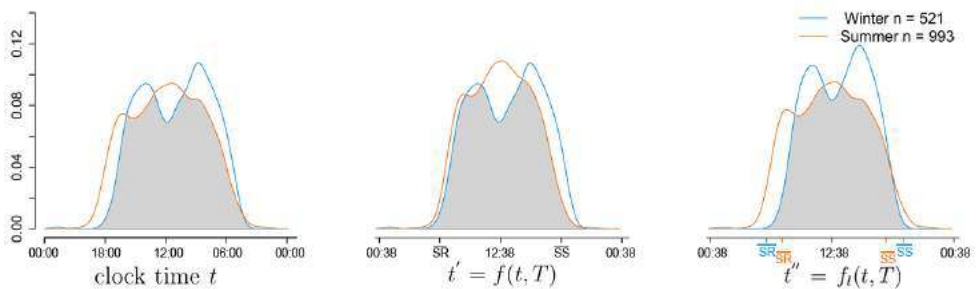
(h) Cape mountain zebra, midnight-centred diel activity rhythm



(i) Cape porcupine, midnight-centred diel activity rhythm

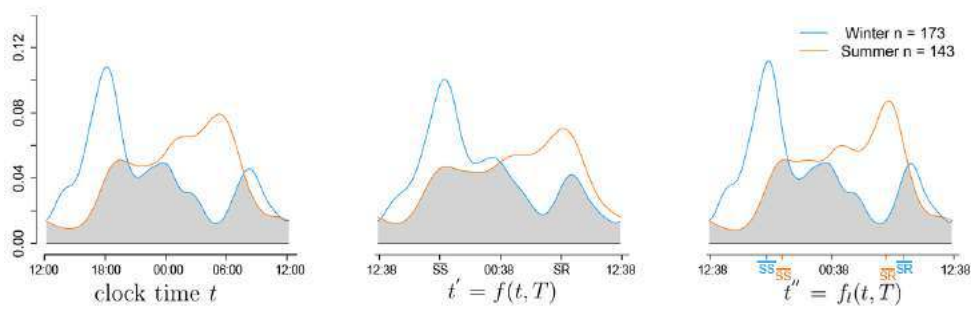


(j) Caracal, midnight-centred diel activity rhythm

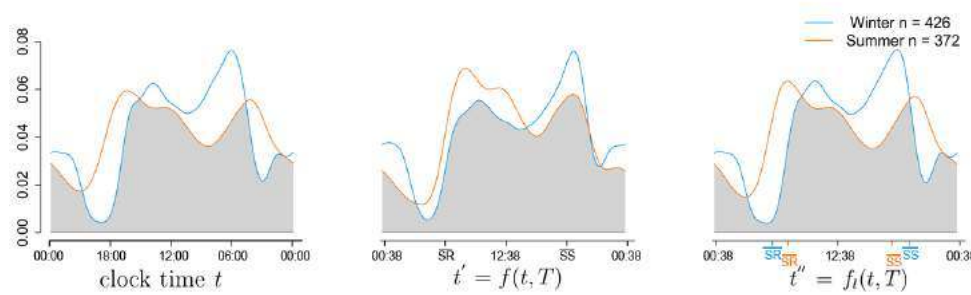


(k) Chacma baboon, noon-centred diel activity rhythm

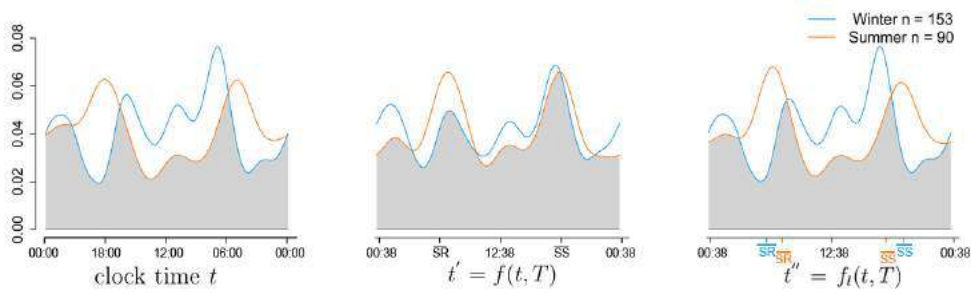
Figure 2.7: Seasonal shift in diel activity rhythms (continued)
 A full caption is provided on p74.



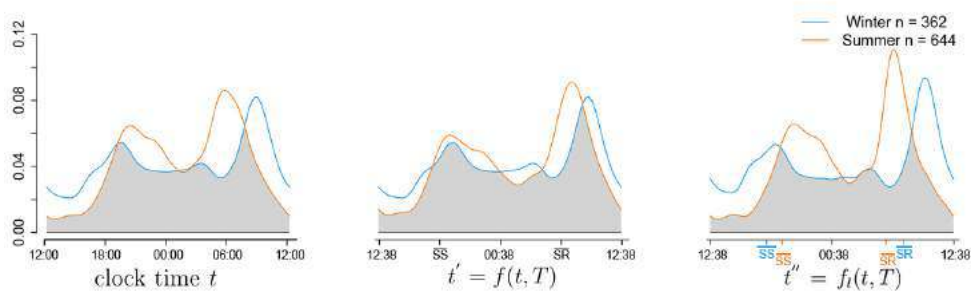
(l) Eland, midnight-centred diel activity rhythm



(m) Gemsbok, noon-centred diel activity rhythm



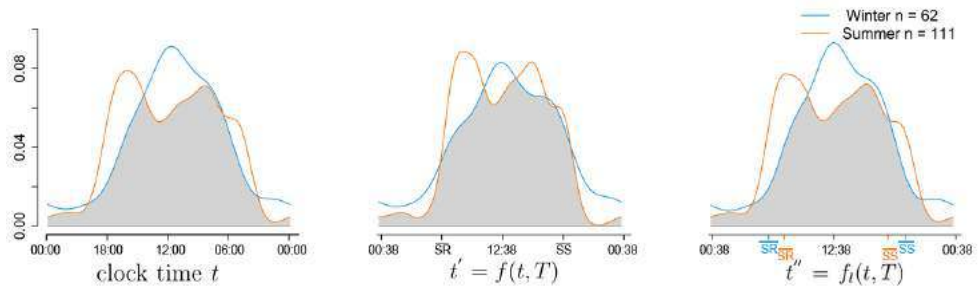
(n) Greater kudu, noon-centred diel activity rhythm



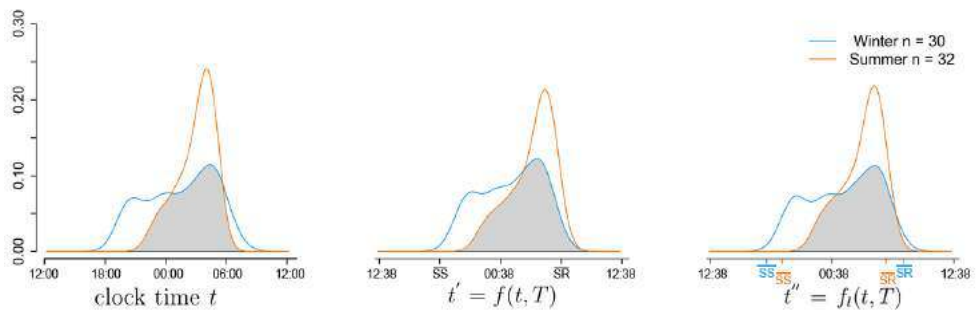
(o) Grey duiker, midnight-centred diel activity rhythm

Figure 2.7: Seasonal shift in diel activity rhythms (continued)

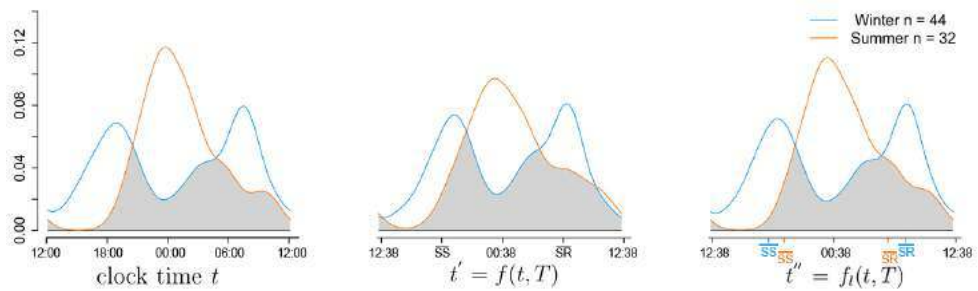
A full caption is provided on p74.



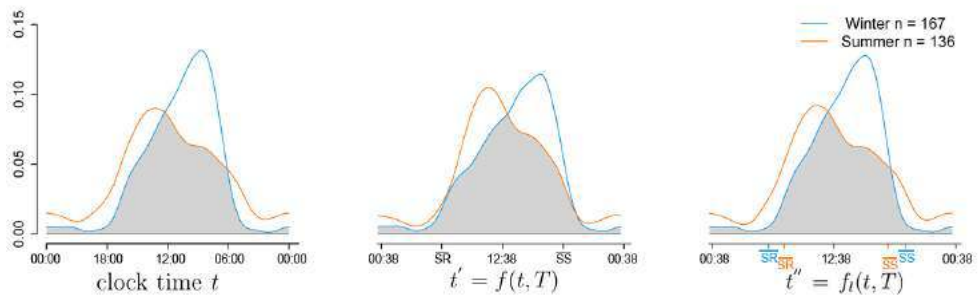
(p) Grey rhebuck, noon-centred diel activity rhythm



(q) Hewitt's red rock rabbit, midnight-centred diel activity rhythm

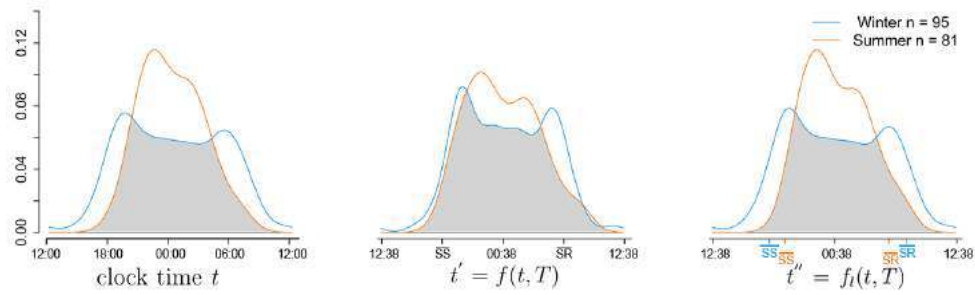


(r) Honey badger, midnight-centred diel activity rhythm

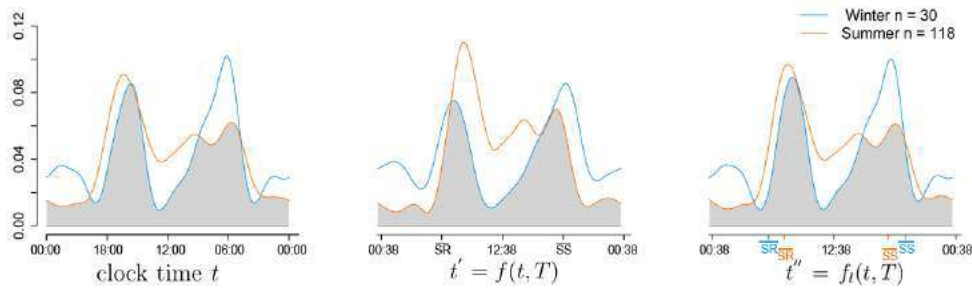


(s) Klipspringer, noon-centred diel activity rhythm

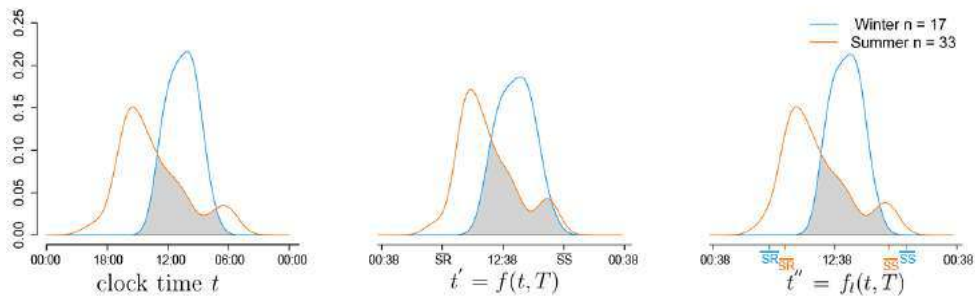
Figure 2.7: Seasonal shift in diel activity rhythms (continued)
A full caption is provided on p74.



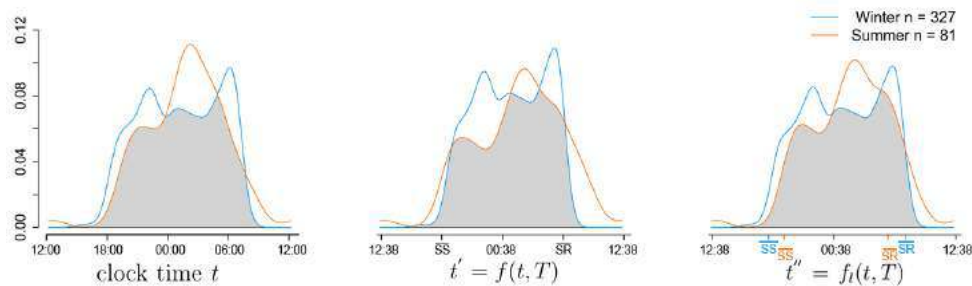
(t) Leopard, midnight-centred diel activity rhythm



(u) Red hartebeest, noon-centred diel activity rhythm



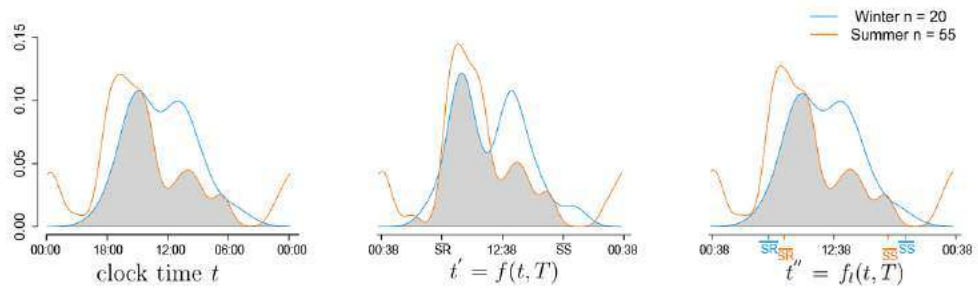
(v) Rock hyrax, noon-centred diel activity rhythm



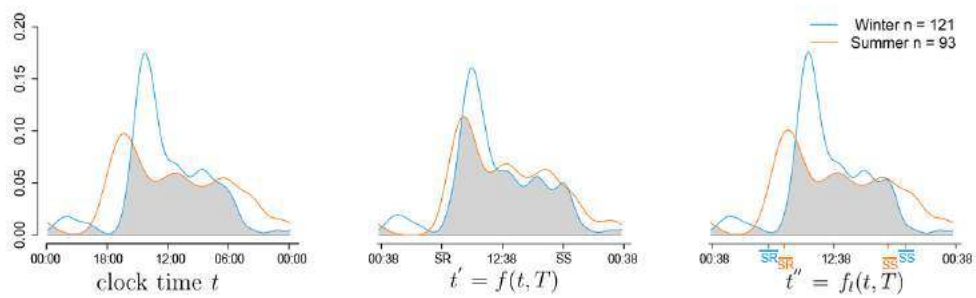
(w) Scrub hare, midnight-centred diel activity rhythm

Figure 2.7: Seasonal shift in diel activity rhythms (continued)

A full caption is provided on p74.

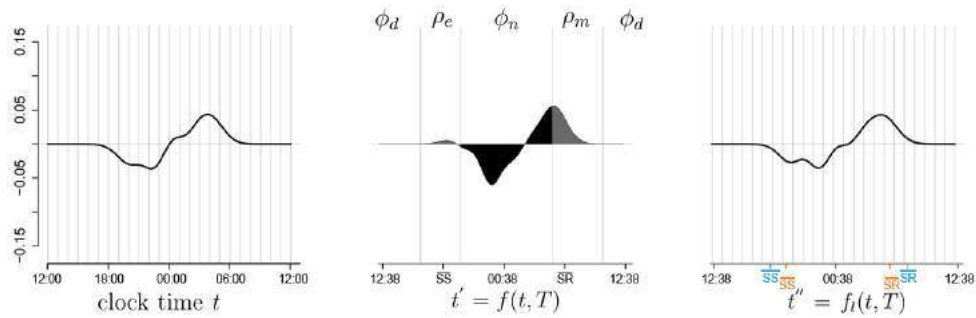


(x) Springbok, noon-centred diel activity rhythm

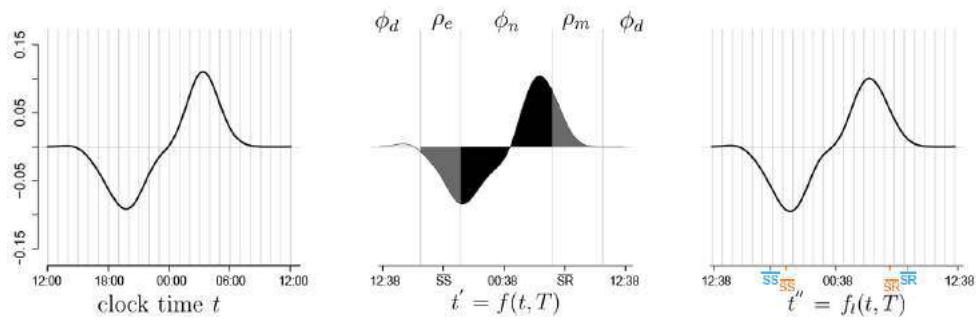


(y) Steenbok, noon-centred diel activity rhythm

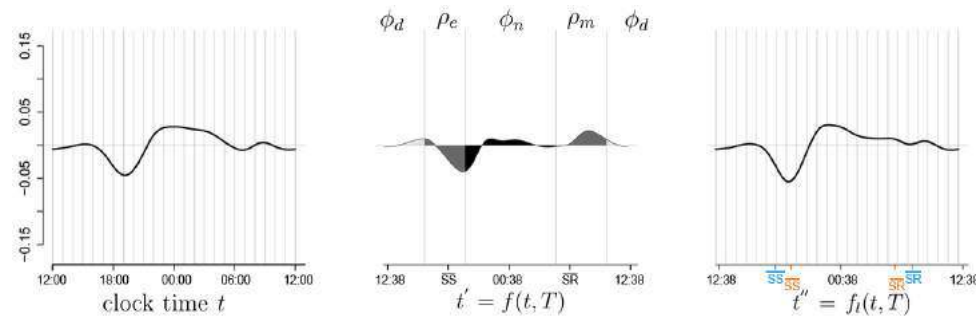
Figure 2.7: Seasonal shift in diel activity rhythms (continued)
 A full caption is provided on p74.



(a) Aardvark, midnight-centred diel activity rhythm



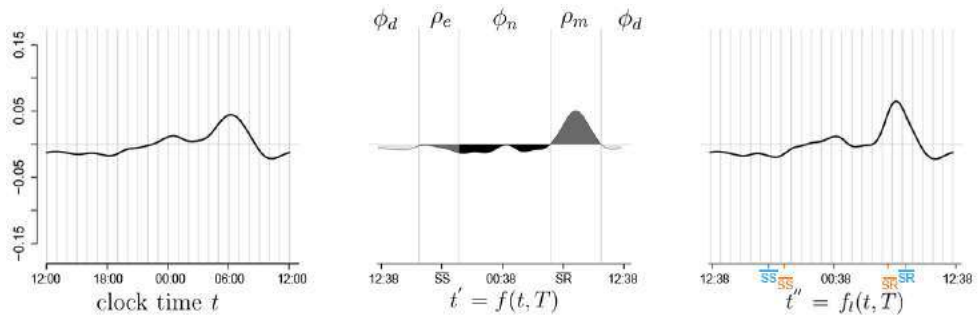
(b) Aardwolf, midnight-centred diel activity rhythm



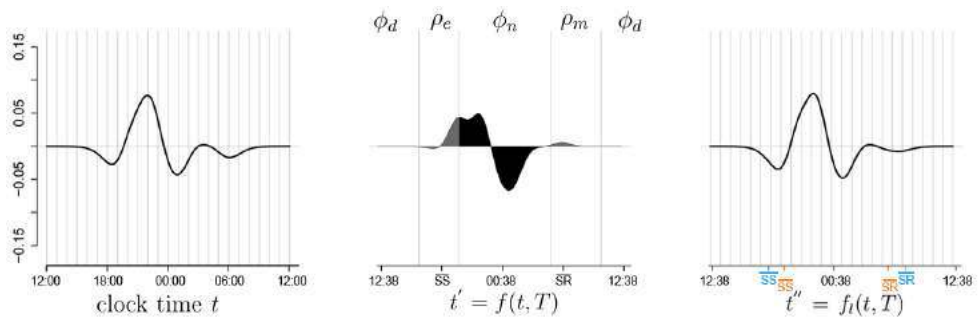
(c) African wildcat, midnight-centred diel activity rhythm

Figure 2.8: Seasonal shift in diel activity rhythms: summer – winter

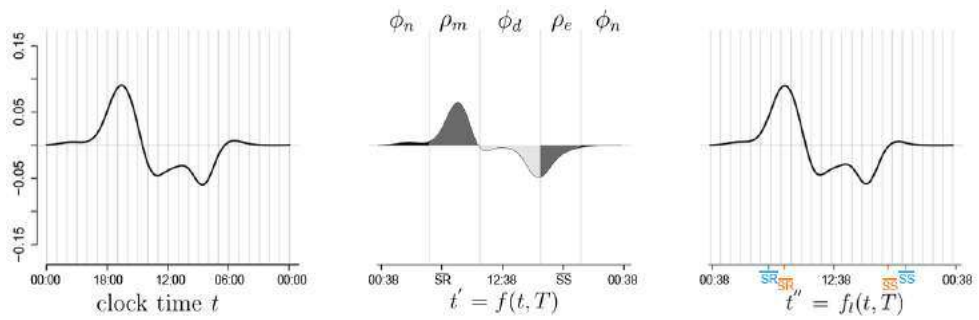
The seasonal change in diel activity rhythms between summer and winter is quantified for 25 mammal species s in the Little Karoo, and in the three different time metrics: traditional 24-hour human clock-time t and two ecological times with standardised sunrise and sunset times t' and t'' . The functions $S_{s,t}$, $S'_{s,t}$ and $S''_{s,t}$ are positive when the proportion of daily activity is higher in summer than in winter; vice versa for negative values.



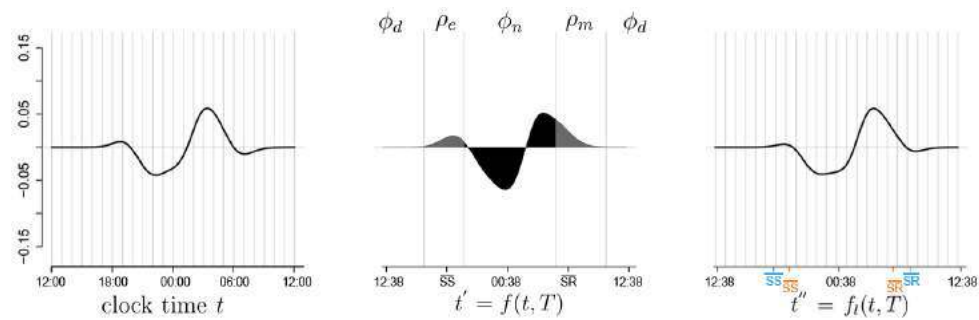
(d) black-backed jackal, midnight-centred diel activity rhythm



(e) Brown hyena, midnight-centred diel activity rhythm



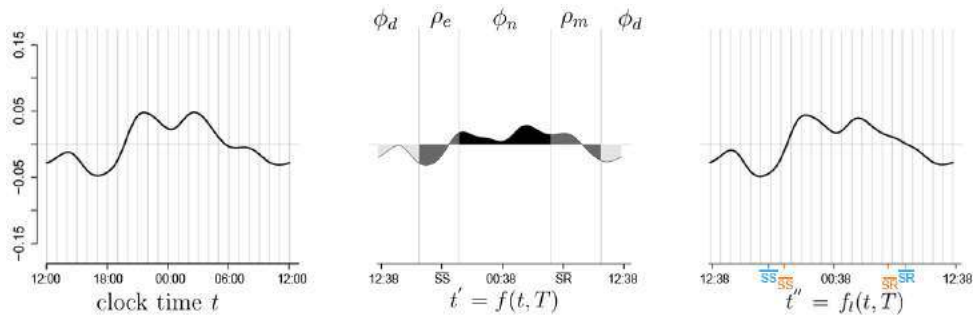
(f) Cape gray mongoose, noon-centred diel activity rhythm



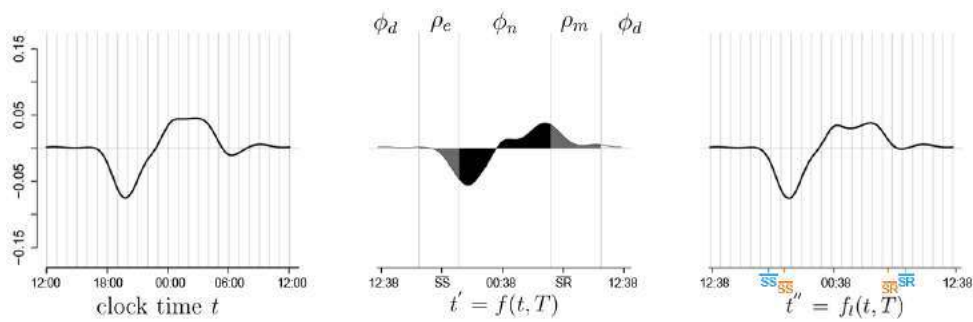
(g) Cape hare, midnight-centred diel activity rhythm

Figure 2.8: Seasonal shift in diel activity rhythms: summer – winter (continued)

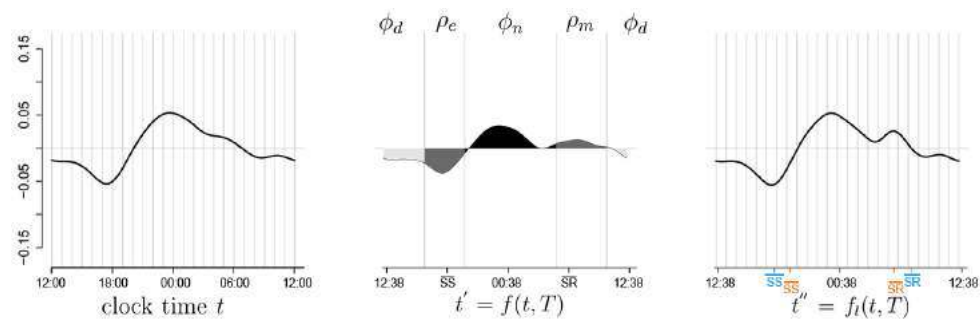
A full caption is provided on p81.



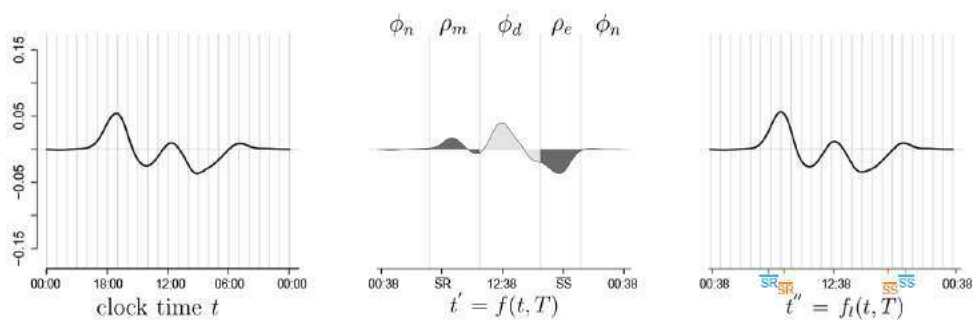
(h) Cape mountain zebra, midnight-centred diel activity rhythm



(i) Cape porcupine, midnight-centred diel activity rhythm



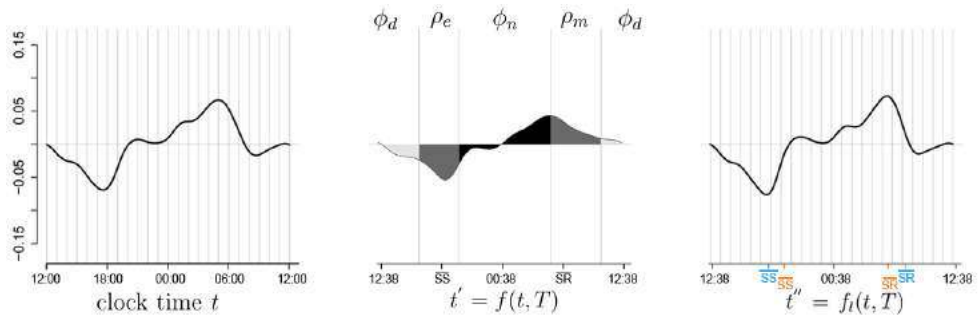
(j) Caracal, midnight-centred diel activity rhythm



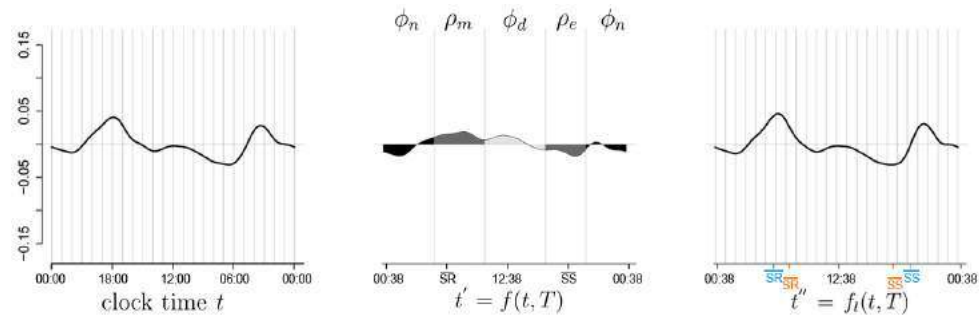
(k) Chacma baboon, noon-centred diel activity rhythm

Figure 2.8: Seasonal shift in diel activity rhythms: summer – winter (continued)

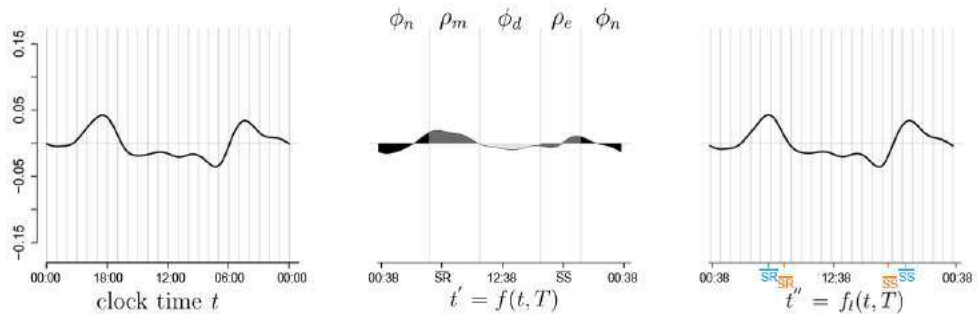
A full caption is provided on p81.



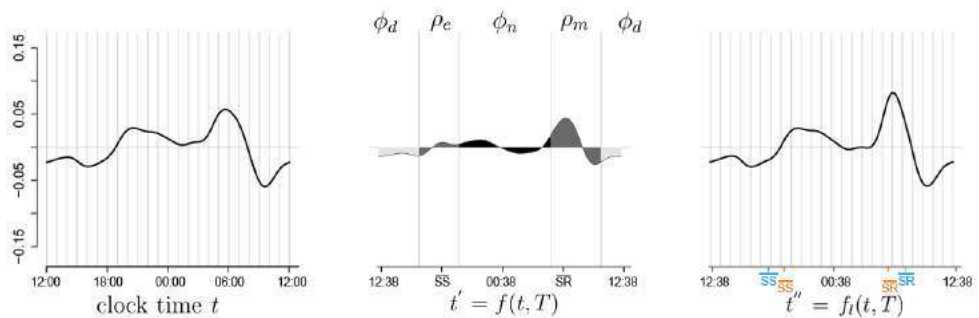
(l) Eland, midnight-centred diel activity rhythm



(m) Gemsbok, noon-centred diel activity rhythm



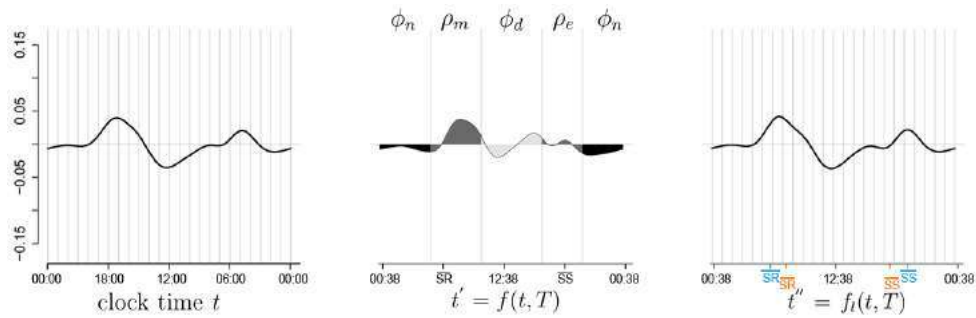
(n) Greater kudu, noon-centred diel activity rhythm



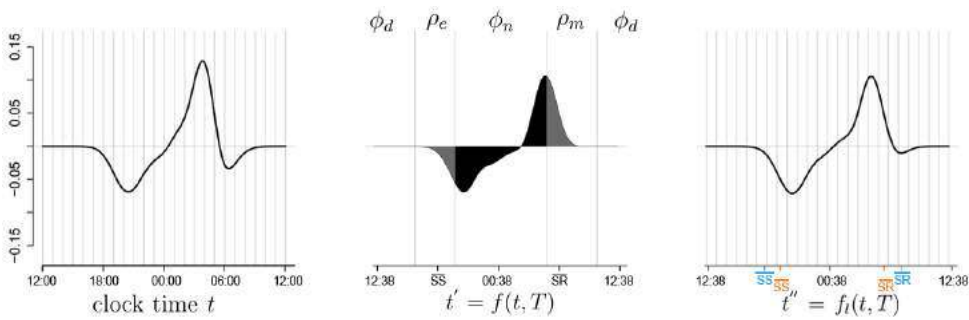
(o) Grey duiker, midnight-centred diel activity rhythm

Figure 2.8: Seasonal shift in diel activity rhythms: summer – winter (continued)

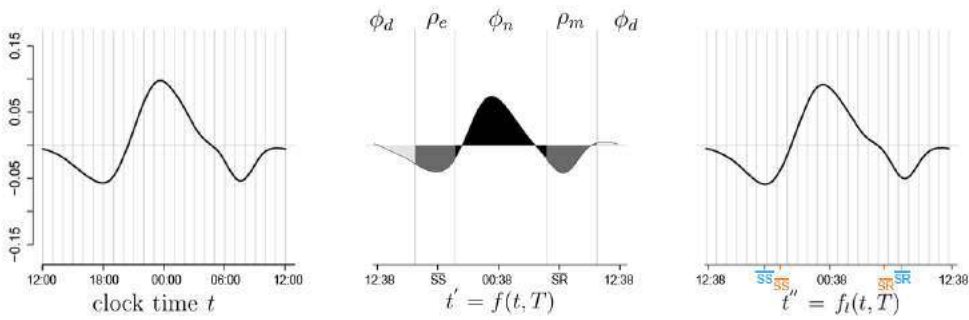
A full caption is provided on p81.



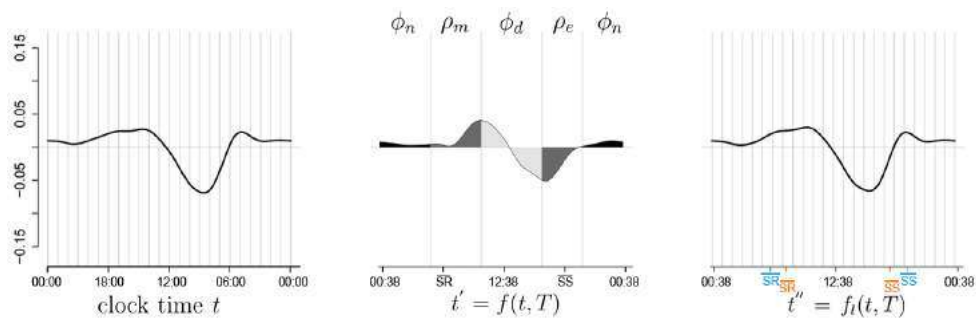
(p) Grey rhebuck, noon-centred diel activity rhythm



(q) Hewitt's red rock rabbit, midnight-centred diel activity rhythm



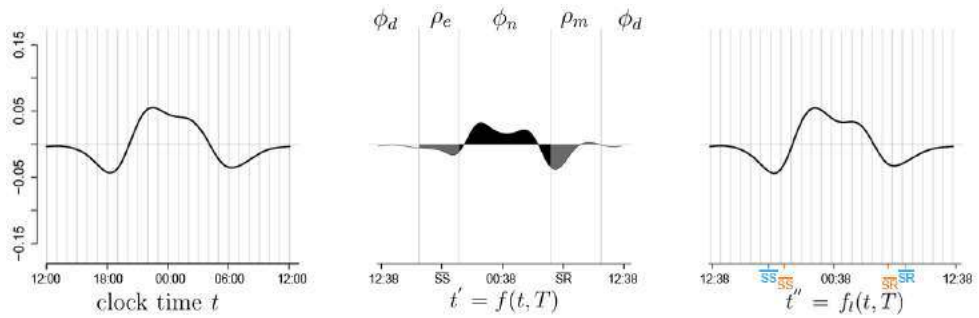
(r) Honey badger, midnight-centred diel activity rhythm



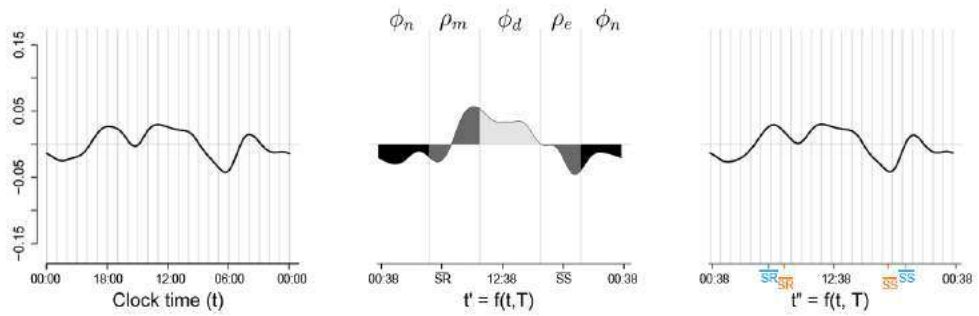
(s) Klipspringer, noon-centred diel activity rhythm

Figure 2.8: Seasonal shift in diel activity rhythms: summer – winter (continued)

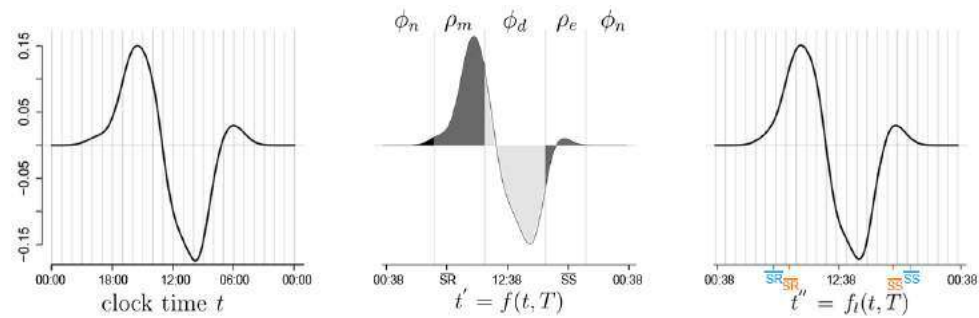
A full caption is provided on p81.



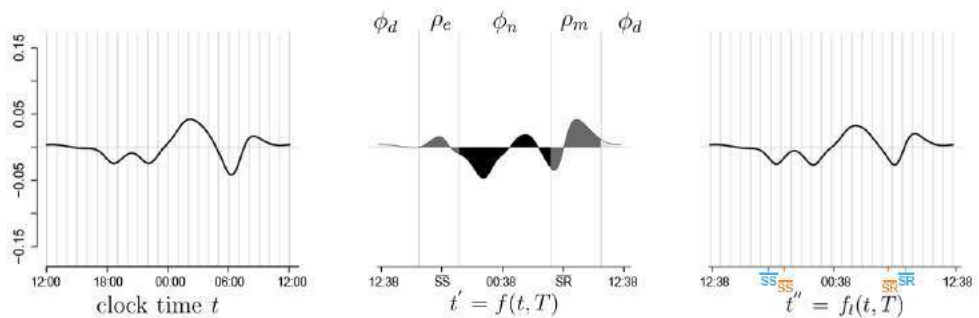
(t) Leopard, midnight-centred diel activity rhythm



(u) Red hartebeest, noon-centred diel activity rhythm



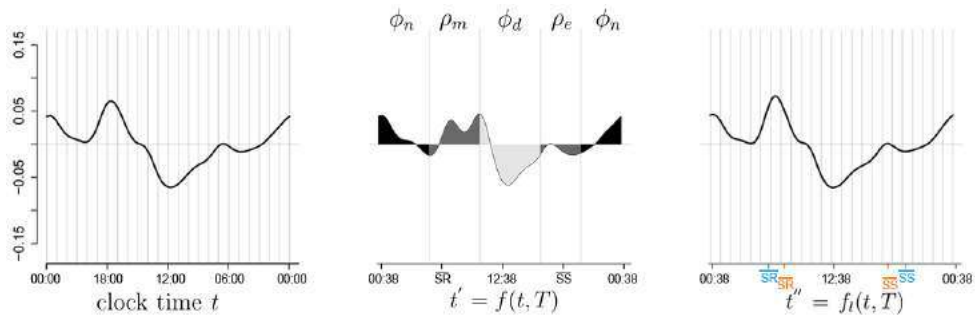
(v) Rock hyrax, noon-centred diel activity rhythm



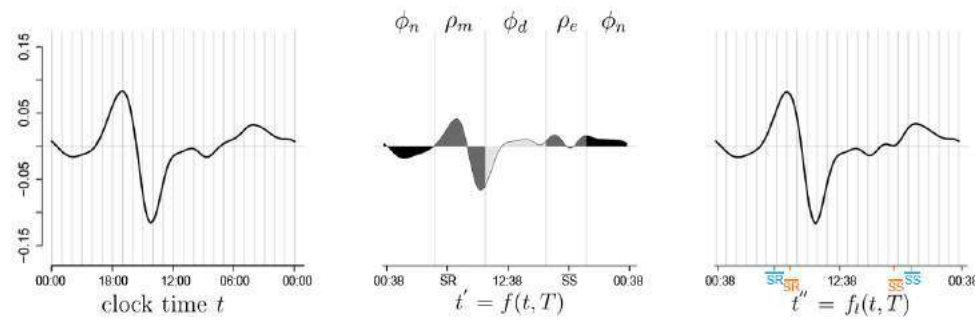
(w) Scrub hare, midnight-centred diel activity rhythm

Figure 2.8: Seasonal shift in diel activity rhythms: summer – winter (continued)

A full caption is provided on p81.



(x) Springbok, noon-centred diel activity rhythm



(y) Steenbok, noon-centred diel activity rhythm

Figure 2.8: Seasonal shift in diel activity rhythms: summer – winter
(continued)

A full caption is provided on p81.

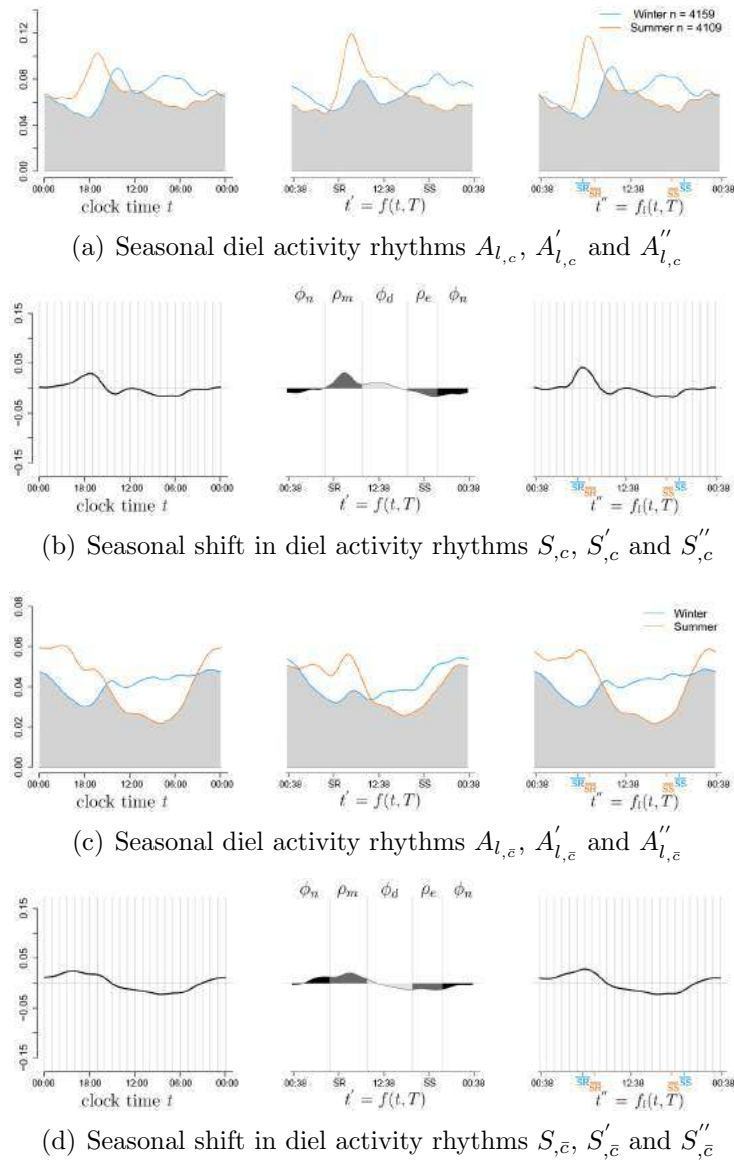


Figure 2.9: Seasonal shift in diel activity rhythms of the mammal community

Winter and summer diel activity rhythms of the mammal community in the Little Karoo are displayed in (a) and (c), using three different time metrics: traditional 24-hour human clock-time t and two ecological times with standardised sunrise and sunset times t' and t'' ; the grey area being the overlap between the two probability density functions. In (a) the density functions were built using the raw camera trap data collected for the mammal community c : 4159 photo-captures in winter and 4208 photo-captures in summer. In (c) the density functions were built after attributing the same weight to every species s of the community c , independently of its photo-capture frequency.

The seasonal shifts in diel activity rhythms of the mammal community, between summer and winter, were quantified in the three different time metrics, as well as before (c) and after (e) equalising every species weight to build the community diel activity rhythms (displayed in (b) and (d)). Functions $S_{c,c}$, $S'_{c,c}$ and $S''_{c,c}$, as well as $S_{\bar{c},\bar{c}}$, $S'_{\bar{c},\bar{c}}$ and $S''_{\bar{c},\bar{c}}$, were positive when the proportion of daily activity was higher in summer than in winter; vice versa for negative values.

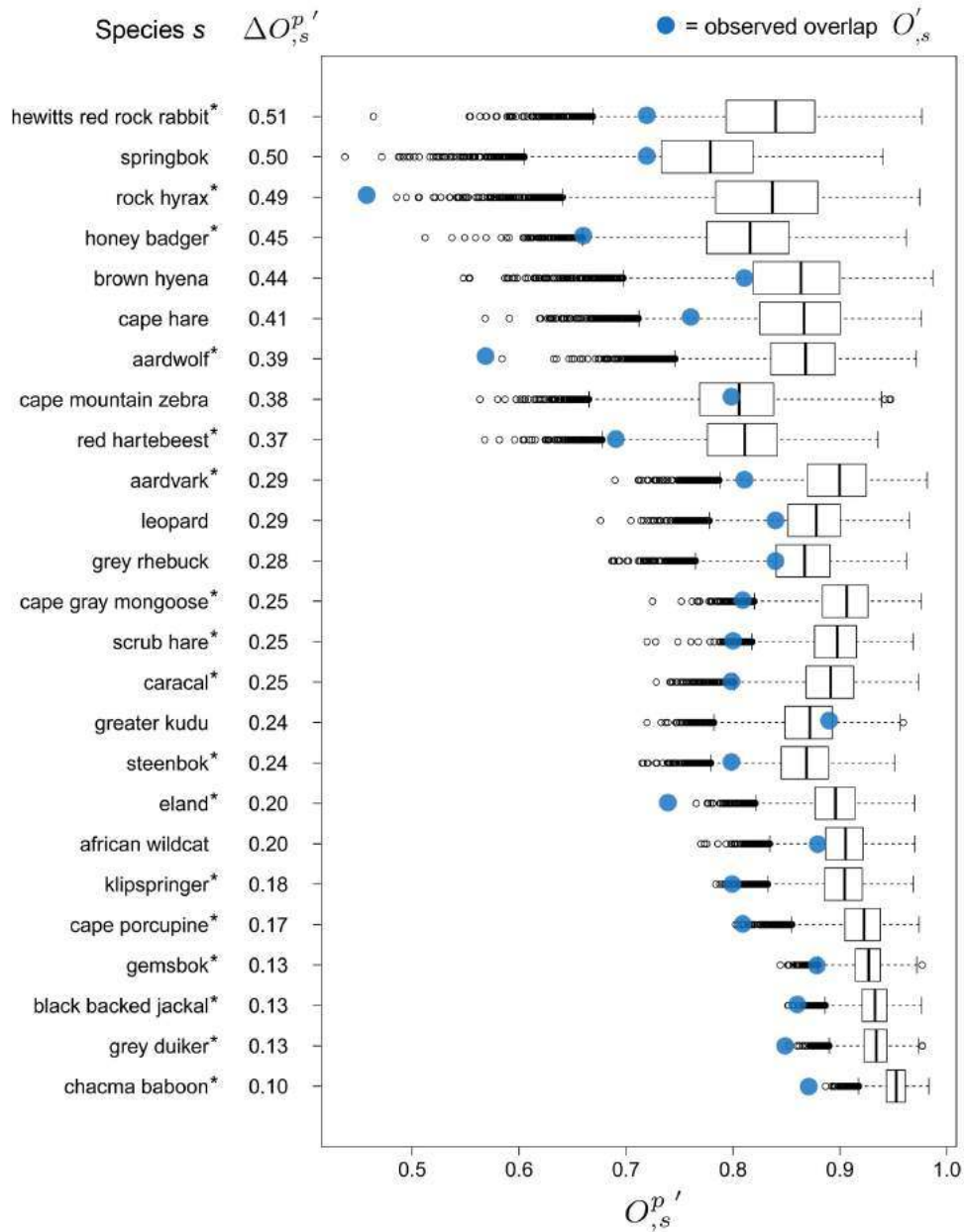


Figure 2.10: Bootstrap boxplots for each of the 25 species in the Little Karoo. Boxplots summarise the structure of the 25 $O_{s,s}^{p'}$ variables, each being defined as the overlap coefficient calculated between two diel activity rhythms of species s , built with two data samples randomly selected from the original dataset collected for species s . The bootstrap analysis used $r = 10,000$ permutations p , producing 10,000 $O_{s,s}^{p'}$ values [Chapter 2 section 2.3.3.3]. The 25 species were sorted in descending order with respect to the degree of dispersion (spread) of $O_{s,s}^{p'}$, which was quantified by $\Delta O_{s,s}^{p'}$, and which represents the versatility of the diel activity rhythm of species s , throughout a 365-day cycle. The second and third quartiles of the $O_{s,s}^{p'}$ variable, are represented by the box, the median being the vertical line within the box. The blue points represent the observed value of $O_{s,s}^{p'}$ calculated between the diel activity rhythms of species s in summer and in winter. * is showing next to the names of species with a significant seasonal change ($P'_{s} < 0.05$).

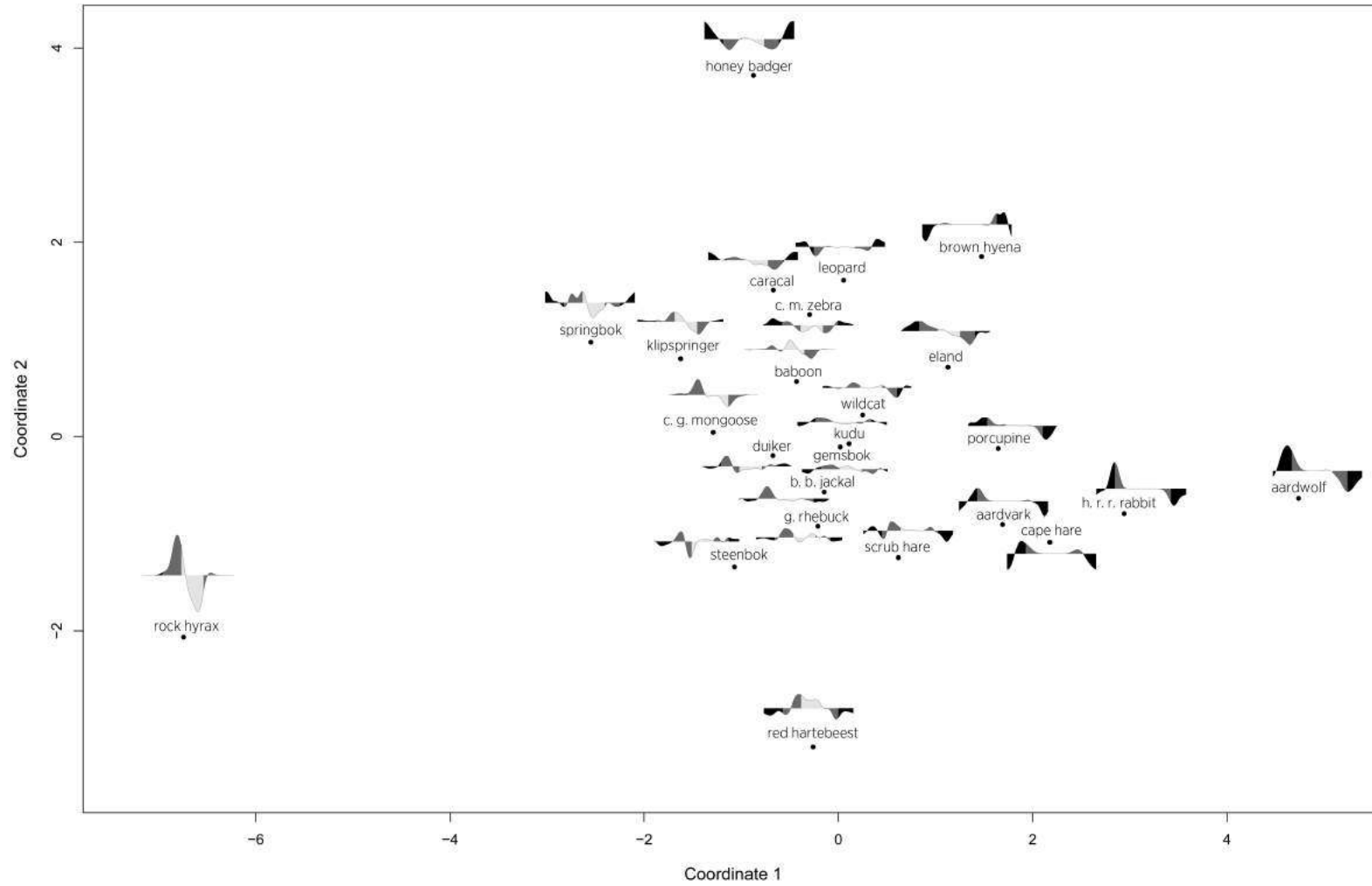


Figure 2.11: Non-metric Multi-Dimensional Scaling

NMDS plot summarising the dissimilarity data between the $S'_{s'}$ -curves. These curves are those of the middle column of Fig. 2.8, but are all midday centred. They illustrate the seasonal shift in diel activity rhythm of 25 mammal species s of the Little Karoo, between summer and winter.

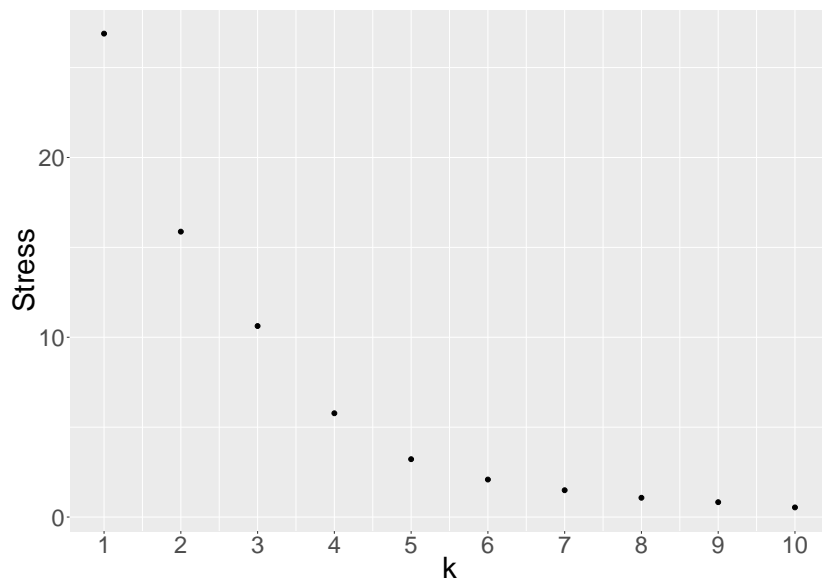


Figure 2.12: Stress values in relation to the number of dimensions k

The measure of lack of fit in NMDS is known as the 'stress' of the configuration. Non-zero stress values occur with insufficient dimensionality, and as the number of dimensions increases, the stress value will either decrease or remain stable.

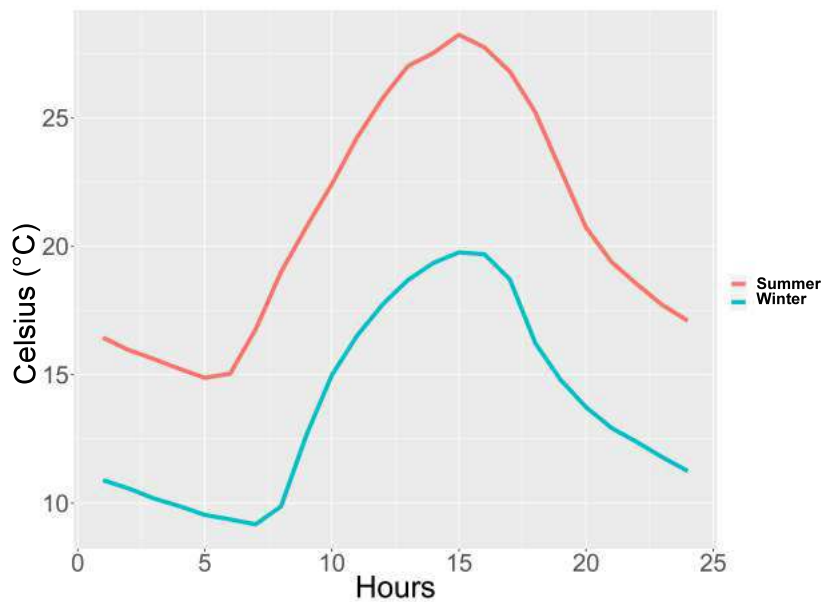


Figure 2.13: Seasonal temperatures

Hourly temperatures collected in Ladismith (Little Karoo) during winter and summer were provided by the South African Weather Service. They were averaged throughout the study period (March 2014 - August 2015).

Splendours of the Little Karoo

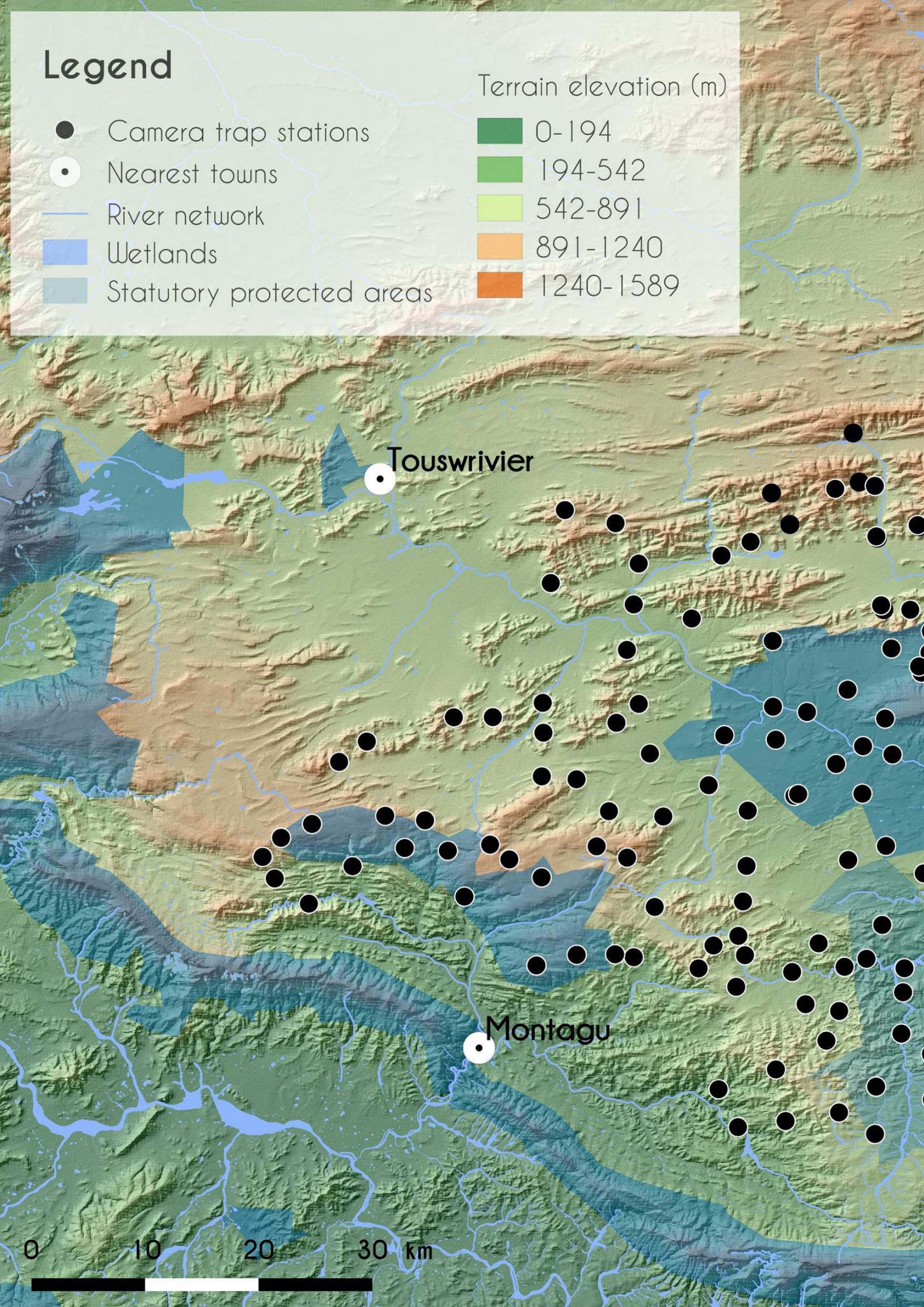
Photos: Elsa Bussière

Legend

- Camera trap stations
- Nearest towns
- River network
- Wetlands
- Statutory protected areas

Terrain elevation (m)

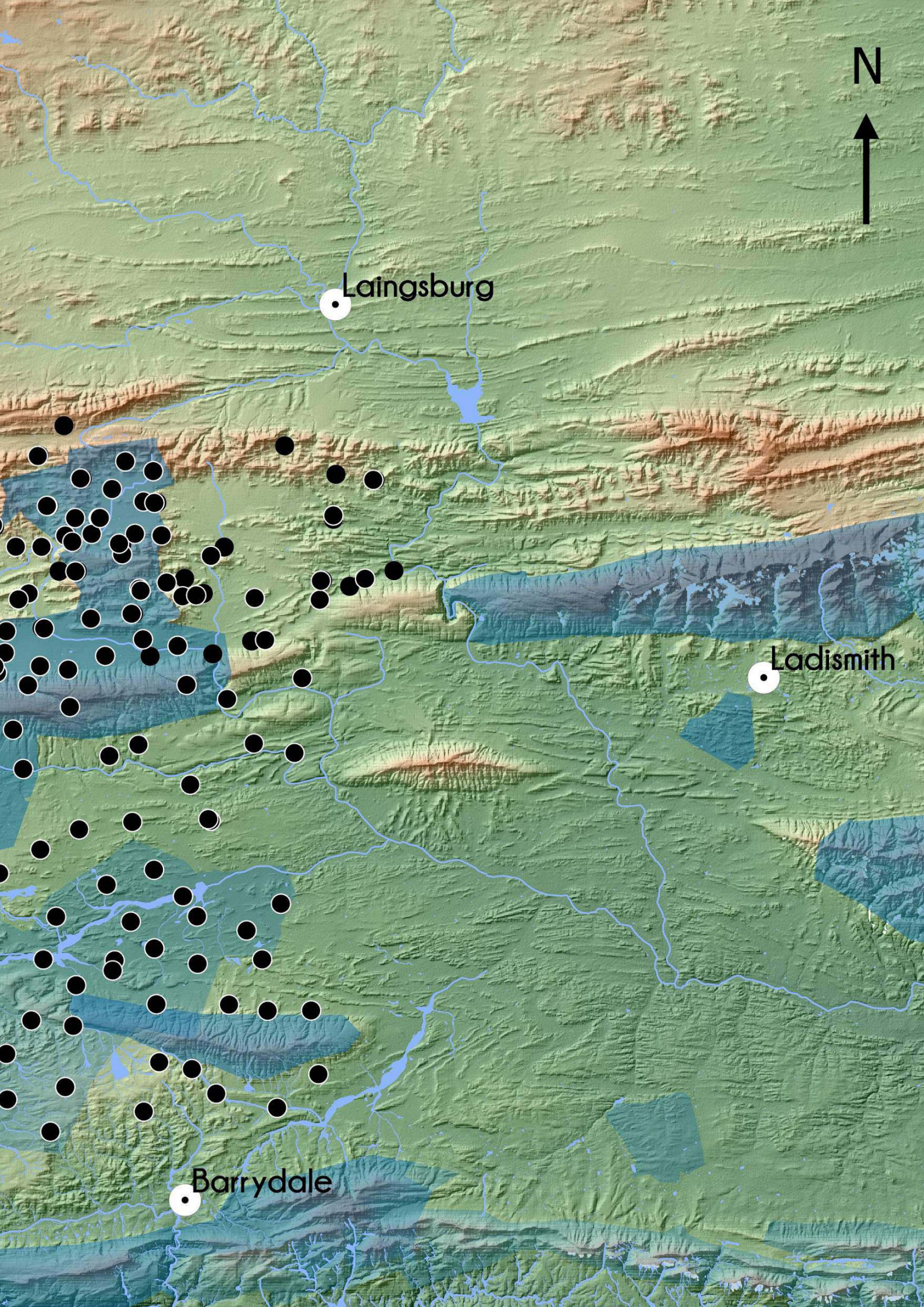
- 0-194
- 194-542
- 542-891
- 891-1240
- 1240-1589



Touswrievier

Montagu

0 10 20 30 km



Laingsburg

Ladismith

Barrydale









Two fluffy black ears are sticking out a thorny bush. I have been looking for you, caracal, gorgeous desert lynx. I imagine your mesmerizing eyes staring at me through the twigs. I am calling you. Please join me; I long to see you leap across the arid and hostile landscape as if it was the most exceptional playground one could possibly dream of. I miss the sound of your purr, the dynamism of your youth, and the ravishing colours of your coat. Go tear-up my landy leather seats; I know you cannot help it. Jump and catch my long tangled hair locks; it makes me laugh. Anything you want, but please, take me with you along the riverline, to your favourite spots, show me the shady places where you rest, and the pools where you drink. Let me be a caracal too, a creature of the Little Karoo, help me forget the void of my human life and find comfort in being part of the wilderness.











Imagine a creature which neither the shape, the traits nor the calls bring any familiarity to your world. Fear is innate to all novelty, but so is curiosity. To many, brown hyenas ought to be little more than a chimera, the result of a wildly implausible mind, an omen for calamity. To me, brown hyenas help reconnect with the child within oneself by triggering the first and fundamental emotion which we discover in the human intellect: curiosity. An emotion that keeps us moving forward and opening new doors leading down new paths. Hand in hand with imagination, curiosity is a powerful driving force: the cradle of creativity.



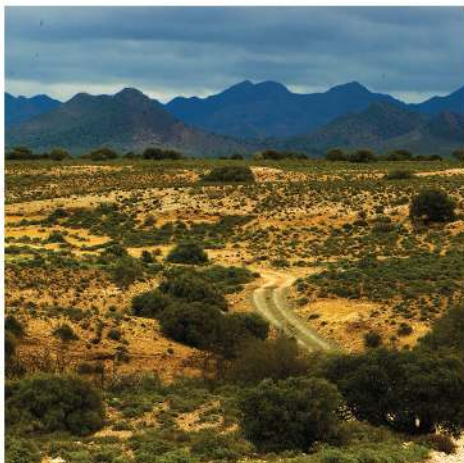
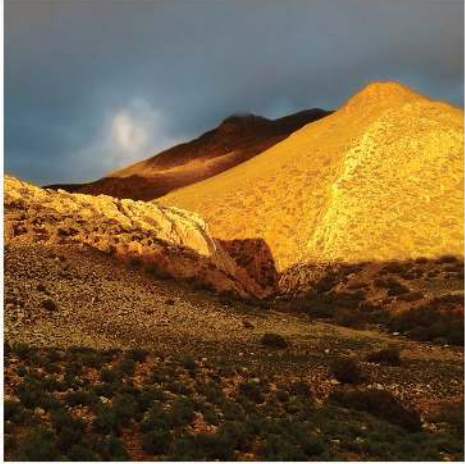








On a scorching hot summer day in the Little Karoo, sitting at the top of a rugged and red koppie, I wipe the sweat off my face. The hostility of this arid region is getting under my skin now that I am found alone surrounded by elemental divinities: wind, sun and mountains. I hear nothing but the silence of a no man's land, smashing all routines, shattering all rituals of my capitalist existence and throwing me out of my bourgeois security. It would be futile to attempt building ramparts against the desert, because right here, nothing can subdue awareness of my human condition. I am left pondering unanswerable questions, on a wandering planet.



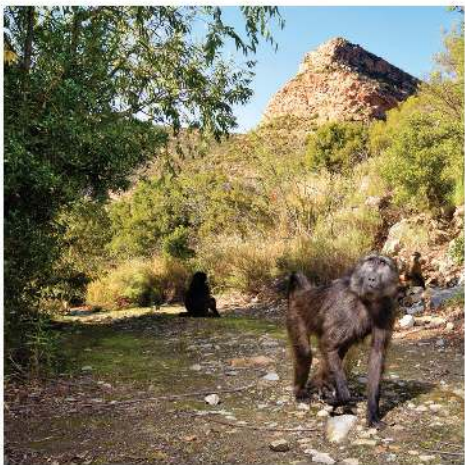








Quickly! My camera is out and the chargers plugged-in. Porcupine quills, cobra's hood, gemsbok's horns and kestrel's talons, I have got you all in my lens' view. Cheeky you, unobtrusive Little Karoo, complotting against me so that I would miss your treasures... got you! My photographs will adorn my desk and walls; I will carry them in my pocket and display them to one and all. They will help me take a little time everyday to reminisce of yesterday. With time, they will eventually become worn and ragged images, yet the lasting love deep in my heart will be what they leave behind.





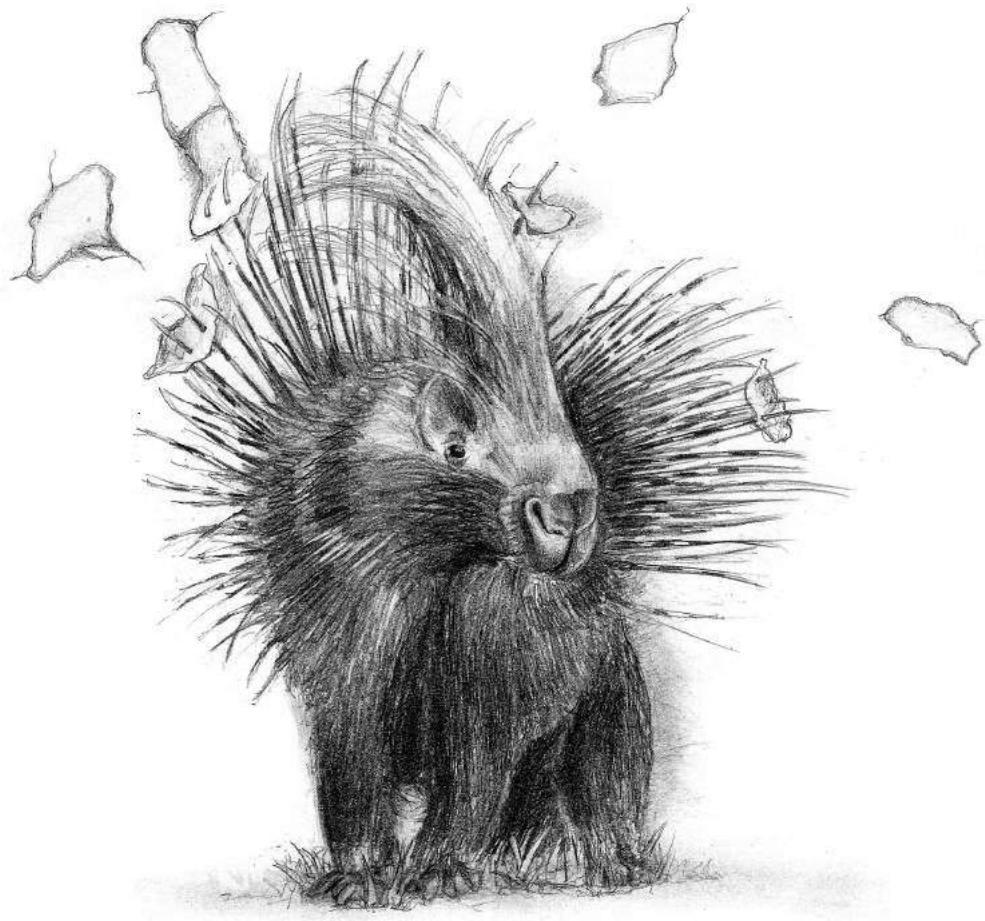






Many species of the mammal kingdom owe their beauty to their fur, this prodigious coat occasionally printed with aesthetic graphic designs. Spotted, striped – or showing more complex patterns with rosettes and other odd shapes – these magnificent artistic creations are the results of millions of years of natural selection. Somehow, these sophisticated outfits provided a natural advantage to their owners: camouflage. A game of hind and seek begins where both predator and prey merge with their habitat. Those that excel in the art of blending in take advantage over others, pressuring the natural world's stylist to continuously become more creative. Nature is harsh, rules are strict and punishments are often deadly. Every wild creation must be efficient; no extra energy can be spent on useless artifices. These designs play a key role in the lives of these animals and even though fur patterns seem to be highly regular; they are in fact – for some species – extremely variable. Every leopard, brown hyena or aardwolf has got its own personalised version, each being a Pop Art masterpiece. The patterns work like human fingerprints and can be used for individual identification. Spots, stripes and other shapes make an important contribution to science, offering new opportunities to study and preserve those that need it the most: cryptic and invisible creatures, shadows in the landscape. But these stylish Cape mammals are presenting themselves in the flickering of camera trap flashes; so let's attend the greatest Haute Couture Fashion Show this wild world has to offer!





Multivariate analyses enable visualisation of temporal resource partitioning in local mammal communities

3.1 Abstract

An important ecological goal is to understand the forces driving species coexistence in local animal communities, and ecologists have focused their attention on resource-partitioning to gain insights into the mechanisms driving sympatry. Interspecific competition takes place when resources are limiting, but coexistence can still be possible if sympatric species use different food sources and/or use them in different areas and/or at different times. Animals have evolved different diel activity rhythms to adapt to the time structure of the environment, which consists of 24-hour periodicity. The ecological implications that these diel activity rhythms have on the interactions and structure of ecological communities are still poorly understood. The nocturnal bottleneck hypothesis, that the majority of mammal species is nocturnal as a result of an ancestral characteristic of the group, has become commonplace in textbooks; nonetheless, behavioural differences among terrestrial mammals were documented, with species using different periods of the 24-hour sleep-wake cycle in complex and diverse ways. In this study, three multivariate statistical approaches were applied to camera trap data, to visually interpret a large multivariate ecological dataset. Each of these three methods is part of an exploratory data analysis philosophy aiming to produce graphical displays, which provide insights into, makes suggestions about, and even answer ques-

tions dealing with temporal partitioning in animal communities. The three multivariate analyses provided similar two-dimensional graphical display explaining the essential structure of the data, which showed that the results are not sensitive to the choice of statistical method. These investigations enabled subtle nuances in the spectrum of diel activity rhythms to be visualised. The graphical outputs show a variety of temporal niche breadths and of activity onset/offset timings, which allowed diel activity rhythms to diversify and the mammal community to partition the temporal resources. By locating species along a continuum rather than in categories, these methods enable us to compare species in such a way that it leads to a better understanding of the forces driving species coexistence in local animal communities.

3.2 Introduction

An important ecological goal is to understand the forces driving species coexistence in local animal communities [133, 193, 357]. Ecologists have focused their attention on resource-partitioning to gain insights into the mechanisms driving sympatry [298]. The subdivision of food, space and time are the three essential means that facilitate species coexistence [160, 174, 176, 277, 298, 339].

Animals have evolved different diel activity rhythms to adapt to the time structure of the environment, which consists of 24-hour periodicity [73, 160, 370]. The ecological implications that these diel activity rhythms have on the interactions and structure of ecological communities are still poorly understood. However the main goal of resource-partitioning studies is to understand the limits that interspecific competition place on the number of species that can stably coexist [298]. Temporal partitioning of short time periods (e.g. diel) probably involves the interplay of competition and predation, in order to facilitate coexistence between competitors and between predators and their prey [58, 280, 298, 363]. Interspecific competition takes place when resources are limiting, but coexistence can still be possible if sympatric species differ in behaviour and morphology, and consequently if they use different food sources and/or use them in different areas and/or at different times [49, 75, 76, 298].

The nocturnal bottleneck hypothesis, that the majority of mammal species is nocturnal as a result of an ancestral characteristic of the group, has become commonplace in textbooks [116]. Early mammals of the Mesozoic area, being subjected to predation pressure from ectothermic and diurnal reptiles (e.g. dinosaurs), evolved endothermic metabolisms, a major adaptation enabling them to restrict their activities to periods of darkness,

leading to considerable changes in photoreception [64, 71, 223, 354]. Although the ecology of diel time partitioning remains a grey area, many behavioural differences among terrestrial mammals were documented, with species converging their peak periods of activity to coincide with the periods of daylight, darkness or twilight, and with species using different periods of the 24-hour sleep-wake cycle in complex and diverse ways [26]. Among the many factors which can impact diel activity rhythms, the more influential one seems to be: daylength [26, 277], temperature [26], rainfall [24], competition [135] and human activities [173]. To unravel the underlying processes governing diel activity rhythms, it is crucial to collect basic quantitative data on these rhythms among sympatric mammal species. The use of remotely triggered cameras enables scientists to collect large datasets and information on diel activity rhythms of sympatric species [43, 80, 103, 135]. Most research in this area has been conducted on a restricted number of species, mainly carnivorous ones [77, 103, 352]. For example, Di Bitetti et al. (2009) [80] showed that temporal partitioning favours the coexistence of two competitors, one reducing its activity when that of the presumably dominant one is high. Harmsen et al. (2011) [135] also showed that predators have similar diel activity rhythms as their most important prey species, and have negligible overlap with less frequently consumed prey species.

In this study, three multivariate statistical approaches (non-metric multidimensional scaling, covariance biplot and correspondence analysis) were applied to camera trap data, in order to visually interpret a large multivariate ecological dataset, and to gain insights into the diel activity rhythms of the mammal community of the Little Karoo. Each of these three methods is part of an exploratory data analysis philosophy [217, 341], aiming to produce graphical displays, which provide insights into, makes suggestions about, and even answer questions dealing with temporal partitioning in animal communities.

3.3 Material and Methods

3.3.1 Study area

The Little Karoo is a semi-arid desert located at the southern tip of the African continent [Appendix 1A], within the Cape Fold Belt. It is also described as a mega-ecotone, where the succulent Karoo and the Cape Floristic Provinces intermingle [Introduction, Chapter 1 section 1.3.1].

3.3.2 Data collection

Camera trap data were deployed between March 2014 and August 2015 [Chapter 1 section 1.3.2] as part of a research project on large carnivores – brown hyenas *Hyaena brunnea* and leopards *Panthera pardus* – within a study area of 4,327 km² (minimum convex polygon).

3.3.3 Analysis

3.3.3.1 Kernel density estimation

The times t recorded for every photo-capture i made throughout the 365-day cycle, provided information on the diel activity rhythm of species s , the later being displayed using a 24-hour kernel density function; a probability density function $A_{,s}$ of the species' activity [309]:

$$A_{,s} = \sum_{i=1}^n k(t_{i,s}) \quad \text{with} \quad \int_0^{24} A_{,s} \cdot dt = 1 \quad (3.1)$$

The probability density functions $A_{,s}$ are representations of circular distributions. Their graphical display was either noon- or midnight-centred, depending on the time period of the 24-hour cycle, in which most of the species daily activity is allocated.

Every photo-capture was either defined as a capture-event or as a duplicate [Chapter 1 section 1.3.3]. All duplicates were discarded for this study as they could significantly inflate the density function in certain areas of the curve, as well as the photo-capture counts per unit of time, which become no longer comparable between species. For this study, mammal species for which at least 50 photo-captures were collected, were included [Chapter 1 section 1.3.3].

3.3.3.2 Data heterogeneity

The northern section of Sanbona Wildlife Reserve differed from the rest of the study area due to its unique species diversity. It also constituted a biological system suspected to have evolved fairly independently, due to the high game fence delimitating its border [Chapter 1 section 1.3.1]. The northern section of Sanbona Wildlife Reserve was sampled in the middle of winter and the datasets were too small to run a bootstrap analysis [235] [Chapter 1 section 2.3.3.3] and search for any significant change in species' diel activity rhythm between Sanbona and the rest of the study site, in winter only. The data

collected within the northern section of the Sanbona Wildlife Reserve were consequently discarded for this study.

3.3.3.3 Data pre-processing

The diel activity rhythms of the mammals of the Little Karoo were not analysed using clock-time because sunrise and sunset times vary throughout the year and across study areas. The time variable t was transformed (t') so that daily sunrise and sunset times were standardised to the annual averages of sunrise and sunset times [Chapter 2 section 2.3.3.2]. Using t' as circular data, the probability density functions describing the diel activity rhythms $A'_{,s}$ of species s were computed.

3.3.3.4 Coefficient of overlap

Kernel density functions such as $A'_{,s}$ have an area under the curve equal to 1, which offers the opportunity to compare them against one another (e.g. species s_1 and s_2), by calculating their coefficient of overlap $O_{s_1}^{s_2}$ ranging from 0 (no overlap) to 1 (identical curves) [226, 283], with the *overlapEst* function from the *overlap* R-package [226]:

$$\begin{aligned} O_{s_1}^{s_2'} &= O_v(A'_{,s_1}, A'_{,s_2}) \\ &= \int_0^{24} \min(A'_{,s_1}, A'_{,s_2}) \cdot dt' \end{aligned} \quad (3.2)$$

3.3.3.5 Temporal partitioning

Non-metric Multi-Dimensional Scaling (NMDS) [32], covariance biplot [114] and correspondence analysis [27] are three statistical tools, each providing a means of displaying and summarising a set of data into a low-dimensional Euclidean space [126, 180, 181]. In two dimensions, the results are displayed in a plane (flat surface), which is the most visually intuitive and therefore most useful of all. They can, for example, be used as a first stage in the exploration of niche overlap in sympatric species. Temporal data collected for the 27 mammal species were analysed using the three approaches, by compiling all information into three matrixes: an Overlap Distance Matrix (ODM) which was used in the NMDS analysis, a Smoothed Community Matrix (SCM) used in the biplot analysis, and a Count Community Matrix (CCM) used in the correspondence analysis.

Overlap Distance Matrix: a symmetric matrix with $n_1 = 27$ rows and $p_1 = 27$ columns (total number of species). Every ODM element $ODM[s_1, s_2]$ quantifies the dissimilarity between the diel activity rhythms of species s_1 and s_2 :

$$ODM[s_1, s_2] = 1 - O_{s_1}^{s_2'} \quad (3.3)$$

Smoothed Community Matrix: for every species s , 128 points were extracted at regular time intervals from the kernel density function $A'_{,s}$. SCM consisted of $n_2 = 27$ rows of species and $p_2 = 128$ columns of time variables. Because the probability density functions are smooth, the choice of alternative values of p_2 makes no difference in the results.

Count Community Matrix: counts of photo-captures were extracted for every x -minutes time slots of the day. CCM consisted of $n_3 = 27$ rows of species and $p_3 = 24 \cdot \frac{60}{x}$ columns of time variables. Three CCMs were built using respectively 15, 30 and 60 as x values.

3.3.3.6 Non-metric Multi-Dimensional Scaling (NMDS)

NMDS is a statistical tool which provides a means of displaying and summarising a square symmetric matrix of dissimilarities into a low-dimensional Euclidean space [126, 180, 181]. The objective in NMDS is to find a configuration of points so that the ordering of the interpoint distances matches, as closely as possible, the ordering of the dissimilarities in the matrix of dissimilarities. Summarising a set of data into a two-dimensional graph might not be feasible and a certain amount of distortion might be created. The measure of lack of fit in NMDS is known as the ‘stress’ of the configuration. Non-zero stress values occur with insufficient dimensionality, and as the number of dimensions increases, the stress value will either decrease or remain stable [32, 180, 181].

Using the *isoMDS* function from the *MASS* R-package [285], an NMDS ordination was performed on ODM, a matrix of dissimilarity data which estimated the dissimilarities of diel activity rhythms between each pair of species in the mammal community of the Little Karoo. The objective of the ordination is to find the configuration with minimum ‘stress’ for a given number of dimensions. The operation was therefore repeated several times, each time with a different number of chosen dimensions k , and a screeplot (stress versus k) was plotted in order to identify the point beyond which additional dimensions do not substantially lower the stress value.

The output data information was then summarised into a two-dimensional graphical display, which maximised the rank correlation between the cal-

culated species dissimilarities/distances and the plotted distances between species [32].

3.3.3.7 Covariance biplot

A biplot is a multivariate technique proposed by Gabriel (1971) [114], which summarises into a low-dimensional graph the relationships between two continuous and/or categorical variables that are defined within a data matrix, using the singular value decomposition [123].

The covariance biplot analysis was applied to SCM in statistical software Genstat [351]. The term ‘bi’ refers to the simultaneous display of both rows and columns, not to a two-dimensionality of the plot. The data were collapsed into a two-variable scatterplot, where both species and time information were displayed simultaneously, in the same plane. It showed the relations and interrelations among the rows (species) and columns (time) in the two dimensions, which accounted for the maximum amount of variation in SCM [114].

Summarising a set of data into a two-dimensional graph might not be feasible and a certain amount of distortion might be created. An increase of the number of dimensions will increase the amount of variation in the data matrix, which is accounted for.

3.3.3.8 Correspondence analysis

The correspondence analysis is a multivariate technique developed by Benzécri (1973) [27] after being proposed by Hirschfeld, in 1935 [143]. Similarly to the covariance biplot analysis, it aims to summarise the data into a graphical display of the rows and columns of the CCM contingency table. It is an extension of a chi-square test, where the null hypothesis being tested is whether rows (species) and columns (time) are independent. In other words, whereas the chi-square test answers the question “is the type of species photo-captured independent to the time of capture?”, the correspondence analysis aims to provide insights into the nature of the dependence between species and time. The correspondence analysis was performed on CCM (also called a contingency table), using the *ca* function from the *ca* R-package [245].

Summarising a set of multidimensional data into a two-dimensional graph might not be feasible and a certain amount of distortion is inevitably created. An increase of the number of dimensions will increase the amount of variation in the data matrix, which is accounted for.

3.4 Results

The trapping effort of 16,409 camera trap nights resulted in 25,211 photo-captures (10,991 independent photo-capture events) of 86 wild species: including 46 mammals, 39 birds and 1 reptile. Twenty-seven of the 46 mammal species had more than 50 photo-captures to enable the analysis to be conducted [Appendix 2A].

3.4.1 Kernel density functions $A'_{,s}$

The midnight-centred diel activity rhythms $A'_{,s}$ of the 27 mammal species s – calculated using camera trap data collected throughout two consecutive years – are provided in Fig. 3.1; \overline{SS} and \overline{SR} being the annual average times of sunrise and sunset, \overline{MD} and \overline{MN} being true midday and midnight in the study area, given the inclination angle of the rotation axis of the Earth (as compared to its orbital plane). The time periods shaded in light grey represent the daily hours of twilight (one hour before and after sunrise and sunset), while the time period shaded in dark grey represents the daily hours of darkness (from one hour after sunset until one hour before sunrise), according to previous studies [151].

The kernel density functions showed that while some species seemed to constrain their peak periods of activity to concur with the periods of daylight (e.g. rock hyrax *Procavia capensis*), darkness (e.g. Cape hare *Lepus capensis*) or twilight (e.g. grey duiker *Sylvicapra grimmia*), other species used different periods of the 24-hour sleep-wake cycle in complex and diverse ways (e.g. springbok). Species' diel activity rhythms also differed according to the species' temporal niche breadth (variety of temporal resources used by a given species). While certain species displayed a wide temporal niche breadth (e.g. caracal *Caracal caracal*), others exploited a short temporal window (e.g. *aardvark* *Orycteropus afer*) of the 24-hour cycle.

3.4.2 Non-metric Multi-Dimensional Scaling (NMDS)

The NMDS iterative algorithm captured, in two dimensions, the essential structure of the dissimilarity matrix data (Table 3.1). It produced the NMDS plot (Fig. 3.3), which represents, as closely as possible, the dissimilarity between species' diel activity rhythms in a two-dimensional space. For example, leopards had closer diel activity rhythms to African wildcats than they had to caracals, although the graph does not quantify this difference.

The NMDS screeplot, provided in Fig. 3.6(a), showed a decrease in ordination stress with an increase in the number of ordination dimensions allowed, which revealed that attempting an ordination with one NMDS axis yielded reasonably high stress (0.061), however two dimensions was more suitable. The stress value equaled 0.032 in two dimensions and, like all stress values equal to or below 0.05, it indicated good fit. The NMDS plot showed a clear and gradual left-right transition along the first (horizontal) axis, from species with strictly nocturnal diel activity rhythms to species with strictly diurnal diel activity rhythms. Cathemeral species – active throughout the 24-hour cycle – were found in the centre of the graph, although the timing of their activity peaks might have differed.

The second (vertical) axis explained less of the data structure and might have also picked up noise in the data. This was to be expected given the small decrease in stress between an ordination with one and an ordination with two NMDS axis.

3.4.3 Correspondence analysis

The correspondence analysis, applied to the three CCMs, built with the time slots $x = 15, 30$ and 60 minutes respectively, summarised the data and produced graphical displays of the cross tabulations. The two-dimensional ordinations respectively explained 66.5%, 77.2% and 86.1% of variance in the data of the three CCMs. These percentages increased by 3% (Fig. 3.6(b)) after adding a third dimension, suggesting that the CA graphical display in two dimensions was adequate, especially because the first axis always explained most of the variance in the data (respectively 58.9%, 69.2% and 77.0%). Fig. 3.7 provides for the 27 mammal species a quality value, a percentage of reliability of the data structure displayed in two dimensions. Greater kudu *Tragelaphus strepsiceros* and grysbok *Raphicerus melanotis* were the two species with the lowest quality values (respectively 31% and 33%), indicating that a substantial part of their data structure was explained in higher dimensions (≥ 3). The next lowest quality value (48%) were that of springbok *Antidorcas marsupialis* and Cape mountain zebra *Equus zebra zebra*. The 15.9% of variance in the data, explained in dimensions higher than 2, was not evenly spread over all 27 species, but mainly over greater kudu and grysbok.

The graphical results of the correspondence analysis were very similar for the three different CCMs. The 60-minute correspondence analysis was the selected version because of the reduced number of time points which facilitated the readability of the output plot. The latter, a two-dimensional plot (Fig. 3.4), represented both variables, species and time, in the same plane. The

species points formed an arch along which, a gradual left-right transition from strictly nocturnal species to strictly diurnal species, was observed. Species displaying similar temporal preferences and therefore similar diel activity rhythms were plotted side-by-side (e.g. Cape porcupine *Hystrix africaeaus-tralis* and small spotted genet *Genetta genetta*). For each 60-minute time slot of the 24-hour cycle, a time-profile summarising the activity level of the 27 species within the mammal community was defined and then plotted in blue in Fig. 3.4 (the details of the 24 time-profiles of the daily cycle are provided in Fig. 3.2). Forming also an arch, the time points followed the same trend as the species points. Species concentrating their activity to the night were found close to the time-profiles of the darkest hours of the 24-hour cycle, whereas species concentrating their activity to the day, were close to the time-profiles of the brightest hours. Species with larger temporal niche breadth – and therefore exploiting a wider range of temporal resources – were found along the lower section of the arch, close to the time-profiles matching hours with rapid changes in light intensities. 60-minute time slots with similar time-profiles (similar composition of diel activity rhythms among the 27 mammal species of the community) were plotted side-by-side (e.g. 04:00 and 05:00).

Following the chronological order of the hours within the 24-hour cycle, two clusters of time points were observed; one gathering the time-profiles of the dark hours starting 1h20 after sunset and ending 1h38 before sunrise ($20:00 < t' < 05:00$), the second one gathering the time-profiles of the bright hours starting 3h22 after sunrise and ending 2h38 before sunset ($10:00 < t' < 16:00$). Within each of these two time periods, the time-profile remained stable, indicating that – within the mammal community – little variation of species activity occurred during the darkest and brightest hours of the daily cycle. On the contrary, during the remaining hours of the daily cycle, the activity of the species in the mammal community underwent high-amplitude variations. The imaginary curves connecting the morning ($05:00 < t' < 10:00$) and evening ($16:00 < t' < 20:00$) hours overlapped, indicating that the variations undergone by the time-profiles of the morning hours followed a pattern which was conversely reproduced by the time-profiles of the evening hours. Consequently, the activity of the 27 species within the mammal community minutes after sunrise ($t' = 07:00$) and minutes before sunset ($t' = 18:00$) were nearly identical, so as that roughly two hours after sunrise ($t' = 09:00$) and two hours before sunset ($t' = 17:00$).

3.4.4 Covariance biplot

The covariance biplot, applied to SDM, summarised the data into a scatter-plot representing the two sets of variables – species and time – in the same plane (Fig. 3.5). The two-dimensional ordination explained 88.6% of variance in the data of the SDM, most of which was explained by the first axis (82%). The percentage of variance explained, increased by 5% (Fig. 3.6(c)) after adding a third dimension, suggesting that the biplot in two dimensions was adequate. Fig. 3.8 provides for the 27 species a quality value, a percentage of reliability of the data structure displayed in two dimensions. Grysbok was the species with the lowest quality value (27%), indicating that a substantial part of its data structure was explained in higher dimensions (≥ 3). The 11.4% of variance in the data, explained in dimensions higher than 2, was not evenly spread over all 27 mammal species, but mainly over grysbok. This indicated that within the multidimensional space, grysbok was the farthest from the plane, among all other species.

Similarly to the CA graphical display, the species points formed an arch along which a gradual left-right transition from strictly nocturnal species to strictly diurnal species was observed. The cosin of the angle between two vectors extending from the origin to a species point estimated the correlation between the diel activity rhythms of the two species in question. In other words, species displaying similar temporal preferences (e.g. diel activity rhythms) were plotted in such a way that their respective position vectors pointed nearly to the same direction (e.g. brown hyena *Hyaena brunnea* and aardwolf *Proteles cristatus*). On the contrary, species with divergent temporal preferences displayed position vectors pointing to opposite directions (e.g. chacma baboon *Papio ursinus* and leopard *Panthera pardus*). The length of the species vector gave insights into the variability of the diel activity rhythm. The longer it was, the more variability was found within the data.

The time-profile – summary of the activity level of all species in the community at time t' – represented by time points (in blue in Fig. 3.5), goes through a periodic cycle within 24-hours, which pattern is built around four specific times: \overline{MD} , \overline{MN} , \overline{SR} and \overline{SS} . Time points plotted side-by-side in Fig. 3.5 indicate that, at those different times, the time-profiles of the mammal community were similar (e.g. 15h45 and 09h45). Two clusters of time points were observed; one gathering the time-profiles of the dark hours starting 3h20 after sunset and ending 1h38 before sunrise ($22:00 < t' < 05:00$), the second one gathering the time-profiles of the bright hours starting 3h22 after sunrise and ending 2h38 before sunset ($10:00 < t' < 16:00$). Within each of these two time periods, the time-profile remained stable, indicating that –

within the mammal community – little variation of species activity occurred during the darkest and brightest hours of the daily cycle. On the contrary, during the remaining hours of the daily cycle, the activity of the species in the mammal community underwent high-amplitude variations. The imaginary curves connecting the morning ($05:00 < t' < 10:00$) and evening ($16:00 < t' < 22:00$) hours overlapped, indicating that the variations undergone by the time-profiles of the morning hours followed a pattern which was conversely reproduced by the time-profiles of the evening hours. Consequently, the activity of the 27 mammal species within the mammal community minutes after sunrise ($t' = 07:00$) and minutes before sunset ($t' = 18:00$) were nearly identical, so as that roughly two hours after sunrise ($t' = 09:00$) and two hours before sunset ($t' = 16:30$). These results were remarkably similar to those of the CA analysis.

The relative positioning of species points to time points depended on the species' temporal preferences. For example, strictly diurnal species tended to be plotted in the same direction from the origin as that of the \overline{MD} time point (e.g. rock hyrax). The length of \vec{ij} , linking species point i and time point j , was calculated as follow: $z_{ij} = ||i|| \cdot ||j|| \cdot \cos(\theta_{ij})$

3.5 Discussion

Each of the three multivariate analyses provided a two-dimensional graphical display which explained most of the data structure. The collapse and summary of the complex initial data table allowed for an intuitive and visual exploration of the data. Although not identical, the relative spatial positioning of all 27 mammal species within the plane was similar in the three analyses. From this it can be inferred that the data are robust in relation to statistical method. In other words, the results are not sensitive to the choice of method. These investigations did not only enable to classify species as diurnal, nocturnal, crepuscular, or cathemeral but also to grasp subtle nuances in the spectrum of diel activity rhythms. The species were located along a continuum rather than simply categorised. These methods enable us to compare species in such a way that it leads to a better understanding of the forces driving species coexistence in local animal communities.

A variety of temporal niche breadths and of activity onset/offset timings allowed diel activity rhythms to diversify and the mammal community to partition the temporal resources. Both phylogenetic and environmental factors are crucial to elucidate the biological principles underlying the diversity of diel activity rhythms [116, 122, 175, 223, 224, 317, 345]. Several studies indicated

that while a circadian clock – an endogenous timing mechanism built on the foundation of an oscillator providing a time tracking system – can regulate diel activity rhythm in organisms, the latter are not slaves to the physiological and biochemical processes of their circadian clock [65, 73, 169, 170, 291, 365]. The niche occupied by an animal within the community results from the interactions this animal may have with the biological and physical factors which contribute to its survival and reproduction [147]. The Earth's daily rotation prevents the influence of these factors to be uniform throughout the day-night cycle, which is why the diel structure of a niche is as fundamental as its spatial, chemical, energetic and social structures in order to understand the segregation of the activities of individuals to specific times of day, as well as the diversity of species that inhabit a community [147, 298].

There is evidence for light-entrained activity (synchronisation of activities with the light-dark cycle) [263, 346], due to genetic [266, 301], latitudinal [262] and seasonal [65, 170] differences in the responsiveness of the circadian system to light. Entrainment is then defined by a stable relationship between determined environmental occurrences (e.g. sunrise or sunset) and specific behaviour (e.g. the onset or offset of activity). In Fig. 3.4, it is observed that within the 24-hour cycle, the time-profile (summary of the activity level of all species in the community at time t') goes through a periodic cycle characterised by four periods. Two stable ones, matching the darkest and brightest hours of the cycle. Outside those hours, the time-profile goes through two transitional periods during which it varies rapidly to get from one stable state to another. The transitional periods are considered to be the crepuscular hours of the daily cycle (periods of rapidly changing light intensities). The synchronisation of the community activity cycle with the light-dark cycle, supports the assumption of light-entrained activity within the mammal community of the Little Karoo.

There is also evidence for non-photic influences on circadian rhythms, resulting into the partition of the temporal environment within a community, to maximise species energy intake while minimizing species exposure to predation and/or to other stressors (e.g. competitors) [168, 179, 239]. Kotler et al. (1993) [179] conducted research studies on granivorous gerbils in the Israeli desert, and showed that the smaller species (*Gerbillus allenbyi*) emerges from underground to forage after the retreat of the larger species (*Gerbillus pyramidum*), which had by then reduced the seed densities to suboptimal levels. Without *G. pyramidum* within the community, *G. allenbyi* shifts its activity to an earlier time, supporting the hypothesis that the temporal feeding partitioning between these species of gerbils is maintained by aggressive encounters. Species positioned close to one another in the plane of multi-

variate analysis (e.g. caracal and black-backed jackal *Canis mesomelas*) in Fig. 3.3, 3.4, and 3.5, belonged to the same temporal niche, and coexistence was either possible because resources were abundant and the resource competition was weak, or facilitated by the partitioning of resources in different niches (e.g. space and/or food).

3.6 Table

Table 3.1: Overlap Distance Matrix ODM (%)

This ODM was built for 27 mammal species in the Little Karoo. Every ODM element $ODM[s_1, s_2]$ quantifies the dissimilarity between the diel activity rhythms of species s_1 and s_2 : $1 - O_{s_1}^{s_2'}$. $ODM[s_1, s_2] < 20\%$ are showing in bold.

	aardvark	aardwolf	African wildcat	black backed jackal	brown hyena	Cape gray mongoose	Cape hare	Cape mountain zebra	Cape porcupine	caracal	chacma baboon	eland	gemsbok	greater kudu	grey duiker	grey rhebuck	grysbok	Hewitts red rock rabbit	honey badger	klipspringer	leopard	red hartebeest	rock hyrax	scrub hare	small spotted genet	springbok	steenbok
aardvark	100	-	-	-	-	-	-	-	-	-	-	-	-	-	-	-	-	-	-	-	-	-	-	-	-	-	-
aardwolf	11	100	-	-	-	-	-	-	-	-	-	-	-	-	-	-	-	-	-	-	-	-	-	-	-	-	-
African wildcat	31	22	100	-	-	-	-	-	-	-	-	-	-	-	-	-	-	-	-	-	-	-	-	-	-	-	-
black backed jackal	52	44	23	100	-	-	-	-	-	-	-	-	-	-	-	-	-	-	-	-	-	-	-	-	-	-	-
brown hyena	24	15	24	41	100	-	-	-	-	-	-	-	-	-	-	-	-	-	-	-	-	-	-	-	-	-	-
Cape gray mongoose	99	95	79	60	93	100	-	-	-	-	-	-	-	-	-	-	-	-	-	-	-	-	-	-	-	-	-
Cape hare	16	18	27	46	30	94	100	-	-	-	-	-	-	-	-	-	-	-	-	-	-	-	-	-	-	-	-
Cape mountain zebra	52	42	31	28	41	56	51	100	-	-	-	-	-	-	-	-	-	-	-	-	-	-	-	-	-	-	-
Cape porcupine	15	10	22	44	17	96	14	44	100	-	-	-	-	-	-	-	-	-	-	-	-	-	-	-	-	-	-
caracal	47	39	18	10	37	62	41	24	40	100	-	-	-	-	-	-	-	-	-	-	-	-	-	-	-	-	-
chacma baboon	97	91	74	53	89	16	92	49	93	55	100	-	-	-	-	-	-	-	-	-	-	-	-	-	-	-	-
eland	70	62	41	21	57	49	64	34	63	23	38	100	-	-	-	-	-	-	-	-	-	-	-	-	-	-	-
gemsbok	75	67	48	27	63	39	69	36	69	29	27	12	100	-	-	-	-	-	-	-	-	-	-	-	-	-	-
greater kudu	71	64	44	24	59	44	66	35	65	26	32	11	8	100	-	-	-	-	-	-	-	-	-	-	-	-	-
grey duiker	56	48	26	7	45	60	50	31	48	15	53	21	26	24	100	-	-	-	-	-	-	-	-	-	-	-	-
grey rhebuck	93	86	67	45	83	27	87	46	88	49	14	31	25	26	43	100	-	-	-	-	-	-	-	-	-	-	-
grysbok	54	46	27	15	43	58	47	32	48	12	49	19	24	20	18	44	100	-	-	-	-	-	-	-	-	-	-
Hewitts red rock rabbit	26	26	28	46	35	97	16	51	20	42	94	64	71	68	50	89	50	100	-	-	-	-	-	-	-	-	-
honey badger	57	49	30	17	46	60	51	27	50	15	47	20	26	23	21	42	20	52	100	-	-	-	-	-	-	-	-
klipspringer	94	90	74	55	87	11	90	48	91	56	9	41	31	36	55	18	51	92	50	100	-	-	-	-	-	-	-
leopard	26	16	8	31	18	87	23	36	15	26	82	48	55	51	34	75	33	25	38	82	100	-	-	-	-	-	-
red hartebeest	87	80	61	40	77	28	82	46	83	43	19	26	16	19	37	13	37	84	40	23	69	100	-	-	-	-	-
rock hyrax	96	91	74	53	88	11	91	53	92	55	12	43	32	35	52	20	52	94	56	10	82	21	100	-	-	-	-
scrub hare	28	21	15	33	25	91	23	41	18	30	86	50	60	56	34	76	39	20	42	87	12	72	85	100	-	-	-
small spotted genet	23	16	15	37	20	95	18	41	12	34	90	55	63	60	40	83	41	17	45	90	9	77	89	9	100	-	-
springbok	92	87	68	46	84	28	86	53	88	50	26	37	29	32	43	20	47	88	52	26	76	15	22	76	84	100	-
steenbok	89	83	66	46	80	22	84	53	85	47	22	37	25	29	45	23	43	86	49	21	74	15	19	79	82	18	100

3.7 Figures

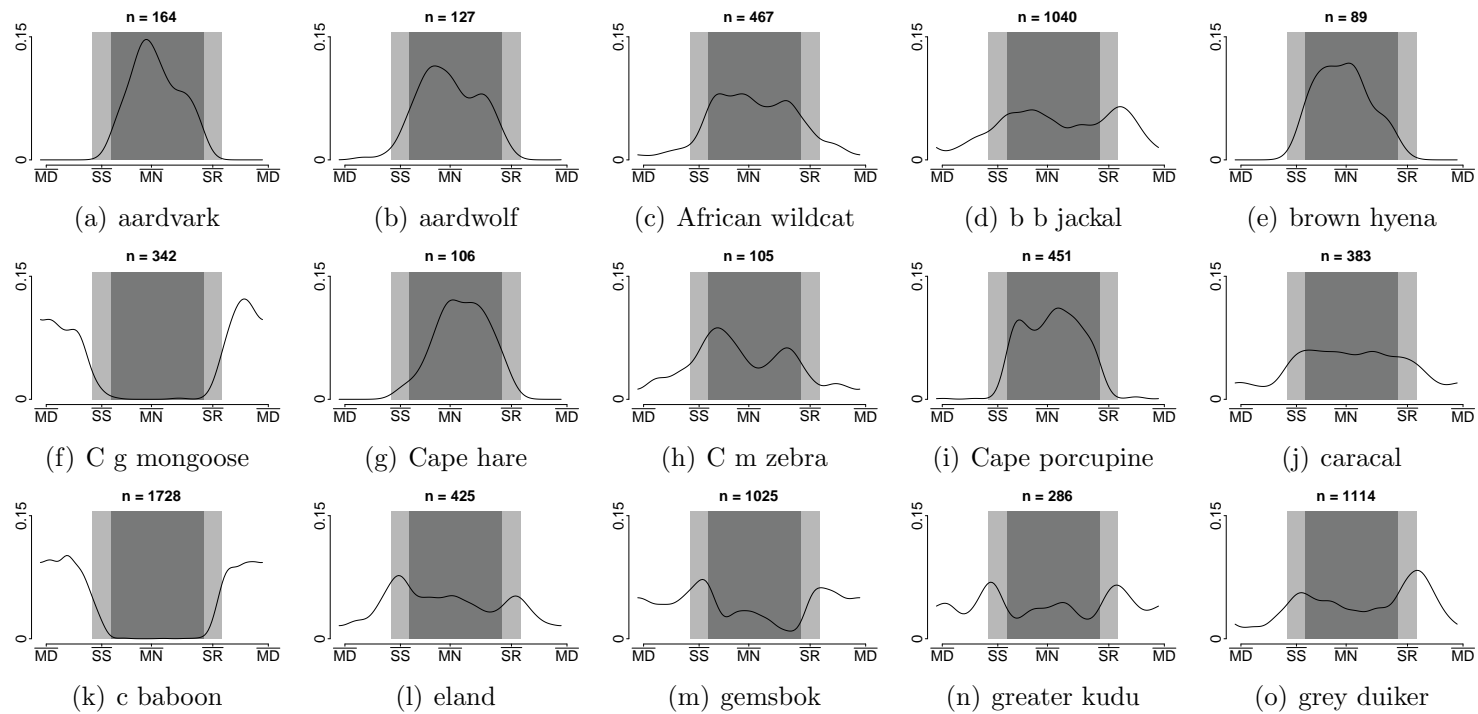


Figure 3.1: Diel activity rhythm of the 27 mammal species in the Little Karoo, throughout the year. Kernel density functions were midnight-centred. \overline{SS} and \overline{SR} represent the annual average times of sunrise and sunset. \overline{MD} and \overline{MN} are true midday and midnight in the study area. The time periods shaded in light grey represent the daily hours of twilight (one hour before and after sunrise and sunset), while the time period shaded in dark grey represents the daily hours of darkness (from one hour after sunset until one hour before sunrise); these were defined in previous studies [151]. The number of photo-captures on which each kernel density function is based is provided at the top of each plot.

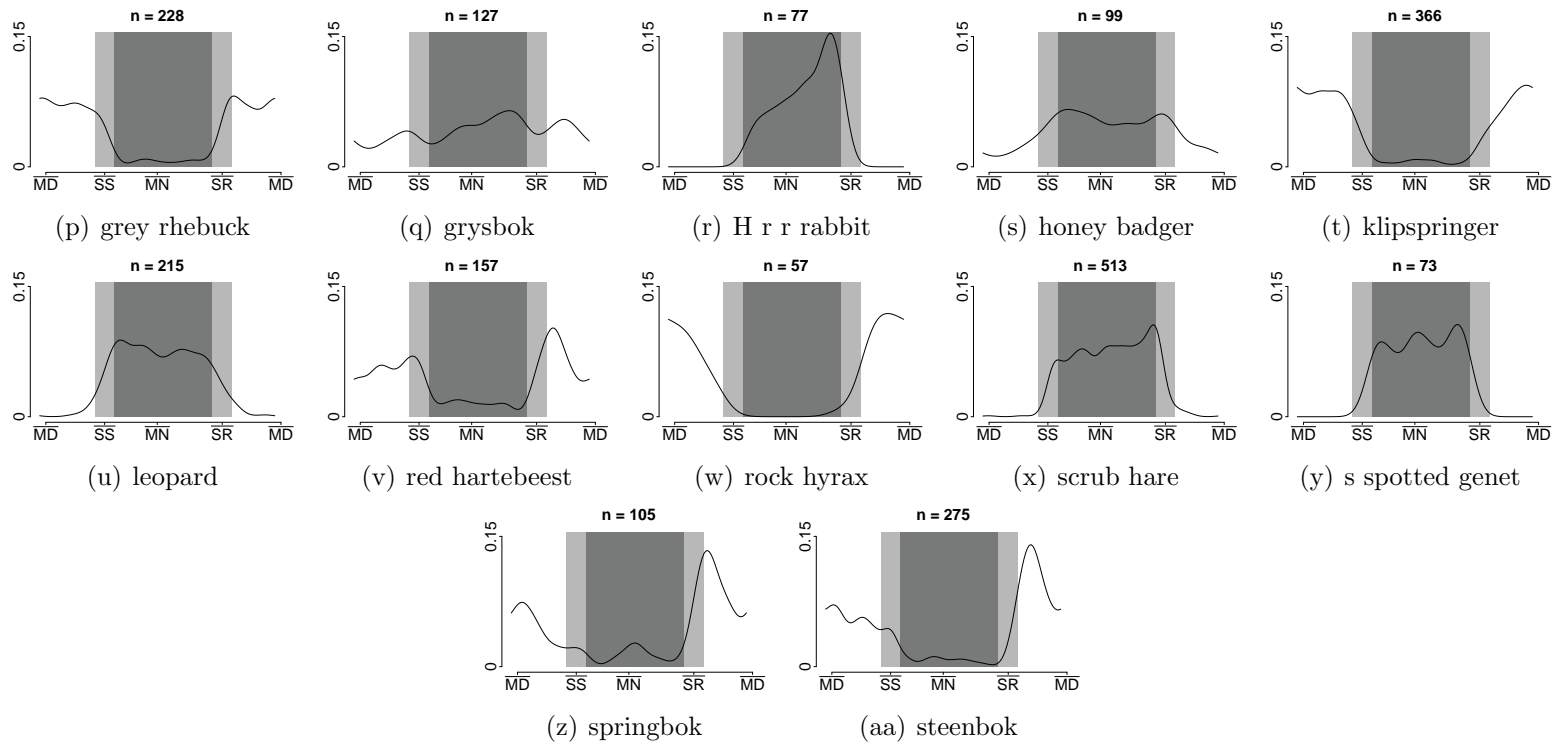


Figure 3.1: Diel activity rhythm of the 27 mammal species in the Little Karoo, throughout the year (continued).
 A full caption is provided on p144

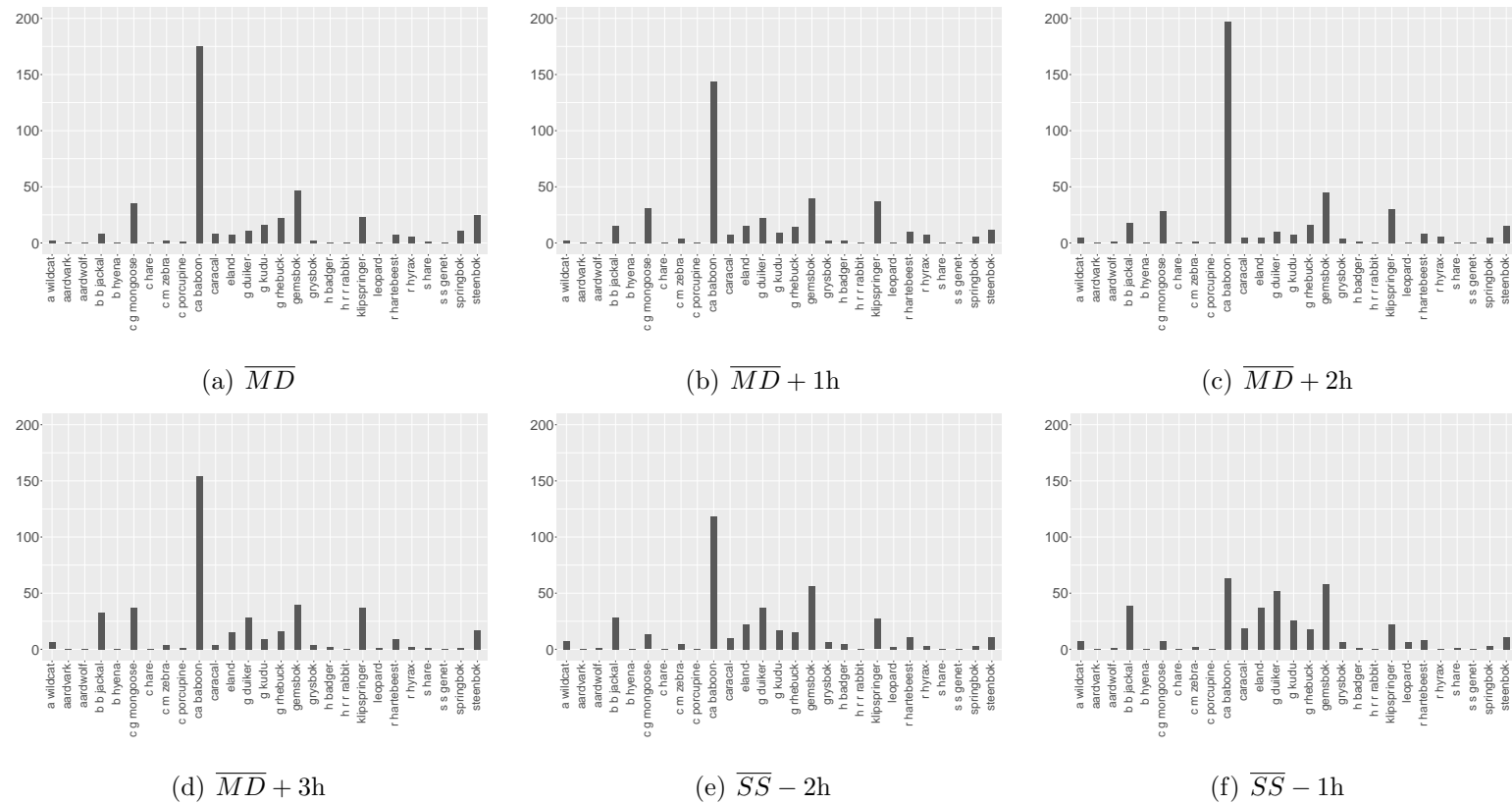
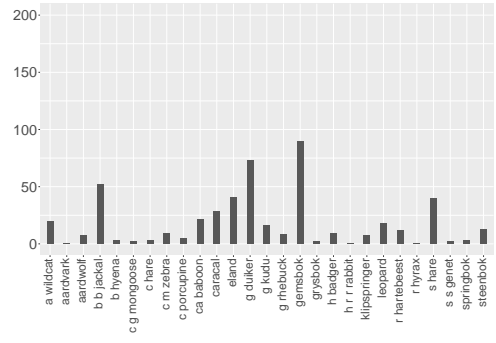
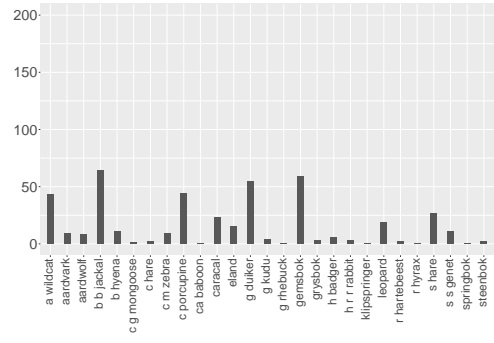


Figure 3.2: Time-profile of mammal activity throughout the 24-hour cycle.

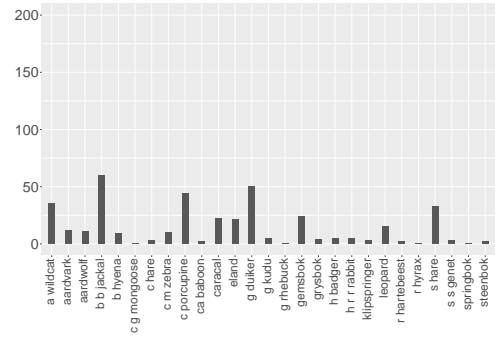
A time-profile is a snapshot of the activity level of the 27 mammal species in the community at time t . The 24 hourly time-profiles provided, for the 27 mammal species, the number of photo-captures recorded during hour H , throughout the study conducted in the Little Karoo.



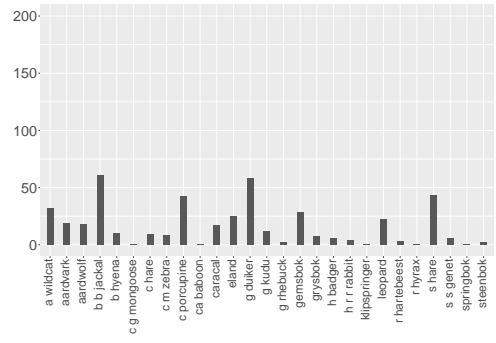
(g) \overline{SS}



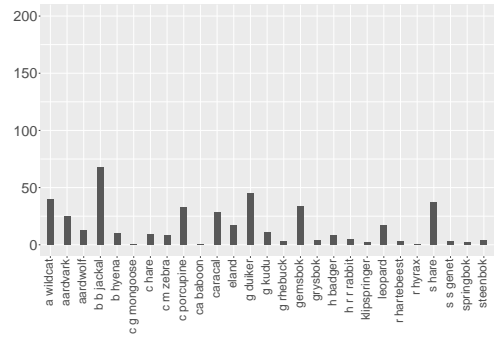
(h) $\overline{SS} + 1h$



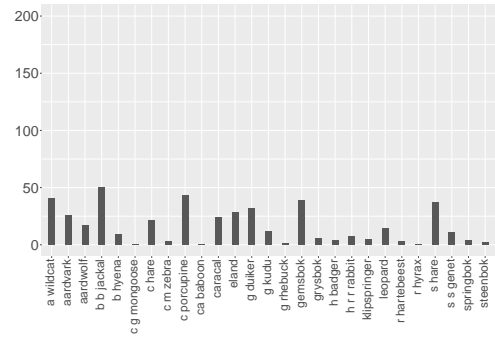
(i) $\overline{SS} + 2h$



(j) $\overline{SS} + 3h$



(k) $\overline{MN} - 2h$



(l) $\overline{MN} - 1h$

Figure 3.2: Time-profile of mammal activity throughout the 24-hour cycle (continued).
A full caption is provided on p146.

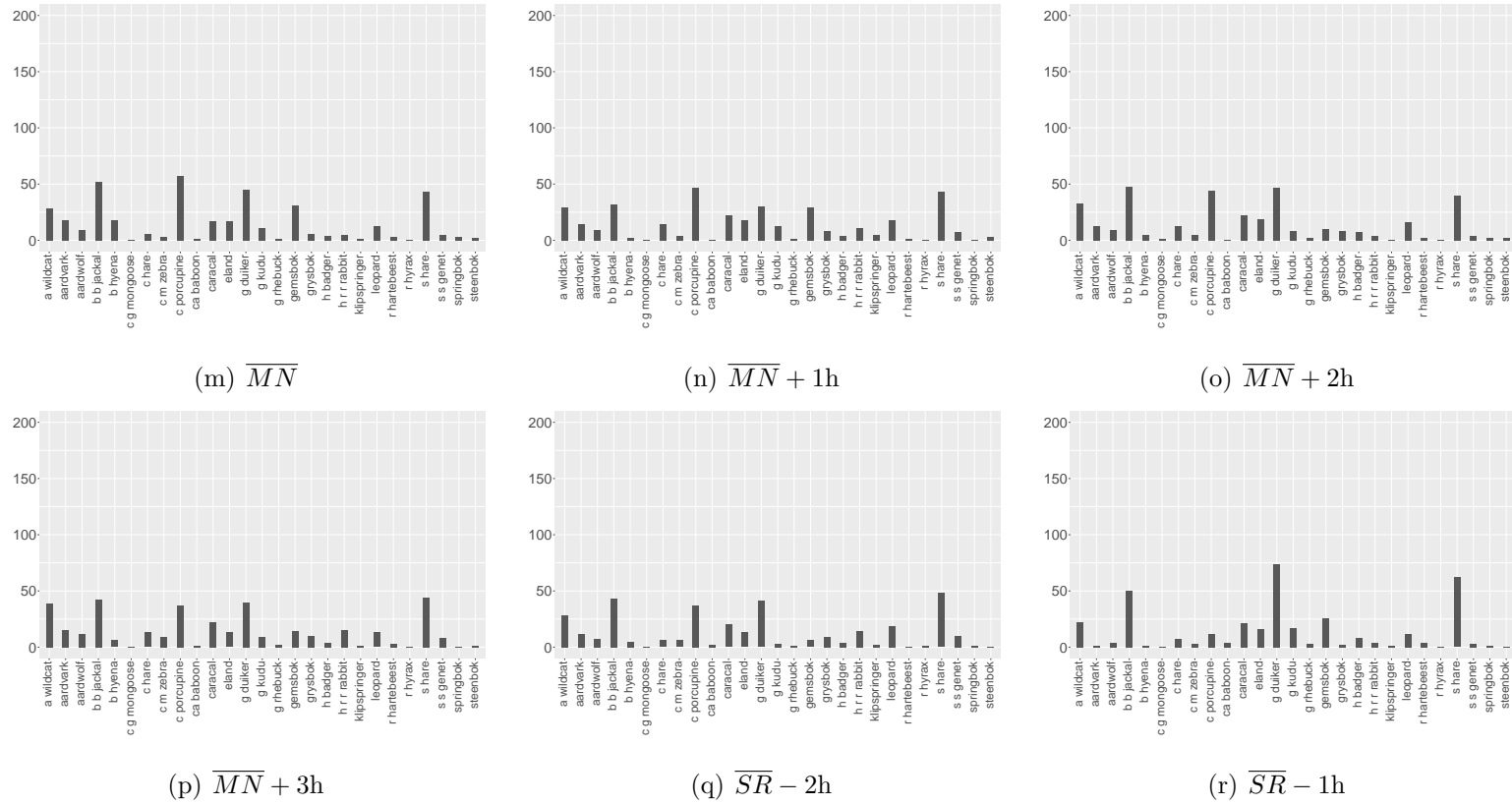
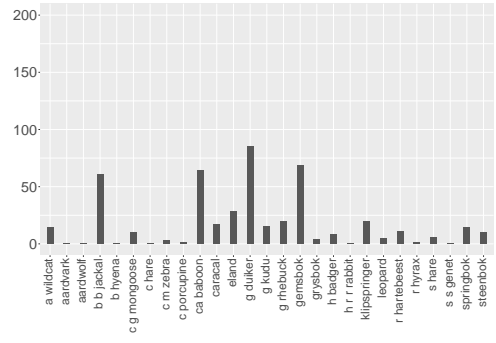
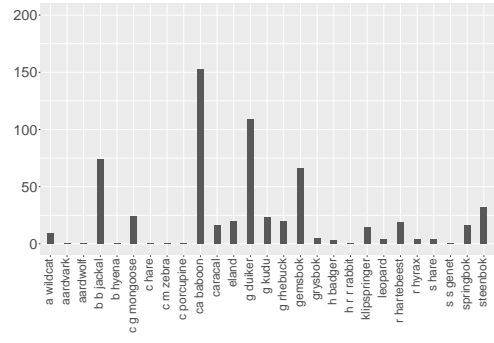


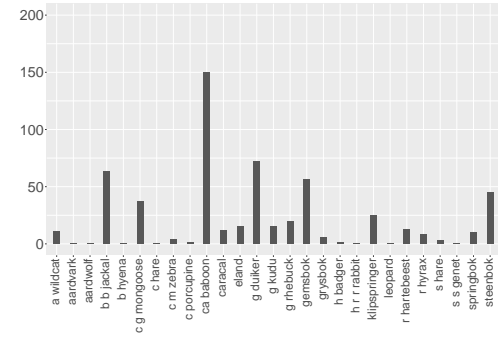
Figure 3.2: Time-profile of mammal activity throughout the 24-hour cycle (continued).
A full caption is provided on p146.



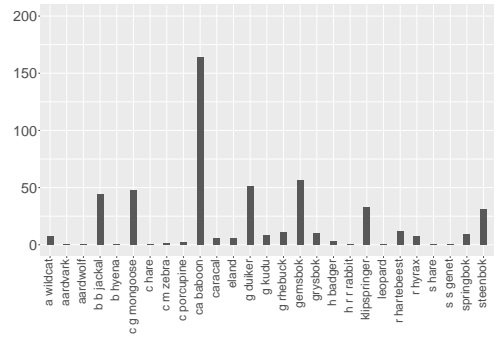
(s) \overline{SR}



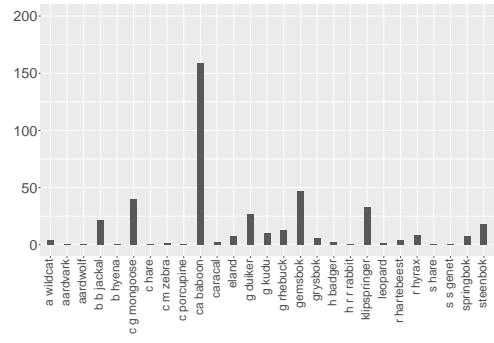
(t) $\overline{SR} + 1h$



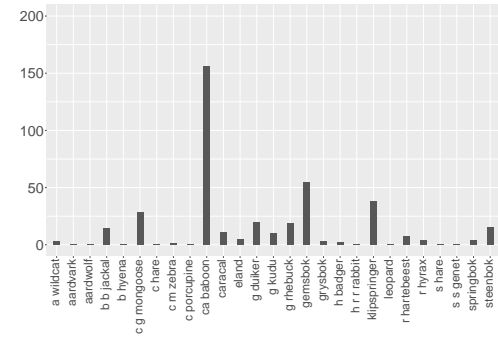
(u) $\overline{SR} + 2h$



(v) $\overline{SR} + 3h$



(w) $\overline{MD} - 2h$



(x) $\overline{MD} - 1h$

Figure 3.2: Time-profile of mammal activity throughout the 24-hour cycle (continued).
A full caption is provided on p146.

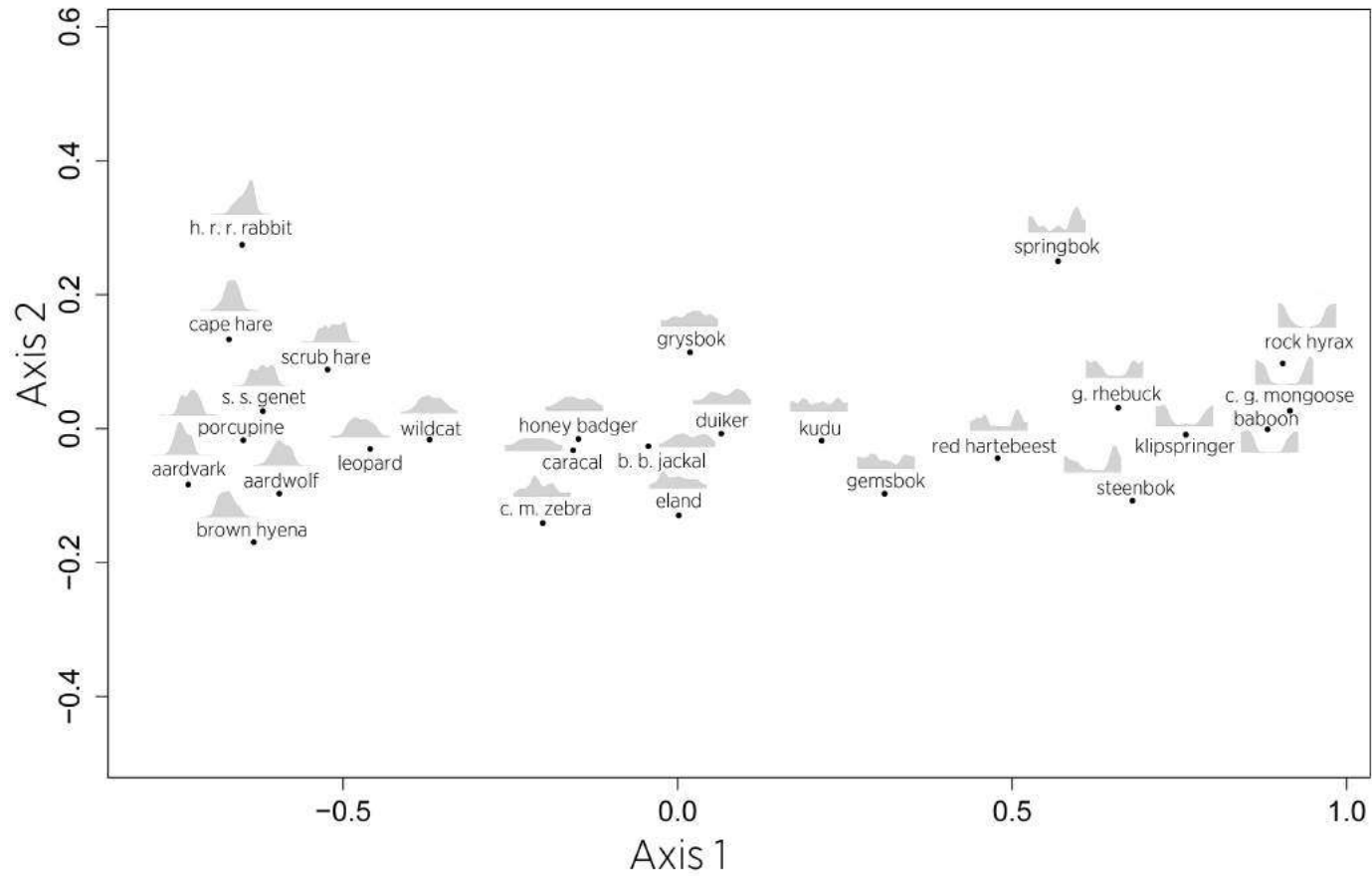


Figure 3.3: Non-metric Multi-Dimensional Scaling.

Dissimilarity study of the 27 mammals' diel activity rhythms in the Little Karoo. The stress value (0.032) indicated good fit. The kernel density functions of the diel activity rhythm of each species have been added to the NMDS display.

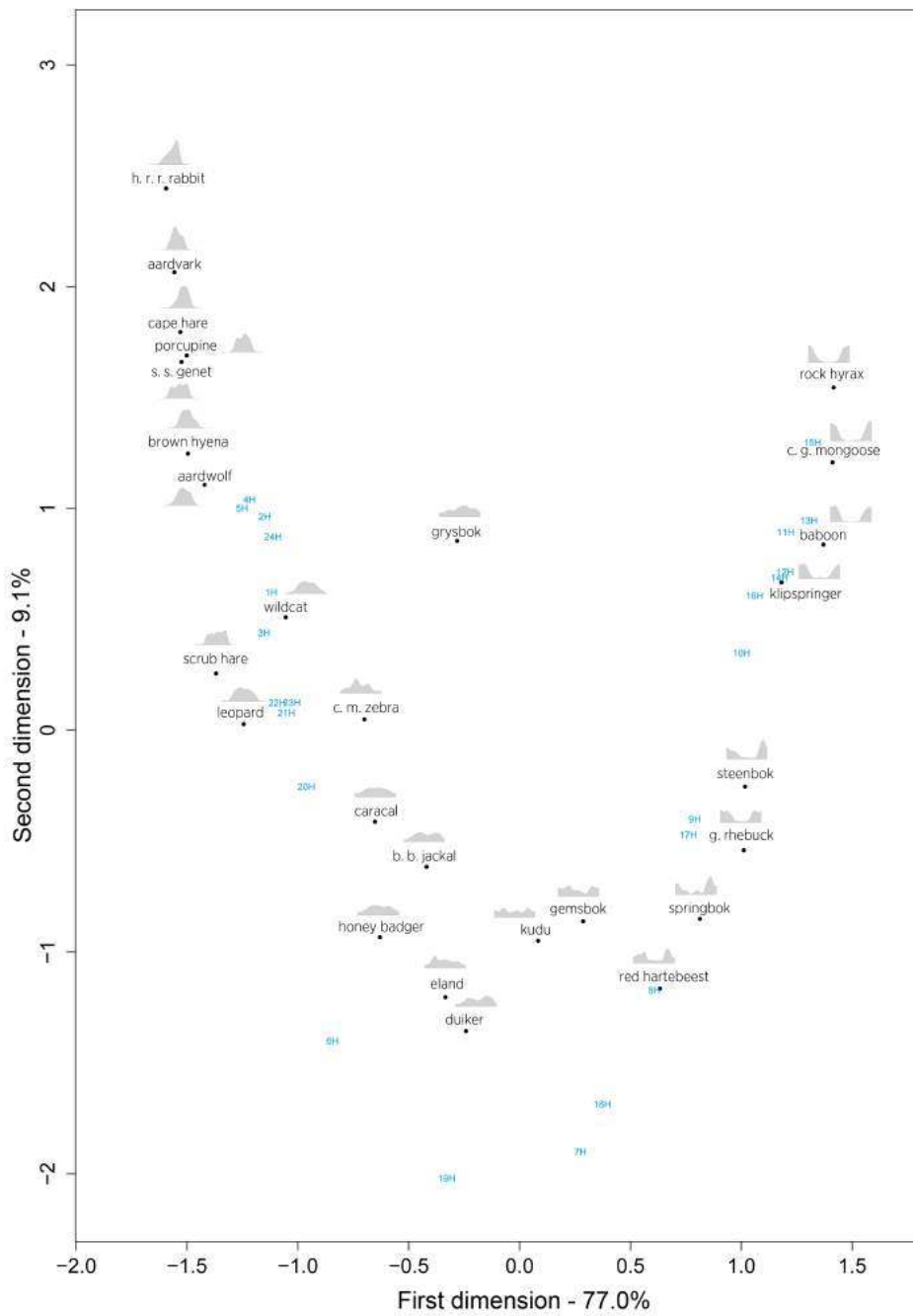


Figure 3.4: Correspondence analysis.

The kernel density functions of the diel activity rhythm of 27 mammal species in the Little Karoo, have been added onto the plot. For each 60-minute time period of the 24-hour cycle of time t' , a time-profile (e.g. Fig. 3.2 p146) summarising the activity level of all species in the community, was plotted in blue. \overline{SR} and \overline{SS} represent the annual average of sunrise and sunset times; \overline{MD} and \overline{MN} represent true midday and midnight for the study area.

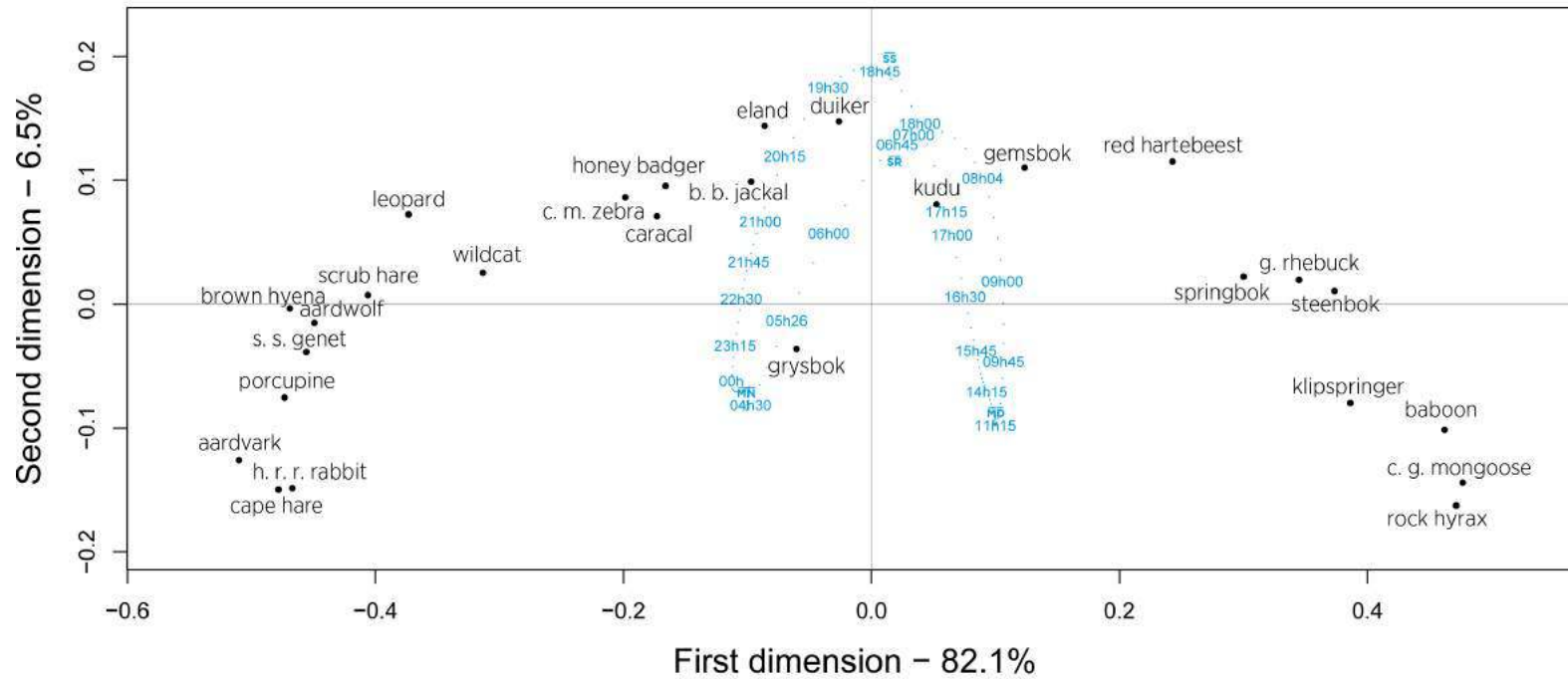
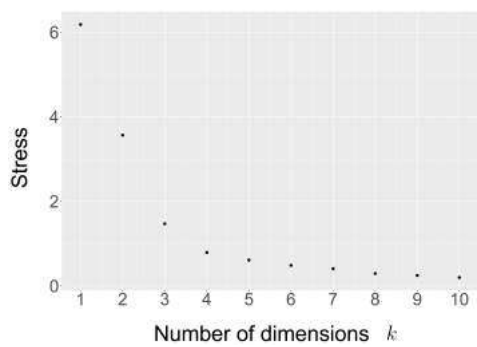
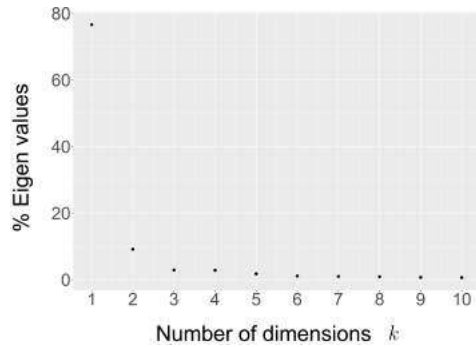


Figure 3.5: Covariance biplot.

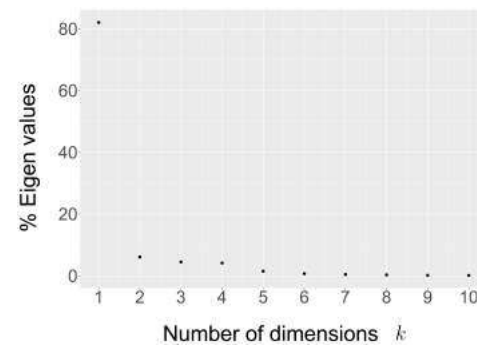
The kernel density functions of the diel activity rhythm of 27 mammal species in the Little Karoo, have been added onto the plot. For each time interval (about 11 minutes) of the 24-hour cycle of time t' , a time-profile (e.g. Fig. 3.2 p146) summarising the activity level of all species in the community, was plotted in blue. \overline{SR} and \overline{SS} represent the annual average of sunrise and sunset times; \overline{MD} and \overline{MN} represent true midday and midnight for the study area.



(a) NMDS



(b) CA



(c) Covariance biplot

Figure 3.6: Screeplots.

Screeplots show, in descending order of magnitude, the eigenvalues of a correlation matrix (or the stress value of an NMDS analysis); they help to visualise the relative importance of the factors and to decide on the adequate number of dimensions used in the analysis.

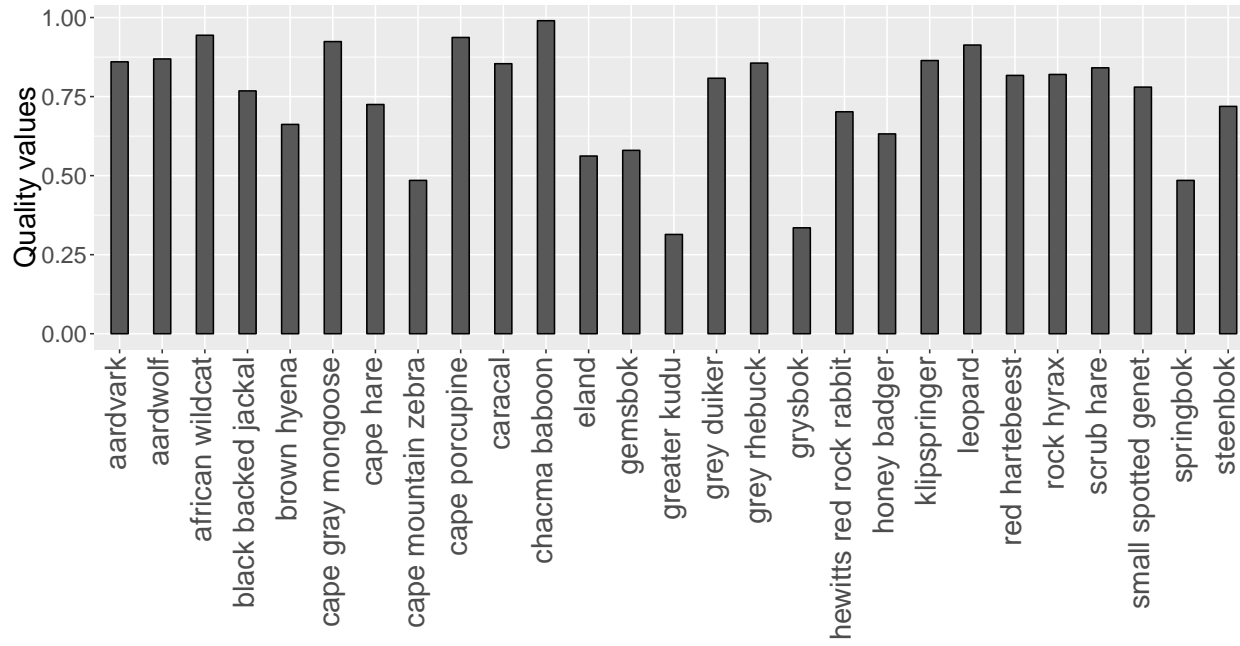


Figure 3.7: Quality values from the correspondence analysis, for the 27 mammal species of the Little Karoo.

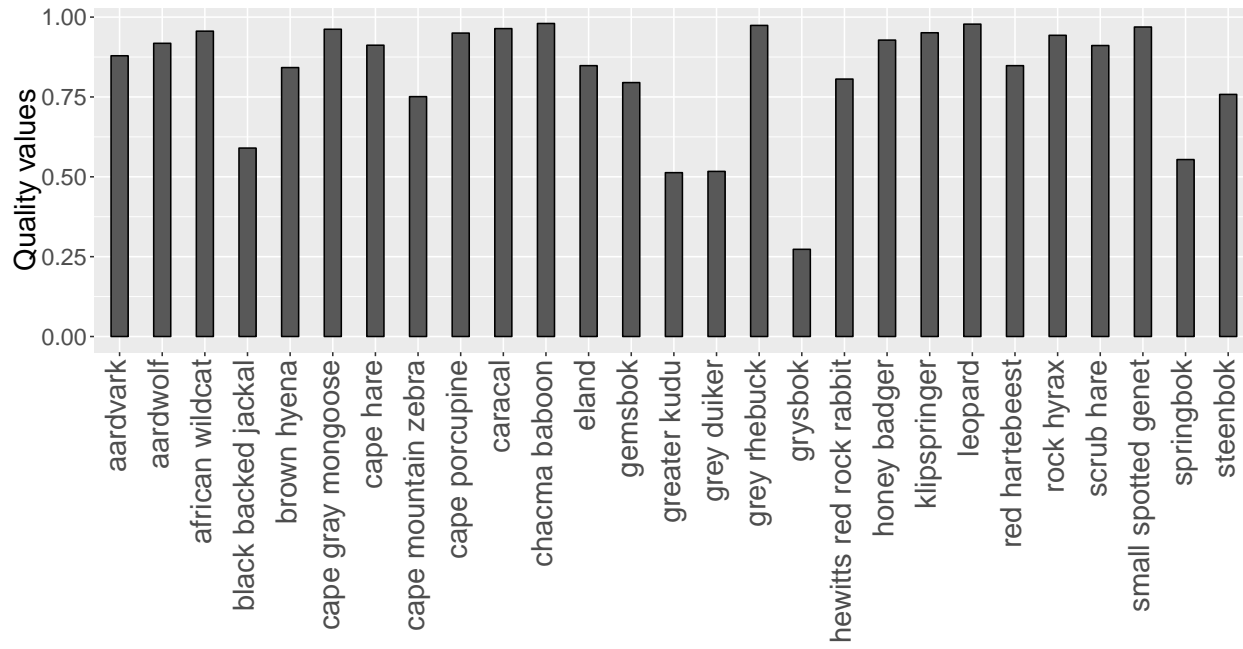
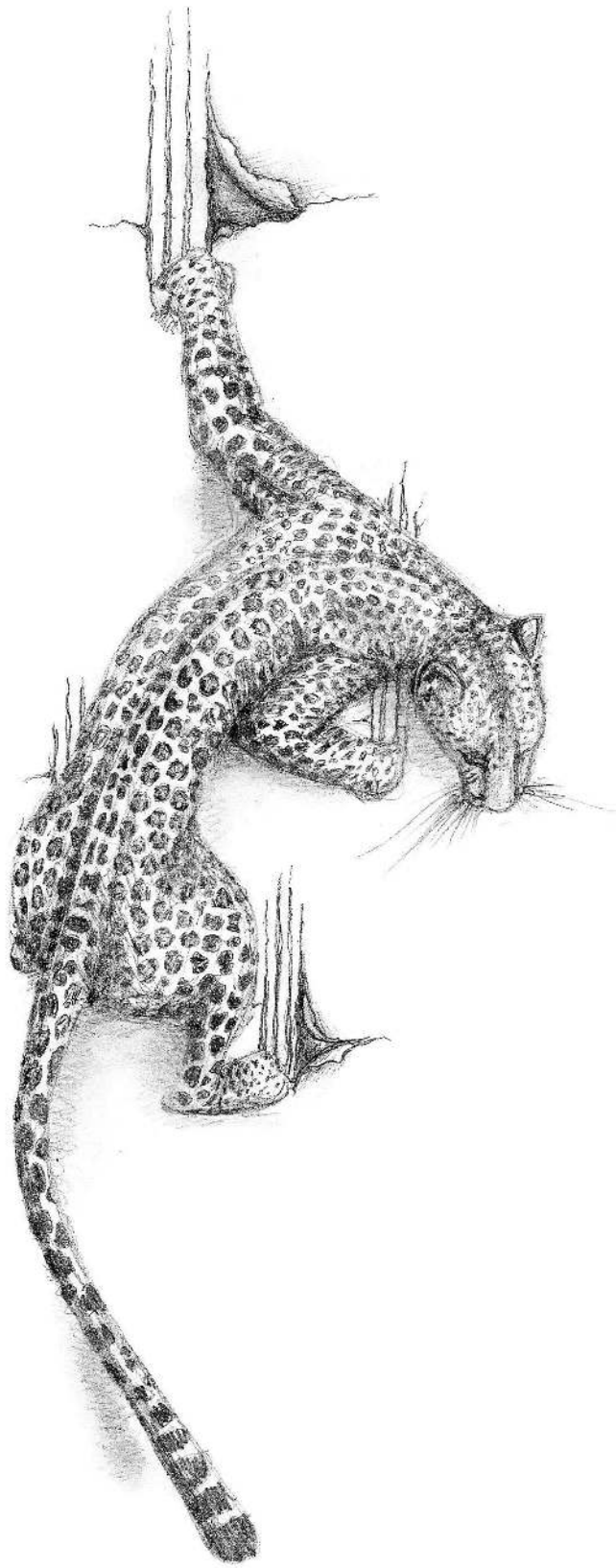


Figure 3.8: Quality values from the covariance biplot analysis, for the 27 mammal species of the Little Karoo.



Estimating leopard population density in relation to terrain ruggedness with spatially explicit capture-recapture models

4.1 Abstract

The best known international system of classifying species at high risk of global extinction is the IUCN (International Union for Conservation of Nature) Red List, which aims to provide an explicit and objective framework to define species conservation status, and which is based on criteria heavily dependent on population size. In the animal kingdom, large carnivorous mammals are of great scientific and conservation interest; however, demographic information is often scarce. In South Africa, leopard *Panthera pardus* demographic data are sparse and usually collected within protected areas; nonetheless, the leopard population is generally thought to be in decline. Most of the Western Cape studies focused on the Cederberg Mountains and few of them investigated topics dealing with habitat preferences and population density. In this study, camera trap systems were used to collect capture-recapture data and to estimate leopard population density in the Little Karoo, using Spatially Explicit Capture-Recapture (SECR) models. Model selection showed that leopard density varied with topographic relief; it increased with ruggedness of the terrain up to an optimum, and followed a reversed trend as the terrain roughness kept increasing. The parameter estimates of the best-

performing model's detection function showed that the leopard population in the Little Karoo was composed of two groups of individuals with significantly different home range sizes, potentially explained by gender duality in movement. The study estimated the leopard population density to be low; density estimates ranged from 0.49 to 0.82 individual per 100 km².

4.2 Introduction

The conservation movement is believed to have started in 1662 when John Evelyn – an English writer, gardener and diarist – submitted a book highlighting the importance of conserving forests to the Royal Society [100]. Due to a number of social and economic factors, the conservation movement only started to gather momentum much later during the 19th century, with the goal to preserve and promote the sustainable use of natural resources [111]. In 1978, an eclectic group of scientists congregated, at what is now called the First International Conference on Conservation Biology, to join forces and save species that were of conservation concern [117]. This event led to a landmark publication in 1980, *Conservation biology: an evolutionary-ecological perspective* [318], and resulted in the creation of a new discipline: conservation biology [347]. One of the most urgent challenges was to develop methods to quantify risk of extinction in order to evaluate whether a species should be listed as endangered. Today, the best known international systems of classifying species at risk of global extinction is the IUCN (International Union for Conservation of Nature) Red List, which aims to provide an explicit and objective framework to define conservation status of species, and which is based on criteria heavily dependent on population size [152].

In the animal kingdom, large carnivorous mammals are of great scientific and conservation interest; however, demographic information is scarce due to challenges rising when conducting research studies on elusive, wide-ranging and low density species [16]. Direct observations and species counts of large carnivores are logistically testing, expensive and time-consuming; several alternative sampling techniques have therefore been developed to estimate their population abundance/density [300, 364]. The most common substitute was to rely on track counts [23, 136, 311], although the methodology remained controversial [20, 66, 322]. Capture-recapture sampling using camera trap data is a method that was first developed to monitor tiger *Panthera tigris* populations in India [163], and is now used extensively worldwide to estimate population density of other individually identifiable species [33, 138, 154, 306, 314, 316, 340].

In southern Africa, leopards are commonly found to be the apex predator outside protected areas, due to their ability to adapt and persist in fragmented habitats and areas that undergo anthropogenic land-use changes [274, 328]. Apex predators are of great ecological importance because they profoundly influence ecosystem structure [69, 286, 335]; however, they commonly are vulnerable and of great conservation concern [14, 274, 335].

In South Africa, leopard demographic data are sparse and usually collected within protected areas [17]; nonetheless, the leopard population is generally thought to be in decline [140, 329]. Scientists focused their leopard research work in the northern parts of the country [17]; the Western Cape Province received relatively little attention [210–213, 248–251, 273, 324, 325]. Most of the Western Cape studies focused on the Cederberg Mountains [210–213, 249] and suffered from small sample sizes and technological limitations [249]. Few of them investigated topics dealing with habitat preferences and population density, although there is an urgent need to provide and monitor baseline estimates of leopard population densities outside protected areas [17].

In this study, camera trap systems were used to collect capture-recapture data and to estimate leopard population density in the Little Karoo, using Spatially Explicit Capture-Recapture (SECR) models [90]. The study considered the impact of specific covariates on density, several submodels were fitted and compared using the Akaike Information Criterion (AIC), an estimator of the relative quality of the collection of statistical models given the data [51, 164, 353]. Submodels were ranked and averaged using Akaike weights. Finally, using the best submodel of the collection, the estimated detection function as well as the relationship between density and selected covariates were quantified and plotted.

4.3 Material and methods

4.3.1 Study area

The Little Karoo is a semi-arid desert located at the southern tip of the African continent [Appendix 1A], within the Cape Fold Belt. It is also described as a mega-ecotone, where the succulent Karoo and the Cape Floristic Provinces intermingle [Introduction, Chapter 1 section 1.3.1].

4.3.2 Data collection

Camera trap data were collected between March 2014 and August 2015 within a study area of 4,327 km² (minimum convex polygon). Digital automated cameras (Cuddeback Attack and Ambush, Cuddeback Inc., Green Bay, Wisconsin, USA) were deployed in units called camera trap stations. Each unit consisted of two camera traps facing one another (slightly off-set to avoid simultaneous flash triggers), positioned at an average height of 40 cm, and at a 90° angle with a linear channel such as gravel roads, animal paths and riverlines, along which large felids are habitually known to move [9, 16, 162, 313]. All camera traps were set to take photos with a one-second delay between consecutive triggers, and with an incandescent flash at night.

The camera trap study was undertaken as a series of six (A, B, C, D, E and F) regional surveys (spatially and temporally separated, Table 4.1, Fig. 4.1). Each survey is referred to as a session.

Temporal constraints: SECR models assume population closure, an assumption which can be troublesome and easily violated [124, 313]. The trend is to restrict the length of the survey period in order to reduce the risks of assumption violation [163, 306]. The leopard's life span (*c.* 10–15 years) is similar to that of other large felids, such as tiger and jaguar *Panthera onca* [146, 326], which is why the use of a short sampling period of three months made the closure assumption tenable [293, 366]. Each sampling block, or session, ran for *c.* three months and camera trap stations were checked once (*c.* 1.5 months, halfway through the survey) to change batteries.

Spatial constraints: Defining the size of the study area and selecting a spatial sampling design were partly driven by a) SECR model assumptions, b) bibliographic knowledge about the home range size of leopards, and c) field-collected information. SECR models assume that all individuals of the targeted population can be detected (i.e. all leopards inhabiting the study area have a probability greater than zero to be photo-captured) [163, 252]. Leopards are well studied in Africa [274] including the northern parts of South Africa [17], and leopard home ranges vary substantially with the productivity of the area in which they occur [11, 35, 189, 233, 320]. Relatively few leopard studies were conducted in the Western Cape, but research in the Cederberg Mountains provided home range estimates spanning from 74 to several hundred square kilometers [210].

Survey A was the first survey of the study. It followed a deployment design using a regular grid that was positioned to maximise the number of camera stations falling onto riverlines [Introduction]. Random locations provided

few to no data at all, and camera trap stations located along river beds were not nearly as successful as that on roads, both in terms of capture frequency and capture diversity. Because of the high number of camera trap stations along river, the region's unpredictable flash floods threatened the study to suffer from recurrent equipment and data losses. The spatial deployment of camera traps was adjusted throughout survey A and the newly developed design was then consistently applied across survey B, C, D, E and F: camera trap stations were deployed on roads and animal paths to maximise chances of photo-capturing medium to large-bodied animals, with a density of two camera trap stations per 50 km². This was achieved using QGIS 2.10.1 software [268] in order to design and place, for each session, a 7 × 7 km grid across the associated portion of the study area, and to select the two final camera trap sites in each grid cell. The design ensured relatively even sampling effort, to satisfy data collection protocols used to estimate population density using SECR models [16, 56, 57, 110]

The first and last surveys (survey A and F) spatially overlapped; survey F consisted of a replicate of survey A, using the newly chosen and standardised protocol.

Data entry was facilitated by the software Camera Base [338]. The final database was exported into Excel and analysed in R Studio, using the R software 3.2.4 [269].

4.3.3 Density Analysis

Population density estimates were provided by SECR models: a statistical method of estimating population density, which is appropriate for data collected with an array of 'detectors' (camera trap stations) [90].

4.3.3.1 SECR background

Capture-recapture studies are commonly used in ecology to estimate animal population size. Conventional capture-recapture models provide species abundance estimates without incorporating any spatial component in inference. To estimate density, an estimate of the Effective Trapping Area (ETA) is required, which is achieved using ad hoc methods subjected to problematic edge effects [29, 89, 110, 256]. The necessity for a spatial component arose from the observation that animal capture probabilities depend on differential utilisation of space [29]. The SECR approach incorporates spatial information on the location of capture into the capture histories and estimates population density directly without needing to estimate an ETA (i.e. density is an explicit parameter appearing in the likelihood function [90]).

4.3.3.2 SECR inference

SECR models can either be implemented into a maximum-likelihood or Bayesian framework [29]; the former method, which allows the use of likelihood-based methods of model selection, was chosen for this analysis [31, 96]. The likelihood can be defined as the joint distribution of the individuals photo-captured and their capture histories [31, 87]. The spatially-explicit maximum likelihood-based approach combines a state model (abundance and distribution of animal home ranges within the landscape) and an observation model (also called spatial detection model). The latter describes the decline in detection probability with distance from the detector to the animal home range centre (activity centre). Among the different functional forms that can be specified for the detection function, the commonly used halfnormal function was selected for this study [96]. Because activity centres are not directly observed, distance is treated like a random effect and conventional distance sampling methods are not used [94].

In this study, models were fitted, using the *secur.fit* function from the *secur* R-package version 3.1.0 [94], by maximizing the full likelihood; which involved integrating all random effects out (i.e. integrating the individuals' activity centres over the unknown locations) [96]. Practically, this was computed by summation over grid cells in the area of integration.

The output of a basic model using a halfnormal detection function gives three parameter estimates: density (D) and two that jointly define the model detection function: g_0 (the intercept; probability to photo-capture an individual if the sensor was located onto the individual's activity centre) and σ (scale parameter indicating how quickly the halfnormal detection function falls away as the distance to detector increases) [94].

4.3.3.3 Sampling occasions

Although camera trap data are usually collected continuously, standard SECR models divide the dataset into discrete sampling occasions (e.g. 24-hour periods), which leads to the so-called midnight problem [161]: individuals photo-captured only a few minutes either side of the cut-off time would be recorded twice in their capture history. In this study, the length of each sampling occasion was defined as a 24-hour trap night (starting from 12:00 (noon) to 11:59 on the following day). Leopards are mainly active during the dark hours of the 24-hour daily cycle – between dusk and dawn [16, 165, 210, 271] [Chapter 2 Fig. 2.7(t) and Chapter 3 Fig. 3.1(u)] – making the chosen sampling occasion match the active period of the leopard's diel activity rhythm.

Due to camera failures, the detector sampling effort varied between occasions. These variations were recorded within a usage matrix $K \times S$, where K is the number of detectors and S the number of occasions. The usage matrix was then used as an attribute of the detector dataset in SECR models and camera failures were taken into account when estimating the parameters of interest [91, 95].

4.3.3.4 Data required

SECR models require two types of primary data (i) the locations of the detectors, and (ii) the detection histories of known individuals on one or more sampling occasions (each entry records the detector at which a known individual was photo-captured at each sample occasion).

With traditional traps (causing animal detention), individuals cannot possibly be caught at more than one trap (i.e. detector) during a sampling occasion; therefore, the detection histories show a 2D structure: individual \times occasion matrix. Camera traps, however, are considered to be ‘proximity detectors’, which means that it is possible for an individual to be caught at more than one detector during a sampling occasion, prompting the detection history to have a 3D structure.

With camera traps, it is also possible for individuals to be photo-captured at a detector more than once per sampling occasion; the records of the detection history are count data and follow a Poisson distribution [94], these models are called encounter rate models. In this study, the leopards were rarely photo-captured more than once per sampling occasion which discouraged their use. Instead, each record followed a Bernoulli distribution and each ‘cell’ of the history contained a binary vector coding presence or absence at each detector [94].

In SECR models, the study area is represented by a ‘mask’, known as the area of integration: a fine net of points across which values are summed and the likelihood is evaluated [31, 92]. The *secr.fit* function in *secr* R-package version 3.1.0 [94] automatically generates a habitat mask by buffering around the detectors. In this study, the automatic mask process was overridden by the use of the *make.mask* function from the *secr* R-package version 3.1.0 [94], which enabled the construction of the habitat mask from a shape file. Using the *addCovariates* function from the same R-package, specific spatial information (e.g. ruggedness) was defined as spatial covariate attributes to the mask [92].

A sequence of preliminary runs was undertaken, using increasing buffer width values to construct the habitat mask of the likelihood integration.

The buffer argument of the *secr.fit* function depends on the scale of animal movement. Making the region too wide should not significantly affect final estimates because activity centres that are distant from the detectors bring minor contribution to the likelihood. Large buffers can however affect the numerical maximisation of the likelihood and lead to slow computation [90]. The smallest buffer value from which the likelihood and estimates were found stable was then used when fitting multiple density submodels.

4.3.3.5 Age and gender

It was not always feasible to reliably age nor to distinguish the sex of photo-captured leopards. Reliably sexing leopards from photographs is possible due to the striking sexual dimorphism of the species [326]. Without a clear view of the external genitalia, it remains feasible to sex leopards by relying on other morphological measurements: cranial morphology, neck circumferences, body length, shoulder height and chest girth [11]. Depending on the photographs and the posture of the leopard, relative dimensions looked unclear and it sometimes became difficult to gauge body size. Balme et al. (2012) showed that while differentiating mature male leopards (≥ 4 year-old) is unambiguous, distinguishing female leopards from young males can create considerable confusion [15]. Due to similar challenges faced in this study, the sexes were analysed together. However, due to expected gender heterogeneity in movement, a different approach (i.e. finite mixture models) was used to account for such heterogeneity [this is dealt with in more detail in Chapter 4 section 4.3.3.7].

4.3.3.6 Leopard identification

Every photo-capture was either defined as a capture-event or as a duplicate [Chapter 1 section 1.3.3], and all duplicates were discarded for this study. Leopard individuals were identified using their fur patterns, which are unique natural markers made of spots and rosettes, comparable to human finger prints. The markers are visible across the body and the inter-individual variation is sufficient to assign identities [4].

4.3.3.7 Covariates

A variety of submodels can be built by allowing the three principal parameters of the model (D , g_0 and σ) to vary with known factors and covariates; examples of model arguments are provided in Table 4.2 and comprehensive instructions and descriptions of these models are provided in Efford. et al (2013) [94].

Fifteen submodels were fitted as part of a first exploratory stage. Only one of the three principal parameters was then allowed to vary with known covariates such as *ruggedness* and *session*. Using the first results of the AIC model selection [51, 164, 353], a set of 12 additional submodels was defined to assess whether more complicated models – assuming more complex biological explanations – would receive more AIC weight. Model computations were performed using facilities provided by the University of Cape Town’s ICTS High Performance Computing team (UCT HPC Cluster): <http://hpc.uct.ac.za>.

ruggedness: spatial covariate

Heterogeneous topographic relief – especially in mountainous regions – often is an essential constituent of the niche of a species [50, 246, 361]. In the Little Karoo, leopards’ strongly avoid even terrain [Chapter 1 section 1.8(u)]; the Terrain Roughness (ruggedness) Index (TRI) [284], calculated using QGIS 2.10.1 software [268], was used as a geospatial covariate of density in SECR models. Using the *addCovariates* function from the *secr* R-package version 3.1.0 [94], spatial covariate TRI was added to the constructed habitat mask.

session: sampling blocks

The study was undertaken as a series of six regional surveys (temporally and spatially separated). In SECR modelling, the six sampling blocks are called ‘sessions’ and are treated independently, ignoring individual photo-recaptures across sessions [93]. The *secr.fit* function fits a multi-session model by maximising the product of session-specific likelihoods [96], and the default is to treat all parameters (D , g_0 and σ) constant across sessions; however, models with session-specific parameters can also be specified. Distinct values of density (D) and detection probabilities (g_0) were also fitted, enabling to calculate different estimates for the six sessions.

Modelling sessions independently implied a loss of information because individual photo-recaptures across sessions were ignored. Alternatively, specifying a single session model would have led to problems with the assumption of demographic closure, which is why this option was not explored.

b: behavioural effect

Models in capture-recapture studies of carnivores commonly include a behavioural effect whereby the detection probability changes after initial capture, especially when it involves retention of the species of interest [61, 102, 256]. Camera traps are non-invasive and although it is not expected that they could affect leopard behaviour, several studies using camera traps to estimate population density confirmed a behavioural response among individuals [30, 355, 356]. In Royle et al. (2009) and Borchers et al. (2014), this response was interpreted as a factor related to trail use rather than an actual

behavioural effect [30, 292]. The hypothesis of a learning process within the animals with respects to detectors was tested in this study by fitting formula ‘ b ’ on g_0 in SECR models [86].

h2: individual heterogeneity

Compared to standard capture-recapture models, SECR models account for some individual heterogeneity due to the incorporation of differential space use among targeted individuals; however, one of the most tenacious problems in capture-recapture studies remains individual heterogeneity: the variation in detection probability among individuals [88]. Whenever possible, this variation is accounted for by grouping individuals into homogeneous classes, e.g. based on gender (male, female) or age (juvenile, adult). When heterogeneity remains, SECR provides finite mixture models that assume latent individual classes. These models calculate, for each class: 1) different detection parameters and 2) the proportion of individuals in the different latent classes [31, 88, 264]. In this study, g_0 and σ were the two parameters modelled with two-class finite mixture models (*h2*). Three-class (*h3*) finite mixture models were also used to test the hypothesis of having capture probabilities varying with three homogeneous classes: 1) adult male, 2) adult female and 3) juveniles. It was chosen not to present the results because *h3* models were not yet fully tested. The *h3* model developer also highlighted the risk of getting stuck on a local maximum of the likelihood during convergence and advised against their use [Efford (2017) personal communication]. Moreover, the standard errors of the parameter estimates were not always estimated or took abnormally high values, suggesting that the models were unstable and did not converge successfully.

4.4 Results

The trapping effort of 17,631 camera trap nights resulted in 26,312 photo-captures of 91 different species. Fifty one (56.04%) species were mammals and 1.34% of all photo-captures were leopards [Appendix 2A].

4.4.1 Descriptive statistics

The study provided 219 photo-captures of leopards, collected at 79 (35%) camera trap stations (Fig. 4.2). Six of these photographs were considered to be dependent events and were discarded; all photographs of the same individual collected within the same trap night following the first photo-capture, at the same location, are considered to be duplicates [Chapter 1 section 1.3.3]. Leopard capture rate was 1.21 in 100 camera trap nights.

Six of the photographs were taken during early mornings, shortly after the automatic deactivation of the incandescent flash, resulting in blurry images and preventing any possible individual identification. These photos were discarded for the purpose of this analysis.

The number of photo-captures collected for each identified individual leopard varied noticeably across the study as a whole (Table 4.3), and across regional surveys (Table 4.4). Among the 219 leopard photo-captures recorded when both cameras of a camera trap station were active, 150 were recorded by both cameras and the remainder by one camera only. It provided a set of 369 photographs (instead of 438 assuming perfect detection). These figures indicate a possible detection failure rate of 15.7% per camera trap, and of 2.4% (0.157^2) per camera trap station.

Based on 207 ($219 - 6 - 6$) photo-captures, twenty nine leopards were identified. Due to detection failures, not all capture events provided simultaneous photos of both flanks of the individuals. This problem was overcome by the collection of photo-recaptures, except for one individual for which only the right flank was recorded. The photo-capture counts and capture histories for the 29 individuals, are respectively provided in Table 4.5 and 4.6.

4.4.2 SECR model selection

The smallest buffer value from which the likelihood and estimates were found to be stable was 10,000 meters; it was therefore defined as such in all sub-models of the first and secondary exploratory stages. Models were ranked according to Akaike's Information Criterion, and AIC weights were calculated [51]. In the first exploratory stage, the finite mixture model that used $h2$ as a covariate of parameter σ (Model 2) was the best-performing one (Table 4.7). In the second exploratory stage, the models that used regression splines for density surface modelling, along with $h2$ and session as covariates of parameter σ (Models 21 and 22) were the best-performing ones (Table 4.8). There was little difference between the AIC weights of Models 21 and 22 (0.01), suggesting that they both fitted the data similarly [332].

4.4.3 Detection function

The two best-performing models, Models 21 and 22, produced respectively 12 and 13 β coefficients estimated on the link scale (Appendix 5A.1 and 5A.2); the real parameter values (fitted values) were calculated by back-transforming the β parameters on the scale given by the link function: log-transformation of D and σ , and logit transformation of $g0$ and $pmix$ (Table 4.9). In this

analysis, the detection function was jointly defined by g_0 (detection probability) and σ (index of home range size), and modelled as a halfnormal function. Models 21 and 22 had the same specified detection functions and their shapes were very similar (Fig. 4.3). In each graph, 12 detection functions were represented further to σ varying with two classes of individuals ($\sim h_2$) and with six sessions ($\sim session$). Two of the 12 curves were difficult to distinguish because they overlapped with other two (very little difference in σ between session B and F). All curves had the same intercept: g_0 (the probability to detect an individual over a 24-hour occasion when the detector is located at its activity centre) which was defined as a constant parameter in both model formulas (Table 4.8) and estimated at 0.029, 95% confidence interval 0.023–0.036 (Table 4.9). Parameter σ varied substantially between the two latent classes of individuals that are quantified by parameter $pmix$ (Table 4.9). In Model 21, with class $h_2 = 1$ making 69% of the population, σ ranged from 1412.04 to 1966.38 m; with class $h_2 = 2$ making 31% of the population, σ ranged from 4414.09 to 7411.48 m. The estimated σ was 3.13 times ($e^{1.14}$, Table 4.9) greater for class 2 compared to class 1, resulting into different shapes of their respective detection functions: in the case of class 2, the function fell away more gradually with distance (class 2 individuals were more detectable at greater distances). The $pmix$ parameter estimated what proportion of the population fell into these latent classes (Table 4.9). Model 21 estimated 69% (95% confidence interval 51–84%) of the population to be in class 1 and 31% (95% confidence interval 16–49%) to be in the second class that has wider ranging movement. Model 22 produced very similar estimates.

4.4.4 Number of individuals

The expected number of leopards N in each of the six regional surveys (A, B, C, D, E and F), estimated by the *region.N* function from the *secr* R-package version 3.1.0 [94], was close between Models 21 and 22 (Table 4.9). With model 22, it ranged from 9.49 individuals in session C (95% confidence interval 6.36–14.11) to 17.11 in session F (95% confidence interval 11.61–25.19). With the multi-session approach, the estimation of leopard abundance was constrained to each session independently, preventing the estimation of a single abundance number of leopards for the study area as a whole. It was not viable to add up the expected number of leopards from each survey due to habitat mask overlap and the fact that individuals caught across more than one survey would be counted twice. The averaged leopard density estimates \bar{D} , computed for each session by dividing the expected number of leopard N by the area of the session's habitat mask, ranged from 0.49 to 0.82 individual

per 100 km² with Model 21, and from 0.51 to 0.82 individual per 100 km² with Model 22 (Table 4.10).

4.4.5 Density maps

The best-performing models, Models 21 and 22, allowed density to vary with spatial covariate *ruggedness* (Table 4.10). Fig. 4.4 shows, for both models, the relationship between the leopard population density in the Little Karoo and the Terrain Ruggedness Index (*ruggedness*). There was a quadratic effect of *ruggedness* on leopard density. With Model 22, the leopard density was estimated around 0.08 leopards per 100 km² in flat terrain, TRI = 10. This density estimate increased with terrain ruggedness (7.73 leopards per 100 km² in moderately-rugged terrain, TRI = 50) up to 20.62 leopards per 100 km² in optimal terrain, TRI = 89. The trend was then reversed and leopard density was estimated around 17.57 leopards per 100 km² in highly-rugged terrain, TRI = 110). Using the constructed habitat masks for the six regional surveys A, B, C, D, E and F (Fig. 4.5), predicted density maps were produced for Model 22 (Fig. 4.6). These maps are choropleth maps: shaded graphical representations in which each geographical area (habitat mask grid cell) had a *ruggedness* value, and was shaded according to its associated density estimate.

4.5 Discussion

Using remote camera trapping in conjunction with SECR modelling, this chapter estimated leopard density in the Little Karoo. The study enabled us to identify 29 leopard individuals in an arid and inaccessible landscape, highlighting the feasibility of using linear channels such as roads and animal paths to sample wide-ranging, low density species such as leopards in the Little Karoo.

Model selection showed that leopard density varied with topographic relief, which is often an essential constituent of the niche of a species [50,246,361]. Leopard density estimates increased with ruggedness of the terrain up to an optimum (20.6 leopards per 100km² in terrain with TRI = 89); it followed a reversed trend as the terrain roughness kept increasing. The two best models were almost identical apart from one extra degree of freedom used in the spline function of Model 22 compared to that of Model 21, which allowed the density-*ruggedness* relationship to fall away more gradually after reaching its optimal peak. These results support the observation developed by Skinner et al. (1990) that leopards of the Western Cape

Province prefer to hunt in rugged and rocky terrain where prey is abundant and where the landscape is more appropriate to stalk, kill [310], and store food items under rocky overhangs. However, this affinity for rugged mountain terrain decreased when TRI exceeded 100, which usually translated into a barren landscape with steep slopes; the decline in leopard density might be explained by a drop of prey presence due to the reduction in vegetation cover, and by difficulties in manoeuvring successful hunts in steep and rugged rockslide areas.

The parameter estimates of the best-performing model's detection function showed that the leopard population in the Little Karoo was composed of two groups of individuals with significantly different σ parameters (3.13 to 1 ratio), which can be used as an index of home range. Using the estimated values of σ and the formula $HR = 2.45^2 \cdot \pi \cdot \sigma^2$ [53], the 95% home range area for the individuals of the two latent classes ranged from 37.88 km² to 106.72 km² (less mobile group), and from 370.18 km² to 1043.53 km² (more mobile group) across the six sessions. In the Cederberg Mountains, male leopards were found to range across areas 4.4 times larger than that of females, and female home ranges were entirely incorporated into that of males [213]. Gender differences in movement could also be explained by males moving in a more linear fashion to patrol their territories and keep other competing males away from potential mating females [213], while females were observed to move in an unpredictable and undefined manner while searching for food [184]. This gender duality in home range sizes could also explain the individual heterogeneity observed in the Little Karoo as well as the associated and uneven population ratio (69–31%); slightly more than two third of the leopard population would be females with home ranges incorporated into that of territorial males, the latter making for slightly less than one third of the population. This could however not be tested because it was not always feasible to reliably sex photo-captured leopards.

Model selection showed that g_0 , the probability to detect an individual over a 24-hour occasion when the detector is located at its activity centre, was constant and did not vary with latent classes (h_2). This was expected because of the absence of explicit biological explanation to justify individual heterogeneity in detection probability at the activity centre.

The parameter estimates of the best-performing model's detection function also showed that σ (i.e. leopard home range) varied across sessions. Because the series of six sessions was spatially and temporally separated, several factors could have affected leopard movement including seasonality (the view that leopards use the landscape differently in summer and winter is

widely held by farmers [249]), land-use, prey availability/catchability (Balme et al. showed a degree of specialisation in leopard's feeding habitat selection likely to influence local use of the landscape [13]) and other spatial covariates differing from ruggedness.

Differences in ruggedness between the habitat masks of each session could have led to the density parameter estimate (D) varying between sessions. However, *ruggedness* was used in the spatial model for density, and, in the presence of this covariate, the *session* variable did not appear to contain further important information about density, explaining why *session* was then not selected as a factor affecting density.

Leopard density being defined as a function of ruggedness, it was more appropriate to provide density maps than a single accurate estimate of density for the study area as a whole. However, in order to compare those results to bibliographical leopard density estimates previously calculated within the Western Cape Province, averaged leopard density estimates \bar{D} were computed. Those estimates, ranging from 0.49 to 0.82 leopard individuals per 100 km², were similar but smaller than those provided by Martins (2010) for the leopard population of the Cederberg Mountains (1.1–1.5 individuals per 100 km²), and by Mann (2014) for the leopard population of the eastern section of the Little Karoo (1.18 individuals per 100 km²) [208, 213]. Martins (2010) surveyed portions of the Cederberg Mountains where the human population (<http://www.statssa.gov.za>, 2017) and the degree of human disturbance were smaller than in the Little Karoo [213], which could have contributed to greater leopard densities. The eastern section of the Little Karoo, surveyed by Mann (2014), is more mountainous than our study site and might provide more suitable habitat for leopards.

Carnivore population density is usually closely related to the density of available prey [57]. The landscapes of the Western Cape Province cannot support large herds of herbivores because the nutrient-poor soils on which the vegetation grows do not provide enough nitrogen for the protein requirements of large herds, and prey densities remain low [34, 196, 270]. This could explain the low density of leopard population in the Little Karoo [212, 213, 251], as well as the small body size of the leopards in the Cape Fold Belt [11, 213].

4.6 Tables

Table 4.1: Camera trap deployment

Given the vastness of the study area in the Little Karoo, the camera trap study was undertaken as a series of six regional surveys: A, B, C, D, E and F. For example, survey C consisted of 34 camera trap stations deployed following a grid-layout, with an average camera spacing of 3265 m. It ran for 102 nights, during which 19 leopard photo-captures were collected and four leopard individuals were identified.

	A	B	C	D	E	F
Camera trap stations	57	38	34	31	30	32
Camera spacing (m)	2122	3330	3265	3253	3817	3531
Occasions	120	103	102	113	95	104
Detections	45	26	19	23	46	48
Individuals	6	5	4	7	10	10

Table 4.2: Model arguments in *secur.fit*

The formula for any detection parameter (g_0 , D , σ) may be constant (~ 1 , the default) or some combination of terms in standard R formula notation. For example, $g_0 \sim b+h2$ specifies a model with a learned response and a 2-class finite mixture for heterogeneity.

Parameter predictors	Information
g_0, detection probabilities	
~ 1	g_0 is constant across animals, occasions and detectors
$\sim session$	session-specific g_0
$\sim b$	learned response
$\sim h2$	2-class finite mixture for heterogeneity in g_0
D, density	
~ 1	density is constant
$\sim session$	session-specific density
$\sim ruggedness$	ruggedness affects density in a linear manner
$\sim ruggedness + ruggedness^2$	ruggedness affects density in a quadratic manner
$\sim spline(ruggedness, k)$	ruggedness affects density according to a spline regression
sigma, detection function	
~ 1	sigma is constant across animals, occasions and detectors
$\sim h2$	2-class finite mixture for heterogeneity in sigma
$\sim session$	session-specific sigma

Table 4.3: Photo-capture heterogeneity

The total number of photo-captures collected in the Little Karoo for each identified individual leopard varied noticeably, ranging from one to 54. For example, seven individuals were photo-captured once, while four other individuals were photo-captured twice. The most photo-captured individual of all identified leopards was photographed 54 times.

Photo-capture categories	1	2	3	5	7	8	11	12	13	14	20	22	54
Number of individuals	7	4	4	5	1	1	1	1	1	1	1	1	1

Table 4.4: Photo-capture heterogeneity in each survey

The number of identified leopard individuals in the Little Karoo and associated photo-captures varied across surveys. For example, 20 photo-captures collected throughout survey C enabled to identify four leopard individuals. Two of them were photo-captured twice, one was photo-captured three times, whereas the fourth one was photo-captured 13 times.

Survey	Number.of	Cat1	Cat2	Cat3	Cat4	Cat5	Cat6	Tot.capt	Tot.ind
Survey A	captures	1	2	3	7	31		45	
	individuals	2	1	1	1	1			6
Survey B	captures	1	4	9	11			26	
	individuals	2	1	1	1				5
Survey C	captures	2	3	13				20	
	individuals	2	1	1					4
Survey D	captures	1	2	3	5	10		23	
	individuals	3	1	1	1	1			7
Survey E	captures	1	2	3	5	12	13	49	
	individuals	1	2	3	2	1	1		10
Survey F	captures	1	2	3	7	8	23	50	
	individuals	4	1	2	1	1	1		10

Table 4.5: Photo-capture counts

Several leopard individuals of the Little Karoo were photo-captured across several surveys (e.g. LEO 10 was photo-captured nine times throughout survey B and 13 times throughout survey C). NONID accounts for photo-captures that did not allow individual identification.

Individual	A	B	C	D	E	F	Total	Individual	A	B	C	D	E	F	Total
LEO 01	2						2	LEO 16				1	13		14
LEO 02	31					23	54	LEO 17				3	5		8
LEO 03	1						1	LEO 18				2			2
LEO 04	7				12	1	20	LEO 19				1			1
LEO 05	1						1	LEO 20					5		5
LEO 06	3					8	11	LEO 21					3		3
LEO 07		11		1		1	13	LEO 22					1		1
LEO 08		4				1	5	LEO 23					2		2
LEO 09		1					1	LEO 24					2	3	5
LEO 10		9	13				22	LEO 25					3	2	5
LEO 11		1					1	LEO 26					3		3
LEO 12			2	10			12	LEO 27						3	3
LEO 13			2				2	LEO 28						7	7
LEO 14			3				3	LEO 29						1	1
LEO 15				5			5	NONID	1	1		1	2	1	6

Table 4.6: Photo-capture histories

After assigning leopard identities in the Little Karoo, photo-capture histories were built by listing for each photo-capture: 1) the camera trap station (e.g. A43) and 2) the sampling occasion (e.g. 009). The first letter of the camera trap station ID indicates the survey ID (e.g. A43 is a camera trap station deployed during survey A). Leopard LEO 01 was photo-captured twice during survey A, at camera trap station A43 on the 9th camera trap night, as well as at camera trap station A42 on the 72nd camera trap night.

Individual	History						
LEO 01	A43 (009)	A42 (072)					
LEO 02	A04 (005)	A02 (011)	A43 (030)	A04 (035)	A29 (041)	A33 (046)	A29 (052)
	A29 (061)	A33 (065)	A04 (066)	A20 (067)	A43 (069)	A29 (069)	A04 (071)
	A33 (074)	A23 (081)	A24 (084)	A39 (085)	A43 (086)	A29 (093)	A11 (094)
	A24 (095)	A29 (096)	A24 (102)	A23 (102)	A11 (102)	A11 (103)	A23 (106)
	A11 (111)	A11 (114)	A39 (117)	F16 (009)	F22 (017)	F17 (032)	F28 (033)
	F16 (036)	F17 (037)	F16 (042)	F11 (043)	F20 (047)	F17 (053)	F11 (064)
	F04 (064)	F14 (067)	F14 (067)	F26 (072)	F20 (072)	F17 (083)	F16 (090)
	F06 (094)	F17 (095)	F04 (095)	F20 (101)	F16 (101)		
LEO 03	A01 (110)						
LEO 04	A06 (013)	A17 (085)	A39 (086)	A11 (094)	A11 (095)	A39 (96)	A01 (117)
	E04 (020)	E14 (026)	E20 (033)	E20 (033)	E12 (034)	E02 (041)	E07 (041)
	E13 (043)	E07 (060)	E08 (075)	E02 (079)	E11 (082)	F13 (086)	
LEO 05	A05 (097)						
LEO 06	A29 (011)	A29 (051)	A29 (073)	F16 (011)	F17 (022)	F16 (049)	F17 (054)
	F16 (067)	F17 (095)	F17 (095)	F17 (099)			
LEO 07	B03 (024)	B06 (031)	B11 (032)	B03 (033)	B03 (051)	B03 (059)	B05 (061)
	B12 (062)	B03 (075)	B06 (089)	B12 (091)	D05 (075)	F31 (058)	
LEO 08	B03 (006)	B03 (021)	B03 (029)	B01 (078)	F19 (014)		
LEO 09	B06 (087)						
LEO 10	B35 (022)	B36 (023)	B37 (053)	B36 (054)	B37 (089)	B36 (089)	B37 (090)
	B36 (093)	B37 (094)	C26 (002)	C16 (014)	C15 (017)	C15 (017)	C26 (021)
	C15 (030)	C22 (034)	C26 (045)	C18 (051)	C16 (064)	C19 (065)	C19 (086)
	C16 (091)						
LEO 11	B36 (100)						
LEO 12	C08 (021)	C08 (039)	D28 (007)	D29 (019)	D28 (026)	D28 (037)	D31 (041)
	D31 (046)	D28 (079)	D29 (092)	D28 (095)	D31 (097)		
LEO 13	C25 (063)	C25 (087)					
LEO 14	C29 (047)	C19 (076)	C29 (082)				
LEO 15	D31 (007)	D28 (012)	D28 (024)	D28 (025)	D28 (094)		
LEO 16	D19 (028)	E29 (018)	E22 (022)	E27 (028)	E29 (029)	E29 (041)	E29 (041)
	E21 (043)	E25 (043)	E29 (047)	E22 (059)	E29 (063)	E29 (073)	E29 (088)
LEO 17	D14 (008)	D15 (009)	D14 (040)	E15 (021)	E20 (024)	E20 (033)	E20 (063)
	E20 (085)						
LEO 18	D29 (039)	D29 (075)					
LEO 19	D15 (028)						
LEO 20	E27 (009)	E28 (023)	E26 (032)	E30 (068)	E27 (086)		
LEO 21	E29 (004)	E29 (011)	E25 (019)				
LEO 22	E22 (013)						
LEO 23	E30 (039)	E30 (071)					
LEO 24	E02 (046)	E02 (046)	F03 (017)	F02 (066)	F03 (078)		
LEO 25	E04 (020)	E03 (047)	E03 (085)	F13 (028)	F09 (029)		
LEO 26	E12 (009)	E14 (026)	E10 (091)				
LEO 27	F27 (041)	F27 (046)	F27 (095)				
LEO 28	F17 (006)	F16 (029)	F17 (054)	F16 (071)	F21 (084)	F17 (085)	F17 (095)
LEO 29	F09 (070)						
NON ID	A04 (043)	B36 (086)	D20 (007)	E03 (076)	E07 (083)	F20 (084)	

Table 4.7: AIC model selection, phase one

Fifteen models – where only one of the three principal parameters (g_0 , D , σ) was allowed to vary with covariates, were fitted and then compared using the Akaike Information Criterion (AIC), an estimator of the relative quality of the collection of statistical models given the data [51, 164, 353].

Model	$g_0 \sim$	$D \sim$	$\sigma \sim$	ΔAIC	AIC weight
1	1	1	1	31.82	0
2	1	1	h_2	0.00	1
3	<i>session</i>	1	1	27.67	0
4	<i>b</i>	1	1	31.20	0
5	h_2	1	1	16.73	0
6	$b + h_2$	1	1	16.18	0
7	1	<i>session</i>	1	30.07	0
8	1	<i>ruggedness</i>	1	29.55	0
9	1	<i>ruggedness + ruggedness²</i>	1	29.55	0
10	1	<i>spline(ruggedness, k=3)</i>	1	25.03	0
11	1	<i>spline(ruggedness, k=4)</i>	1	25.00	0
12	1	<i>ruggedness + session</i>	1	28.26	0
13	1	<i>ruggedness + ruggedness² + session</i>	1	28.26	0
14	1	<i>spline(ruggedness, k=3) + session</i>	1	25.03	0
15	1	<i>spline(ruggedness, k=4) + session</i>	1	24.99	0

Table 4.8: AIC model selection, phase two

Twenty-seven models were fitted and then compared using the Akaike Information Criterion (AIC), an estimator of the relative quality of the collection of statistical models given the data [51, 164, 353].

Model	$g_0 \sim$	$D \sim$	$\sigma \sim$	ΔAIC	AIC weight
1	1	1	1	47.21	0.00
2	1	1	$h2$	15.39	0.00
3	<i>session</i>	1	1	43.05	0.00
4	b	1	1	46.59	0.00
5	$h2$	1	1	32.12	0.00
6	$b + h2$	1	1	31.57	0.00
7	1	<i>session</i>	1	45.45	0.00
8	1	<i>ruggedness</i>	1	44.94	0.00
9	1	<i>ruggedness + ruggedness²</i>	1	44.94	0.00
10	1	<i>spline(ruggedness, k=3)</i>	1	40.41	0.00
11	1	<i>spline(ruggedness, k=4)</i>	1	40.39	0.00
12	1	<i>ruggedness + session</i>	1	43.65	0.00
13	1	<i>ruggedness + ruggedness² + session</i>	1	43.65	0.00
14	1	<i>spline(ruggedness, k=3) + session</i>	1	40.41	0.00
15	1	<i>spline(ruggedness, k=4) + session</i>	1	40.38	0.00
16	1	1	$h2 + session$	9.00	0.00
17	1	1	$h2 * session$	4.57	0.04
18	1	<i>session</i>	$h2 + session$	6.28	0.02
19	1	<i>ruggedness</i>	$h2 + session$	5.77	0.02
20	1	<i>ruggedness + ruggedness²</i>	$h2 + session$	5.77	0.02
21	1	<i>spline(ruggedness, k=3)</i>	$h2 + session$	0.08	0.42
22	1	<i>spline(ruggedness, k=4)</i>	$h2 + session$	0.00	0.43
23	1	<i>session</i>	$h2$	13.47	0.00
24	1	<i>ruggedness</i>	$h2$	11.91	0.00
25	1	<i>ruggedness + ruggedness²</i>	$h2$	11.91	0.00
26	1	<i>spline(ruggedness, k=3)</i>	$h2$	6.67	0.02
27	1	<i>spline(ruggedness, k=4)</i>	$h2$	6.61	0.02

Table 4.9: Parameter estimates

The table provides, for Model 21 (left) and 22 (right), the real parameter estimates (fitted value) for g_0 , σ and the mixing proportion $pmix$ of the two classes defined by h_2 . It also gives estimates of the expected number N of leopard individuals occurring in each session taking place in the Little Karoo.

	Estimate	SE	LCL	UCL	Estimate	SE	LCL	UCL
g_0	0.029	0.003	0.023	0.036	0.029	0.003	0.023	0.036
σ , session A, $h_2 = 1$	1412.042	212.918	1052.490	1894.423	1413.060	213.700	1052.300	1897.400
σ , session A, $h_2 = 2$	4414.093	378.506	3732.373	5220.328	4408.654	376.734	3729.927	5210.888
σ , session B, $h_2 = 1$	1869.391	316.400	1344.770	2598.678	1875.100	316.615	1349.976	2604.674
σ , session B, $h_2 = 2$	5843.785	613.525	4759.632	7174.887	5850.349	613.203	4766.598	7180.550
σ , session C, $h_2 = 1$	2370.888	407.251	1697.307	3311.780	2376.426	409.934	1698.897	3324.157
σ , session C, $h_2 = 2$	7411.480	970.639	5739.864	9569.919	7414.259	964.712	5751.452	9557.802
σ , session D, $h_2 = 1$	1559.817	276.636	1104.789	2202.258	1572.580	278.900	1138.330	2220.293
σ , session D, $h_2 = 2$	4876.045	807.224	3532.675	6730.259	4906.352	801.702	3569.331	6744.202
σ , session E, $h_2 = 1$	1966.382	344.681	1398.269	2765.318	1969.800	347.937	1397.287	2777.089
σ , session E, $h_2 = 2$	6146.980	574.513	5120.108	7379.798	6145.840	581.544	5107.596	7395.133
σ , session F, $h_2 = 1$	1865.298	232.937	1461.711	2380.310	1863.453	233.525	1459.025	2379.985
σ , session F, $h_2 = 2$	5830.987	542.622	4860.730	6994.920	5813.826	539.125	4849.508	6969.897
$pmix$	0.696	0.086	0.507	0.836	0.694	0.085	0.508	0.834
N , session A	15.256	2.971	10.453	22.266	15.425	3.012	10.558	22.535
N , session B	10.342	2.261	6.772	15.794	10.022	2.172	6.586	15.251
N , session C	9.649	1.936	6.537	14.244	9.486	1.943	6.375	14.113
N , session D	10.691	2.345	6.991	16.350	10.435	2.190	6.947	15.675
N , session E	14.615	2.983	9.837	21.715	14.489	2.901	9.824	21.370
N , session F	16.710	3.533	11.091	25.174	17.105	3.412	11.614	25.192

Table 4.10: Averaged density estimates \bar{D}

The table provides, for Model 21 (left) and 22 (right), the expected number N of leopard individuals occurring in each session of the Little Karoo, as well as the resulting averaged leopard density estimate, \bar{D} , given in number of individuals per 100 km².

	Mask Area (km ²)	N	\bar{D}	N	\bar{D}
session A	1870	15.26	0.82	15.42	0.82
session B	2036	10.34	0.51	10.02	0.49
session C	1860	9.65	0.52	9.49	0.51
session D	1880	10.69	0.57	10.44	0.56
session E	2190	14.62	0.67	14.49	0.66
session F	2076	16.71	0.81	17.11	0.82

4.7 Figures

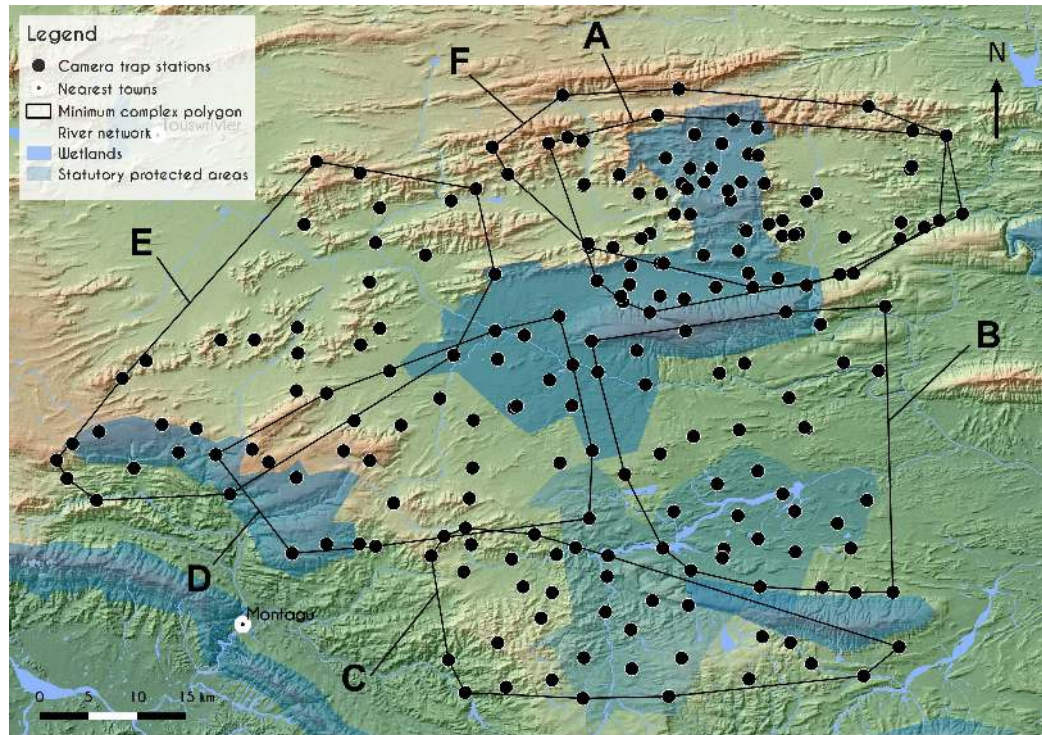
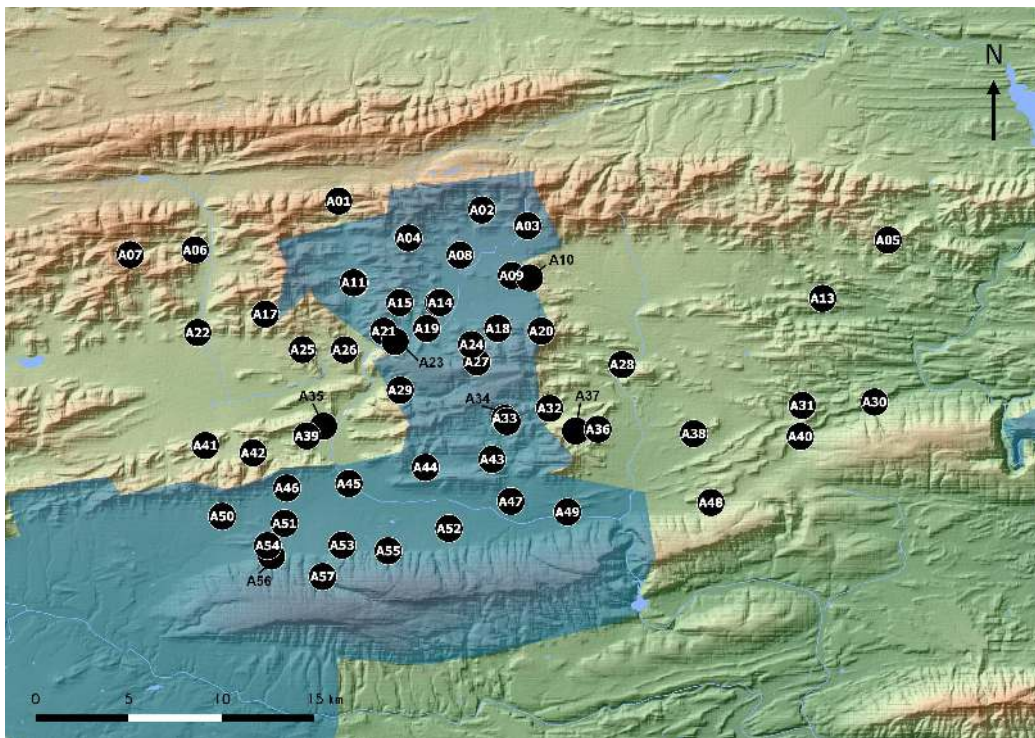
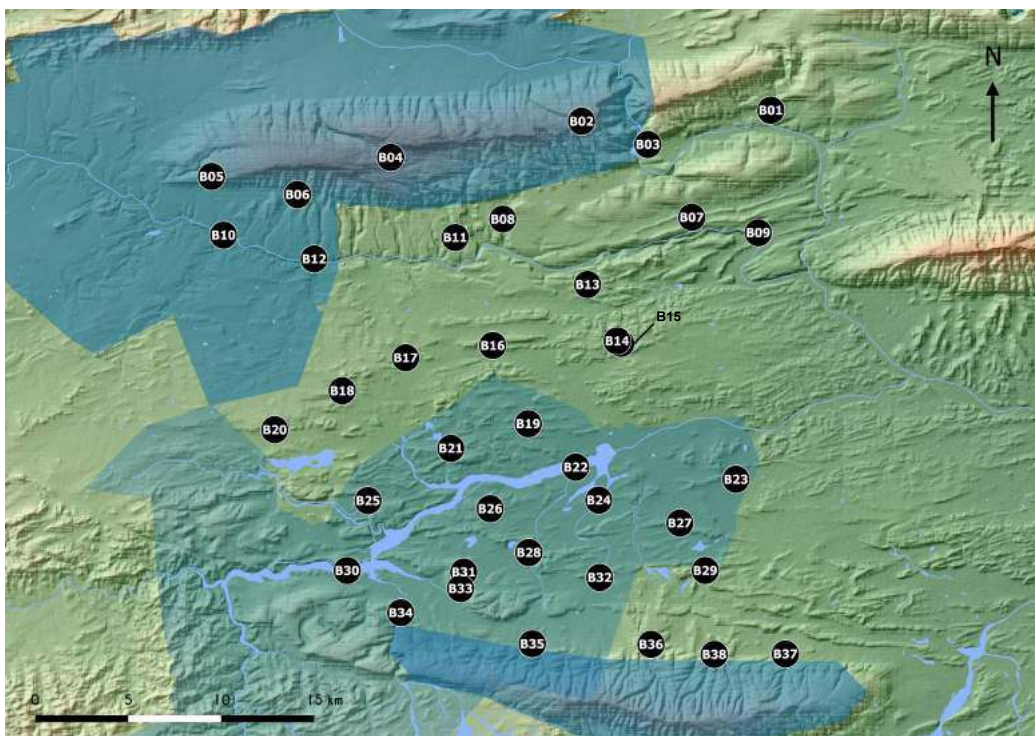


Figure 4.1: Sampling design.

Given the vastness of the study area ($4,327 \text{ km}^2$) in the Little Karoo, the camera trap study was conducted as a series of six, three-month long, regional surveys (temporally and spatially separated): survey A, B, C, D, E and F. Every dot represents a camera trap station. Two months in survey A, the Little Karoo was hit by the worst flooding since 1981. The water level washed away 20 camera traps (a third), which were never to be found again. Survey A then led to redraw the scientific design and camera trap deployment protocol of the project. Camera trap stations were then all deployed on roads and animal paths, with a density of two camera trap stations per 50 km^2 . Survey F consists of a replicate of survey A, using the newly chosen and standardised protocol which was then used throughout the project.

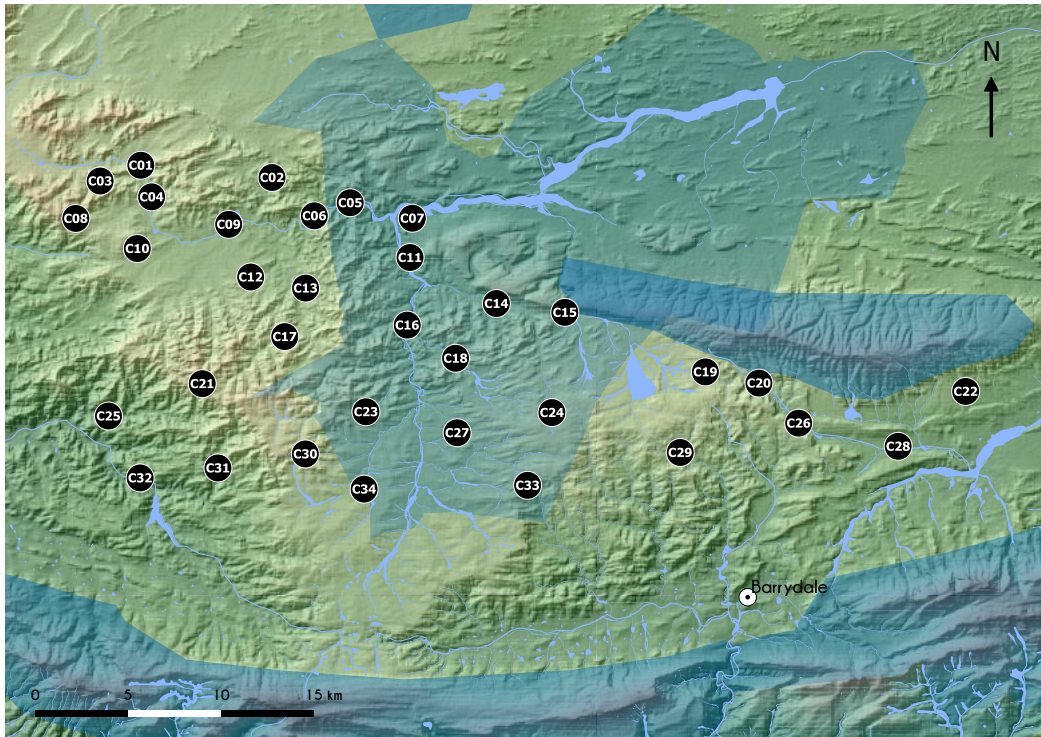


(a) Session A

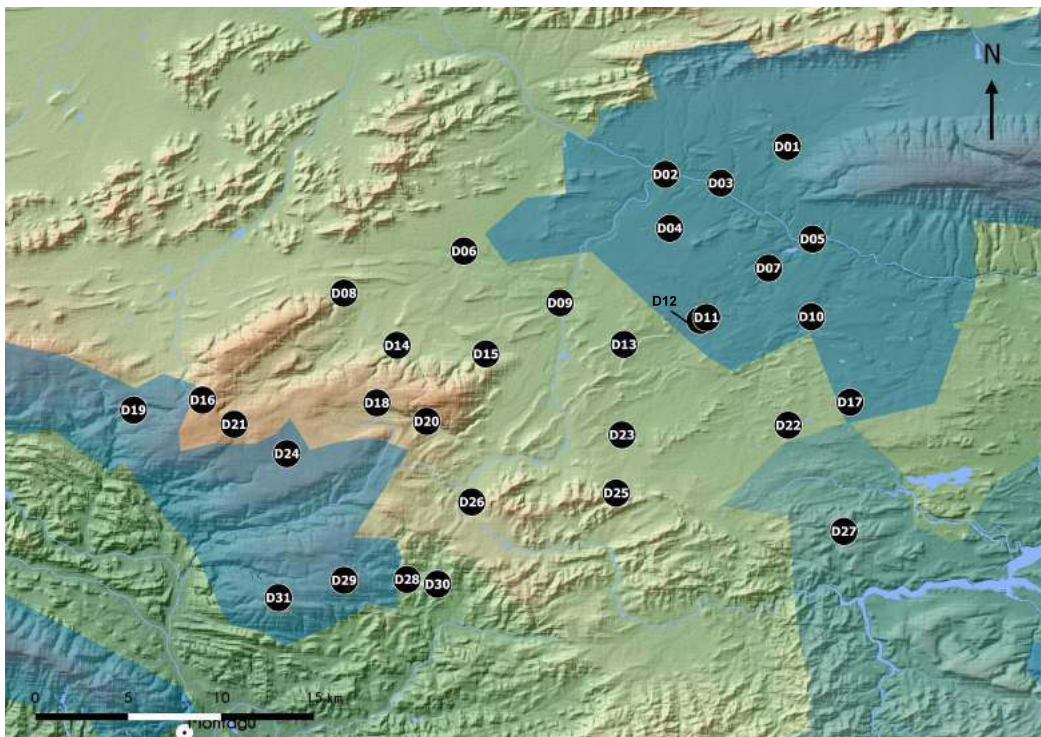


(b) Session B

Figure 4.1: Sampling design (continued).
A full caption is provided on p182.

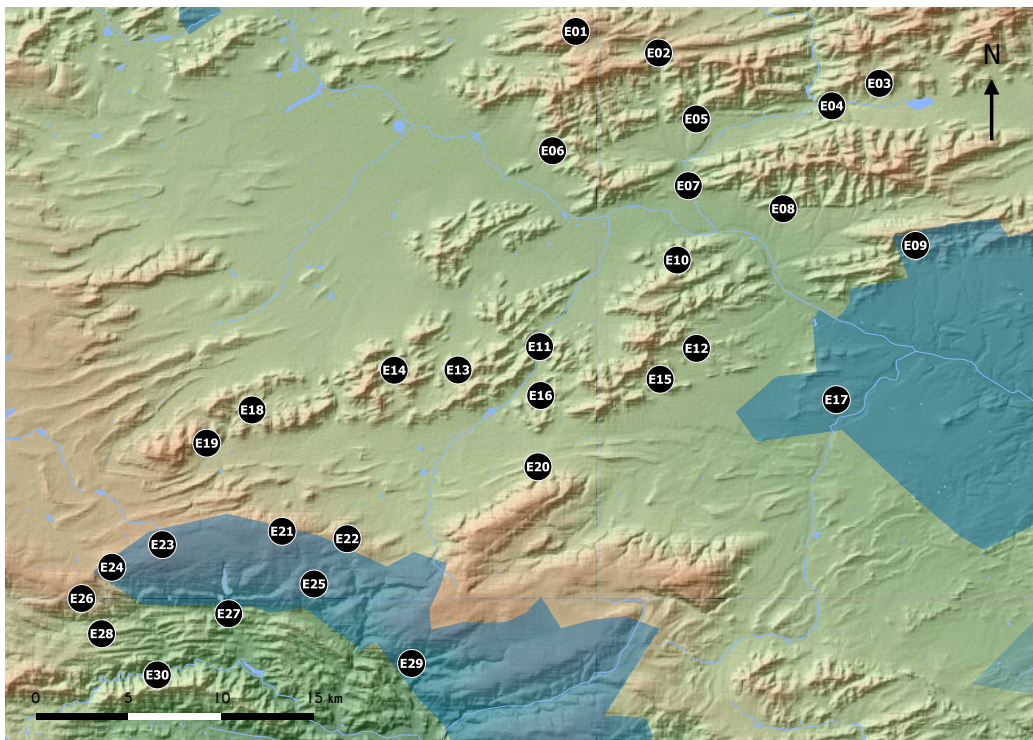


(c) Session C

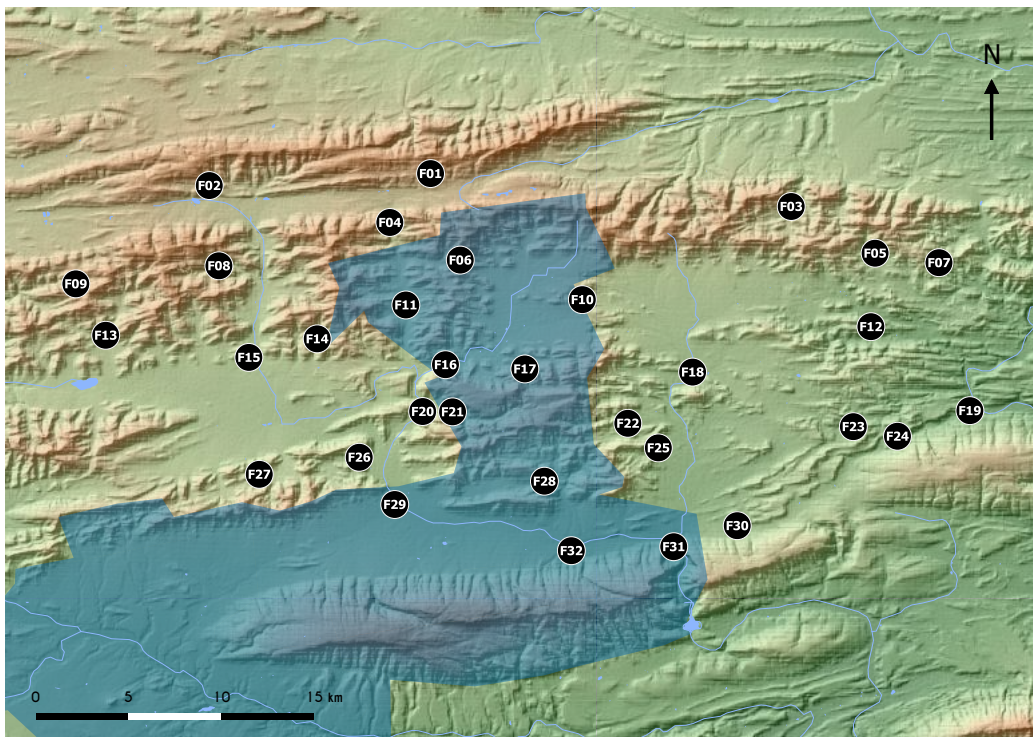


(d) Session D

Figure 4.1: Sampling design (continued).
A full caption is provided on p182.



(e) Session E



(f) Session F

Figure 4.1: Sampling design (continued).
A full caption is provided on p182.

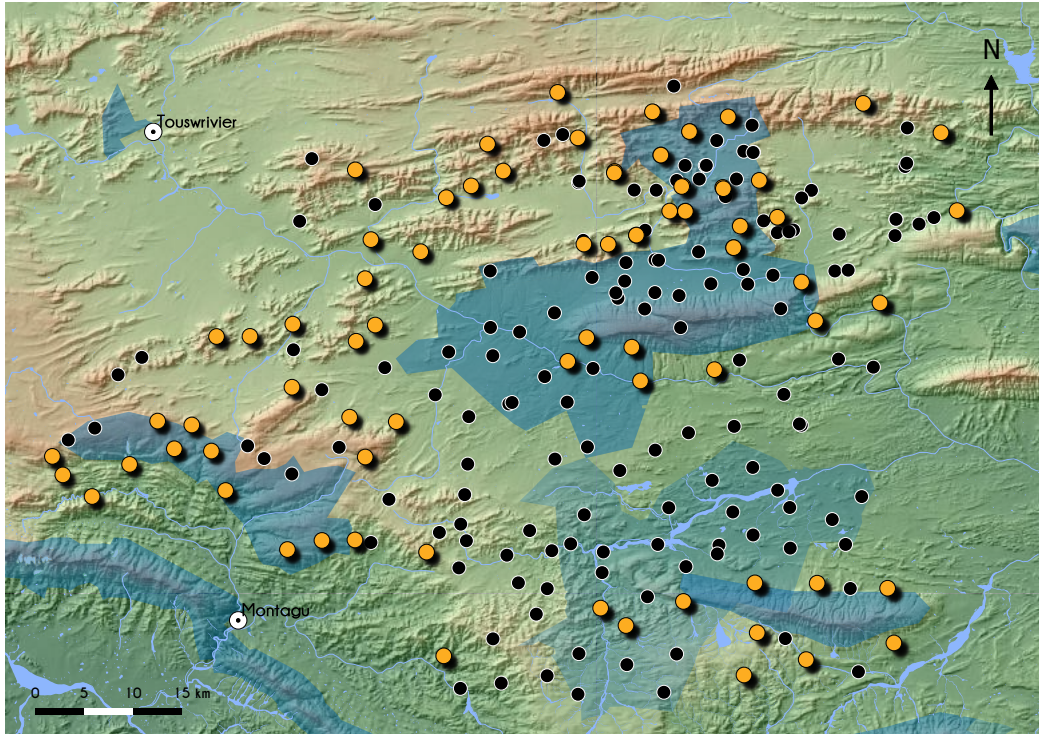


Figure 4.2: Photo-capture leopards.

The study provided 219 photo-captures of leopards in the Little Karoo, collected at 79 (35%) camera trap stations. Each point represents a camera trap station; the orange ones being those where leopards were photo-captured.

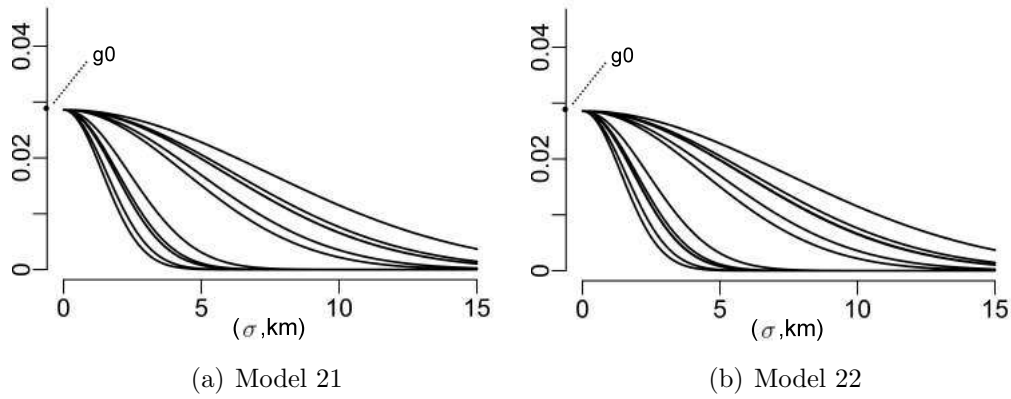


Figure 4.3: Detection functions.

The detection function is jointly defined by g_0 (detection probability) and σ (index of home range size), and modelled as a halfnormal function. Each graph shows 12 curves (two classes h_2 , six sessions $session$); g_0 (~ 1) being the sole intercept.

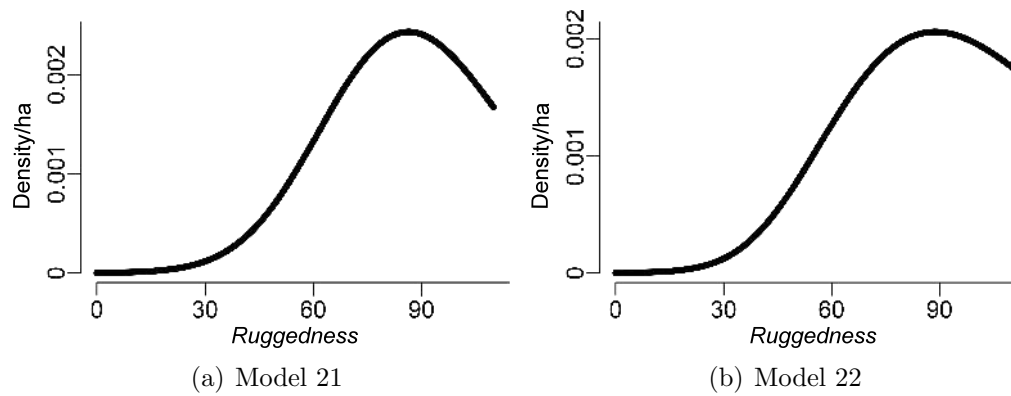


Figure 4.4: Density spline relationship with spatial covariate (ruggedness).

The curves show the relationship between the population density (second axis) and the terrain roughness (first axis).

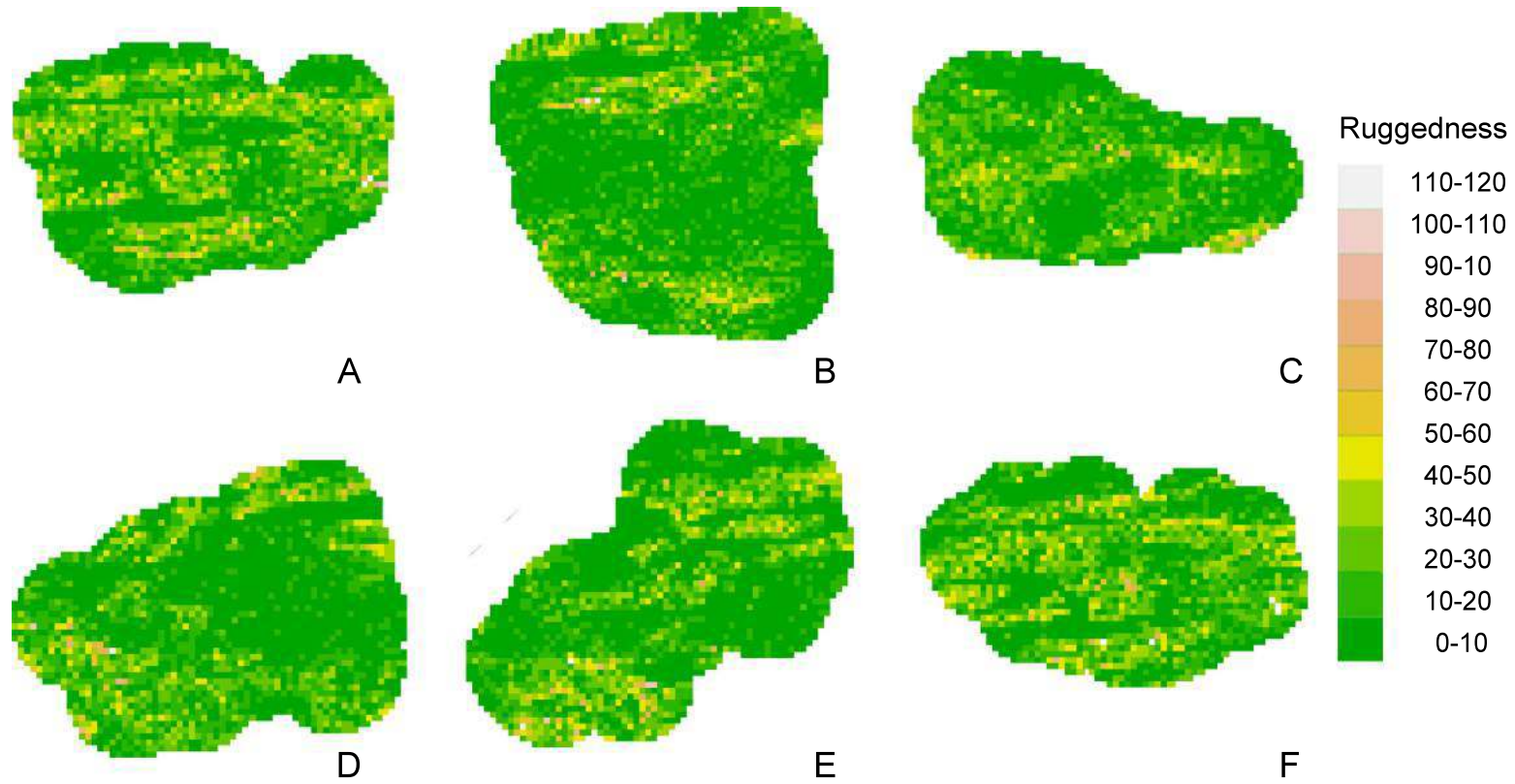


Figure 4.5: Ruggedness maps.

This figure shows the six habitat masks with ruggedness data (spatial covariate) that were constructed by the *secur.fit* function from the *secur* R-package version 3.1.0 [94], for the six regional surveys that took place in the Little Karoo.

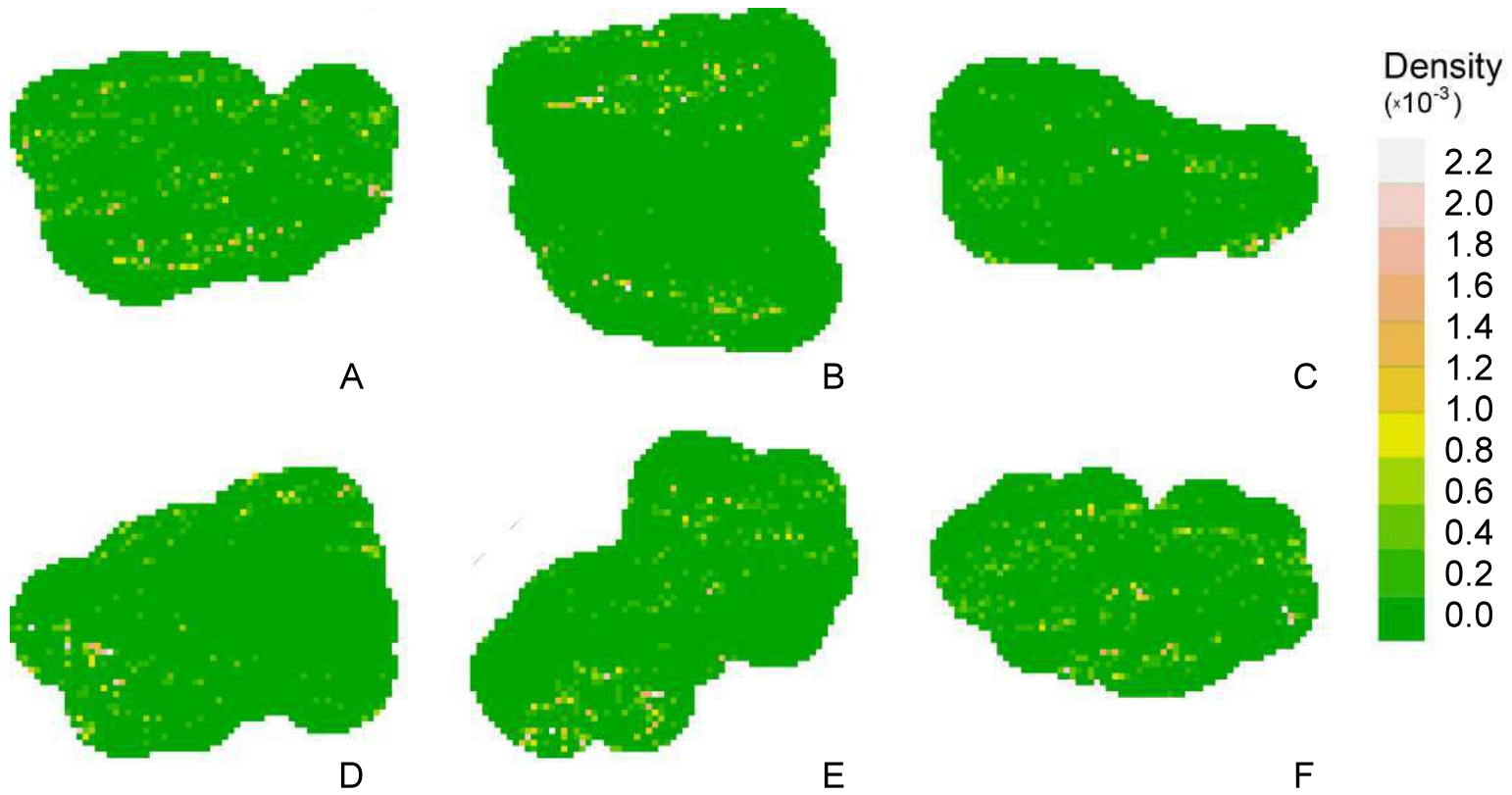
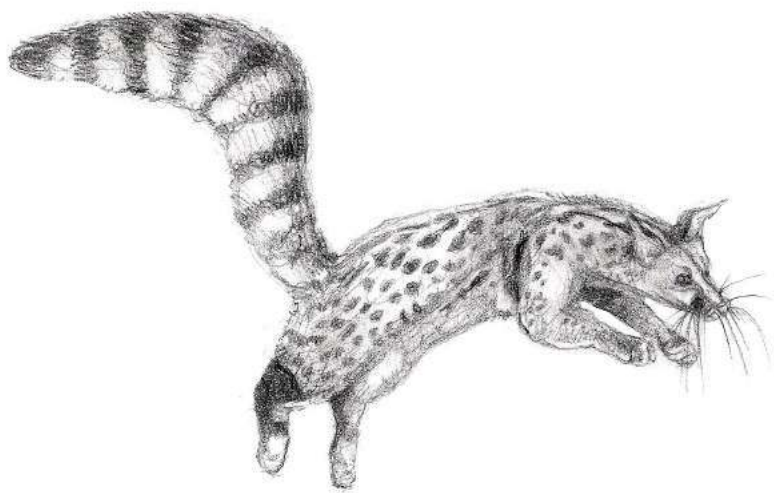


Figure 4.6: Density maps.

This figure shows the six predicted density maps from best-performing Model 22, for the six regional surveys that took place in the Little Karoo.



Conclusion

Camera trapping technology has led to a surge in the collection of large ecological datasets. This provides an unmissable opportunity to study rare, protected and sensitive species, as well as to help resolve numerous of the burning ecological questions that are crucial in dealing with ecological communities. This thesis showed that camera traps can provide good sensor networks for the space-time monitoring of terrestrial mammal communities; it also provided new analytical methods to explore large camera trap datasets and attain deeper knowledge of the mammal community assembly and structure, over space and time. This methodology can be transposed, adjusted and applied to other camera trap studies, conducted on different areas and/or at different times.

Hutchinson (1965) developed the term ‘ecological theatre’; in this theatre, ‘acts’ are played out on different spatial and temporal scales [149]. Understanding the full extent of the drama requires us to watch it on the appropriate sampling scales. Although geologists, geographers, oceanographers, physicists and mathematicians address scaling as a primary focus of their investigations, ecologists have taken much longer to recognise that ecological processes and patterns are sensitive to differences in scales [145, 192, 362]. Local communities, such as that of the mammal species of the Little Karoo, are neither closed nor isolated, which is why it will be insightful to embrace the metacommunity concept and explain these patterns of distribution, abundance and interaction at multiple scales of spatio-temporal organisation [192].

The activity level (movement) of mammal species is optimised throughout the day and endogenous schedules are adjusted by environmental (exogenous) conditions. This explains why species are expected to show variations in their diel activity rhythm throughout different latitudes and landscapes. Investigating the environmental processes influencing the diel activity rhythm of mammal species at different locations and various spatial scales would provide great insights into the mammal community assembly and structure.

Studies of seasonal shifts in diel activity rhythm among mammal communities would benefit from datasets that compile information collected over several consecutive years. Inter-year comparisons would enable us to determine whether observed versatilities within seasons are stable with respect to different years.

It would be precarious to extrapolate the results and findings of the study of species' habitat preferences to a broader landscape than that of the Little Karoo. However, if similar studies were conducted on habitat-use patterns within mammal communities inhabiting a variety of study sites in the Western, Eastern and Northern Cape Provinces, it should be possible to build a distribution map with suitable habitat for each species, based on ruggedness preferences. Additional camera trap studies would then need to be implemented in order to ground truth projections. Similarly, if supplemental spatially explicit capture-recapture studies were conducted on the density-ruggedness relationship within leopard populations inhabiting multiple study sites in the three Cape Provinces, it ought to be feasible to produce leopard density maps and to delimit the area in which leopards occur regularly.

References

- [1] ADAMS, C. S., RYBERG, W. A., HIBBITTS, T. J., PIERCE, B. L., PIERCE, J. B., AND RUDOLPH, D. C. Evaluating effectiveness and cost of time-lapse triggered camera trapping techniques to detect terrestrial squamate diversity. *Herpetological Review* 48 (2017), 44–48.
- [2] AHUMADA, J. A., SILVA, C. E. F., GAJAPERSAD, K., HALLAM, C., HURTADO, J., MARTIN, E., MCWILLIAM, A., MUGERWA, B., O'BRIEN, T., ROVERO, F., SHEIL, D., SPIRONELLO, W. R., WINARNI, N., AND ANDELMAN, S. J. Community structure and diversity of tropical forest mammals: data from a global camera trap network. *Philosophical Transactions of the Royal Society* 366 (2011), 2703–2711.
- [3] ALEXY, K. J., BRUNJES, K. J., GASSETT, J. W., AND MILLER, K. V. Continuous remote monitoring of gopher tortoise burrow use. *Wildlife Society Bulletin* 31 (2003), 1240–1243.
- [4] ALLEN, W. L., CUTHILL, I. C., SCOTT-SAMUEL, N. E., AND BADDELEY, R. Why the leopard got its spots: relating pattern development to ecology in felids. *Proceedings of the Royal Society B* (2010), doi:10.1098/rspb.2010.1734.
- [5] ANDERSEN, D. M., AND KEAFER, B. A. An endogenous annual clock in the toxic marine dinoflagellate *Gonyaulax tamarensis*. *Nature* 325 (1987), 616–617.
- [6] ANGELSTAM, P. Conservation of communities - the importance of edges, surroundings and landscape mosaic structure. In *Ecological principles of nature conservation. Application in temperate and boreal environments*, L. Hansson, Ed. Springer, New York, 1992, pp. 9–70.
- [7] APPS, C. D., MCLELLAN, B. N., WOODS, J. G., AND PROCTOR, M. F. Estimating grizzly bear distribution and abundance relative to habitat and human influence. *Journal of Wildlife Management* 68 (2004), 138–152.
- [8] ARROYO-ARCE, S., THOMSON, I., FERNÁNDEZ, C., AND SALOM-PÉREZ, R. Relative abundance and activity patterns of terrestrial mammals in Pacuare Nature Reserve, Costa Rica. *Cuadernos de Investigacion UNED* 9 (2017), 15–21.
- [9] AZLAN, J. M., AND SHARMA, D. S. K. The diversity and activity patterns of wild felids in a secondary forest in Peninsular Malaysia. *Oryx* 40 (2006), 1–6.
- [10] BAILEY, L. L., SIMONS, T. R., AND POLLOCK, K. H. Estimating site occupancy and detection probability parameters for terrestrial salamanders. *Ecological Applications* 14 (2004), 692–702.
- [11] BAILEY, T. N. *The African leopard: ecology and behaviour of a solitary felid*. The Blackburn Press, Caldwell, 1993.
- [12] BAKER, J. R. The evolution of breeding seasons. In *Evolution: essays on aspects of evolutionary biology*, G. R. Beer, Ed. Oxford University Press, 1938, pp. 161–177.
- [13] BALME, G., HUNTER, L., AND SLOTOW, R. Feeding habitat selection by hunting leopards *Panthera pardus* in a woodland savanna: prey catchability versus abundance. *Animal Behaviour* 74 (2007), 589–598.

-
- [14] BALME, G., AND HUNTER, L. T. B. Mortality in a protected leopard population, Phinda Private Game Reserve, South Africa: a population in decline? *Ecological Journal* 6 (2004), 1–6.
- [15] BALME, G. A., HUNTER, L., AND BRACZKOWSKI, A. R. Applicability of age-based hunting regulations for African leopards. *PLoS ONE* 7 (2012), e35209.
- [16] BALME, G. A., HUNTER, L. T. B., AND SLOTOW, R. Evaluating methods for counting cryptic carnivores. *Journal of Wildlife Management* 73 (2009), 433–441.
- [17] BALME, G. A., LINDSEY, P. A., SWANEPOEL, L. H., AND HUNTER, L. T. B. Failure of research to address the rangewide conservation needs of large carnivores: leopards in South Africa as a case study. *Conservation Letters* 7 (2013), 3–11.
- [18] BANNARI, A., MORIN, D., BONN, F., AND HUETE, A. R. A review of vegetation indices. *Remote Sensing Reviews* 13 (1995), 95–120.
- [19] BARAS, E. Day – night alternation prevails over food availability in synchronising the activity of *Piaractus brachypomus* (Characidae). *Aquatic Living Resources* 13 (2000), 115–120.
- [20] BART, J., DROEGE, S., GEISSLER, P., PETERJOHN, B., AND RALPH, C. J. Density estimation in wildlife surveys. *Wildlife Society Bulletin* 32 (2004), 1242–1247.
- [21] BATSCHLET, E. *Circular statistics in biology*. Academic Press, New York, 1981.
- [22] BECKER, R. A., CHAMBERS, J. M., AND WILKS, A. R. *The new S language*. Wadsworth & Brooks, Pacific Grove, California, 1988.
- [23] BEIER, P., AND CUNNINGHAM, S. C. Power of track surveys to detect changes in cougar populations. *Wildlife Society Bulletin* 24 (1996), 540–546.
- [24] BEIER, P., AND MCCULLOUGH, D. R. Factors influencing white-tailed deer activity patterns and habitat use. *Wildlife Monographs* 109 (1990), 5–51.
- [25] BELOVSKY, G. E., AND SLADE, J. B. Time budgets of grassland herbivores: body size similarities. *Oecologia* 70 (1986), 53–62.
- [26] BENNIE, J. J., DUFFY, J. P., INGER, R., AND GASTON, K. J. Biogeography of time partitioning in mammals. *Proceedings of the National Academy of Sciences* 111 (2014), 13727–13732.
- [27] BENZÉCRI, J.-P. *L'analyse des données*. Dunod, Paris, 1973.
- [28] BOND, W., FERGUSON, M., AND FORSYTH, G. Small mammals and habitat structure along altitudinal gradients in the southern Cape mountains. *South African Journal of Zoology* 15 (1979), 34–43.
- [29] BORCHERS, D. A non-technical overview of spatially explicit capture-recapture models. *Journal of Ornithology* 152 (2010), 435–444.
- [30] BORCHERS, D., DISTILLER, G., FOSTER, R., HARMSSEN, B., AND MILAZZO, L. Continuous-time spatially explicit capture-recapture models, with an application to a jaguar camera-trap survey. *Methods in Ecology and Evolution* 5 (2014), 656–665.
- [31] BORCHERS, D. L., AND EFFORD, M. G. Spatially explicit maximum likelihood methods for capture-recapture studies. *Biometrics* 64 (2008), 377–385.
- [32] BORG, I., AND GROENEN, P. J. F. *Modern multidimensional scaling: theory and applications*. Springer, New York, 1997.
- [33] BORON, V., TZANOPOULOS, J., GALLO, J., BARRAGAN, J., JAIMES-RODRIGUEZ, L., SCHALLER, G., AND PAYAN, E. Jaguar densities across human-dominated landscapes in Colombia: the contribution of unprotected areas to long term conservation. *PLoS ONE* 11 (2016), e0153973.

- [34] BOSHOFF, A. F., KERLEY, G. I. H., AND COWLING, R. M. A pragmatic approach to estimating the distributions and spatial requirements of the medium- to large-sized mammals in the Cape Floristic Region, South Africa. *Diversity and Distributions* 7 (2001), 29–43.
- [35] BOTHMA, J. D. P., KNIGHT, M. H., LE RICHE, E. A. N., AND VAN HENSBERGEN, H. J. Range size of southern Kalahari leopards. *South African Journal of Wildlife Research* 27 (1997), 94–100.
- [36] BOWKETT, A., ROVERO, F., AND MARSHALL, A. R. The use of camera-trap data to model habitat use by antelope species in the Udzungwa Mountain forests, Tanzania. *African Journal of Ecology* 46 (2008), 479–487.
- [37] BOYCE, M. S., AND MCDONALD, L. L. Relating population to habitats using resource selection functions. *Trends in Ecology and Evolution* 14 (1999), 268–272.
- [38] BRADSHAW, W. E., AND HOLZAPFEL, C. M. Evolution of animal photoperiodism. *Annual Review of Ecology, Evolution and Systematics* 38 (2007), 1–25.
- [39] BRADSHAW, W. E., AND HOLZAPFEL, C. M. Light, time, and the physiology of biotic response to rapid climate change in animals. *Annual Review of Physiology* 72 (2010), 147–166.
- [40] BRÄNNÄS, E., AND ALANÄRÄ, A. Is diel dualism in feeding activity influenced by competition between individuals? *Canadian Journal of Zoology* 75 (1997), 661–669.
- [41] BRIDGES, A. S., FOX, J. A., OLFENBUTTEL, C., AND VAUGHAN, M. R. American black bear denning behavior: observations and applications using remote photography. *Wildlife Society Bulletin* 32 (2004), 188–193.
- [42] BRIDGES, A. S., AND NOSS, A. J. Behaviour and activity patterns. In *Camera traps in animal ecology*, A. F. O’Connell, J. D. Nichols, and K. U. Karanth, Eds. Springer, Tokyo, 2011, pp. 57–69.
- [43] BRIDGES, A. S., VAUGHAN, M. R., AND KLENZENDORF, S. Seasonal variation in American black bear *Ursus americanus* activity patterns: quantification via remote photography. *Wildlife Biology* 10 (2004), 277–284.
- [44] BRIEN, T. G. O. On the use of automated cameras to estimate species richness for large- and medium- sized rainforest mammals. *Animal Conservation* 11 (2008), 179–181.
- [45] BRODY, S. *Bioenergetics and growth*. Reinhold, New York, 1945.
- [46] BRONSON, F. H. Mammalian reproduction: an ecological perspective. *Biology of Reproduction* 33 (1985), 1–26.
- [47] BROOKS, T. M., BAKAAR, M. I., BOUCHER, T., DA FONSECA, G. A. B., HILTON-TAYLOR, C., HOEKSTRA, J. M., MORITZ, T., OLIVIERI, S., PARRISH, J., PRESSEY, R. L., RODRIGUES, A. S. L., SECHREST, W., STATTERSFIELD, A., STRAHM, W., AND STUART, S. N. Coverage provided by the global protected-area system: is it enough? *BioScience* 54 (2004), 1081–1091.
- [48] BROWN, J. H. Mammals on mountainsides: elevational patterns of diversity. *Global Ecology and Biogeography* 10 (2001), 101–109.
- [49] BROWN, W. L., AND WILSON, E. O. Character displacement. *Systematic Zoology* 5 (1956), 49–64.
- [50] BURNETT, M. R., AUGUST, P. V., BROWN, J. H., AND KILLINGBECK, K. T. The influence of geomorphological heterogeneity on biodiversity I. A patch-scale perspective. *Conservation Biology* 12 (1998), 363–370.
- [51] BURNHAM, K. P., AND ANDERSON, D. R. *Model selection and multimodel inference: a practical information-theoretic approach*. Springer, New York, 2002.
- [52] CADÉE, N., PIERSMA, T., AND DAAN, S. Endogenous circannual rhythmicity in a non-passerine migrant, the Knot *Calidris canutus*. *Ardea* 84 (1996), 75–84.

-
- [53] CALHOUN, J. B., AND CASBY, J. U. Calculation of home range and density of small mammals. *Public Health Monograph* 55 (1958).
- [54] CAPEN, D. E. Time-lapse photography and computer analysis of behavior of nesting white-faced ibises. In *Wading birds. National Audubon Society Research Report 7*, A. Sprunt, J. C. Ogden, and S. Winckler, Eds. National Audubon Society, New York, 1978, pp. 41–43.
- [55] CARBONE, C., CHRISTIE, S., CONFORTI, K., COULSON, T., FRANKLIN, N., GINSBERG, J. R., GRIF-FITHS, M., HOLDEN, J., KAWANISHI, K., KINNAIRD, M., LAIDLAW, R., LYNAM, A., MACDONALD, D. W., MARTYR, D., MCDUGAL, C., NATH, L., O'BRIEN, T., SEIDENSTICKER, J., SMITH, D. J. L., SUNQUIST, M., TILSON, R., AND WAN SHAHRUDDIN, W. N. The use of photographic rates to estimate densities of tigers and other cryptic mammals. *Animal Conservation* 4 (2001), 75–79.
- [56] CARBONE, C., COWLISHAW, G., ISAAC, N. J. B., AND ROWCLIFFE, J. M. How far do animals go? Determinants of day range in mammals. *The American Society of Naturalists* 165 (2005), 290–297.
- [57] CARBONE, C., AND GITTLEMAN, J. A common rule for the scaling of carnivore density. *Science* 295 (2002), 2273–2276.
- [58] CAROTHERS, J. H., AND JAKSIC, F. M. Time as a niche difference: the role of interference competition. *Oikos* 42 (1984), 403–406.
- [59] CARTHEW, S. M., AND SLATER, E. Monitoring animal activity with automated photography. *Journal of Wildlife Management* 55 (1991), 689–692.
- [60] CAVENDER-BARES, J., KOZAK, K. H., FINE, P. V. A., AND KEMBEL, S. W. The merging of community ecology and phylogenetic biology. *Ecology Letters* 12 (2009), 693–715.
- [61] CHAO, A., CHU, W., AND HSU, C.-H. Capture-recapture when time and behavioral response affect capture probabilities. *Biometrics* 56 (2000), 427–433.
- [62] CHAPMAN, F. M. Who treads our trails? *National Geographic Magazine* 52 (1927), 331–345.
- [63] CHASE, J. M., AND LEIBOLD, M. A. *Ecological niches. Linking classical and contemporary approaches*. University of Chicago Press, Chicago, 2003.
- [64] CLARK, A., AND PÖRTNER, H.-O. Temperature, metabolic power and the evolution of endothermy. *Biological Reviews* 85 (2010), 703–727.
- [65] CLAYPOOL, L. E. *The environmental and physiological determinants of activity patterns in Microtus montanus the montane vole*. PhD thesis, Univeristy of Utah, Salt Lake City, UT, 1984.
- [66] CONROY, M. J. Abundance indices. In *Measuring and monitoring biological diversity: standard methods for mammals*, D. E. Wilson, F. R. Cole, J. D. Nichols, R. Rudran, and M. S. Foster, Eds. Institution Press, Washington, 1996, pp. 179–192.
- [67] COVE, M. V., SIMONS, T. R., GARDNER, B., MAURER, A. S., AND CONNELL, A. F. O. Evaluating nest supplementation as a recovery strategy for the endangered rodents of the Florida Keys. *Restoration Ecology* 25 (2016), 1–8.
- [68] CRAIG, G. H., AND CRAIG, J. L. An automatic nest recorder. *Ibis* 116 (1974), 557–561.
- [69] CREEL, S., AND CHRISTIANSON, D. Wolf presence and increased willow consumption by Yellowstone elk: implications for trophic cascades. *Ecology* 90 (2009), 2454–2466.
- [70] CRITICAL ECOSYSTEM PARTNERSHIP FUND. Ecosystem profile: the succulent Karoo hotspot Namibia and South Africa. Tech. rep., South African National Biodiversity Institute, Cape Town, 2003.
- [71] CROMPTON, A. W. Biology of the earliest mammals. In *Comparative physiology: primitive mammals*, K. Schmidt-Nielsen, L. Bolis, and C. R. Taylor, Eds. Cambridge University Press, New York, 1980.

- [72] CUTLER, T. L., AND SWANN, D. E. Using remote photography in wildlife ecology: a review. *Wildlife Society Bulletin* 27 (1999), 571–581.
- [73] DAAN, S. Adaptive daily strategies in behavior. In *Biological rhythms*, Jürgen Aschoff, Ed. Springer US, 1981, pp. 275–298.
- [74] DAAN, S., AND ASCHOFF, J. Circadian rhythms of locomotor activity in captive birds and mammals: their variations with season and latitude. *Oecologia* 18 (1975), 269–316.
- [75] DAVIES, T. J., MERI, S., BARRACLOUGH, T. G., AND GITTLEMAN, J. L. Species co-existence and character divergence across carnivores. *Ecology Letters* 10 (2007), 146–152.
- [76] DAYAN, T., AND SIMBERLOFF, D. Ecological and community-wide character displacement: the next generation. *Ecology Letters* 8 (2005), 875–894.
- [77] DE ALMEIDA JACOMO, A. T., SILVEIRA, L., AND DINIZ-FILHO, J. A. F. Niche separation between the maned wolf (*Chrysocyon brachyurus*), the crab-eating fox (*Dusicyon thous*) and the hoary fox (*Dusicyon vetulus*) in central Brazil. *Zoological Society of London* 262 (2004), 99–106.
- [78] DE CANDOLLE, A. P. A. *Constitution dans le règne végétal de groupes physiologiques applicables à la géographie ancienne et moderne*. Archives des sciences des la Bibliothèque universelle, Genève, 1874.
- [79] DE LA VEGA, C., LEBRETON, B., SIEBERT, U., GUILLOU, G., DAS, K., ASMUS, R., AND ASMUS, H. Seasonal variation of harbor seal’s diet from the Wadden sea in relation to prey availability. *PLoS ONE* (2016), e0155727.
- [80] DI BITETTI, M. S., DI BLANCO, Y. E., PEREIRA, J. A., AND PAVIOLO, A. Time partitioning favors the coexistence of sympatric crab-eating foxes (*Cerdocyon thous*) and pampas foxes (*Lycalopex gymnocercus*). *Journal of Mammalogy* 90 (2009), 479–490.
- [81] DICKINSON, J. L., AND BONNEY, R. *Citizen science. Public participation in environmental research*. Cornell University Press, New York, 2012.
- [82] DOWNES, S. J. Trading heat and food for safety: costs of predator avoidance in a lizard. *Ecology* 82 (2001), 2870–2881.
- [83] DRISCOLL, K., LACEY, M., AND GREATHOUSE, J. Use of camera trapping to determine spatial distribution, habitat use, and environmental factors affecting mesopredators on reclaimed mine lands at the wilds. *Journal American Society of Mining and Reclamation* 6 (2017), 15–33.
- [84] DU PREEZ, B. D., LOVERIDGE, A. J., AND MACDONALD, D. W. To bait or not to bait: A comparison of camera-trapping methods for estimating leopard *Panthera pardus* density. *Biological Conservation* 176 (2014), 153–161.
- [85] DUTHIE, A., SKINNER, J., AND ROBINSON, T. The distribution and status of the riverine rabbit, *Bunolagus monticularis*, South Africa. *Biological Conservation* 47 (1989), 195–202.
- [86] EBERHARDT, L. L. Population estimates from recapture frequencies. *Journal of Wildlife Management* 33 (1969), 28–39.
- [87] EFFORD, M. Density estimation in live-trapping studies. *Oikos* 3 (2004), 598–610.
- [88] EFFORD, M. *Finite mixture models in secr*. University of Otago, Dunedin, 2010.
- [89] EFFORD, M. *SECR overview*. University of Otago, Dunedin, 2013.
- [90] EFFORD, M. *SECR: Spatially Explicit Capture-Recapture in R*. University of Otago, Dunedin, 2013.
- [91] EFFORD, M. *Adjustment for varying effort in secr 3.0*. No. X. University of Otago, Dunedin, 2017.
- [92] EFFORD, M. *Habitat masks in the package secr*. University of Otago, Dunedin, 2017.

-
- [93] EFFORD, M. *Multi-session models in secr 3.0*. University of Otago, Dunedin, 2017.
- [94] EFFORD, M. *secr package: Spatially Explicit Capture-Recapture in R*. The Comprehensive R Archive Network, Version 3.1.0. Vienna, Austria, 2017.
- [95] EFFORD, M. G. Varying effort in capture–recapture studies. *Methods in Ecology and Evolution* 4 (2013), 629.
- [96] EFFORD, M. G., BORCHERS, D. L., AND BYROM, A. E. Density estimation by spatially explicit capture–recapture: likelihood-based methods. In *Modeling demographic processes in marked populations*, D. L. Thomson, E. G. Cooch, and M. J. Conroy, Eds. Springer, Boston, 2009, pp. 255–269.
- [97] ELLIOTT, J. A., AND GOLDMAN, B. D. Seasonal reproduction: photoperiodism and biological clocks. In *Neuroendocrinology of reproduction*. 1981, pp. 377–423.
- [98] EMERSON, B. C., AND GILLESPIE, R. G. Phylogenetic analysis of community assembly and structure over space and time. *Trends in Ecology and Evolution* 23 (2008), 619–630.
- [99] ENDERSON, J. H., TEMPLE, S. A., AND SWARTZ, L. G. Time-lapse photographic records of nesting peregrine falcons. *Living Bird* 11 (1972), 113–128.
- [100] EVELYN, J. *Sylvia, or a discourse of forest-trees, and the propagation of timber in his majesties dominions*. Royal Society, London, 1664.
- [101] FABRICIUS, C., AND COETZEE, K. Geographic information systems and artificial intelligence for predicting the presence or absence of mountain reedbeek. *South African Journal of Wildlife Research* 22 (1992), 80–86.
- [102] FARCOMENI, A., AND SCACCIATELLI, D. Heterogeneity and behavioral response in continuous time capture–recapture, with application to street cannabis use in Italy. *Annals of Applied Statistics* 7 (2013), 2293–2314.
- [103] FEDRIANI, J. M., FULLER, T. K., SAUVAJOT, R. M., AND YORK, E. C. Competition and intraguild predation among three sympatric carnivores. *Oecologia* 125 (2000), 258–270.
- [104] FEIERABEND, D., AND KIELLAND, K. Movements, activity patterns, and habitat use of snowshoe hares (*Lepus americanus*) in interior Alaska. *Journal of Mammalogy* 95 (2014), 525–533.
- [105] FERNANDEZ-DUQUE, E. Influences of moonlight, ambient temperature and food availability on the diurnal and nocturnal activity of owl monkeys (*Aotus azarai*). *Behavioral Ecology and Sociobiology* 54 (2014), 431–440.
- [106] FISCHER, J. T., ANHOLT, B., BARDBURY, S., WHEATLEY, M., AND VOLPE, J. P. Spatial segregation of sympatric marten and fishers: the influence of landscapes and species-scapes. *Ecography* 36 (2013), 240–248.
- [107] FISCHER, L. A., AND GATES, C. C. Competition potential between sympatric woodland caribou and wood bison in southwestern Yukon, Canada. *Canadian Journal of Zoology* 83 (2005), 1162–1173.
- [108] FISHER, N. I. *Statistical analysis of circular data*. Cambridge University Press, Cambridge, 1993.
- [109] FOSTER, R. G., AND KREITZMAN, L. *Seasons of life: the biological rhythms that enable living things to thrive and survive*. Yale University Press, New York, 2009.
- [110] FOSTER, R. J., AND HARMSEN, B. J. A critique of density estimation from camera-trap data. *The Journal of Wildlife Management* 76 (2012), 224–236.
- [111] FOX, S. *The american conservation movement. John Muir and his legacy*. The University of Wisconsin Press, Madison, 1981.
- [112] FRECKLETON, R. P., AND WATKINSON, A. R. Large-scale spatial dynamics of plants: metapopulations, regional ensembles and patchy populations. *Journal of Ecology* 90 (2002), 419–434.

-
- [113] FULLER, A., HETEM, R. S., MALONEY, S. K., AND MITCHELL, D. Adaptation to heat and water shortage in large, arid-zone mammals. *Physiology* 29 (2014), 159–167.
- [114] GABRIEL, K. R. The biplot graphic display of matrices with application to principal component analysis. *Biometrika* 58 (1971), 453–467.
- [115] GALLO, J. A., PASQUINI, L., REYERS, B., AND COWLING, R. M. The role of private conservation areas in biodiversity representation and target achievement within the Little Karoo region, South Africa. *Biological Conservation* 142 (2009), 446–454.
- [116] GERKEMA, M. P., DAVIES, W. I. L., FOSTER, R. G., MENAKER, M., AND HUT, R. A. The nocturnal bottleneck and the evolution of activity patterns in mammals. *Proceedings of the Royal Society B* 280 (2013), 20130508.
- [117] GIBBONS, A. Conservation biology in the fast track. *Science* 255 (1992), 20–22.
- [118] GIBSON, L. A. The importance of incorporating imperfect detection in biodiversity assessments: a case study of small mammals in an Australian region. *Diversity and Distributions* 17 (2011), 613–623.
- [119] GLEASON, H. A. The structure and development of the plant association. *Bulletin of the Torrey Botanical Club* 44 (1917), 463–481.
- [120] GLEASON, H. A. The individualistic concept of the plant association. *American Midland Naturalist* 21 (1939), 92–110.
- [121] GOLDMAN, B. D. The circadian timing system and reproduction in mammals. *Steroids* 64 (1999), 679–685.
- [122] GOLDMAN, B. D. Mammalian photoperiodic system: formal properties and neuroendocrine mechanisms of photoperiodic time measurement. *Journal of Biological Rhythms* 16 (2001), 283–301.
- [123] GOLUB, G. H., AND REINSCH, C. Singular value decomposition and least squares solutions. *Numerical Mathematics* 14 (1970), 403–420.
- [124] GRANT, T. *Leopard population density, home range size and movement patterns in a mixed landuse area of the Mangwe district of Zimbabwe*. No. February. MSc thesis, Rhodes University, Grahamstown, 2012.
- [125] GRAY, T. N. E., AND PHAN, C. Habitat preferences and activity patterns of the larger mammal community in Phnom Prich Wildlife Sanctuary, Cambodia. *The Raffles Bulletin of Zoology* 59 (2011), 311–318.
- [126] GREENACRE, M. J., AND UNDERHILL, L. G. Scaling a data matrix in a low dimensional Euclidian space. In *Topics in applied multivariate analysis*, D. M. Hawkins, Ed. Cambridge University Press, Cambridge, 1982, pp. 183–268.
- [127] GRIFFITHS, M., AND VAN SCHAİK, C. P. Camera-trapping: a new tool for the study of elusive rain forest animals. *Tropical Biodiversity* 1 (1993), 131–135.
- [128] GRIFFITHS, M., AND VAN SCHAİK, C. P. The impact of human traffic on the abundance and activity periods of sumatran rain forest wildlife. *Conservation Biology* 7 (1993), 623–626.
- [129] GUGGISBERG, C. A. W. *Early wildlife photographer*. Taplinger Pub. Co, New York, 1977.
- [130] GUISAN, A., AND THUILLER, W. Predicting species distribution: offering more than simple habitat models. *Ecology Letters* 8 (2005), 993–1009.
- [131] GWINNER, E. *Circannual rhythms*. Springer, Heidelberg, Germany, 1986.
- [132] HAECKEL, E. *Generelle Morphologie der Organismen*. Berlin, 1866.

-
- [133] HALL, S. J., AND RAFFAELLI, D. G. Food webs: theory and reality. *Advances in Ecological Research* 24 (1993), 187–239.
- [134] HANSSON, L. Why ecology fails at application: should we consider variability more than regularity? *Oikos* 100 (2003), 624–627.
- [135] HARMSÉN, B. J., FOSTER, R. J., SILVER, S. C., OSTRO, L. E. T., AND DONCASTER, C. P. Jaguar and puma activity patterns in relation to their main prey. *Mammalian Biology* 76 (2011), 320–324.
- [136] HAYWARD, G. D., MIQUELLE, D. G., SMIRNOV, E. N., AND NATIONS, C. Monitoring Amur tiger populations: characteristics of track surveys in snow. *Wildlife Society Bulletin* 30 (2002), 1150–1159.
- [137] HEARN, A. J., ROSS, J., BERNARD, H., ABU BAKAR, S., HUNTER, L. T. B., AND MACDONALD, D. W. The first estimates of marbled cat *Pardofelis marmorata* population density from Bornean primary and selectively logged forest. *PLoS ONE* 11 (2016), e0151046.
- [138] HEILBRUN, R. D., SILVY, N. J., PETERSON, M. J., AND TEWES, M. E. Estimating bobcat abundance using automatically triggered cameras. *Wildlife Society Bulletin* 34 (2006), 69–73.
- [139] HELM, B., AND LINCOLN, G. A. Circannual rhythms anticipate the Earth’s annual periodicity. In *Biological timekeeping: clocks, rhythms and behaviour*, V. Kumar, Ed. Springer India, New Delhi, 2017, pp. 545–569.
- [140] HENSCHÉL, P., HUNTER, L. T. B., BREITENMOSER, U., PACKER, C., KHOROZYAN, I. G., BAUER, H., MARKER, L. L., SOGBOHOSSOU, E., AND BREITENMOSER-WÜRSTEN, C. *Panthera pardus*. In *IUCN Red List of threatened species*. IUCN Species Survival Commission, Gland, 2008.
- [141] HERNÁNDEZ, D., ROLLINS, D., AND CANTU, R. An evaluation of Trailmaster camera systems for identifying ground-nest predators. *Wildlife Society Bulletin* 25 (1997), 848–853.
- [142] HERVEY, G. R. Physiological mechanisms for the regulation of energy balance. *Proceedings of the Nutrition Society* 30 (1965), 119–122.
- [143] HIRSCHFELD, H. O. A connection between correlation and contingency. *Mathematical Proceedings of the Cambridge Philosophical Society* 31 (1935), 520–524.
- [144] HOFFMAN, M. T., COUSINS, B., MEYER, T., PETERSEN, A., AND HENDRICKS, H. Historical and contemporary land use and the desertification of the Karoo. In *The Karoo, ecological patterns and processes*, W. Richard, J. Dean, and S. Milton, Eds. Cambridge University Press, 1999, pp. 257–273.
- [145] HOLYOAK, M., LEIBOLD, M. A., AND HOLT, R. D. The effects of spatial processes on two species interactions. In *Metacommunities. Spatial dynamics and ecological communities*, no. October 2016. University of Chicago Press, London, 2005, pp. 35–67.
- [146] HOOGESTEIJN, R., AND MONDOLFI, E. *The jaguar*. Armitano Editores, Caracas, 1992.
- [147] HORTON, T. H. Conceptual issues in the ecology and evolution of circadian rhythms. In *Handbook of behavioral neurobiology. Vol. 12. Circadian clocks*, J. S. Takahashi, F. W. Turek, and R. Y. Moore, Eds. Plenum Press, New York, 2001, pp. 45–57.
- [148] HUNT, R. H., AND OGDEN, J. J. Selected aspects of the nesting ecology of American alligators in the Okefenokee Swamp. *Journal of Herpetology* 25 (1991), 448–453.
- [149] HUTCHINSON, E. G. *Ecological theatre and the evolutionary play*. Yale University Press, New Haven, 1965.
- [150] III, J. W. C., KRAUSMAN, P. R., ROSENSTOCK, S. S., AND TURNER, J. C. Mechanisms of thermoregulation and water balance in desert ungulates. *Wildlife Society Bulletin* 7648 (2015), 570–581.

- [151] IKEDA, T., UCHIDA, K., MATSUURA, Y., TAKAHASHI, H., YOSHIDA, T., KAJI, K., AND KOIZUMI, I. Seasonal and diel activity patterns of eight sympatric mammals in northern Japan revealed by an intensive camera-trap survey. *PLoS ONE* 11 (2016), e0163602.
- [152] IUCN. *IUCN Red List categories and criteria*. IUCN Species Survival Commission, Gland, 2012.
- [153] JABLONSKI, D., ROY, K., AND VALENTINE, J. W. Out of the tropics: evolutionary dynamics of the latitudinal diversity gradient. *Science* 314 (2006), 102–106.
- [154] JACKSON, R. M., ROE, J. D., WANGCHUK, R., AND HUNTER, D. O. Estimating snow leopard abundance using photographic identification and capture-recapture techniques. *Wildlife Society Bulletin* 34 (2006), 772–781.
- [155] JACOBS, J. Quantitative measurement of food selection: a modification of the forage ratio and Ivlev's electivity index. *Oecologia* 14 (1974), 413–417.
- [156] JAMMALAMADAKA, S. R., AND SENGUPTA, A. *Topics in circular statistics*. World Scientific Publishing, Singapore, 2001.
- [157] JARMAN, P. J. Behaviour of topi in a shadeless environment. *Zoologica Africana* 12 (1977), 101–111.
- [158] JAY A . ALDERMAN, P. R. . K., AND LEOPOLD, B. D. . Diel activity of female desert bighorn sheep in Western Arizona. *Journal of Wildlife Management* 53 (1989), 264–271.
- [159] JOHNSON, D. D. P., BAKER, S., MORECROFT, M. D., AND MACDONALD, D. W. Long-term resource variation and group size: a large-sample field test of the resource dispersion hypothesis. *BioMed Central Ecology* 1 (2001), 25–34.
- [160] JONES, M., MANDELIK, Y., AND DAYAN, T. Coexistence of temporally partitioned spiny mice: roles of habitat structure and foraging behavior. *Ecology* 82 (2001), 2164–2176.
- [161] JORDAN, M. J., BARRETT, R. H., AND PURCELL, K. L. Camera trapping estimates of density and survival of fishers (*Martes pennanti*). *Wildlife Biology* 17 (2011), 266–276.
- [162] KARANTH, K. U. Estimation of tiger densities in india using photographic captures and recaptures. *Biological Conservation* 79 (1995), 333–338.
- [163] KARANTH, K. U., AND NICHOLS, J. D. Estimation of tiger densities in India using photographic captures and recaptures. *Ecology* 79 (1998), 2852–2862.
- [164] KARANTH, K. U., NICHOLS, J. D., AND KUMAR, N. S. Estimating tiger abundance from camera trap data: field surveys and analytical issues. In *Camera traps in animal ecology: methods and analyses*, A. F. O'Connell, J. D. Nichols, and K. U. Karanth, Eds. Springer, Japan, 2011, pp. 97–117.
- [165] KARANTH, K. U., AND SUNQUIST, M. E. Behavioural correlates of predation by tiger (*Panthera tigris*), leopard (*Panthera pardus*) and dhole (*Cuon alpinus*) in Nagarahole, India. *Zoological Society of London* (2000), 255–265.
- [166] KAYS, R., TILAK, S., KRANSTAUBER, B., JANSEN, P. A., CARBONE, C., ROWCLIFFE, M., FOUNTAIN, T., EGGERT, J., AND HE, Z. Camera traps as sensor networks for monitoring animal communities. *International Journal of Research and Reviews in Wireless Sensor Networks* 1 (2011), 19–29.
- [167] KELLY, M. J., AND HOLUB, E. L. Camera trapping of carnivores: trap success among camera types and across species, and habitat selection by species, on salt pond mountain, Giles county, Virginia. *Northeastern Naturalist* 15 (2008), 249–262.
- [168] KENAGY, G. J. Daily and seasonal patterns of activity and energetics in a heteromyid rodent community. *Ecology* 54 (1973), 1201–1219.
- [169] KENAGY, G. J. The periodicity of daily activity and its seasonal changes in free-ranging and captive kangaroo rats. *Oecologia* 24 (1976), 105–140.

-
- [170] KENAGY, G. K. Seasonality of endogenous circadian rhythms in a diurnal rodent *Ammospermophilus leucurus* and a nocturnal rodent *Dipodomys merriami*. *Journal of Comparative Physiology* 128 (1978), 21–36.
- [171] KENT, V. T., AND HILL, R. A. The importance of farmland for the conservation of the brown hyaena *Parahyaena brunnea*. *Oryx* 47 (2013), 431–440.
- [172] KETEN, A. Distribution and habitat preference of roe deer (*Capreolus capreolus L.*) in Düzce Province (Turkey). *Journal of the Faculty of Forestry Istanbul University* 67 (2017), 22–28.
- [173] KILGO, J. C., LABISKY, R. F., AND FRITZEN, D. E. Influence of hunting on the behavior of white-tailed deer: implication for conservation of the florida panther. *Conservation Biology* 12 (1998), 1359–1364.
- [174] KITCHEN, A. M., GESE, E. M., AND SCHAUSTER, E. R. Resource partitioning between coyotes and swift foxes: space, time, and diet. *Canadian Journal of Zoology* 77 (1999), 1645–1656.
- [175] KLEIN, D. C., COON, S. L., ROSEBOOM, P. H., WELLER, J. L., BERNARD, M., GASTEL, J. A., ZATZ, M., IUVONE, P. M., RODRIGUEZ, I. R., BÉGAY, V., FALCON, J., CAHILL, G. M., CASSONE, V. M., AND BALER, R. The melatonin rhythm-generating enzyme: molecular regulation of serotonin N-acetyltransferase in the pineal gland. *Recent Progress in Hormone Research* 52 (1997), 307–358.
- [176] KNEITEL, J. M., AND CHASE, J. M. Trade-offs in community ecology: linking spatial scales and species coexistence. *Ecology Letters* 7 (2004), 69–80.
- [177] KOEHLER, G. M., AND HORNOCKER, M. G. Influences of season on bobcats in Idaho, USA. *Journal of Wildlife Management* 53 (1989), 197–202.
- [178] KOPROWSKI, J. L., AND CORSE, M. C. Time budgets, activity periods, and behavior of mexican fox squirrels. *Journal of Mammalogy* 86 (2005), 947–952.
- [179] KOTLER, B. P., BROWN, J. S., AND SUBACH, A. Mechanisms of species coexistence of optimal foragers: temporal partitioning by two species of sand dune gerbils. *Oikos* 67 (1993), 548–556.
- [180] KRUSKAL, J. B. Multidimensional scaling by optimizing goodness of fit to a nonmetric hypothesis. *Psychometrika* 29 (1964), 1–27.
- [181] KRUSKAL, J. B. Nonmetric multidimensional scaling: a numerical method. *Psychometrika* 29 (1964), 115–129.
- [182] KUCERA, T. E., AND BARRETT, R. H. In my experience: the trailmaster camera system for detecting wildlife. *Wildlife Society Bulletin* 21 (1993), 505–508.
- [183] KUCERA, T. E., AND BARRETT, R. H. A history of camera trapping. In *Camera traps in animal ecology: methods and analyses*, A. F. O’Connell, J. D. Nichols, and K. U. Karanth, Eds., no. January 2011. Springer, London, 2011, pp. 9–26.
- [184] KURE, N. *Living with leopards*. Sunbird, Cape Town, 2003.
- [185] LAURENCE, W. F., AND GRANT, J. D. Photographic identification of ground-nest predators in Australian tropical rainforest. *Wildlife Research* 21 (1994), 241–247.
- [186] LAWTON, J. H. *Community ecology in a changing world*. Ecology Institute, Oldendorf (Luhe), Germany, 1996.
- [187] LAWTON, J. H. Are there general laws in ecology? *Oikos* 84 (1999), 177–192.
- [188] LE MAITRE, D. C., MILTON, S. J., JARMAN, C., COLVIN, C. A., VLOK, J. H. J., MAITRE, D. C. L., MILTON, S. J., JARMAN, C., COLVIN, C. A., SAAYMAN, I., AND VLOK, J. H. J. Linking ecosystem services and water resources: landscape-scale hydrology of the Little Karoo. *Frontiers in Ecology and the Environment* 5, 5 (2007), 261–270.

- [189] LE ROUX, P. G., AND SKINNER, J. D. A note on the ecology of the leopard (*Panthera pardus Linnaeus*) in the Londolozi Game Reserve, South Africa. *African Journal of Ecology* 27 (1989), 167–171.
- [190] LEE, T. M., CARMICHAEL, M. S., AND ZUCKER, I. Circannual variations in circadian rhythms of ground squirrels. *American Journal of Physiology* 250 (1986), 831–836.
- [191] LEE, T. M., HOMES, W. G., AND ZUCKER, I. Temperature dependence of circadian rhythms in golden-mantled ground squirrels. *Journal of Biological Rhythms* 5 (1990), 25–34.
- [192] LEIBOLD, M. A., HOLYOAK, M., MOUQUET, N., AMARASEKARE, P., CHASE, J. M., HOOPES, M. F., HOLT, R. D., SHURIN, J. B., LAW, R., TILMAN, D., LOREAU, M., AND GONZALEZ, A. The meta-community concept: a framework for multi-scale community ecology. *Ecology Letters* 7 (2004), 601–613.
- [193] LEWIN, R. Supply-Side Ecology. *Science* 234 (1986), 25–27.
- [194] LINCOLN, G. A., CLARKE, I. J., HUT, R. A., AND HAZLERIGG, D. G. Characterizing a mammalian circannual pacemaker. *Science* 314 (2006), 1941–1944.
- [195] LINDSEY, P. A., MASTERSON, C. L., BECK, A. L., AND ROMANACH, S. Ecological, social and financial issues related to fencing as a conservation tool in Africa. In *Fencing for conservation: restriction of evolutionary potential or a riposte to threatening processes?*, no. January 2012. Springer New York, 2012, pp. 215–234.
- [196] LOMBARD, A. T., COWLING, R. M., VLOK, J. H. J., AND FABRICUS, C. Designing conservation corridors in production landscapes: assessment methods, implementation issues, and lessons learned. *Ecology and Society* 15 (2010), 7.
- [197] LOMOLINO, M. Elevation gradients of species diversity: historical and prospective views. *Global Ecology and Biogeography* 10 (2001), 3–13.
- [198] LOVEGROVE, B. The deserts of southern Africa. In *The living deserts of southern Africa*. Fernwood Press, Vlaeberg, 1993, pp. 18–19.
- [199] LOW, A. B., AND ROBELO, A. G. *Vegetation of South Africa, Lesotho and Swaziland*. Department of Environmental Affairs and Tourism, Pretoria, South Africa, 1996.
- [200] MAC NALLY, R. C. *Ecological versatility and community ecology*. Cambridge University Press, Cambridge, UK, 1995.
- [201] MACCARINI, T. B., ATTIAS, N., MEDRI, I. M., MARINHO-FILHO, J., AND MOURAO, G. Temperature influences the activity patterns of armadillo species in a large neotropical wetland. *Mammal Research* 60 (2015), 403–409.
- [202] MACE, R. D., MINTA, S. C., MANLEY, T. L., AND AUNE, K. E. Estimating grizzly bear population size using camera sightings. *Wildlife Society Bulletin* 22 (1994), 74–83.
- [203] MAFFEI, L., CUÉLLAR, E., AND NOSS, A. One thousand jaguars (*Panthera onca*) in Bolivia's Chaco? Camera trapping in the Kaa-Iya National Park. *Zoological Society of London* 262 (2004), 295–304.
- [204] MAFFEI, L., AND NOSS, A. J. How small is too small? Camera trap survey areas and density estimates for ocelots in the Bolivian Chaco. *Biotropica* 40 (2008), 71–75.
- [205] MAFFEI, L., NOSS, A. J., CUÉLLAR, E., AND RUMIZ, D. I. Ocelot (*Felis pardalis*) population densities, activity, and ranging behaviour in the dry forests of eastern Bolivia: data from camera trapping. *Journal of Tropical Ecology* 21 (2005), 349–353.
- [206] MAHER, R., AND LOTT, F. Definitions of territoriality used in the study of variation in vertebrate spacing systems. *Animal Behaviour* 49 (1995), 1581–1597.

-
- [207] MAJOR, R. E., AND GOWING, G. An inexpensive photographic technique for identifying nest predators at active nests of birds. *Wildlife Research* 21 (1994), 657–666.
- [208] MANN, G. *Aspects of the ecology of leopards (panthera pardus) in the Little Karoo, South Africa*. PhD thesis, Rhodes University, 2014.
- [209] MARDIA, K. V., KENT, J. T., AND BIBBLY, J. M. *Multivariate analysis*. Academic Press, London, 1979.
- [210] MARTINS, Q., AND HARRIS, S. Movement, activity and hunting behaviour of leopard in the Cederberg mountains, South Africa. *African Journal of Ecology* 51 (2013), 571–579.
- [211] MARTINS, Q., HORSNELL, W. G. C., TITUS, W., RAUTENBACH, T., AND HARRIS, S. Diet determination of the Cape mountain leopards using global positioning system location clusters and scat analysis. *Journal of Zoology* 283, 2 (2011), 81–87.
- [212] MARTINS, Q., AND MARTINS, N. Leopards of the Cape: conservation and conservation concerns. *International Journal of Environmental Studies* 63, 5 (2006), 579–585.
- [213] MARTINS, Q. E. *The ecology of the leopard Panthera pardus in the Cederberg Mountains*. PhD thesis, University of Bristol, Bristol, UK, 2010.
- [214] MCCAIN, C. M. The mid-domain effect applied to elevational gradients: species richness of small mammals in Costa Rica. *Journal of Biogeography* 31 (2004), 19–31.
- [215] MCCAIN, C. M. Elevational gradients in diversity of small mammals. *Ecology* 86 (2005), 366–372.
- [216] MCCAIN, C. M., AND BECK, J. Species turnover in vertebrate communities along elevational gradients is idiosyncratic and unrelated to species richness. *Global Ecology and Biogeography* 25 (2015), 299–310.
- [217] MCCULLAGH, P. John Wilder Tukey. *Biographical Memoirs of Fellows of the Royal Society* 49 (2003), 537–555.
- [218] MCINTOSH, R. P. *The background of ecology: concept and theory*. Cambridge University Press, 1985.
- [219] MCNAB, B. K. Bioenergetics and the determination of home range size. *American Naturalist* 97 (1963), 133–140.
- [220] MECHTLY, E. A. *The International System of Units. Physical constants and conversion factors*. National Aeronautics and Space Administration, Washington, 1973.
- [221] MEEK, P. D., BALLARD, G.-A., FLEMING, P. J. S., SCHAEFER, M., WILLIAMS, W., AND FALZON, G. Camera traps can be heard and seen by animals. *PLoS ONE* 9 (2014), e110832.
- [222] MEENTEMEYER, V., AND BOX, E. O. Scale effects in landscape studies. In *Landscape heterogeneity and disturbance*, M. G. Turner, Ed. 1987, pp. 15–34.
- [223] MENAKER, M., MONEIRA, L. F., AND TOSINI, G. Evolution of circadian organization in vertebrates. *Brazilian Journal of Medical and Biological Research* 30 (1977), 305–313.
- [224] MENAKER, M., AND TOSINI, G. The evolution of vertebrate circadian systems. In *Circadian organisation and oscillatory coupling*, K. I. Honma and S. Honma, Eds. Hokkaido University Press, Sapporo, Japan, 1996, pp. 39–52.
- [225] MENZEL, M. A., FORD, W. M., LAERM, J., AND KRISHON, D. Forest to wildlife opening: habitat gradient analysis among small mammals in the southern Appalachians. *Forest Ecology and Management* 114 (1999), 227–232.
- [226] MEREDITH, M., AND RIDOUT, M. *Estimates of coefficient of overlapping for animal activity patterns*. R package version 3.2.4. Vienna, Austria, 2014.

- [227] MERRIAM, C. H. Results of a biological survey of the San Francisco mountain region and desert of the Little Colorado, Arizona. *North American Fauna* 3 (1890), 1–136.
- [228] MERRIAM, C. H. *Life zones and crop zones of the United States*. Government Printing Office, Washington, 1898.
- [229] MILNE, B. T. Heterogeneity as a multiscale characteristic of landscapes. In *Ecological heterogeneity*, J. Kolasa and S. T. A. Pickett, Eds. 1991, pp. 69–84.
- [230] MITTERMEIER, R. A., GIL, P. R., HOFFMAN, M., PILGRIM, J., BROOKS, T., MITTERMEIER, C. G., LAMOREUX, J., AND DA FONSECA, G. A. B. *Hotspots revisited: Earth's biologically richest and most endangered terrestrial ecoregions*. Cemex Books, Mexico, 2005.
- [231] MITTERMEIER, R. A., TURNER, W. R., LARSEN, F. W., BROOKS, T. M., AND GASCON, C. Global biodiversity conservation: the critical role of hotspots. In *Biodiversity hotspots*, F. E. Zachos and J. C. Habel, Eds., no. January. Springer, Verlag Berlin Heidelberg, 2011, pp. 3–22.
- [232] MIYAZAKI, Y., NISIMURA, Y., AND NUMATA, H. Circannual rhythm in the varied carped beetle, *Anthrenus verbasci*. In *The neurobiology of circadian timing*, A. Kalsbeek, M. Merrow, T. Roenneberg, and R. G. Foster, Eds., vol. 199. Elsevier, Amsterdam, 2012, pp. 439–456.
- [233] MIZUTANI, F., AND JEWELL, P. A. Home-range and movements of leopards (*Panthera pardus*) on a livestock ranch in Kenya. *Journal of Zoology* 244 (1998), 269–286.
- [234] MOEBIUS, K. *Die Auster und die Austernwirtschaft*. Ecology Institute, Berlin, 1877.
- [235] MOONEY, C. Z., AND DUVAL, R. D. *Bootstrapping: a non-parametric approach to statistical inference*. SAGE University Paper series, Newbury Park, CA: SAGE, 1993.
- [236] MOORE, I. T., BONIER, F., AND WINGFIELD, J. C. Reproductive asynchrony and population divergence between two tropical bird populations. *Behavioral Ecology* 16 (2005), 755–762.
- [237] MORRISON, M. L., MARCOT, B. G., AND MANNAN, R. W. *Wildlife-habitat relationships: concepts and applications*, third edit ed. Island Press, Washington, 2006.
- [238] MORTON, S. R., STAFFORD SMITH, D. M., FRIEDEL, M. H., GRIFFIN, G. F., AND PICKUP, G. The stewardship of arid Australia: ecology and landscape management. *Journal of Environmental Management* 43 (1995), 195–217.
- [239] MROSOVSKY, N. Locomotor activity and non-photic influences on circadian clocks. *Biological Reviews* 71 (1996), 343–372.
- [240] MYERS, N. Biodiversity hotspots revisited. *BioScience* 53 (2003), 916–917.
- [241] MYERS, N., MITTERMEIER, R. A., MITTERMEIER, C. G., DA FONSECA, A. B., AND KENT, J. Biodiversity hotspots for conservation priorities. *Nature* (2000), 853–858.
- [242] NASA EOSDIS LAND PROCESSES DAAC. *USGS Earth Resources Observation and Science (EROS) Center*. Sioux Falls, 2017.
- [243] NATHAN, R., SPIEGEL, O., FORTMANN-ROE, S., HAREL, R., WIKELSKI, M., AND GETZ, W. Using tri-axial acceleration data to identify behavioral modes of free-ranging animals: general concepts and tools illustrated for griffon vultures. *Journal of Experimental Biology* 215 (2012), 986–996.
- [244] NELSON, R. J., DENLINGER, D. L., AND SOMERS, D. E., Eds. *Photoperiodism: the biological calendar*. Oxford University Press, Oxford, 2010.
- [245] NENADIC, O., AND GREENACRE, M. Correspondence Analysis in R, with two- and three-dimensional graphics: The ca package. *Journal of Statistical Software* 20 (2007), 1–13.

-
- [246] NICHOLS, W. F., KILLINGBECK, K. T., AND AUGUST, P. V. The influence of geomorphological heterogeneity on biodiversity II. A patch-scale perspective. *Conservation Biology* 12 (1998), 371–379.
- [247] NORTON, D. A. Conservation biology and private land: shifting the focus. *Conservation Biology* 14 (2000), 1221–1223.
- [248] NORTON, P. M. Historical changes in the distribution of leopards in the Cape Province, South Africa. *Bontebok* 5 (1986), 1–9.
- [249] NORTON, P. M., AND HENLEY, S. R. Home range and movements of male leopards in the Cedarberg Wilderness Area, Cape Province. *South African Journal of Wildlife Research* 17 (1987), 41–48.
- [250] NORTON, P. M., AND LAWSON, A. B. Radio tracking of leopards and caracals in the Stellenbosch area, Cape Province. *South African Journal of Wildlife Research* 16 (1985), 47–52.
- [251] NORTON, P. M., LAWSON, A. B., HENLEY, S. R., AND AVERY, G. Prey of leopards in four mountainous areas of the south-western Cape Province. *South African Journal of Wildlife Research* 16 (1986), 47–52.
- [252] O’CONNELL, A. F., NICHOLS, J. D., AND KARANTH, K. U. *Camera traps in animal ecology: methods and analyses*. No. January 2011. Springer, London, 2011.
- [253] O’FARRELL, P., LE MAITRE, D., GELDERBLOM, C., BONORA, D., HOFFMAN, T., AND REYERS, B. Applying a resilience framework in the pursuit of sustainable land-use development in the Little Karoo, South Africa. In *Advancing Sustainability Science*. SUN PReSS, Stellenbosch, 2008, pp. 383–432.
- [254] OLIVEIRA-SANTOS, L. G. R., ZUCCO, C. A., AND AGOSTINELLI, C. Using conditional circular kernel density functions to test hypotheses on animal circadian activity. *Animal Behaviour* 85 (2013), 269–280.
- [255] ORPWOOD, J. E., GRIFFITHS, S. W., AND ARMSTRONG, J. D. Effects of food availability on temporal activity patterns on growth of Atlantic salmon. *Journal of Animal Ecology* 75 (2006), 677–685.
- [256] OTIS, D. L., BURNHAM, K. P., WHITE, G. C., AND ANDERSON, D. R. Statistical inference from capture data on closed animal populations. *Wildlife Monographs* 62 (1978).
- [257] PALOMARES, F., AND DELIBES, M. Determining activity types and budgets from movement speed of radio-marked mongooses. *Journal of Wildlife Management* 57 (1993), 164–167.
- [258] PARTECKE, J., HOF, T. J. V., AND GWINNER, E. Underlying physiological control of reproduction in urban and forest-dwelling European blackbirds *Turdus merula*. *Journal of Avian Biology* 36 (2005), 295–305.
- [259] PEARSON, O. P. A traffic survey of *Microtus reithrodontomys* runways. *Journal of Mammalogy* 40 (1959), 169–180.
- [260] PEARSON, O. P. Habits of *Microtus californicus* revealed by automatic photographic recorders. *Ecological Monographs* 30 (1960), 231–250.
- [261] PICMAN, J. An inexpensive camera setup for the study of egg predation at artificial nests. *Journal of Field Ornithology* 58 (1992), 372–382.
- [262] PITTENDRIGH, C. S. The amplitude of circadian oscillations: temperature dependence, latitudinal clines and photoperiodic time measurement. *Journal of Biological Rhythms* 6 (1991), 299–313.
- [263] PITTENDRIGH, C. S., AND DAAN, S. A functional analysis of circadian pacemakers in nocturnal rodents. IV. Entrainment: pacemaker as clock. *Journal of Comparative Physiology* 106 (1976), 291–331.

- [264] PLEDGER, S. Unified maximum likelihood estimates for closed capture-recapture models using mixtures. *Biometrics* 56 (2000), 434–442.
- [265] POOLE, K. G., AND BOAG, D. A. Ecology of gyrfalcons, *Falco rusticolus*, in the central Canadian Arctic: diet and feeding behavior. *Canadian Journal of Zoology* 41 (1988), 31–38.
- [266] POSSIDENTE, B., AND HEGMANN, J. P. Gene differences modify Aschoff’s rule in mice. *Physiology and Behavior* 28 (1982), 199–200.
- [267] PYKE, G. H., PULLIAM, H. R., AND CHARNOV, E. L. Optimal foraging: a selective review of theory and tests. *The Quarterly Review of Biology* 52 (1977), 137–154.
- [268] QUANTUM GIS DEVELOPMENT TEAM. *QGIS Geographic Information System, Open Source Geospatial Foundation Project*. version 2.10.1. Pisa, 2017.
- [269] R DEVELOPMENT CORE TEAM. *R: a language and environment for statistical computing*. R Foundation for Statistical Computing, version 3.2.4. Vienna, Austria, 2016.
- [270] RADLOFF, F. G. T. *The ecology of large herbivores native to the coastal lowlands of the Fynbos Biome in the Western Cape, South Africa*. PhD thesis, Stellenbosch University, Stellenbosch, South Africa, 2008.
- [271] RAMESH, T., SNEHALATHA, V., SANKAR, K., AND QURESHI, Q. Food habits and prey selection of tiger and leopard in Mudumalai Tiger Reserve, Tamil Nadu, India. *Scientific Transactions in Environment and Technovation* 2 (2009), 170–181.
- [272] RASTOGI, A. D., ZANETTE, L., AND CLINCHY, M. Food availability affects diurnal nest predation and adult antipredator behaviour in song sparrows, *Melospiza melodia*. *Animal behaviour* 72 (2006), 933–940.
- [273] RAUTENBACH, T. *Assessing the diet of the Cape leopard (Panthera pardus) in the Cederberg and Gamka Mountains, South Africa*. MSc thesis, Nelson Mandela Metropolitan University, Port Elizabeth, 2010.
- [274] RAY, J. C., HUNTER, L., AND ZIGOURIS, J. Setting conservation and research priorities for larger African carnivores. 2005.
- [275] REEBS, S. G. Plasticity of diel and circadian activity rhythms in fishes. *Reviews in Fish Biology and Fisheries* 12 (2003), 349–371.
- [276] REISS, M. Scaling of home range size: body size, metabolic needs and ecology. *Trends in Ecology and Evolution* 3 (1988), 86–86.
- [277] REVIEWS, A. Partitioning of time as an ecological resource. *Annual Review of Ecology, Evolution and Systematics* 34 (2003), 153–181.
- [278] RICE, C. G. Trailmaster camera system: the dark side. *Wildlife Society Bulletin* 23 (1995), 110–111.
- [279] RICH, L. N., DAVIS, C. L., FARRIS, Z. J., MILLER, D. A. W., TUCKER, J. M., HAMEL, S., FARHADINIA, M. S., STEENWEG, R., DI BITETTI, M. S., THAPA, K., KANE, M. D., SUNARTO, S., ROBINSON, N. P., PAVIOLO, A., CRUZ, P., MARTINS, Q., GHOLIKHANI, N., TAKTEHRANI, A., WHITTINGTON, J., WIDODO, F. A., YOCOZ, N. G., WULTSCH, C., HARMSSEN, B. J., AND KELLY, M. J. Assessing global patterns in mammalian carnivore occupancy and richness by integrating local camera trap surveys. *Global Ecology and Biogeography* 26 (2016), 918–929.
- [280] RICHARDS, S. A. Temporal partitioning and aggression among foragers: modeling the effects of stochasticity and individual state. *Behavioral Ecology* 13 (2002), 427–438.
- [281] RICHARDSON, P. R. K. Food consumption and seasonal variation in the diet of the aardwolf *Proteles cristatus* in southern Africa. *Zeitschrift für Säugetierkunde* 52 (1987), 307–325.

-
- [282] RICKART, E. A. Elevational diversity gradients, biogeography and the structure of montane mammal communities in the intermountain region of North America. *Global Ecology and Biogeography* 10 (2001), 77–100.
- [283] RIDOUT, A. M. S., LINKIE, M., RIDOUT, M. S., AND LINKIE, M. Estimating overlap of daily activity patterns from camera trap data. *Journal of Agricultural, Biological and Environmental Statistics* 14 (2017), 322–337.
- [284] RILEY, S. J., DEGLORIA, S. D., AND ELLIOT, R. A terrain ruggedness index that quantifies topographic heterogeneity. *Intermountain Journal of Sciences* 5 (1999), 23–27.
- [285] RIPLEY, B., VENABLES, B., BATES, D. M., HORNIK, K., GEBHARDT, A., AND FIRTH, D. *Package MASS in CRAN*. R package version 3.2.4. Vienna, Austria, 2016.
- [286] RIPPLE, W. J., AND BESCHTA, R. L. Wolves and the ecology of fear: can predation risk structure ecosystems? *BioScience* 54 (2004), 755–766.
- [287] RISSER, P. G. Landscape ecology: state of the art. In *Landscape heterogeneity and disturbance*, M. G. Turner, Ed. Springer, New York, 1987, pp. 3–14.
- [288] RIVERO, K., RUMIZ, D. I., AND TABER, A. B. Differential habitat use by two sympatric brocket deer species (*Mazama americana* and *M. gouazoubira*) in a seasonal Chiquitano forest of Bolivia. *Mammalia* 69 (2005), 169–183.
- [289] RODRIGUES, A. S. L., ANDELMAN, S. J., BAKARR, M. I., BOITANI, L., BROOKS, T. M., CROWLING, R. M., FISHPOOL, L. D. C., DA FONSECA, G. A. B., GASTON, K. J., HOFFMANN, M., LONG, J. S., MARQUET, P. A., PILGRIM, J. D., PRESSEY, R. L., SCHIPPER, J., SECHREST, W., STUART, S. N., UNDERHILL, L. G., WALLER, R. W., WATTS, M. E. J., AND YAN, X. Effectiveness of the global protected area network in representing species diversity. *Nature* 428 (2004), 640–643.
- [290] ROWCLIFFE, M., KAYS, R., KRANSTAUBER, B., CARBONE, C., AND JANSEN, P. A. Quantifying levels of animal activity using camera-trap data. *Methods in Ecology and Evolution* (2014), 1–10.
- [291] ROWSEMITT, C. N., PETTERBERG, L. J., CLAYPOOL, L. E., HOPPENSTAEDT, F. C., NEGUS, N. C., AND BERGER, P. J. Photoperiodic induction of diurnal locomotor activity in *Microtus montanus*, the montane vole. *Canadian Journal of Zoology* 60 (1982), 2798–2803.
- [292] ROYLE, J. A., KARANTH, K. U., GOPALASWAMY, A. M., AND KUMAR, N. S. Bayesian inference in camera trapping studies for a class of spatial capture-recapture models. *Ecology* 90 (2009), 3233–3244.
- [293] ROYLE, J. A., MAGOUN, A. J., GARDNER, B., VALKENBURG, P., AND LOWELL, R. E. Density estimation in a wolverine population using spatial capture-recapture models. *Journal of Wildlife Management* 75 (2011), 604–611.
- [294] SADLEIR, R. M. F. S. *The ecology of reproduction in wild and domestic mammals*. Methuen and Co., London, 1969.
- [295] SAPPINGTON, J. M., LONGSHORE, K. M., AND THOMPSON, D. Quantifying landscape ruggedness for animal habitat analysis: a case study using bighorn sheep in the Mojave Desert. *Journal of Wildlife Management* 71 (2007), 1419–1426.
- [296] SCHILLINGS, C. G. *With flash-light and rifle: a record of hunting adventures and of studies in wild life in equatorial East Africa*. Harper & Brothers, New York, 1905.
- [297] SCHILLINGS, C. G. *In wildest Africa. Volume I and II*. Hutchinson & Co., London, 1907.
- [298] SCHOENER, T. W. Resource partitioning in ecological communities. *Science* 185 (1974), 27–39.
- [299] SCHRADIN, C., AND PILLAY, N. Female striped mice (*Rhabdomys pumilio*) change their home ranges in response to seasonal variation in food availability. *Behavioral Ecology* 17 (2006), 452–458.

- [300] SCHWARZ, C. J., AND SEBER, G. A. F. Estimating animal abundance. *Statistical Science* 14 (1999), 427–456.
- [301] SHIMOMURA, K., VITATERNA, M. H., LOW-ZEDDIES, S. S., WHITELEY, A. R., AND TAKAHASHI, J. S. *Genetic dissection of strain differences in mouse circadian rhythmicity. Presented at the Annual Meeting of the Society for Research on Biological Rhythms*. Amelia Island Plantation, 1998.
- [302] SHIRAS, G. Photographing wild game with flashlight and camera. *National Geographic Magazine* 17 (1906), 366–423.
- [303] SHIRAS, G. One season's game bag with a camera. *National Geographic Magazine* 19 (1908), 387–446.
- [304] SHIRAS, G. Wild animals that took their own pictures by day and by night. *National Geographic Magazine* 24 (1913), 763–834.
- [305] SHUKOR, M. N. Elevational diversity patterns of small mammals on Mount Kinabalu, Sabah, Malaysia. *Global Ecology and Biogeography* 10 (2001), 41–62.
- [306] SILVER, S. C., OSTRO, L. E. T., MARSH, L. K., MAFFEI, L., NOSS, A. J., KELLY, M. J., WALLACE, R. B., GOMEZ, H., AND AYALA, G. The use of camera traps for estimating jaguar *Panthera onca* abundance and density using capture-recapture analysis. *Oryx* 38 (2004), 148–154.
- [307] SILVERTOWN, J. A new dawn for citizen science. *Trends in Ecology and Evolution* 24 (2009), 467–471.
- [308] SIMBERLOFF, D. Community ecology: is it time to move on? *American Society of Naturalists* 163 (2004), 787–799.
- [309] SIMONOFF, J. S. *Density estimation for statistics and data analysis*. Chapman and Hall, London, 1986.
- [310] SKINNER, J. D., AND SMITHERS, R. H. N. *The mammals of the southern African subregion*. University of Pretoria, Pretoria, 1990.
- [311] SMALLWOOD, K. S., AND FITZHUGH, E. L. A track count for estimating mountain lion *Felis concolor* California population trends. *Biological Conservation* 71 (1995), 251–259.
- [312] SMITH, D. A. E., SMITH, Y. C. E., RAMESH, T., AND DOWNS, C. T. Camera-trap data elucidate habitat requirements and conservation threats to an endangered forest specialist, the spotted ground thrush (*Zoothera guttata*). *Forest Ecology and Management* 400 (2017), 523–530.
- [313] SOISALO, M. K., AND CAVALCANTI, S. M. Estimating the density of a jaguar population in the Brazilian Pantanal using camera-traps and capture-recapture sampling in combination with GPS radio-telemetry. *Biological Conservation* 129 (2006), 487–496.
- [314] SOLLMANN, R., FURTADO, M. M., GARDNER, B., HOFER, H., JACOMO, A. T. A., TÔRRES, N. M., AND SILVEIRA, L. Improving density estimates for elusive carnivores: accounting for sex-specific detection and movements using spatial capture-recapture models for jaguars in central Brazil. *Biological Conservation* 144 (2011), 1017–1024.
- [315] SOLLMANN, R., FURTADO, M. M., HOFER, H., JÁCOMO, A. T. A., TORRES, N. M., AND SILVEIRA, L. Using occupancy models to investigate space partitioning between two sympatric large predators, the jaguar and puma in central Brazil. *Mammalian Biology* 77 (2012), 41–46.
- [316] SOLLMANN, R., GARDNER, B., CHANDLER, R. B., SHINDLE, D. B., ONORATO, D. P., ROYLE, J. A., AND O'CONNELL, A. F. Using multiple data sources provides density estimates for endangered Florida panther. *Journal of Applied Ecology* 50 (2013), 961–968.
- [317] SONI, B. G., AND FOSTER, R. G. A novel and ancient vertebrate opsin. *Federation of European Biochemical Societies Letters* 406 (1997), 279–283.

-
- [318] SOULÉ, M. E., AND WILCOX, B. A. *Conservation biology: an evolutionary-ecological perspective*. Sinauer Associates, Sunderland, 1980.
- [319] SOUTH AFRICAN NATIONAL BIODIVERSITY INSTITUTE. *Little Karoo Biodiversity Assessment*. South African National Biodiversity Institute, Cape Town, 2008.
- [320] STANDER, P. E., HADEN, P. J., KAZECE, I., AND GHU, I. The ecology of asociality in Namibian leopards. *Journal of Zoology* 242 (1997), 343–364.
- [321] STEIDL, R. J., GRIFFIN, C. R., AND NILES, L. J. Differential reproductive success of ospreys in New Jersey. *Journal of Wildlife Management* 55 (1991), 266–272.
- [322] STEPHENS, P. A., ZAUMYSLOVA, O. Y., MIQUELLE, D. G., MYSLENKOV, A. I., AND HAYWARD, G. D. Estimating population density from indirect sign: track counts and the Formozov-Malyshev-Pereleshin formula. *Animal Conservation* 9 (2006), 339–348.
- [323] STRAUSS, S. Y. Indirect effects in community ecology: their definition, study and importance. *Trends in Ecology and Evolution* 6 (1991), 206–210.
- [324] STUART, C. T. Notes on the mammalian carnivores of the Cape Province, South Africa. *Bontebok* 1 (1981), 1–58.
- [325] STUART, C. T., MACDONALD, I. A. W., AND MILLS, M. G. L. History, current status and conservation of large mammalian predators in Cape Province, Republic of South Africa. *Biological Conservation* 31 (1985), 7–19.
- [326] SUNQUIST, M. E., AND SUNQUIST, F. C. *Wild cats of the world*. The University of Chicago Press, Chicago, 2002.
- [327] SUSELBEEK, L., ESENS, W.-J., HIRSCH, B. T., KAYS, R., ROWCLIFFE, J. M., ZAMORA-GUTIERREZ, V., AND JANSEN, P. A. Food acquisition and predator avoidance in a Neotropical rodent. *Animal Behaviour* 88 (2014), 41–48.
- [328] SWANEPEOL, L. H., LINDSEY, P., SOMERS, M. J., VAN HOVEN, W., AND DALERUM, F. Extent and fragmentation of suitable leopard habitat in South Africa. *Animal Conservation* 16 (2013), 41–50.
- [329] SWANEPEOL, L. H. *Viability of leopards Panthera pardus (Linnaeus, 1758) in South Africa*. PhD Thesis. University of Pretoria, Pretoria, 2009.
- [330] SWANN, D. E., HASS, C. C., DALTON, D. C., AND WOLF, S. A. Infrared-triggered cameras for detecting wildlife: an evaluation and review. *Wildlife Society Bulletin* 32 (2004), 357–365.
- [331] SWANSON, A., KOSMALA, M., SWANSON, A., KOSMALA, M., LINTOTT, C., AND SIMPSON, R. Snapshot Serengeti, high-frequency annotated camera trap images of 40 mammalian species in an African savanna. *Scientific Data* 2 (2015), 150026.
- [332] SYMONDS, M. R. E., AND MOUSSALLI, A. A brief guide to model selection, multimodel inference and model averaging in behavioural ecology using Akaike’s information criterion. *Behavioral Ecology and Sociobiology* 65 (2011), 13–21.
- [333] SZOR, G., BERTEAUX, D., AND GAUTHIER, G. Finding the right home: distribution of food resources and terrain characteristics influence selection of denning sites and reproductive dens in arctic foxes. *Polar Biology* 31 (2008), 351–362.
- [334] TAYLOR, C. R. Hygroscopic food: a source of water for desert antelopes? *Nature* 219 (1968), 181–182.
- [335] TERBORGH, J. Maintenance of diversity in tropical forests. *Biotropica* 24 (1992), 283–292.
- [336] TERRIEN, J., PERRET, M., AND AUJARD, F. Behavioral thermoregulation in mammals: a review. *Frontiers in Bioscience* 16 (2011), 1428–1444.

- [337] THOMPSON, I. D., DAVIDSON, I. J., O'DONNELL, S., AND BRAZEAU, F. Use of track transects to measure the relative occurrence of some boreal mammals in uncut forest and regeneration stands. *Revue Canadienne de Zoologie* 67 (1989), 1816–1823.
- [338] TOBLER, M. Camera base user guide, 2013.
- [339] TRACY, C. R., AND CHRISTIAN, K. A. Ecological relations among space, time, and thermal niche axes. *Ecology* 67 (1986), 609–615.
- [340] TROLLE, M., AND KERY, M. Density estimation of ocelot *Leopardus pardalis* in the Brazilian Pantanal using capture-recapture analysis of camera trapping data. *Journal of Mammalogy* 84 (2003), 607–614.
- [341] TUKEY, J. W. *Exploratory data analysis*. Addison-Wesley, Boston, 1977.
- [342] TULLOCH, A. I. T., POSSINGHAM, H. P., JOSEPH, L. N., SZABO, J., AND MARTIN, T. G. Realising the full potential of citizen science monitoring programs. *Biological Conservation* 165 (2013), 128–138.
- [343] TURNER, M. G. Landscape ecology: the effect of pattern on process. *Annual Review of Ecology and Systematics* 20 (1989), 171–197.
- [344] TURNER, M. G., DALE, V. H., AND GARDNER, R. H. Predicting across scales: theory development and testing. *Landscape Ecology* 3 (1989), 245–252.
- [345] UNDERWOOD, H., AND GOLDMAN, B. D. Vertebrate circadian and photoperiodic systems: role of the pineal gland and melatonin. *Journal of Biological Rhythms* 2 (1987), 279–315.
- [346] VAN DER MERWE, I., BENNETT, N. C., HAIM, A., AND OOSTHUIZEN, M. K. Locomotor activity in the Namaqua rock mouse (*Micaelamys namaquensis*) – entrainment by light manipulations. *Revue Canadienne de Zoologie* 92 (2014), 1083–1091.
- [347] VAN DYKE, F. The history and distinctions of conservation. In *Conservation biology. Foundations, concepts and applications*, F. van Dyke, Ed. Springer, Wheaton, 2008, pp. 1–27.
- [348] VAN SCHAIK, C. P., AND GRIFFITHS, M. Activity periods of indonesian rain forest mammals. *Biotropica* 28 (1996), 105–112.
- [349] VILLETTE, P., KREBS, C. J., AND JUNG, T. S. Evaluating camera traps as an alternative to live-trapping to estimate the density of snowshoe hares (*Lepus americanus*) and red squirrels (*Tamiasciurus hudsonicus*). *European Journal of Wildlife Research* 6 (2017), 3.
- [350] VON HUMBOLDT, A. *Ideen zu einer geographie der pflanzen nebat einem naturgemalde der tropen-lander*. Tübingen, 1807.
- [351] VSN INTERNATIONAL. *Genstat for Windows 17th Edition*. VSN International, Hemel Hempstead, 2014.
- [352] WACHER, T., AND ATTUM, O. Preliminary investigation into the presence and distribution of small carnivores in the empty quarter of Saudi Arabia through the use of a camera trap. *Mammalia* 69 (2005), 81–84.
- [353] WAGENMAKERS, E., AND FARRELL, S. AIC model selection using Akaike weights. *Psychonomic Bulletin and Review* 11 (2004), 192–196.
- [354] WALLS, G. L. *The vertebrate eye and its adaptive radiation*. Cranbrook Institute of Science, Bloomfield Hills, 1942.
- [355] WANG, S. W., AND MACDONALD, D. W. The use of camera traps for estimating tiger and leopard populations in the high altitude mountains of Bhutan. *Biological Conservation* 142 (2009), 606–613.
- [356] WEGGE, P., POKHERAL, C. P., AND JNAWALI, S. R. Effects of trapping effort and trap shyness on estimates of tiger abundance from camera trap studies. *Animal Conservation* 7 (2004), 251–256.

-
- [357] WEIHER, E., AND KEDDY, P. *Ecological assembly rules: perspectives, advances, retreat*. Cambridge University Press, Cambridge, 1999.
- [358] WHELAN, C. J., DILGER, M. L., ROBSON, D., HALLYN, N., AND DILGER, S. Effects of olfactory cues on artificial-nest experiments. *Auk* 111 (1994), 945–952.
- [359] WHITE, K. S. Seasonal and sex-specific variation in terrain use and movement patterns of mountain goats in southeastern Alaska. In *Biennial symposium: Northern Wild Sheep and Goat Council*, no. August. Kananaksis, 2006, pp. 183–193.
- [360] WHITTAKER, R. H. Vegetation of the Great Smoky Mountains. *Ecological Monographs* 26 (1956), 1–80.
- [361] WHITTAKER, R. H., LEVIN, S. A., AND ROOT, R. B. Niche, habitat and ecotope. *American Naturalist* 197 (1973), 321–328.
- [362] WIENS, J. A. Spatial scaling in ecology. *Functional Ecology* 3 (1989), 385–397.
- [363] WIENS, J. A., ADDICOTT, J. F., CASE, T. J., AND DIAMOND, J. The importance of spatial and temporal scale in ecological investigations. In *Community Ecology*, J. Diamond and T. J. Case, Eds. Harper & Row, New York, 1986, pp. 145–153.
- [364] WILLIAMS, B. K., NICHOLS, J. D., AND CONROY, M. J. *Analysis and management of animal populations: modeling, estimation, and decision making*. Academic Press, London, 2002.
- [365] WILSON, D. E., AND REEDER, D. M. *Mammal species of the world. A taxonomic and geographic reference*. Smithsonian Institution Press, Washington, DC, 1993.
- [366] WILTING, A., MOHAMED, A., AMBU, L. N., LAGAN, P., MANNAN, S., AND HOFER, H. Sunda clouded leopard *Neofelis diardi* density in two used forests in Sabah, Malaysian Borneo. *Oryx* 46 (2012), 423–426.
- [367] WINSLADE, P. Behavioural studies on the lesser sandeel *Ammodytes marinus* (Raitt) l. The effect of food availability on activity and the role of olfaction in food detection. *Journal of Fish Biology* 6 (1974), 565–576.
- [368] WULF, A. *The invention of nature: the adventures of Alexander von Humboldt, the lost hero of science*. London, 2016.
- [369] YARNELL, R., RICHMOND-COGGAN, L., WILLIAMS, K., BISSETT, C., WELCH, C., AND WIESEL, I. A conservation assessment of *Parahyaena brunnea*. In *The Red List of Mammals of South Africa, Swaziland and Lesotho*. South African National Biodiversity Institute and Endangered Wildlife Trust, South Africa, 2016.
- [370] YERUSHALMI, S., AND GREEN, R. M. Evidence for the adaptive significance of circadian rhythms. *Ecology Letters* 12 (2009), 970–981.
- [371] YIMING, L. Seasonal variation of diet and food availability in a group of Sichuan snub-nosed monkeys in Shennongjia Nature Reserve, China. *American Journal of Primatology* 68 (2006), 217–233.
- [372] ZALEWSKI, A. Seasonal and sexual variation in diel activity rhythms of pine marten *Martes martes* in the Bialowieza National Park (Poland). *Acta Theriologica* 46 (2001), 295–304.
- [373] ZONNEVELD, I. S. The land unit - A fundamental concept in landscape ecology, and its applications. *Landscape Ecology* 3 (1989), 67–86.

Appendix

Appendix 1A

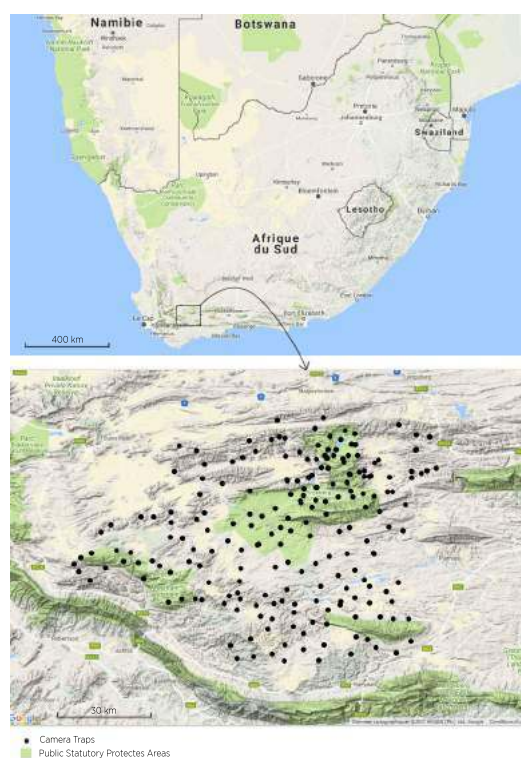


Figure 1A.1: The Little Karoo in South Africa

The Little Karoo of South Africa is a semi-arid inter-montane basin falling into the Cape Floristic Region, where three globally-recognised biodiversity hotspots intermingle [230, 231, 240]. The succulent Karoo biome is one of two international biodiversity hotspots located in arid regions [230]. In South Africa, although these semi-arid rangelands contain some of the most biodiversity rich landscapes in the country, they are also some of the least conserved spaces; falling under the national average of 6% of their area under protection [253].

Appendix 2A

Data Volume

Table 2A.1: Camera trap data volumes.

These statistics describe the amount of data collected throughout the camera trap study, which took place in the Little Karoo.

	Northern Sanbona included	Northern Sanbona excluded
Overall dataset		
Camera trap sites:	222	207
Camera trap nights:	17631	16409
Photo-captures:	26312	25211
Percentage of duplicates:	55	56
Independent photo-captures:	11742	10991
Species:	91	86
Mammals:	51	46
Birds:	39	39
Reptiles:	1	1
Seasonal dataset		
Camera trap sites:		207
Total camera trap nights:		14331
Photo-captures:		21469
Percentage of duplicates:		58
Independent photo-captures:		9057
Species:		80
Mammals:		46
Birds:		33
Reptiles:		1

Appendix 3A

Chloropleth maps

These shaded graphical representations show the preferences in terrain roughness (ruggedness) for 27 mammal species in the Little Karoo [Chapter 1 section 1.3.3.2].

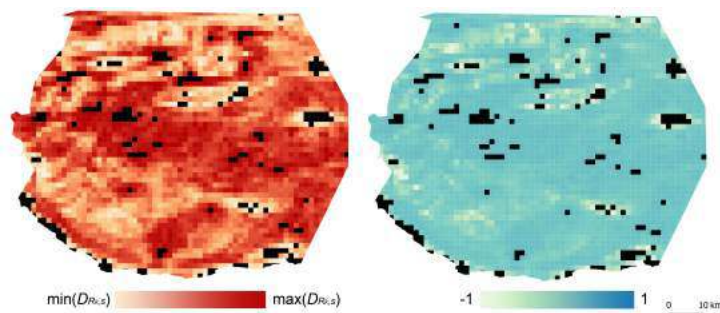


Figure 3A.1: armadillo

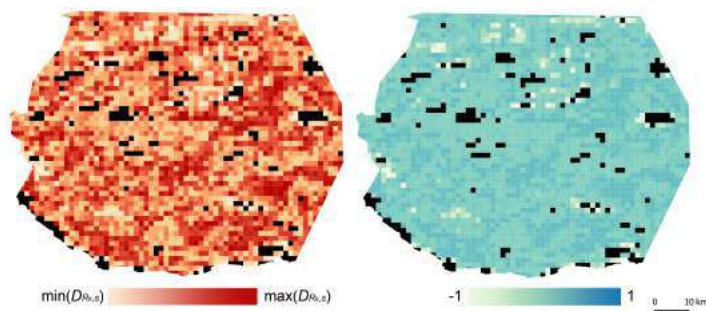


Figure 3A.2: armadillo

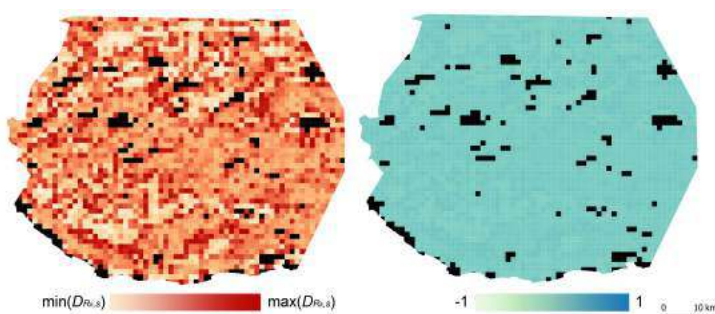


Figure 3A.3: African wildcat

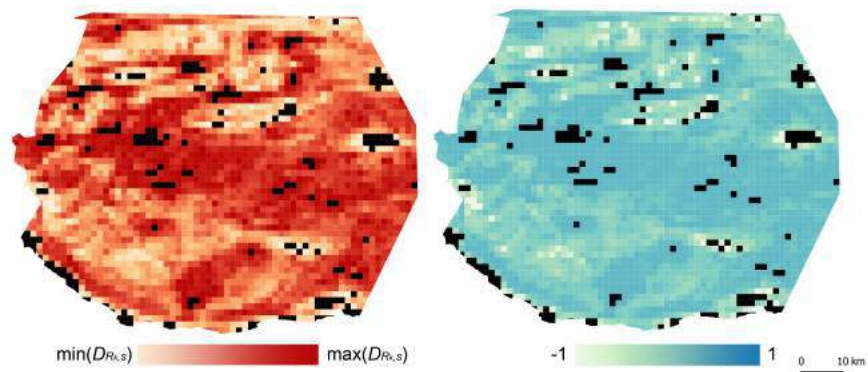


Figure 3A.4: black-backed jackal

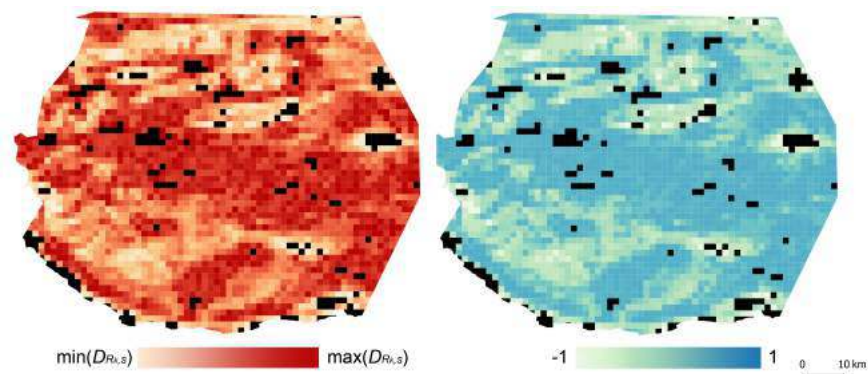


Figure 3A.5: brown hyena

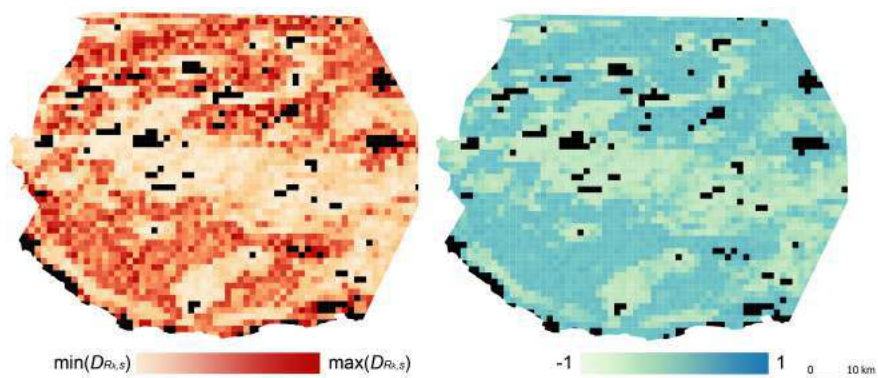


Figure 3A.6: Cape gray mongoose

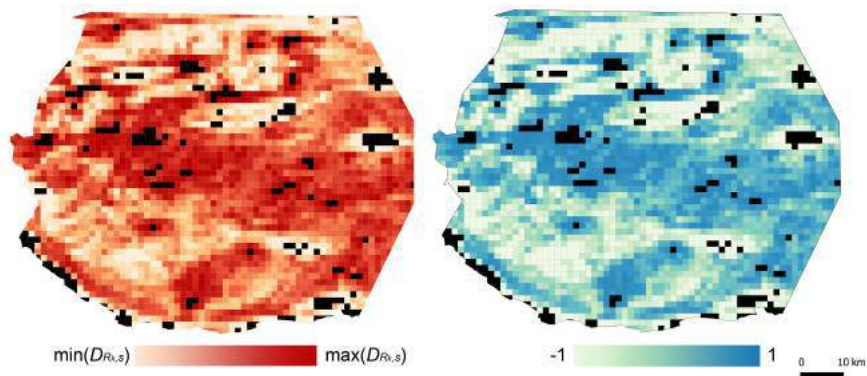


Figure 3A.7: Cape hare

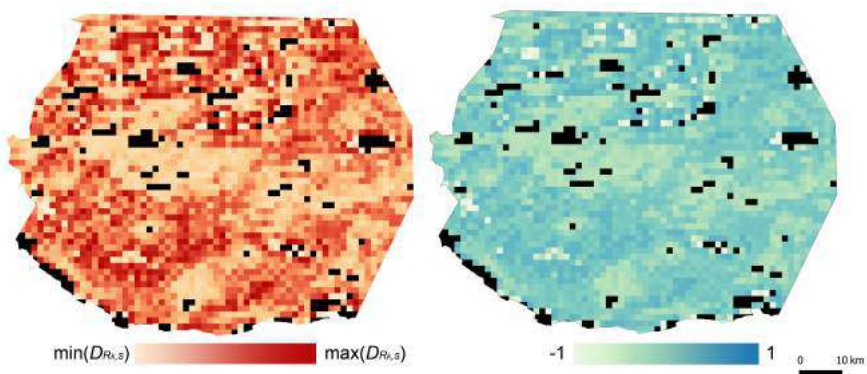


Figure 3A.8: Cape mountain zebra

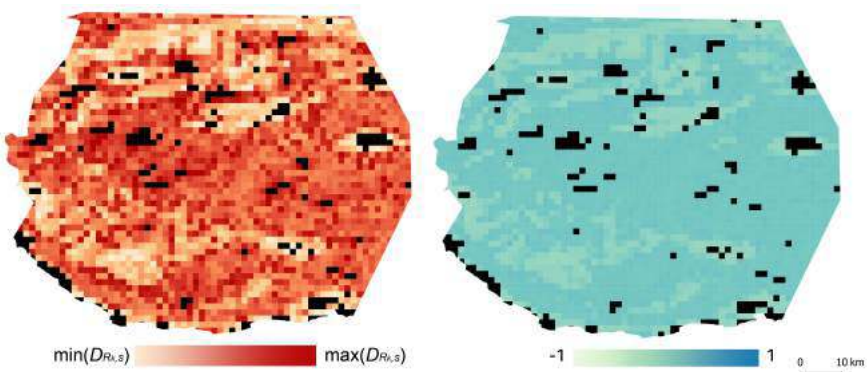


Figure 3A.9: Cape porcupine

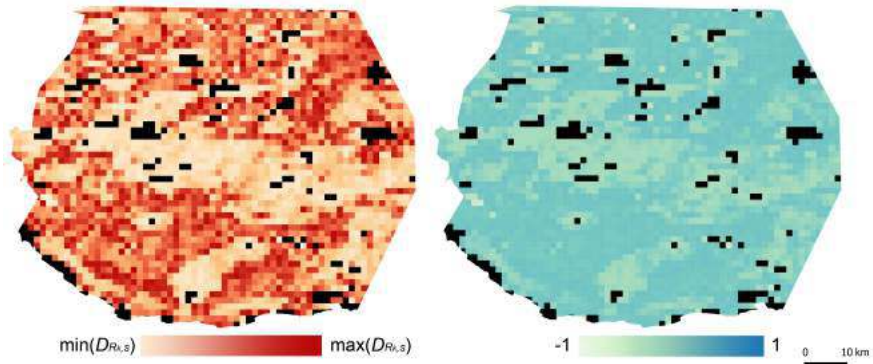


Figure 3A.10: caracal

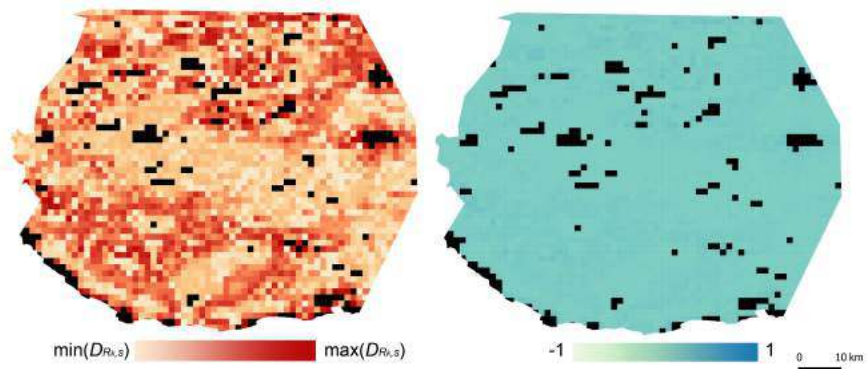


Figure 3A.11: chacma baboon

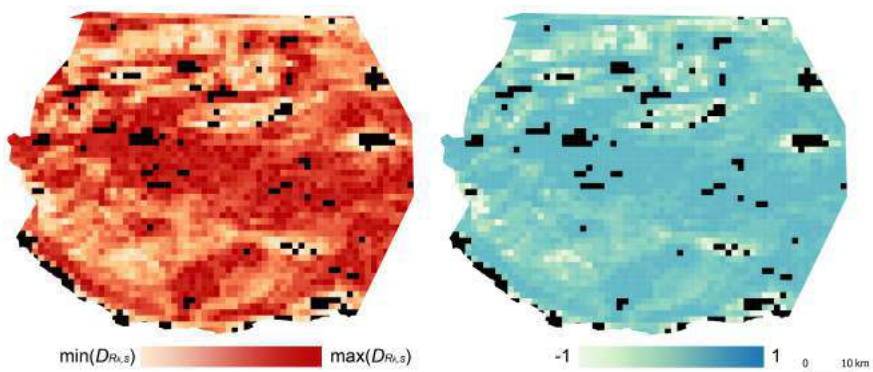


Figure 3A.12: eland

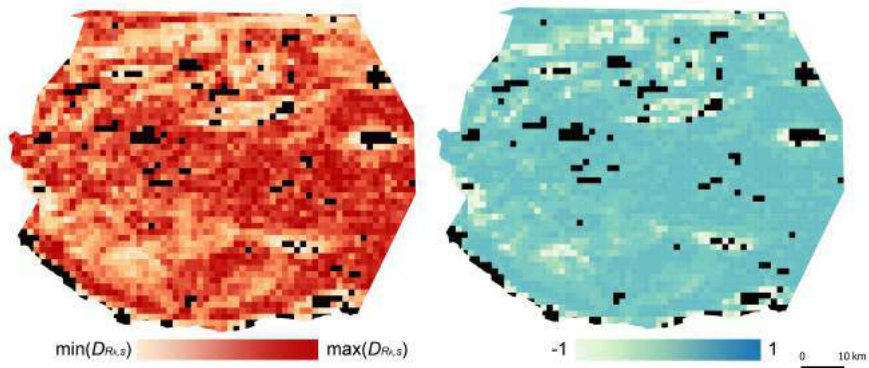


Figure 3A.13: gembok

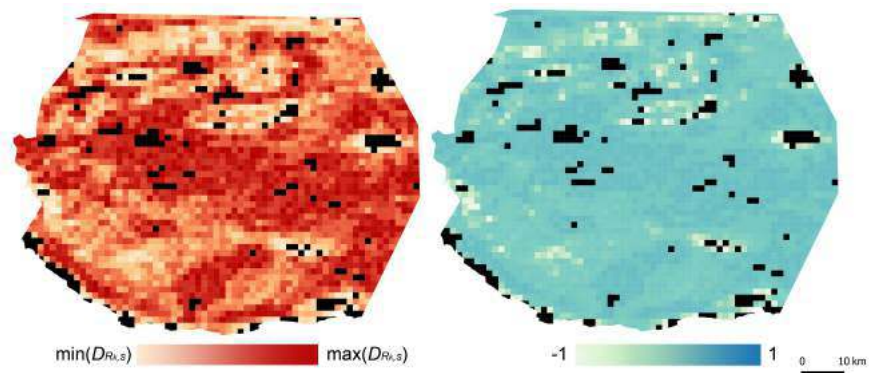


Figure 3A.14: greater kudu

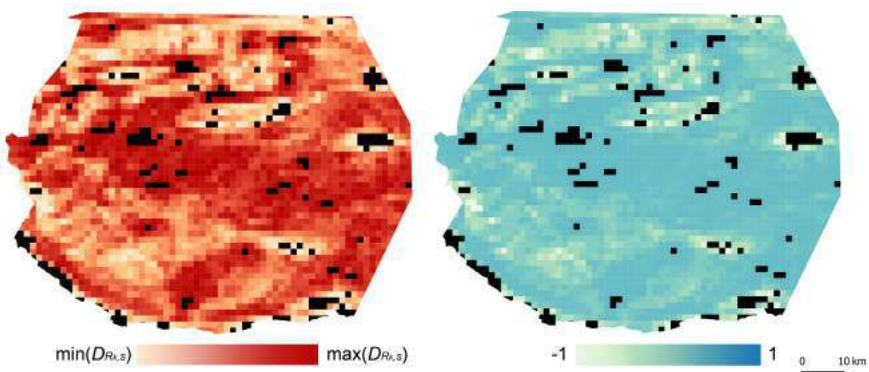


Figure 3A.15: grey duiker

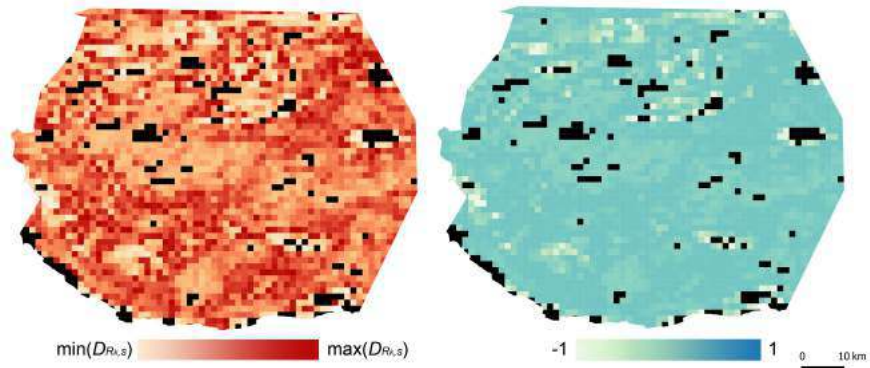


Figure 3A.16: grey rhebuck

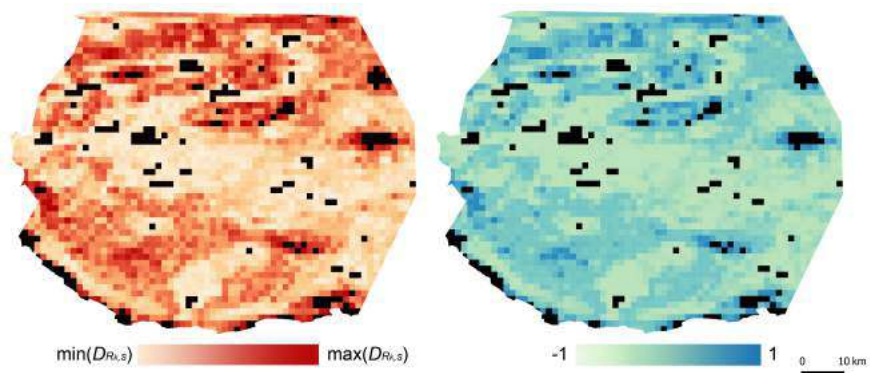


Figure 3A.17: grysbok

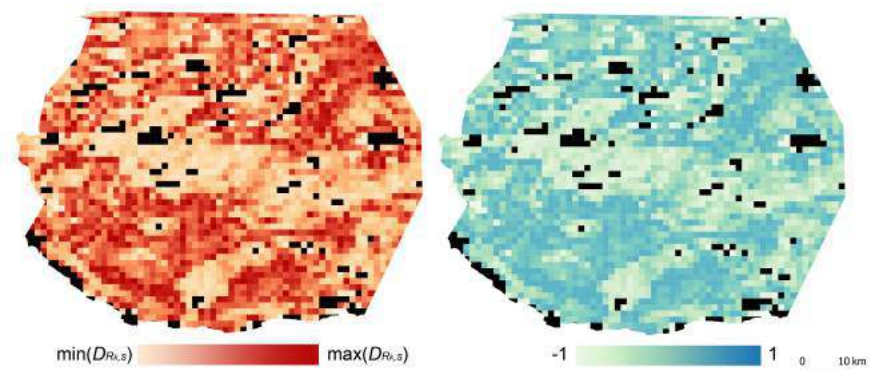


Figure 3A.18: Hewitts red rock rabbit

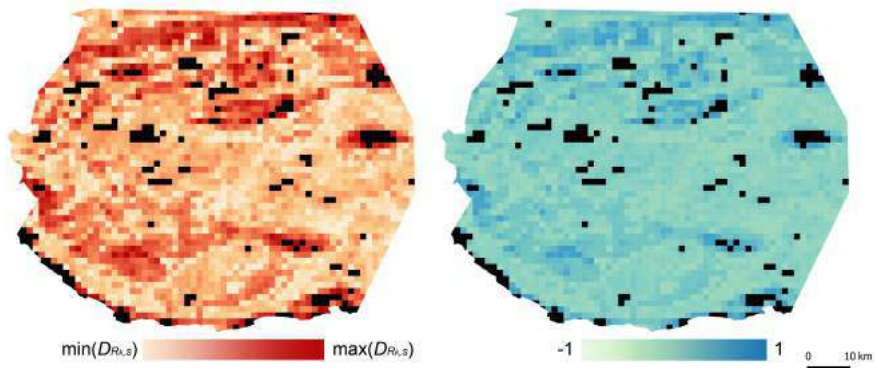


Figure 3A.19: honey badger

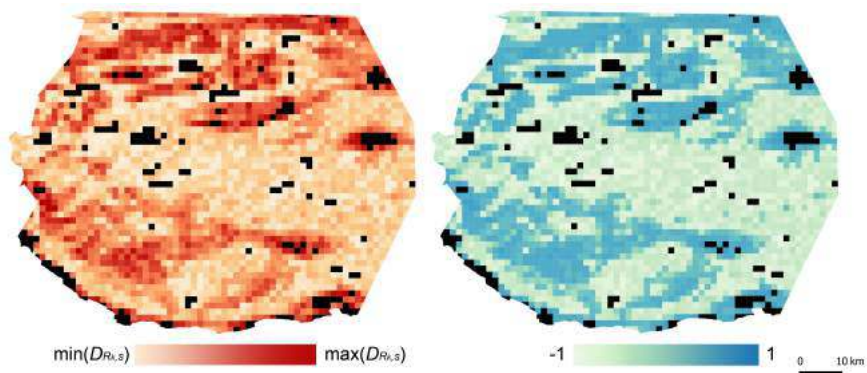


Figure 3A.20: klipspringer

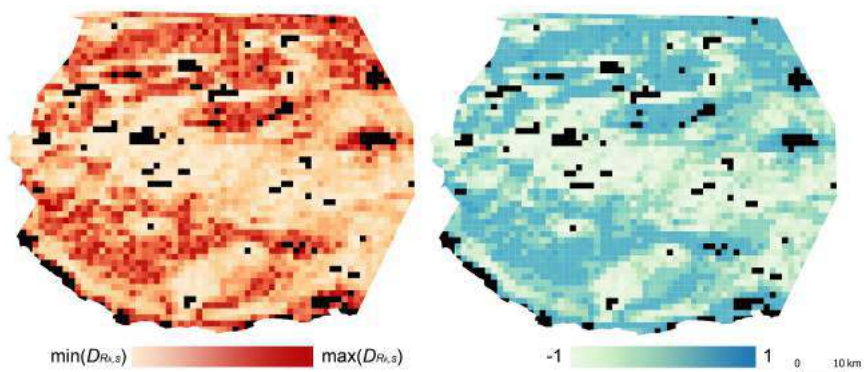


Figure 3A.21: leopard

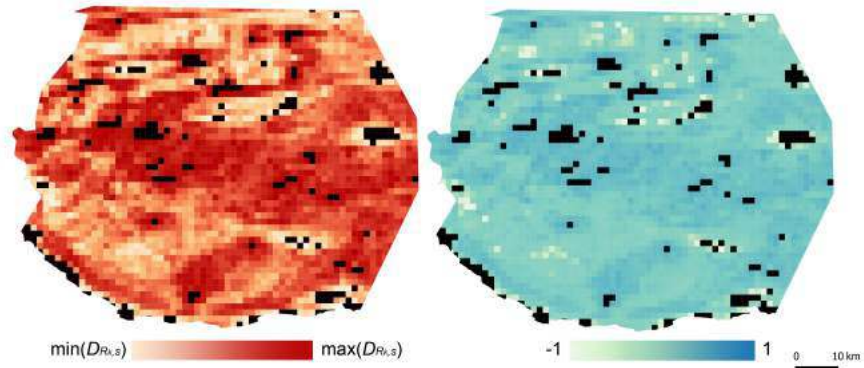


Figure 3A.22: red hartebeest

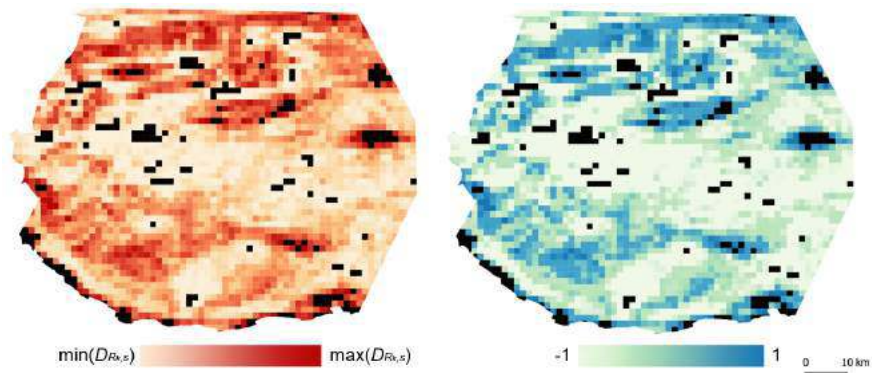


Figure 3A.23: rock hyrax

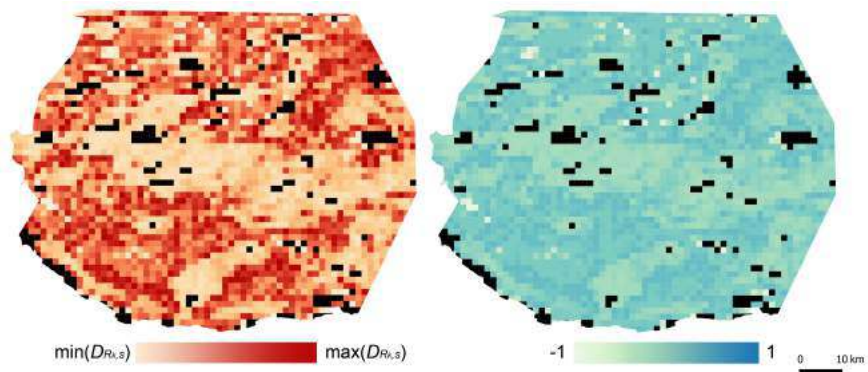


Figure 3A.24: scrub hare

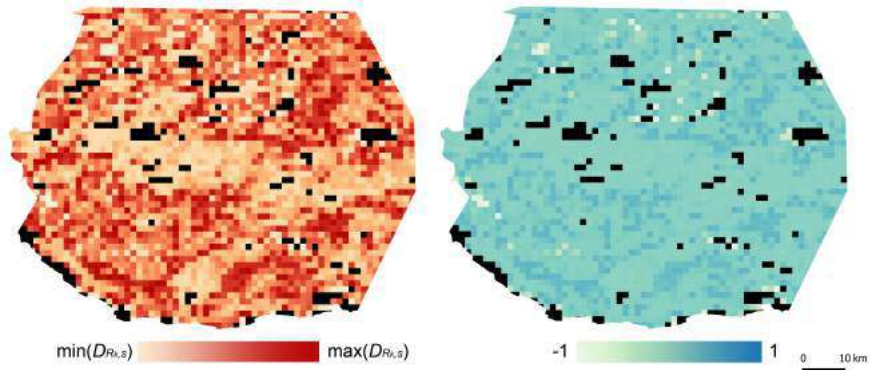


Figure 3A.25: small spotted genet

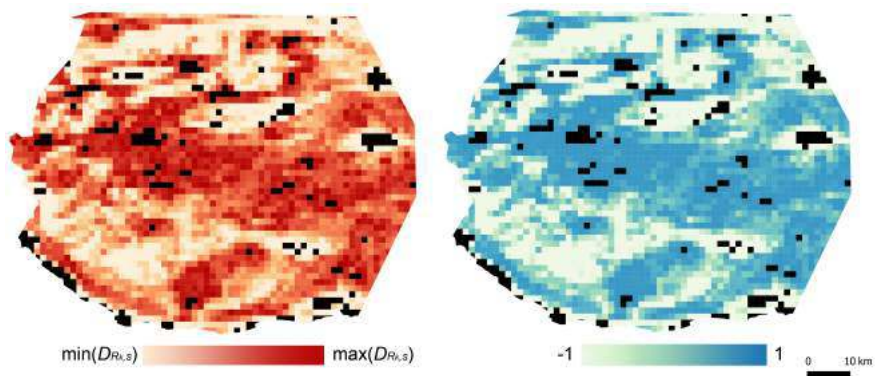


Figure 3A.26: springbok

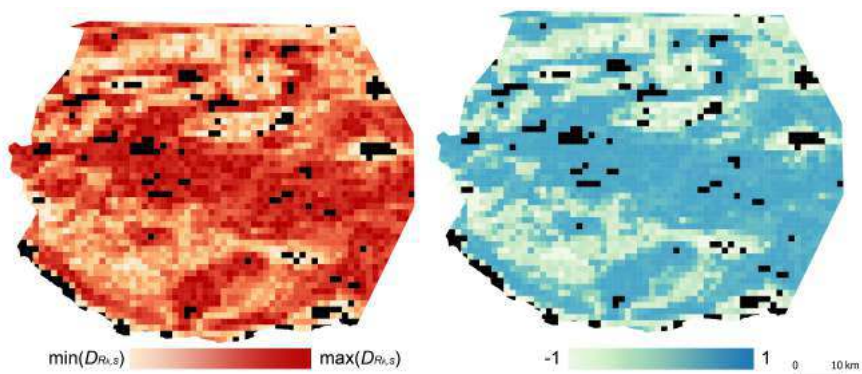


Figure 3A.27: steenbok

Appendix 4A

Demonstration of Eq. 2.11

To lighten the presentation, functions' variables were only annotated at the first occurrence of the function definition.

$t \mapsto A_{e,s}(t)$ and $t \mapsto A_{w,s}(t)$ are probability density functions whose domain is $D = [0, 24]$, therefore:

$$\forall t \in D, A_{e,s} \geq 0, \quad A_{w,s} \geq 0, \quad S_{,s} = A_{e,s} - A_{w,s} \quad \text{and} \quad A_{e,s}, A_{w,s}, S_{,s} \in C^0(D)$$

$$\int_0^{24} A_{e,s} \cdot dt = \int_0^{24} A_{w,s} \cdot dt = 1 \quad \Leftrightarrow \quad \int_0^{24} S_{,s} \cdot dt = 0$$

$$O_{,s} = \int_0^{24} \min(A_{e,s}, A_{w,s}) \cdot dt$$

$$D = D^+ + D^-,$$

$$D^+ = \bigcup_{i=1}^n [a_i, b_i], \quad \forall t \in D^+, A_{e,s} \geq A_{w,s} \Leftrightarrow \int_{a_i}^{b_i} A_{w,s} \cdot dt = \int_{a_i}^{b_i} \min(A_{e,s}, A_{w,s}) \cdot dt$$

$$D^- = \bigcup_{j=1}^m [c_j, d_j], \quad \forall t \in D^-, A_{e,s} \leq A_{w,s} \Leftrightarrow \int_{c_j}^{d_j} A_{e,s} \cdot dt = \int_{c_j}^{d_j} \min(A_{e,s}, A_{w,s}) \cdot dt$$

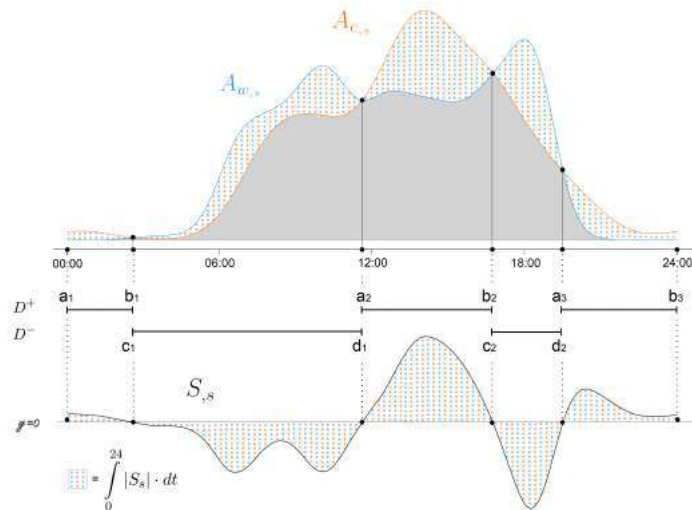


Figure 4A.1: Example showing D^+ and D^- , with $n = 3$ and $m = 2$

$$\begin{aligned}
\int_0^{24} |S_{,s}| \cdot dt &= \int_0^{24} |A_{e,s} - A_{w,s}| \cdot dt \\
&= \sum_{i=1}^n \int_{a_i}^{b_i} A_{e,s} - A_{w,s} \cdot dt - \sum_{j=1}^m \int_{c_j}^{d_j} A_{e,s} - A_{w,s} \cdot dt \\
&= \sum_{i=1}^n \int_{a_i}^{b_i} A_{e,s} - A_{w,s} \cdot dt + \sum_{j=1}^m \int_{c_j}^{d_j} A_{w,s} - A_{e,s} \cdot dt \\
&= \sum_{i=1}^n \int_{a_i}^{b_i} A_{e,s} - A_{w,s} + A_{w,s} - A_{w,s} \cdot dt + \sum_{j=1}^m \int_{c_j}^{d_j} A_{w,s} - A_{e,s} + A_{e,s} - A_{e,s} \cdot dt \\
&= \int_0^{24} A_{e,s} + A_{w,s} \cdot dt - 2 \cdot \sum_{i=1}^n \int_{a_i}^{b_i} A_{w,s} \cdot dt - 2 \cdot \sum_{j=1}^m \int_{c_j}^{d_j} A_{e,s} \cdot dt \\
&= 2 - 2 \cdot \left(\sum_{i=1}^n \int_{a_i}^{b_i} \min(A_{e,s}, A_{w,s}) \cdot dt + \sum_{j=1}^m \int_{c_j}^{d_j} \min(A_{e,s}, A_{w,s}) \cdot dt \right) \\
&= 2 \cdot \left(1 - \int_0^{24} \min(A_{e,s}, A_{w,s}) \cdot dt \right) \\
&= 2 \cdot (1 - O_{,s})
\end{aligned}$$

The demonstration would be the same for $A'_{e,s}$, $A'_{w,s}$, $S'_{,s}$ and $A''_{e,s}$, $A''_{w,s}$, $S''_{,s}$:

$$\begin{aligned}
\int_0^{24} |S_{,s}| \cdot dt &= 2 \cdot (1 - O_{,s}) \\
\int_0^{24} |S'_{,s}| \cdot dt &= 2 \cdot (1 - O'_{,s}) \\
\int_0^{24} |S''_{,s}| \cdot dt &= 2 \cdot (1 - O''_{,s})
\end{aligned}$$

Appendix 5A

Parameter coefficients from best-performing models

Modelling leopard population density in the Little Karoo.

Table 5A.1: β coefficients from Model 21

This table provides the β coefficients estimated on the original scale when Model 21 was fitted. Once transformed on the scale given by the link function, the real parameter values (fitted values) can be accessed: log-transformed density D and σ ; logit-transformed g0 and pmix.

	Estimate	SE	LCL	UCL
D	-11.02	0.92	-12.82	-9.22
D <i>s(ruggedness)</i> 1	8.13	9.16	0.98	26.08
D <i>s(ruggedness)</i> 2	0.34	0.56	-0.76	1.43
g0	-3.52	0.12	-3.77	-3.28
σ	7.25	0.15	6.96	7.55
σ <i>h2</i>	1.14	0.13	0.88	1.40
σ <i>session</i> B	0.28	0.13	0.03	0.53
σ <i>session</i> C	0.52	0.15	0.23	0.81
σ <i>session</i> D	0.10	0.18	-0.25	0.45
σ <i>session</i> E	0.33	0.12	0.10	0.56
σ <i>session</i> F	0.28	0.11	0.06	0.50
pmix <i>h2</i>	-0.83	0.41	-1.63	-0.03

Table 5A.2: β coefficients from Model 22

This table provides the β coefficients estimated on the original scale when Model 22 was fitted. Once transformed on the scale given by the link function, the real parameter values (fitted values) can be accessed: log-transformed density D and σ ; logit-transformed g0 and pmix.

	Estimate	SE	LCL	UCL
D	-11.27	1.10	-13.43	-9.11
D <i>s(ruggedness)</i> 1	0.70	1.71	-2.65	4.05
D <i>s(ruggedness)</i> 2	5.23	5.71	-5.96	16.42
D <i>s(ruggedness)</i> 3	0.66	0.68	-0.67	1.98
g0	-3.53	0.12	-3.77	-3.28
σ	7.25	0.15	6.96	7.55
σ <i>h2</i>	1.14	0.13	0.88	1.40
σ <i>session</i> B	0.28	0.13	0.03	0.53
σ <i>session</i> C	0.52	0.15	0.23	0.81
σ <i>session</i> D	0.11	0.18	-0.24	0.45
σ <i>session</i> E	0.33	0.12	0.10	0.57
σ <i>session</i> F	0.28	0.11	0.06	0.50
pmix <i>h2</i>	-0.82	0.40	-1.61	-0.03

